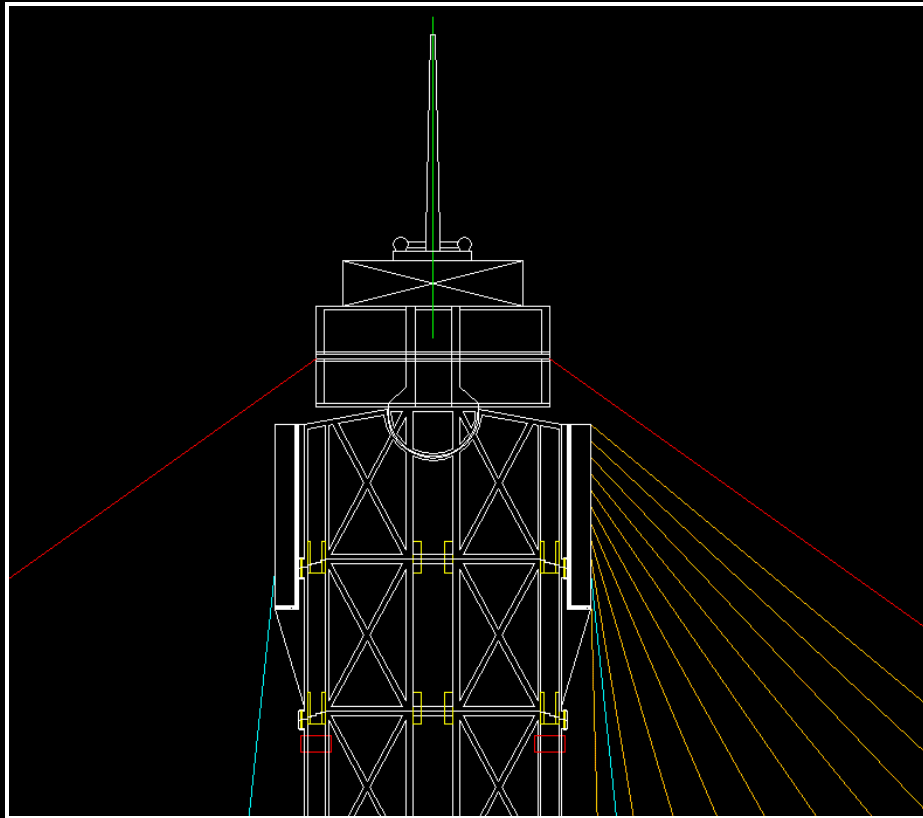


**Giacinto Libertini**

**Project for powerful wind power plants  
with vertical axis of rotation**

**(VertEolo Project)**

**2<sup>nd</sup> edition**



**Copernican Editions**



**Giacinto Libertini**

[\(giacinto.libertini@tin.it](mailto:giacinto.libertini@tin.it)

[www.r-site.org/VertEolo/](http://www.r-site.org/VertEolo/)

[www.r-site.org/ageing/](http://www.r-site.org/ageing/)

**Project for powerful wind power plants  
with vertical axis of rotation**

**(VertEolo Project)**

**2<sup>nd</sup> edition**

**Copyright © January 2013**

**Copernican Editions**

**Naples, Italy**

**ISBN 9788890648625**

# CONTENTS

## Text

Number	Section	Page
1	Summary	8
2	Introduction	9
3	Limits of current wind power plants	16
4	Brief description of the VertEolo 1:1 project	18
4-A	--- Fixed part	18
4-B	--- Rotating part	25
4-C	--- Some technical details	35
5	Construction of the plant	36
6	Short description of VertEolo 2:3 and VertEolo 3:6	40
7	Power of the hypothesized plants	42
8	Conclusion	44
9	References	47
10	Acknowledgements	48

## Table Index

Number	Title	Page
1	World production of electricity (2008)	10
2	World TPES (2008)	10
3	Estimated Levelized Cost of New Generation Resources, 2016	15
4	Required plants to satisfy world Energy needs	44

## Figure Index

Number	Title	Page
1	An Enercon E-126 plant under construction, using a gigantic, powerful crane	17
2	General view of the plant – vertical section	20
3	General view of the plant from above	21
4	A module of the vertical axis	22
5	Lower flexing module	23
6	Head of the vertical axis	23
7	A horizontal axis with its wing-supporting ropes	24
8	An anchorage system	24
9	A wing element	26
10	3D images of a wing element	26
11	A connection arm	27
12	3D image of a ring (partial), a connection arm and two main anchorages	27
13	A yellow transverse rope (single round) and a cyan transverse rope (double round)	29
14	One of the two connection arm anchorages and yellow and cyan ring transverse ropes anchorages	30
15	A main anchorage	30
16	A main anchorage in two 3D-images	31
17	A ring in a horizontal section	32

18	Scheme of the rotary systems	33
19	An anti-swing system with its anti-swing ropes	34
20	Scaffoldings and lifting worms, view from above	37
21	VertEolo 1:1, VertEolo 2:3, VertEolo 3:6 + a scheme of an Enercon E-126	41
22	Exposition of the sails to the wind	42
23	Wind speed/power curves for the three hypothesized wind power plants with vertical axis of rotation compared with that of the most powerful existing plant with horizontal axis of rotation	43
24	Comparison between an array of 40 VertEolo 3:6 and an array of 800 current wind-power plants	46

## APPENDIX

### Section 1 – Images from the original files (available at [www.r-site.org/VertEolo](http://www.r-site.org/VertEolo))

Number	Legend	Page
A1	(from installation_step_01.dwg)	49
A2	(from installation_step_02.dwg) - A	49
A3	(from installation_step_02.dwg) - B	50
A4	(from installation_step_03.dwg)	50
A5	(from installation_step_04.dwg) - A	51
A6	(from installation_step_04.dwg) - B	51
A7	(from installation_step_05.dwg) - A	52
A8	(from installation_step_05.dwg) - B	52
A9	(from installation_step_06.dwg)	53
A10	(from installation_step_07.dwg)	53
A11	(from installation_step_08.dwg)	54
A12	(from installation_step_09.dwg)	54
A13	(from installation_step_10.dwg)	55
A14	(from installation_step_11.dwg) - A	55
A15	(from installation_step_11.dwg) - B	56
A16	(from installation_step_11.dwg) - C	56
A17	(from installation_step_12.dwg)	57
A18	(from installation_step_13.dwg) - A	57
A19	(from installation_step_13.dwg) - B	58
A20	(from installation_step_14.dwg) - A	58
A21	(from installation_step_14.dwg) - B	59
A22	(from installation_step_15.dwg)	59
A23	(from installation_step_16.dwg)	60
A24	(from installation_step_17.dwg)	61
A25	(from installation_step_18.dwg)	62
A26	(from installation_step_19.dwg)	63
A27	(from installation_step_20.dwg)	64
A28	(from installation_step_21.dwg)	65
A29	(from installation_step_22.dwg) - A	66
A30	(from installation_step_22.dwg) - B	67
A31	(from installation_step_22.dwg) - C	67

A32	(from scaffoldings.dwg) - A	68
A33	(from scaffoldings.dwg) - B	68
A34	(from scaffoldings.dwg) - C	69
A35	(from scaffoldings.dwg) - D	69
A36	(from scaffoldings.dwg) - E	70
A37	(from scaffoldings.dwg) - F	70
A38	(from scaffoldings.dwg) - G	71
A39	(from wing_element.dwg) - A	71
A40	(from wing_element.dwg) - B	72
A41	(from wing_element.dwg) - C	72
A42	(from wing_element.dwg) - D	73
A43	(from wing_element.dwg) - E	73
A44	(from ring.dwg) - A	74
A45	(from ring.dwg) - B	74
A46	(from ring.dwg) - C	75
A47	(from ring.dwg) - D	75
A48	(from ring.dwg) - E	76
A49	(from ring.dwg) - F	76
A50	(from ring.dwg) - G	77
A51	(from ring.dwg) - H	77
A52	(from ring.dwg) - I	78
A53	(from ring.dwg) - J	78
A54	A 3D (partial) image of a row and its ropes	79
A55	A 3D (partial) image of a row, a ring and an element of the vertical axis	79

## Section 2 – Technical calculations

Number	Section	Page
1	Characteristics of the ropes used in the draft project	80
2	Approximate dimensions and weight of a ring	81
3	Breaking load of the ring	83
4	Breaking load for each blue / yellow system at each ring	84
5	Weight of rings + blue & yellow systems + 1/2 connection arms	86
6	Ring-supporting ropes	88
7	Weights of the wings	90
8	Breaking load for each wing-wing rope	92
9	Wing-supporting ropes	92
10	Pressure in centripetal direction for each wing	93

## Section 3 – Energy production, consumption, and cost (from Wikipedia)

Number	Section	Page
1	Total world energy consumption by source 2010	94
2	Annual world greenhouse gas emissions, in 2005	95
3	List of countries with source of electricity 2008	96
4	Annual electricity net generation in the world (1980-2009)	97
5	Annual electricity net generation from renewable energy in the world (1980-2009)	97

6	Price of oil per barrel (bbl) at which energy sources are competitive	98
7	Hubbert peak graph showing the world's oil production peak	99
8	Total world nuclear power capacity, in GW, and generation, in TWh, for the years 1980 to 2007	100
9	History of nuclear power generation	101
10	World energy consumption outlook from the International Energy Outlook	102
11	Cost of electricity by source	103
11-A	--- US Department of Energy estimates	103
11-B	--- UK 2010 estimates	106
11-C	--- French 2011 estimates	106
11-D	--- Analysis from different sources	107
12	Environmental impact of electricity generation	110
12-A	--- Water usage	110
13	Hydraulic fracturing	111
13-A	--- Air	111
13-B	--- Water Consumption	111

#### Section 4 – Effects on climate

<b>(from Wikipedia)</b>		
Number	Section	Page
1	Global-Land Ocean Temperature Index, from 1880 to present	114
2	CO <sub>2</sub> emissions per years vs. IPCC scenarios	115
3	Temperature variations in the decade 2000-2009	116
4	Atmospheric CO <sub>2</sub> measured at Mauna Loa, Hawaii, from 1960 to 2008	117
5	Global annual fossil fuel CO <sub>2</sub> emissions, from 1800 to 2007	118
6	Average rate of glacier thickness change, from 1955 to 2004	119
7	Effective glacier thinning, from 1970 to 2004	121
8	Retreat of glaciers	122
8-A	--- Greenland	122
8-B	--- Antarctica	122
8-C	--- Impacts of glacier retreat	123
9	Projected temperature variations in the 21 <sup>st</sup> century on a range of emissions scenarios	126
10	Global average absolute seas level, from 1870 to 2008	128
11	Projected surface temperatures for the period 2050-2059 in different scenarios	129
12	Global warming and irreversible effects	131
12-A	--- Abrupt or irreversible changes	131
12-B	--- Irreversible impacts	131
13	Risks from climate change	132
13-A	--- Current risk	132
14	Impacts of global warming	134
<b>(from National Geographic)</b>		
15	If all the ice melted (Tim Folger, September 2013)	135

# **Project for powerful wind power plants with vertical axis of rotation**

## **(1) Summary**

83% of total world energy production for all purposes is, today, based on the use of non-renewable resources. This is becoming increasingly problematic, both in terms of the gradual depletion of the resources themselves, but even more so because of the progressive climate warming that, within a few decades, could lead to the complete destruction of large part of many of the world's most important cities. A transition to massive use of renewable resources as soon as possible is, therefore, essential.

The use of wind power plants would potentially appear as the best possible solution but today's plants have severe limitations. If, on one hand, we need to build plants that are as powerful as possible, costs grow exponentially, for the type of plant currently in use, in relation to the height (i.e., power) of the plants and so the construction of plants noticeably more powerful than those so far constructed, does not seem feasible.

This work proposes an entirely new type of plants, with a vertical axis of rotation, and with reduced costs, due to the method of construction and to the reduction in materials used.

In addition, the most interesting aspect is the possibility of constructing plants that are much more powerful than those existing at present with a linear increase of the costs/power ratio.

In fact, by building plants with an effective power 20 times greater than that of the most powerful current wind power plants built to date, about 68,000 plants would be sufficient to meet today's world energy needs satisfied by non-renewable sources. Furthermore, in a future scenario with world population increased to 10 billion and average consumption per capita equal to that of the most industrialized countries (but excluding countries with high consumption of energy), the overall energy needs would be covered by about 165,000 plants. The building of these plants would not constitute a heavy economic burden but could, indeed, be amortized in less than two years.

**Keywords:** wind power plants, vertical axis of rotation, renewable resources, fossil fuels



## (2) Introduction

In 2008, world production of electricity was 20,262 TWh, generated by combustion of fossil fuels (67.49%), nuclear power plants (13.48%), and renewable sources (19.03%) [1] (Table 1). The total of electricity generated by non-renewable resources was, therefore, 80.97%.

Since then, the data has changed appreciably for two types of resources:

- In 2010, the production of electricity by wind power plants rose to 344.8 TWh [2], with an increase of 57.4% over two years. From 2008 to 2011, wind power capacity rose from 121 to 238 GW (+96.7%) [3].

- Over the same period, the installed capacity of photovoltaic systems for the production of electricity has increased from 15.7 to 70 GW (+345.9%) [3].

The mean efficiency of electricity production plants was 39% and the balance of 61% was generated heat [4]. Therefore, as 20,262.4 TWh are equivalent to 1,742,252.79 kilo tonnes of oil equivalent (ktoe; 1 TWh = 3,600,000 GJ; 1 ktoe = 41,868 GJ; 1 TWh = 85.98452279 ktoe), the energy consumed in all power plants for electricity production was  $1,742,252.79 \text{ ktoe} / 39 \cdot 100 = 4,467,314.86 \text{ ktoe}$ .

This consumption was 36% of the total for primary energy sources (TPES) of 2008 [4]. Therefore, the TPES was about  $4,467,315 \text{ ktoe} / 36 \cdot 100 = 12,409,208 \text{ ktoe} = 12.409 \text{ Gtoe}$ .

If we consider the broader and more comprehensive picture of TPES in 2010, we find that which is illustrated in Table 2 [3]. As 80.6% of TPES is obtained by fossil fuels, this means that, every year, fossil fuels equivalent to  $12,409 \text{ Gtoe} \cdot 0.806 = 10.00 \text{ Gtoe}$  are burned, i.e. 27.40 Mtoe / day.

The predominant use of non-renewable sources of energy generates two kinds of problems.

1) By definition, these sources are available in a limited quantity and, so, after a certain period in which their cost will progressively increase with a heavy impact on the economy, they must run out. The discussion on this subject is active and sometimes contradictory, but a documented review published in an authoritative journal, has recently provided some interesting elements of assessment [5]. In short, the production of oil has reached a peak of about 75 million barrels per day between 2005-2012. Over these years, the ratio cost/production became "anelastic", i.e. small increases/reductions in demand are opposed by large increases/reductions in the price, a signal of an inability to adapt supply to demand for about 7 years. It does not appear that this gap can be easily filled by the increase in the use of other fossil fuels:

- "Production of oil derived from Canada's tar sands ... is expected to reach just 4.7 million barrels per day by 2035 (Canadian Association of Petroleum Producers. *Report of the Dialogues on the Oil Sands*, CAPP, 2011)."

- "The production from Venezuela's tar sands is currently less than 2 million barrels per day, with little prospect of a dramatic increase (Hirsch, R., Bezdek, R.H., Wendling, R.M. *The Impending World Energy Mess: What it is and What it Means to You!* Apogee Prime Press, 2010)."

- "... several studies suggest that available coal is less abundant than has been assumed"

- "... US shale-gas resources are immense, but recent reports suggest that both reserves and future production rates have been substantially overstated."

As regards the economic consequences: "What does this mean for the global economy, which is so closely tied to physical resources? Of the 11 recessions in the United States since the Second World War, 10, including the most recent, were preceded by a spike in oil prices (Hamilton, J.D. *Causes and Consequences of the Oil Shock of 2007-08*. Brookings Papers on Economic Activity. 215-59, 2009).

It seems clear that it wasn't just the 'credit crunch' that triggered the 2008 recession, but the rarely-talked-about 'oil price crunch' as well. High energy prices erode family budgets and act as a head wind against economic recovery" [5].

**Table 1 – World production of electricity (2008) [1]**

Resources	TWh per year	%
Coal	8,263	40.78
Gas	4,301	21.23
Oil	1,111	5.48
Total fossil fuels:	13,675	67.49
Nuclear	2,731	13.48
Total non-renewable resources:	16,406	80.97
Hydro	3,288	16.23
Wind	219	1.08
Geothermal	65	0.32
Solar photovoltaic	12	0.059
Solar thermal	0.9	0.0044
Tide	0.5	0.0025
Biomasses and other	271	1.34
Total renewable resources:	3,856.4	19.03
Total	20,262.4	100.00

**Table 2 – World TPES (2008) [3]**

Resources	%
Fossil fuels	80.6
Nuclear	2.7
Total non-renewable resources:	83,3
Biomass heat	11.44
Hydropower	3.34
Wind power	0.51
Ethanol	0.50
Biomass electricity	0.28
Solar hotwater	0.17
Biodiesel	0.17
Geothermal heat	0.12
Geothermal electricity	0.07
Solar photovoltaic power	0.06
Solar CSP (concentrating solar thermal power)	0.002
Tide	0.001
Total renewable resources:	16.7
Total	100.00

2) The combustion of fossil fuels produces carbon dioxide (CO<sub>2</sub>) and this has increased the concentration of the gas in the atmosphere from values of 280 parts per million (ppm) in pre-industrial times to 395 ppm in June 2012, with an increment of 2.0 ppm/yr during 2000-09 [6], caused by anthropogenic causes [7]. Global warming is caused by increasing concentrations of greenhouse gases, mainly CO<sub>2</sub>, produced by human activities, in particular the burning of fossil fuels and deforestation [8]. The effects of global warming include a continuing retreat of glaciers, permafrost and sea ice, altered patterns of precipitations, expansion of arid zones, and a rise in sea levels [8].

“Complete deglaciation of the Greenland ice would rise sea level by 7 m and could be irreversible” [8]. The sea level rise caused by the complete melting of the Greenland and Antarctic ice sheets would be 7.1 m and 61.1, respectively (with a total of 68.2 m) [9].

The worst-case scenario envisaged in the IPCC report shows that, with CO<sub>2</sub> concentrations stabilized at values of 855-1130 ppm, there would be a rise in global temperatures of 8° Celsius (!) and an increase in sea level due to thermal expansion of between 1 and 3.7 m [8].

However, the report does not point out the catastrophic effects, in this scenario, of an increase in sea level caused by the certain melting of the Greenland and Antarctic ice sheets in the case of both the worst scenario and of other scenarios. In fact, an increase in sea level of 68.2 m would submerge cities such as London, York, Liverpool, Dublin, Brussels, Lille, Paris, Marseilles, Bordeaux, Nice, Rome, Naples, Palermo, Bari, Catania, Padua, Ferrara, Pisa, Livorno, Cagliari, Barcelona, Valencia, Alicante, Málaga, Lisbon, Hamburg, Hannover, Bremen, Kiel, Gdansk, Riga, Tallin, Oslo, Stockholm, Helsinki, Saint Petersburg, Vladivostok, Odessa, Istanbul, Izmir, Athens, Thessaloniki, Varna, Costantza, New York, Los Angeles, San Francisco, Miami, Orlando, New Orleans, Boston, Philadelphia, Houston, Seattle, Honolulu, Montreal, Veracruz, Buenos Aires, Bangkok, Tokyo, Yokoyama, Hiroshima, Nagasaki, Osaka, Kyoto, Hokkaido, Seoul, Busan, Taipei, Beijing, Tianjin, Shanghai, Guangzhou, Hong Kong, Shenzhen, Macao, Hanoi, Manila, Jakarta, Saigon, Singapore, Phnom Penh, Rangoon, Kolkata, Mumbai, Colombo, Dhaka, Dubai, Kuwait City, Beirut, Tel Aviv, Gaza, Cairo, Alexandria, Tunis, Lagos, Tel Aviv, Sydney, Adelaide, Brisbane, Melbourne, Perth, Wellington, Auckland, and countless other towns, while an increase of even a few meters would be enough to destroy Venice, the whole of the Netherlands and Denmark and a large number of insular states.

In summary, the current predominant use of fossil fuels: a) will be possible only for a limited time; b) has been, is and will be a source of serious economic crises and imbalances; c) is causing serious climatic alterations with potentially catastrophic effects of appalling and unacceptable severity.

A transition from the use of non-renewable to renewable energetic sources is, therefore, essential and inevitable. In addition, this must be accomplished before the increases in costs and the climatic alterations cause serious and unacceptable long-lasting damages.

It is, therefore, necessary to develop and use energy production mechanisms based entirely on renewable sources, capable of producing what is now obtained by fossil fuels, and satisfying the likely increase in demand due to the increasing world population and the adjustment of consumption to the average levels of advanced countries (i.e., without the excesses of countries such as the USA).

This means that it is essential to produce, through renewable sources, a total amount of energy ( $W_t$ ) equal to the sum of:

A) 16,406 TWh of electricity, i.e. the production in 2008 through non-renewable sources, ignoring the increase to the current levels of production;

B) the energy produced by non-renewable sources for other purposes, roughly estimated here as the double of A;

C) the expected increase of A and B due to the combined effects of: 1) increase of world population from 7 to 10 billion; 2) growth of world per capita consumption from 70 GJ (Gigajoules) to 170 GJ, which are the 2011 values of entire world and European mean consumption, respectively [10]; 3) an

optimistic saving of 30% in energy consumption. With these assumptions, the increase could be estimated roughly at +143%.

So, with the above-mentioned estimated coarse values,  $W_t$  would be  $16,406 \cdot 3 \cdot 2.43 = 119,599$  TWh.

As 1 TWh is approximately the energy produced by a power of 0.114 GW for a period of one year, the effective power ( $W_e$ ) required to get this energy would be equal to  $W_t \cdot 0.114 \text{ GW} = 13,634$  GW.

If the mean efficiency of the plants is equal to  $E$  ( $0 < E < 1$ ), the value of  $W_t$  must be divided by  $E$  in order to obtain the necessary nameplate power ( $W_n = W_e / E$ ).

By using non-nuclear plants with a mean  $E = 39\%$  (as for electricity production),  $W_n = 13,634 \text{ GW} / 0.39 = 34,959 \text{ GW}$ .

By using only nuclear power plants with an average efficiency of 90%:  $W_n = 13,634 \text{ GW} / 0.9 = 15,149 \text{ GW}$ , i.e. to produce this power, 15,149 nuclear plants with nameplate power of 1 GW and average efficiency = 90% would be necessary. To get an idea of the magnitude of this figure, all nuclear power plants in operation around the world are 435 and have a nominal capacity of 370 GW [11], i.e. 2.44 % of 15,149 GW.

The possibility of obtaining this energy by mass production of energy through nuclear fission plants is not realistic due to the following: a) the limited availability of nuclear fission fuels, which are non-renewable resources too; b) huge, increasing costs for the construction, safe operation and finally decommissioning of nuclear installations, c) the costs and risks related to plants which are potentially dangerous for the surrounding areas.

As regards the possibility of obtaining this by nuclear fusion plants: a) at present, this option is only hypothetical; b) to ensure that it becomes real, there is a need for further significant investments which have rather been decreasing, in view of the dwindling prospects of success; c) the time predicted for getting the first plant up and running has gradually expanded and is certainly unacceptable given the gravity and urgency of the energy problem; d) systems of this kind, once in operation, will have high costs and will produce radioactive substances with consequent problems of safety and further costs.

Let us examine which renewable sources could be used for the mass production of energy.

- Hydropower is widely used (3.34% of TPES [3]), but the potential to expand the use of this resource appears limited. The sites where it is possible to build new powerful hydroelectric plants are relatively few and often with high environmental impact. However, a doubling of the power generated by this renewable source, a goal hardly attainable, would bring the share of energy produced to 6.68% of the current total, which is not sufficient for an overall solution.

- The use of geothermal energy is limited to particular areas. Currently it provides, as a source of heat and electricity production, only 0.19% of TPES [3], and it is not likely to solve the problem globally.

- Likewise, the use of energy from waves or tides is even more limited (0.001%) [3] and with scant possibilities of expansion.

- The combustion of natural biomasses (firewood) is now largely used to produce heat and for cooking (11.44% of TPES) [3] but this use is unlikely to be expandable. For electricity production, this source is marginal (0.28% of TPES) [3].

- Energy from agricultural products grown specifically to be burned, or for the production of fuels (biodiesel or ethanol; 0.67% TPES [3]) seems an impractical and irrational solution: a) because of the associated energy costs, which make the overall energetic balance only weakly positive or even negative; b) because of the unacceptable effect of increasing the costs of food for human consumption.

- The combustion of waste products is certainly useful, but it cannot be a sufficient solution.

- Hot water from solar energy was 0.17% of TPES in 2010 and electricity produced by solar photovoltaic cells was 0.06% [3]. For the moment, solar energy is too expensive to be used on a large scale for energy production [12] (Table 3). As regards other possible important objections about solar photovoltaic, Ozzie Zehner in his recent book [13] says (references in the text omitted): “The Earth Policy Institute claims solar electricity costs are ‘falling due to economics of scale as rising demands drives industry expansion’ ... But according to the solar industry, prices from the most recent decade have flattened out. Between 2004 and 2009, the installed cost of solar photovoltaic modules actually increased ...” (p. 11)

“Among the CEOs and chief scientists in the solar industry, there is surprisingly little argument that solar systems are expensive. Even an extreme drop in the price of polysilicon, the most expensive technical component, would do little to make solar cells more competitive. Peter Nieh, managing director of Lightspeed Venture Partners, a multibillion-dollar venture capital firm in Silicon Valley, contends that cheaper polysilicon won’t reduce the overall cost of solar arrays much, even if the price of the expensive material dropped to zero. Why? Because the cost of other materials such as copper, glass, plastics, and aluminum, as well as the costs for fabrication and installation, represent the bulk of a solar system’s overall price tag. The technical polysilicon represents only about a fifth of the total.” (p. 24)

“With such high expectations welling up around solar photovoltaics, it is no wonder that newbie solar cell owners are often shocked by the underwhelming performance of their solar arrays in the real world. For example, roof jobs may require that they disconnect, remove, and reinstall their rooftop arrays. Yet an even larger surprise awaits them—within about five to ten years, their solar system will abruptly stop producing power. Why? Because a key component of the solar system, the electrical inverter, will eventually fail. While the solar cells themselves can survive for twenty to thirty years, the associated circuitry does not. Inverters for a typical ten-kilowatt solar system last about five to eight years and therefore owners must replace them two to five times during the productive life of a solar photovoltaic system. Fortunately, just about any licensed electrician can easily swap one out. Unfortunately, they cost about eight thousand dollars each.” (p. 24)

“Soiling is not always so easy to remove. ... many solar installations perch high atop steep roofs. Owners must tango with gravity to clean their panels or hire a stand-in to dance for them. Researchers discovered that soiling routinely cut electrical output of a San Diego site by 20 percent during the dusty summer months. In fact, according to researchers from the photovoltaic industry, soiling effects are ‘magnified where rainfall is absent in the peak-solar summer months, such as in California and the Southwest region of the United States,’ or in other word, right where the prime real estate for solar energy lies.

When it comes to cleanliness, solar cells are prone to the same vulnerability as clean, white dress shirts; small blotches reduce their value dramatically. Due to wiring characteristics, solar output can drop disproportionately if even tiny fragments of the array are blocked, making it essential to keep the entire surface clear of the smallest obstructions, according to manufacturers. Bird droppings, shade, leaves, traffic dust, pollution, hail, ice, and snow all induce headaches for solar cell owners as they attempt to keep the entirety of their arrays in constant contact with the sunlight that powers them. Under unfavorable circumstances, these soiling losses can climb to 80 percent in the field.” (p. 21)

“Not only are solar cells an overpriced tool for reducing CO<sub>2</sub> emissions, but their manufacturing process is also one of the largest emitters of hexafluoroethane (C<sub>2</sub>F<sub>6</sub>), nitrogen trifluoride (NF<sub>3</sub>), and sulfur hexafluoride (SF<sub>6</sub>). Used for cleaning plasma production equipment, these three gruesome greenhouse gases make CO<sub>2</sub> seem harmless. As a greenhouse gas, C<sub>2</sub>F<sub>6</sub> is twelve thousand times more potent than CO<sub>2</sub>, is 100 percent manufactured by humans, and survives ten thousand years once released into the atmosphere. NF<sub>3</sub> is seventeen thousand times more virulent than CO<sub>2</sub>, and SF<sub>6</sub>, the most treacherous greenhouse gas, according to the Intergovernmental Panel on Climate Change, is twenty-five thousand times more threatening. The solar photovoltaic industry

is one of the leading and fastest growing emitters of these gases, which are now measurably accumulating within the earth's atmosphere. A recent study on  $\text{NF}_3$  reports that atmospheric concentrations of the gas have been rising an alarming 11 percent per year." (p. 18)

"The desert outside Masdar City [United Arab Emirates] seems like one of the few ideal locations on the planet for [solar photovoltaic] ... Unfortunately, during the midday hours of the summer, all of the test cells became extremely hot, up to 176 degrees Fahrenheit ( $80^\circ\text{C}$ ), as they baked in the desert sun. Due to the temperature sensitivity of the photovoltaic cells, their output was markedly hobbled across the board, right at the time they should have been producing their highest output. ... In addition to haze, humidity, soiling, misalignment, and temperature sensitivity, silicon solar cells suffer an aging effect that decreases their output by about 1 percent or more per year. Newer thin-film, polymer, paint, and organic solar technologies degrade even more rapidly, with some studies recording degradation of up to 50 percent within a short period of time. This limitation is regularly concealed because of the way reporters, corporations, and scientists present these technologies.

For instance, scientists may develop a thin-film panel achieving, say, 13 percent overall efficiency in a laboratory. However, due to production limitations, the company that commercializes the panel will typically only achieve a 10 percent overall efficiency in a prototype. Under the best conditions in the field this may drop to 7-8.5 percent overall efficiency due just to degradation effects. Still, the direct current (DC) output is not usable in a household until it is transformed. Electrical inverters transform the DC output of solar cells into the higher voltage and oscillating AC that appliances and lights require. Inverters are 70-95 percent efficient, depending on the model and loading characteristics. As we have seen, other situational factors drag performance down even further. Still, when laboratory scientists and corporate PR teams write press releases, they report the more favorable figure, in this case 13 percent. Journalists at even the most esteemed publications will often simply transpose this figure into their articles. Engineers, policy analysts, economists, and others in turn transpose the figure into their assessments." (p. 22)

As regards the energy produced by wind power plants, in 2010 the wind power capacity was 197,637 MW [14] and the energy produced 344.8 TWh [2]. In that year, the mean capacity factor, i.e. the ratio between the energy produced and the rated power was  $344.8 \text{ TWh} / (197,636 \text{ MW} / 114 \text{ MW/TWH}) = 22.4\%$ . The capacity factor is strongly conditioned by the site (Burradale Wind Farm on the Shetland Islands in 2000-2012 has had an average capacity factor of 52%, and, in 2005, had an incredible world record of 57.9% [15]), but also by turbine characteristics and, in particular, by the fact that higher turbines receive more wind. In the USA, the capacity factor for wind power plants coming into service in 2016, has been estimated at 34% [12] (Table 3).

Wind power market penetration for electricity production is expected to reach 3.35 percent by 2013 and 8 percent by 2018 [16, 17]. The share of energy produced by wind is relatively small but growing strongly.

The price of construction and operation of wind power plants built onshore is competitive compared with conventional plants using fossil or nuclear fuels [12]. As for wind power plants built offshore, their cost is considerable and not competitive [12]. However, if one takes into account the warming caused by  $\text{CO}_2$  accumulation in the atmosphere, and the present and future damage caused, in strictly economic terms, the production of energy using wind power plants is greatly cheaper.

However, there are some problems limiting the development of wind power plants and these will be discussed in the next section. A possible solution to many of these difficulties, namely the projects that are the subject of this work, will be proposed in the subsequent sections.

**Table 3. Estimated Levelized Cost of New Generation Resources, 2016 [12]**

Plant Type	Capacity Factor %	U.S. Average Levelized Costs (2009 \$/megawatthour) for Plants Entering Service in 2016				
		Levelized Capital Cost	Fixed O&M	Variable O&M (including fuel)	Transmission Investment	Total System Levelized Cost
Conventional Coal	85	65.3	3.9	24.3	1.2	94.8
Advanced Coal	85	74.6	7.9	25.7	1.2	109.4
Advanced Coal with CCS	85	92.7	9.2	33.1	1.2	136.2
Natural Gas-fired						
Conventional Combined Cycle	87	17.5	1.9	45.6	1.2	66.1
Advanced Combined Cycle	87	17.9	1.9	42.1	1.2	63.1
Advanced CC with CCS	87	34.6	3.9	49.6	1.2	89.3
Conventional Combustion Turbine	30	45.8	3.7	71.5	3.5	124.5
Advanced Combustion Turbine	30	31.6	5.5	62.9	3.5	103.5
Advanced nuclear	90	90.1	11.1	11.7	1.0	113.9
Wind - Onshore	34	83.9	9.6	0.0	3.5	97.0
Wind - Offshore	34	209.3	28.1	0.0	5.9	243.2
Solar Photovoltaic (1)	25	194.6	12.1	0.0	4.0	210.7
Solar Thermal	18	259.4	46.6	0.0	5.8	311.8
Geothermal	92	79.3	11.9	9.5	1.0	101.7
Biomass	83	55.3	13.7	42.3	1.3	112.5
Hydro	52	74.5	3.8	6.3	1.9	86.4

(1) Costs are expressed in terms of net AC power available to the grid for the installed capacity.

### **(3) Limits of current wind power plants**

A modern wind power plant has a horizontal axis of rotation, i.e. it consists of a fixed vertical tower, supporting a horizontal arm with propeller of three stiff blades rotating around it. The electric generator and its housing are arranged around the horizontal axis.

The installation and use of current plants has significant limits that restrain their employment on a large scale:

- 1) The wind is an intermittent source of energy. To counter the discontinuity in energy production, it is necessary to have plants in different areas and to expand the energy transmission links, factors that increase costs considerably.
- 2) The plants must be slowed down or inactivated when the wind is too strong (cut-off). This limits the energy production and, thus, the capacity of the plant. Plants with greater cut-off are, therefore, necessary.
- 3) Onshore built plants are usually located on the crests of hills or, at least, in areas where they are visible from a long distance, which is perceived by many as having a strong environmental impact. Offshore plants mitigate this problem and are also more productive due to the greater intensity and constancy of the wind on the sea, but they are considerably more expensive (about +150% in E.I.A. valuation [12]).
- 4) The tower is basically unstable because it holds a rotating heavy weight with a barycentre that is potentially oscillating and is not on the axis of the barycentre line of the tower. Moreover, the considerable weight of electric generator + its housing + rotor is at the weakest point of the tower, i.e. the top. To ensure the stability of the structure, it is necessary to strengthen it exponentially as the height of the tower and the length of the blades (i.e., the plant power) grow. Furthermore, it is necessary to provide mechanisms to release the wings, in the case of very strong wind, to avoid irreparable damage to the entire structure.
- 5) The largest and most modern plants have a relatively modest power in relation to their considerable cost. The largest wind turbine model built to date is Enercon E-126, manufactured by Enercon GmbH, with 7.58 MW nameplate power. Its dimensions are: hub height 135 m, base diameter 16 m, rotor diameter 127 m, total height 198 m; swept area 12,668 m<sup>2</sup> [18]. Its weights are: foundations 2,500 t; turbine tower 2,800 t, generator and machine housing 348 t, rotor 364 t, total weight about 6,000 t [19]. Enercon GmbH does not make public the cost of the Enercon E-126 manufacture and assembly, but the plant size and the weight of the materials used ensure that costs are considerable.
- 6) To assemble the higher parts of current plants, use of powerful and expensive cranes, capable of lifting considerable weights to the top of the tower, are indispensable. For Enercon E-126, it is necessary to use a crane capable of lifting the heavy parts of the rotor to 135 m and the blades even higher (fig. 1).
- 7) Modern large wind power plants have certain components that are quite large and/or heavy, with considerable difficulties and transportation and installation costs.
- 8) Building wind power plants larger than those as big as the Enercon E-126, means making them even taller, using longer blades and employing greater volumes of materials. Given that this cause costs to rise exponentially the costs, we appear to have come close to the limits of convenience with the type of large wind power plant currently in use.
- 9) Modern plants are made up almost entirely of unique parts that are not easy to manufacture using cost-reducing mass production methods.





**Figure 1 – An Enercon E-126 plant under construction, using a gigantic, powerful crane.**

A project capable of improving this traditional approach should have the following requirements:

- A) a structure that is inherently balanced in its statics, i.e. with a barycentre of the rotating part that is on the same vertical of the barycentre of the fixed part and at a relatively low point;
- B) a significantly greater surface area moved by the wind;
- C) a power one order of magnitude, or more, greater than that of current plants;
- D) high resistance to breakage, even in strong winds;
- E) potentiality to increase plant power with stable or even decreasing cost/power ratio;
- F) electric generator placed near the base and not on the top of the structure;
- G) use of materials in a quantity that is significantly lower with regard to the power of the plant;
- H) no large component which is difficult to transport;
- I) no need to use powerful cranes for lifting any part to considerable heights;
- L) a structure composed of various similar components, in order to exploit the advantages of mass production;
- M) construction procedures that do not involve working at dangerous heights;
- N) relative cheapness and simplicity of construction and management, and highly competitiveness compared both with energy production plants using non-renewable fuels, and with any plant using renewable sources, including modern wind power plants.
- O) the possibility of building very high and powerful structures with the advantages of points A-C, without violating the requirements of points D-N.

This list of characteristics may well seem an unrealistic set of targets, elements of a utopian dream. In this paper, I put forward the draft project of a very powerful type of wind power plant with vertical axis of rotation. The project is based on an approach which is completely different from that used in current systems and one which I believe satisfies all the requirements listed above.

In order to simplify the description of the project, I will briefly describe the draft design of an example with very specific physical dimensions, having arbitrarily chosen width and height of the surface areas (wings or sails) moved by the wind (i.e.: width = 1 unity of wing width = 8 elements, each 5 m wide = 40 m; height = 1 unity of wing height = 50 rows, each 1,68 m high = 84 m). This project is referred to using the abbreviation VertEolo 1:1.

Immediately afterwards, I will move onto the characteristics of two similar projects (VertEolo 2:3 and VertEolo 3:6) with greater dimensions of the surface areas moved by the wind. Clearly, this does not exclude other dimensions.

The description of the project is supported, in the Documentary Appendix to this work, by 2D drawings in dwg format, and by some 3D images in jpg format, of which, for the sake of brevity, only some a limited number of overall views and details are shown in the text.

#### **(4) Brief description of the VertEolo 1:1 project**

A general view of the VertEolo 1:1 project, is given in a vertical section in fig. 2 and in a view from above in fig. 3. The source drawings can be examined in detail, in dwg format, in the Documentary Appendix. The single parts and their functions are described in the following sections.

The plant consists of a fixed part and a rotating part.

##### **(4-A) Fixed part:**

The term “fixed” is to be understood in reference to the inability of this part to perform any rotating movement. However, most of the component is able to perform limited oscillating movements in any direction on a horizontal plane, significantly increasing the ability of the plant as a whole to withstand stresses on that plane.

The fixed part is consists of:

1) a fixed “vertical axis” made up of:

-- foundations. Here, dimensions and design are not specified, and vary in relation to ground characteristics.

-- 89 modules. 87 modules are identical (“standard modules” or simply “modules”, hexagonal in shape on a horizontal plane, height 1.68 m, max. width 2.915 m, fig. 4), while 2 modules are modified (figs. 5 and 6). The lower module is the “base module”, while the top module is the “upper module”. The modules are connected by nuts and bolts and have contact surfaces designed so as to maximize the resistance to bending forces. The two modified modules (“lower flexing module” and “higher flexing module”), on the other end, enable the vertical axis to swing in any direction as a result of bending forces caused by strong winds or even earthquakes. Bending is permitted thanks to a concave lower surface that articulates with a corresponding upper convex surface. The space between the two surfaces is occupied by ball bearings and lubricating liquid.

-- a “pivot part” above the higher flexing module (height = 1.12 m, fig. 6), from which “anchorage ropes” extend;

-- a circular “hanger ring support” around the “upper module” and the overhanging higher flexing module (fig. 6);

-- the “rotor” and the “stator”, around the basis of the vertical axis, which form the “electric generator” (fig. 2).

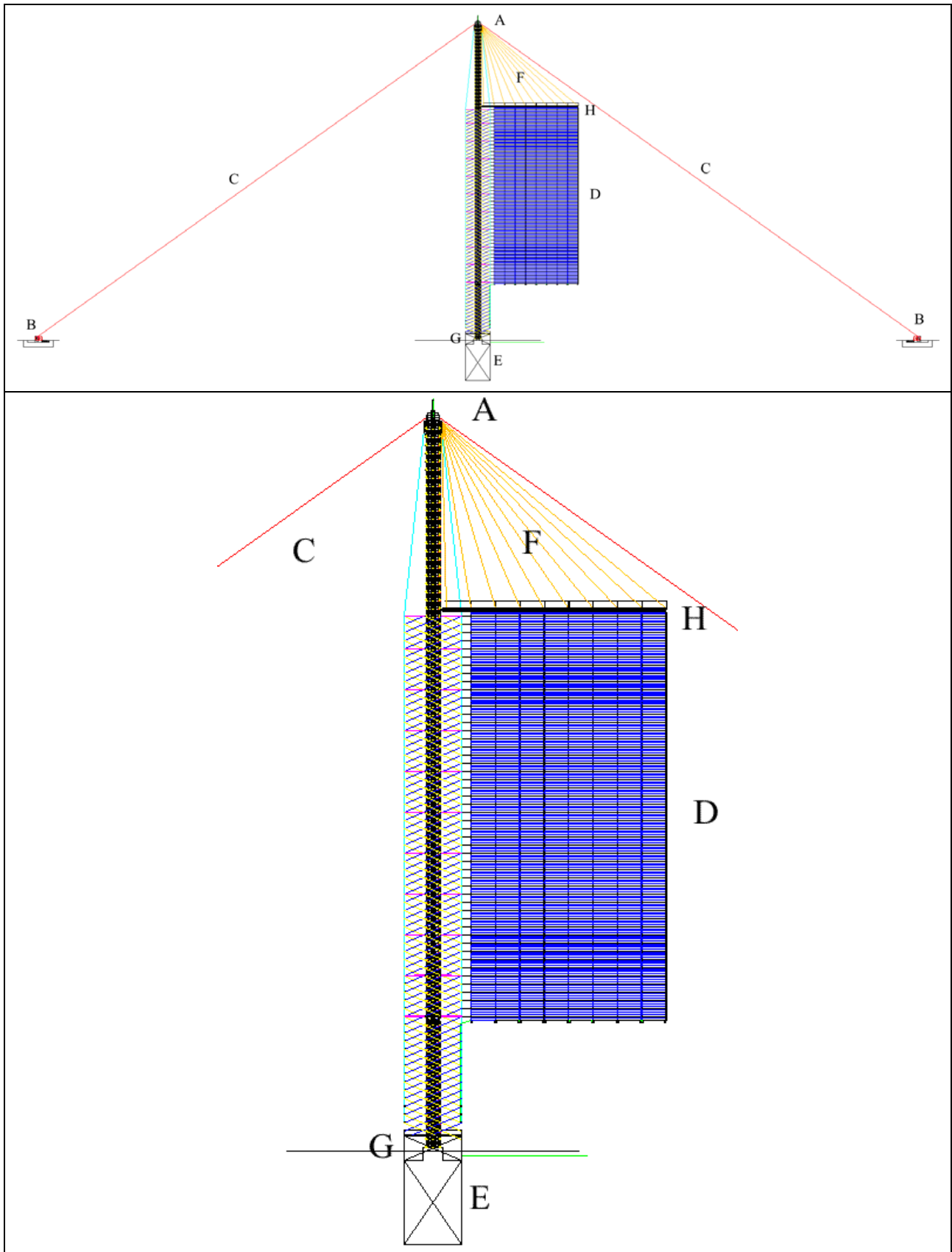


Figure 2 - General view of the plant – vertical section. A: head of the vertical axis; B: anchorage systems; C: anchorage ropes; D: wing or sail; E: foundations; F: wing-supporting ropes; G: electric generator; H: horizontal axis (Documentary Appendix, "general\_scheme\_frontal\_section.dwg")

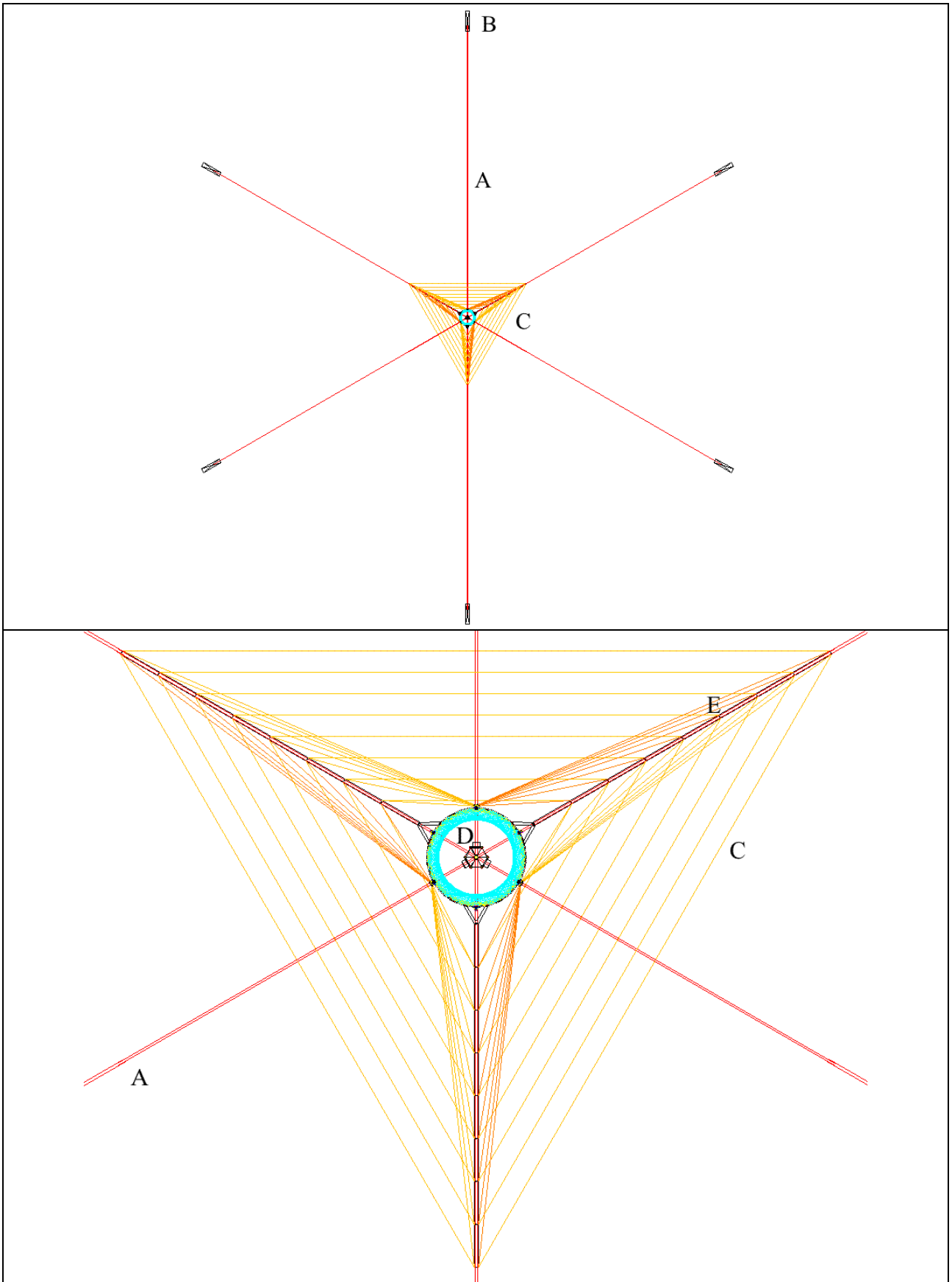
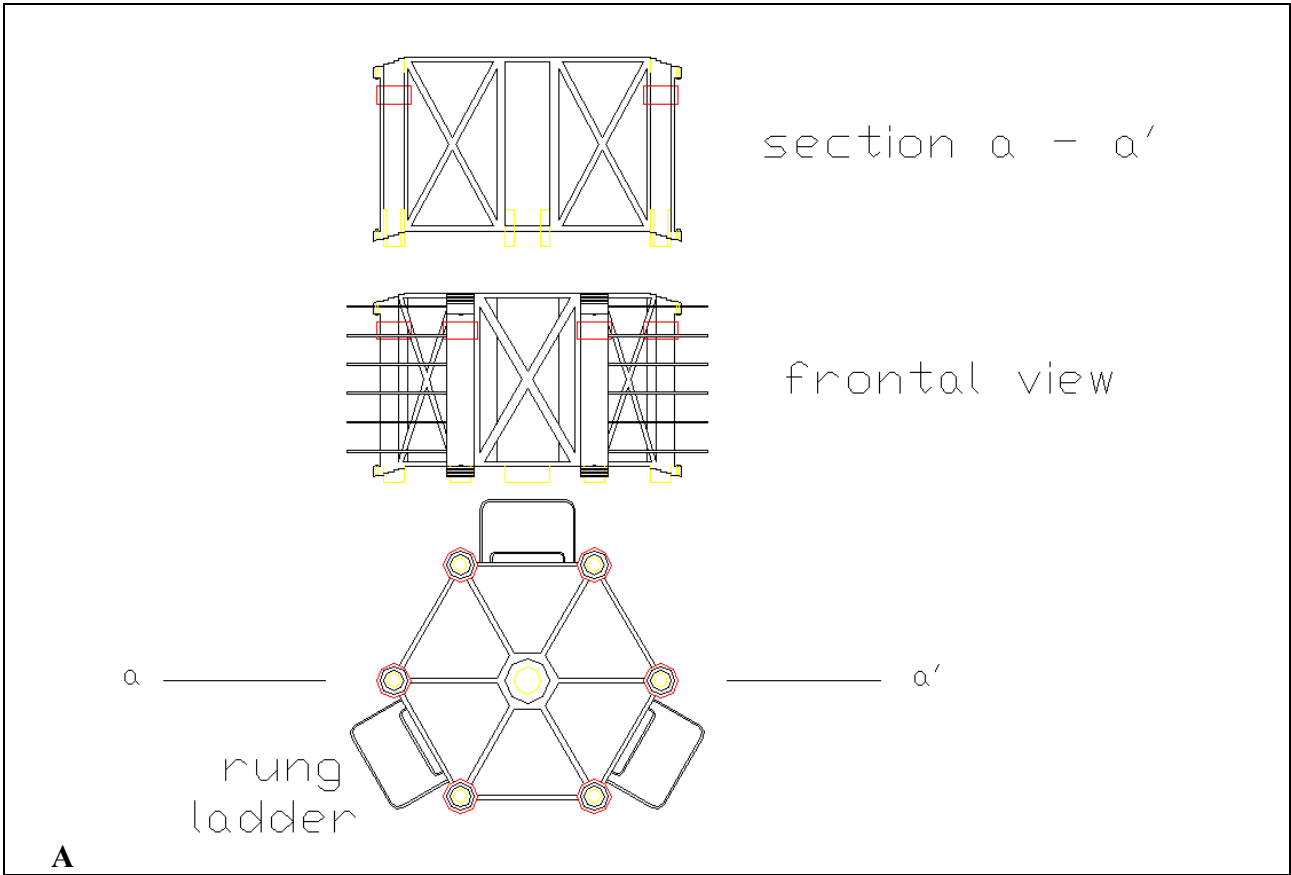


Figure 3 - General view of the plant from above. A: anchorage ropes; B: anchorage system; C: wing-wing ropes; D: ring; E: wing-ring ropes ("general\_scheme\_up\_down.dwg")



**Figure 4 – A module of the vertical axis (detail of "general\_scheme\_frontal\_section.dwg").**

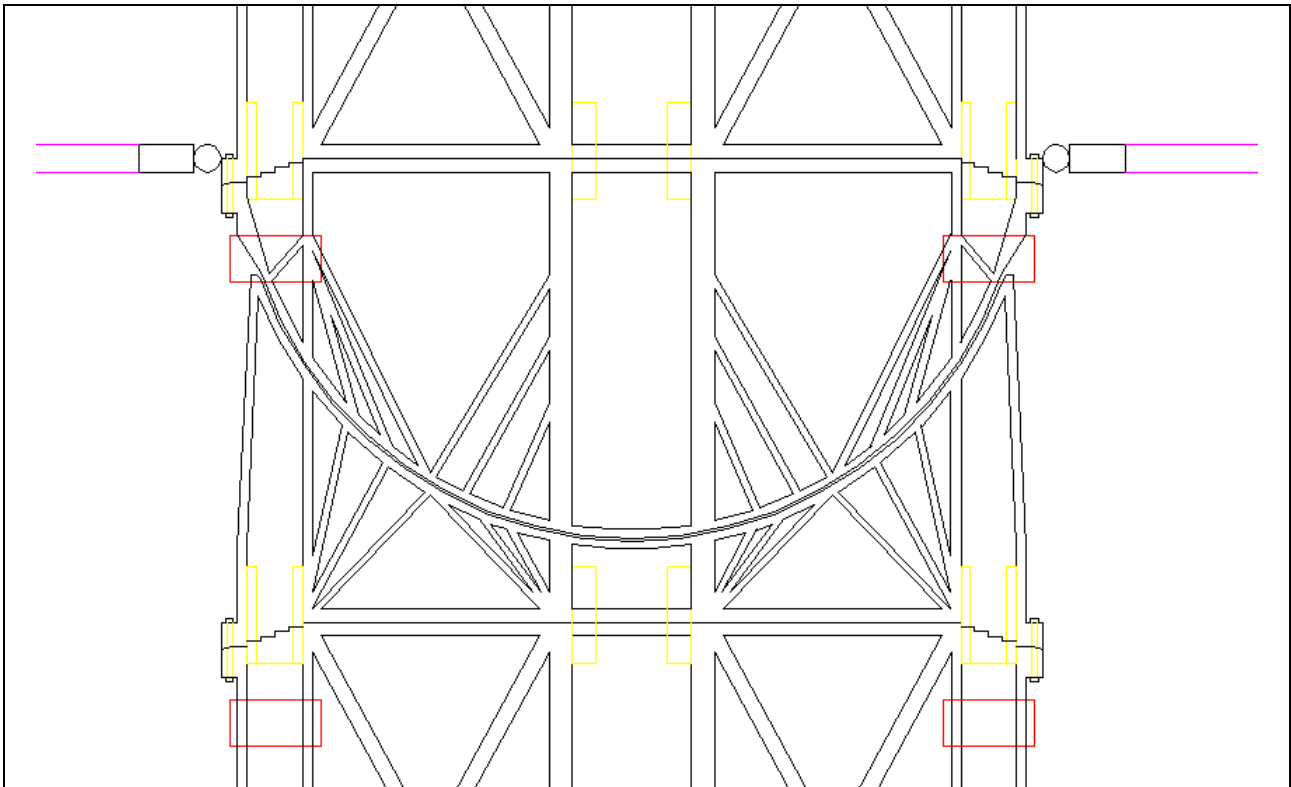


Figure 5 – Lower flexing module (detail of "general\_scheme\_frontal\_section.dwg")

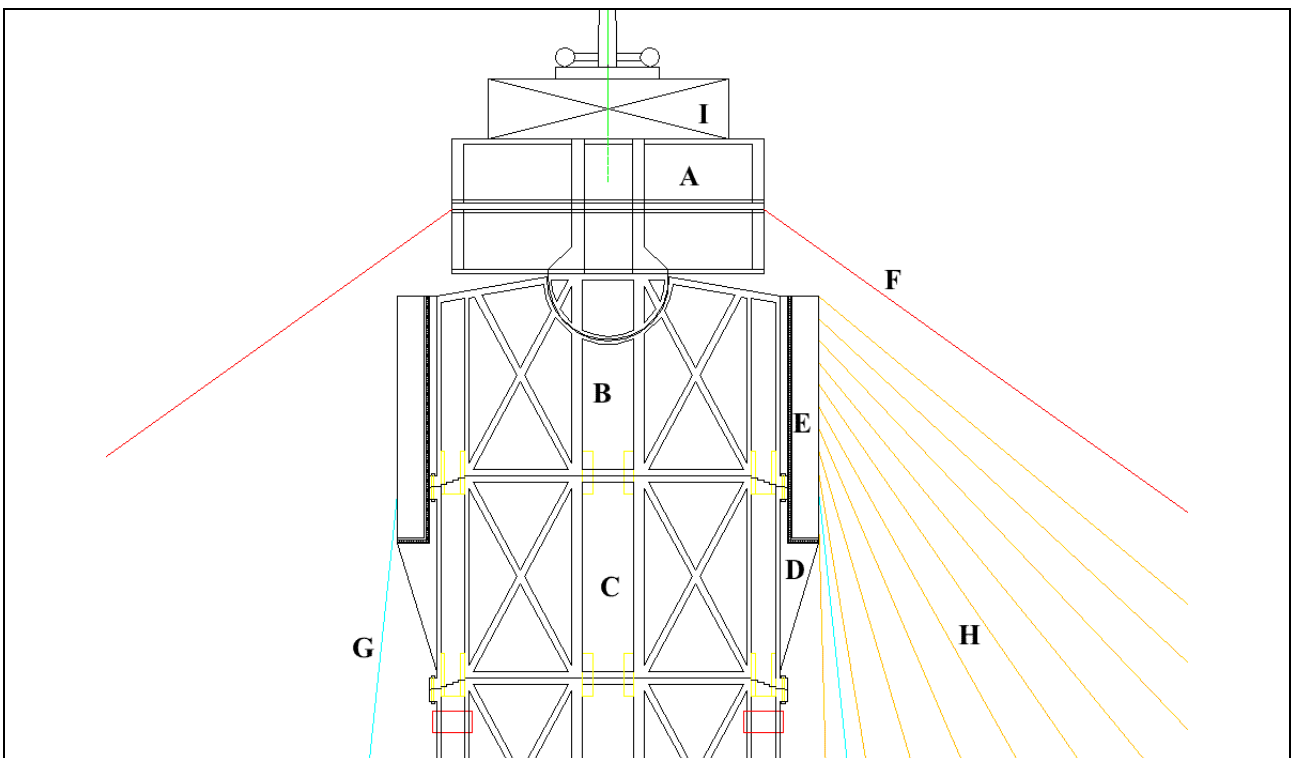
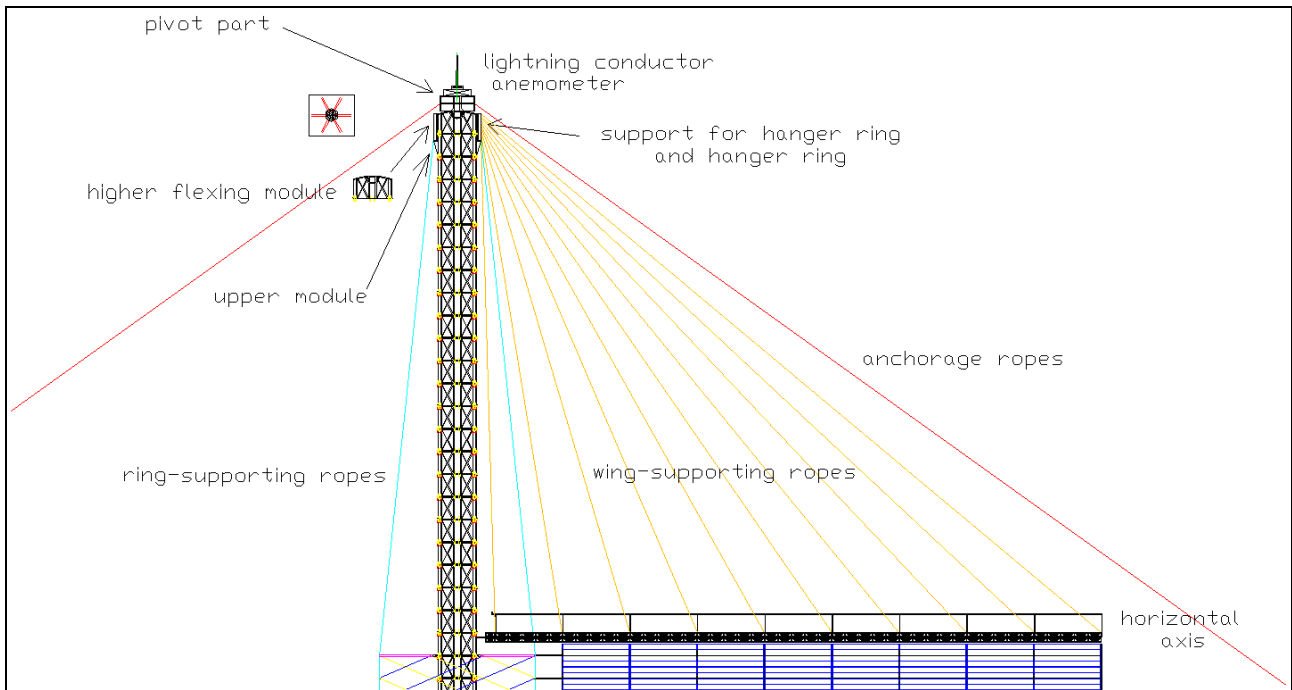
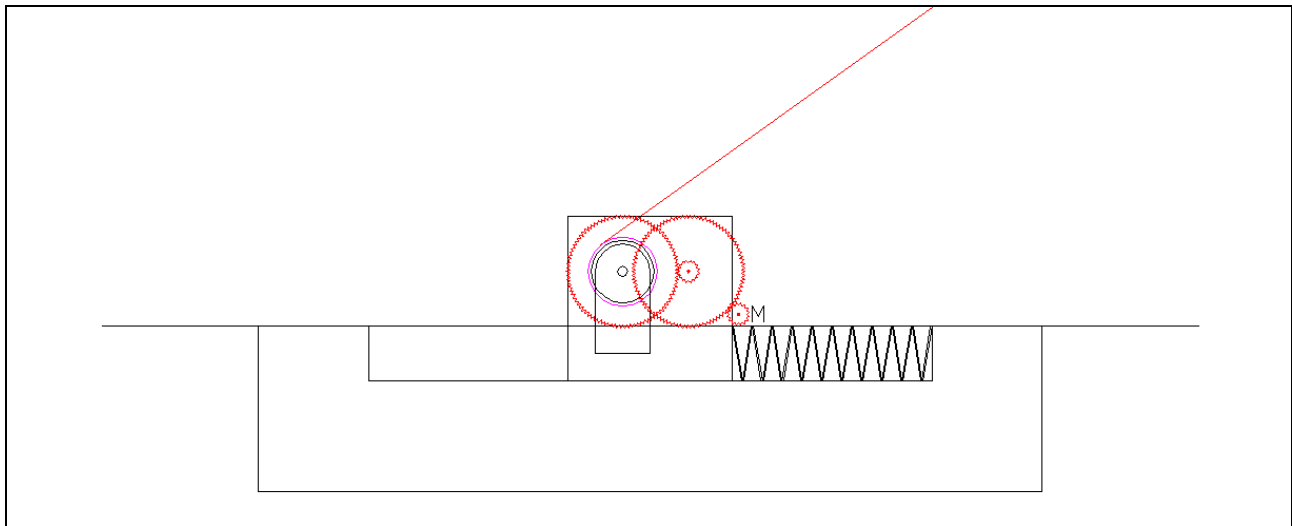


Figure 6 – Head of the vertical axis, composed of: A: pivot part; B: higher flexing module; C: upper module; D: hanger ring support; E: hanger ring. In addition, F: Anchorage ropes, G: ring-supporting ropes; H: wing-supporting ropes; I: anemometer. (detail of "general\_scheme\_frontal\_section.dwg")



**Figure 7 – A horizontal axis with its wing-supporting ropes (detail of "general\_scheme\_frontal\_section.dwg")**



**Figure 8 – An anchorage system (detail of "general\_scheme\_frontal\_section.dwg")**



#### **(4-B) Rotating part:**

This is composed of:

1) Three horizontal axes, rotating around the vertical axis and spaced  $120^\circ$  around it. Each “horizontal axis” is made up of 9 identical modules (“modules of horizontal axis”, length = 5 m) and a small module 0.5 m in length, with a total length of 45.5 m. Each axis supports a “wing” (or “sail”), and is supported by 10 pairs of steel ropes (“wing-supporting ropes”). These ropes are anchored to a central structure (“hanger ring”), rotating around the “hanger ring support” on the vertical axis (fig. 6). Over each horizontal axis, there is a railing for future maintenance.

2) 3 wings (or sails), rotating around the vertical axis, spaced  $120^\circ$  around it and supported by the overlooking horizontal axes (figs. 2-3). Each wing consists of 50 “rows” of 8 “elements”. An equivalent description is that each wing consists of 8 “columns” of 50 elements. Each wing has therefore 400 elements and the total for the three wings is 1,200 elements.

The dimensions of each element are: width = 5 m; height = 1.68 m, depth = 0.44 m. Each element includes 4 plastic “winglets” that may have vertical (ON), horizontal (OFF), and intermediate positions, determined by the action of synthetic fibre ropes (“winglet-rotating ropes”), moved by motors (“winglet-rotating motors”), one for each column in the lower part of the column. In the ON position, the winglets offer the greatest resistance to the wind and push the sail to the maximum. The opposite happens with the OFF position. The winglets, via the aforementioned winglet-rotating ropes, switch from ON to OFF, or vice versa, according to the direction of the wind and the direction in which the sails must rotate (clockwise / anticlockwise). In practice, at any given moment, all the winglets of one or two sails with a favourable wind are in the ON position, while all other winglets are in the OFF position. As the system rotates, winglets change from the ON to the OFF position, or vice versa, depending on whether the wind is the contrary or favourable wind. When the wind is too strong, the ON position may be modified to an intermediate position or even to the OFF position. In the case of winglet-rotating rope or motor failure, the winglets are moved to the OFF position by appropriate passive mechanisms.

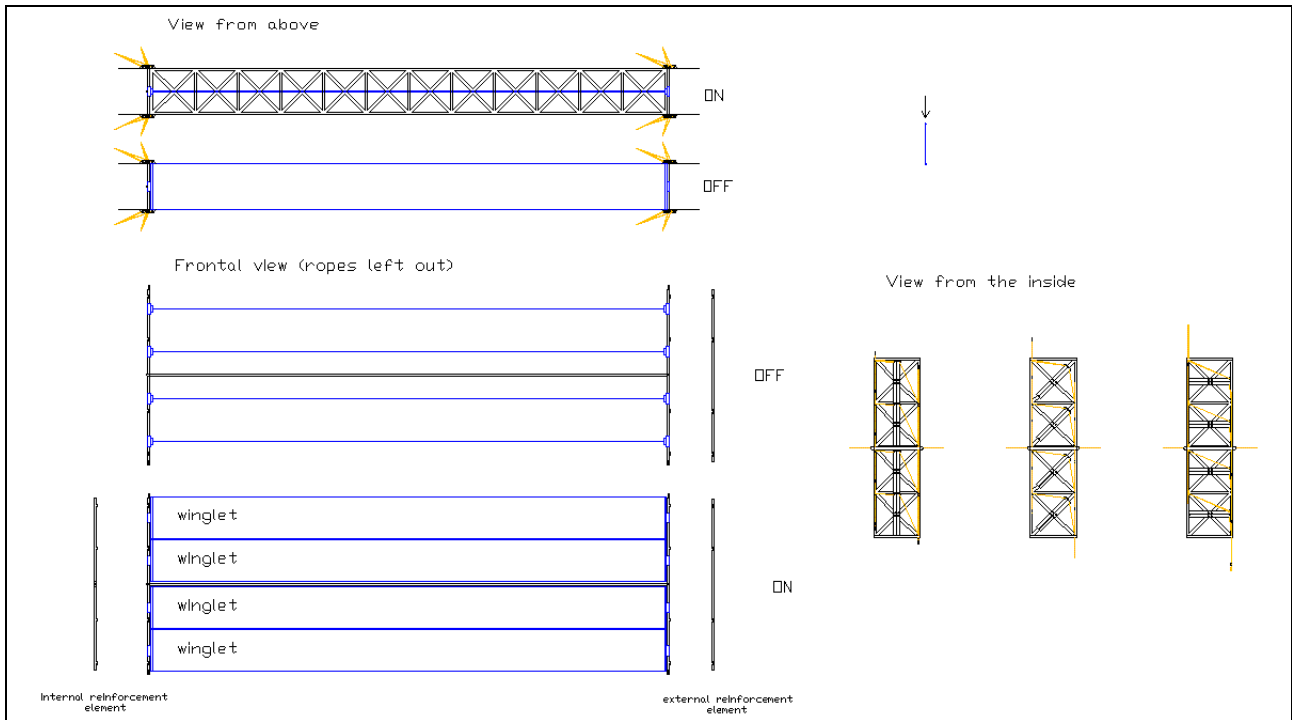
If all the winglets rotate in the same direction (clockwise or counterclockwise), this could originate thrusts in the vertical direction, i.e. directed upward if the wind hits the lower side of the winglets or downward if the wind hits the upper side. To avoid this, the winglets, in alternate rows of the modules, should rotate clockwise or counterclockwise, so that the two above said thrusts are perfectly balanced. Alternatively, for each module, two winglets should rotate clockwise and the others counterclockwise. These measures involve minor changes in the design drawings that have been omitted for simplicity.

The frame of an element (figs. 9 and 10) has a horizontal part and two vertical parts and is made of plastic materials. A number of metallic springs in these parts – not shown in the images – and the elasticity of the material, allow limited elastic flexions of the element. The vertical parts are reinforced by a core of two thin steel ropes. The winglets are made of flexible plastic material with a ticker reinforcing edge (and a very thin steel core if necessary), and are anchored to a rotating rigid support, which is moved by synthetic fibre ropes as it passes from the ON to the OFF position, or vice versa.

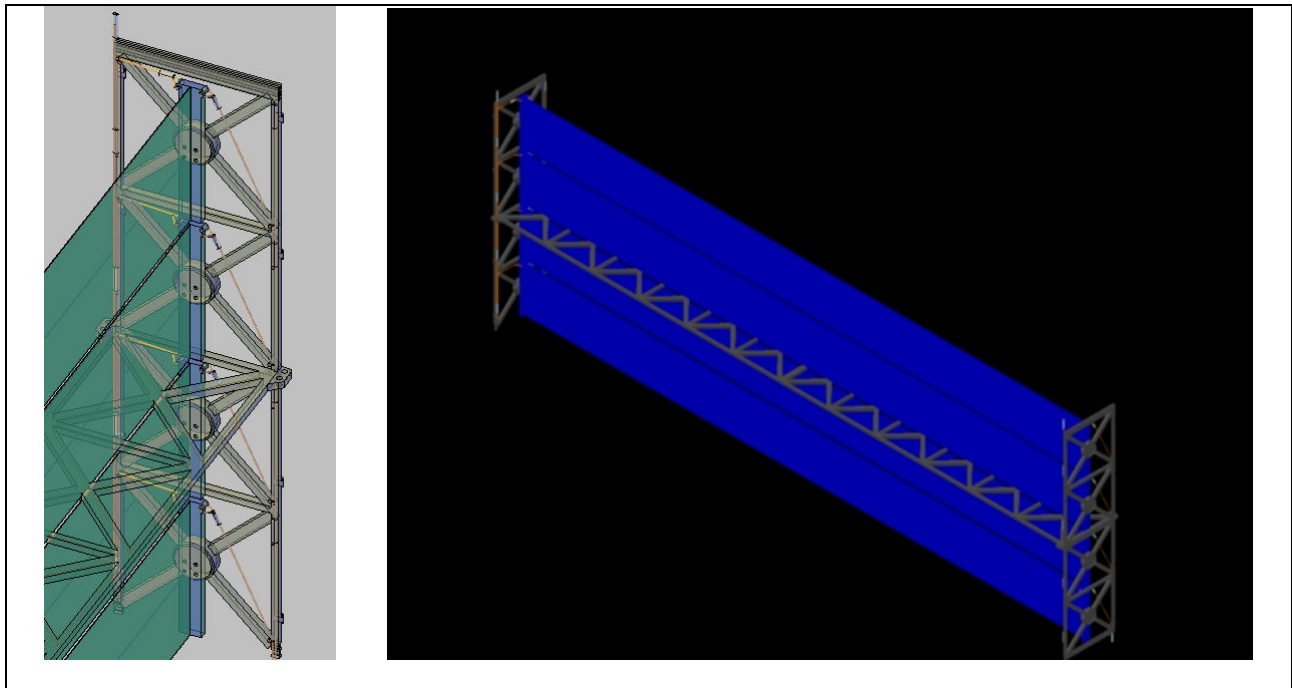
Each wing element has an inferior concave linear anchorage for the corresponding convex superior part of the element below. Moreover, each element has, on the left-hand side, a linear concave anchorage for the corresponding convex surface of the element that is on its left-hand side. The hooking of an element to its neighbouring elements is obtained using a drawer-like insertion and no screws or bolts are used.

The space between the concave and the convex hooking parts of two adjacent elements is minimal in the central part and wider in the non-central parts, so as to allow a limited rotation between two contiguous elements on the horizontal or vertical plane. The possible limited rotations between the

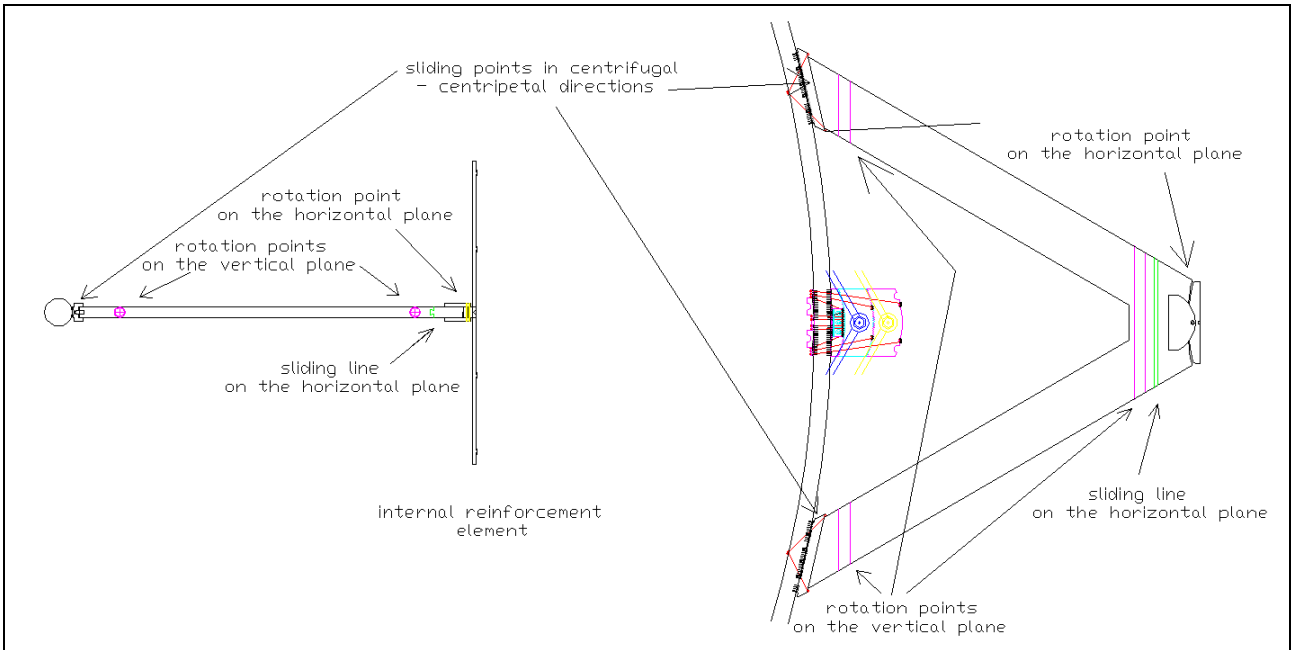
pairs of elements, and the internal elasticity of the elements, ensure a certain deformation of the wing as a whole, making it more resistant to excessive stress due to strong gusts of wind. The external and internal elements of each row are reinforced in the vertical part without adjacent element, by reinforcing elements ("external reinforcement element" and "internal reinforcement element", respectively; fig. 9).



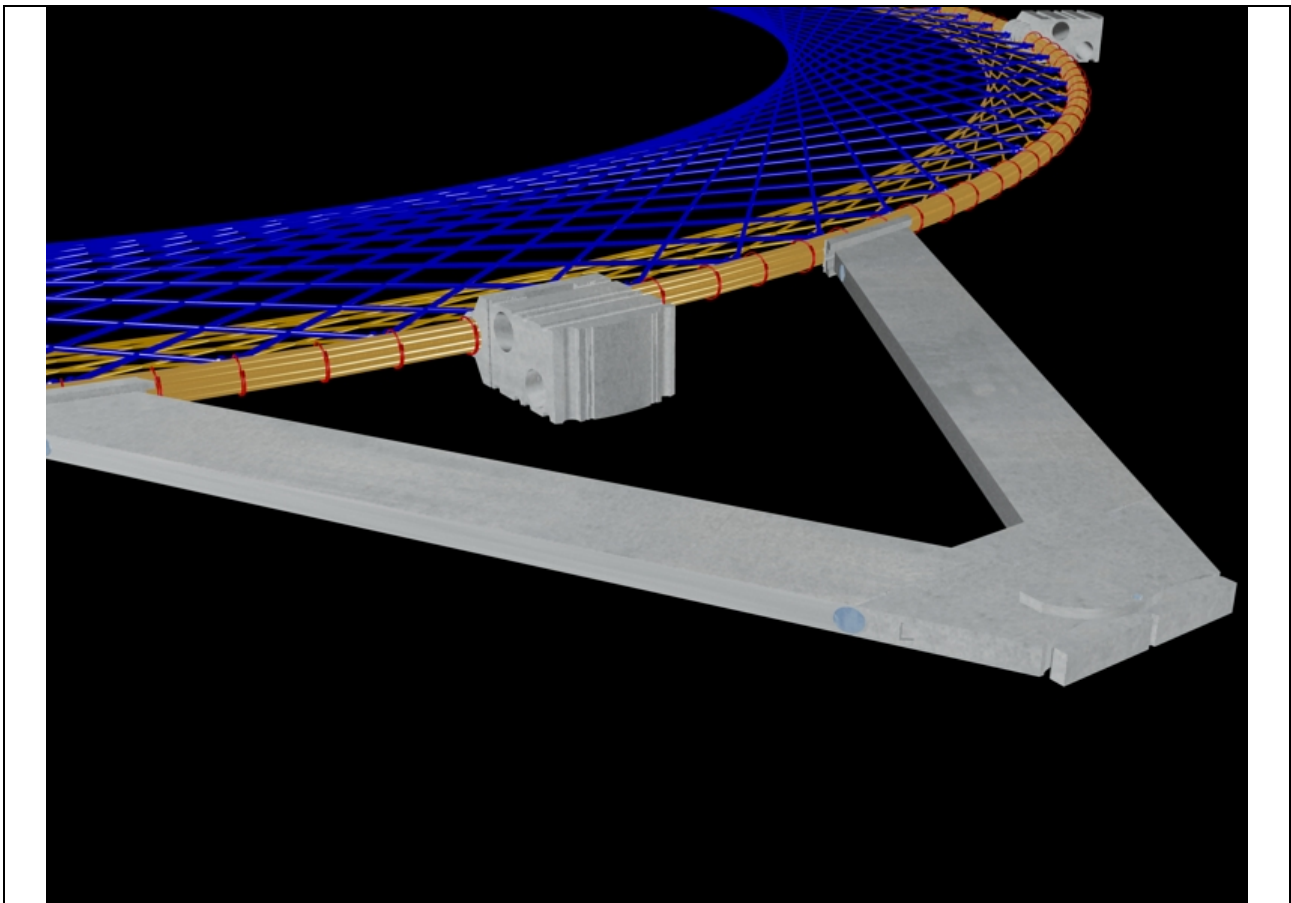
**Figure 9 – A wing element ("wing\_element.dwg", Documentary Appendix)**



**Figure 10 – 3D images of a wing element. The winglets are in the ON position.**



**Figure 11 – A connection arm (detail of "wing\_element.dwg")**



**Figure 12 – 3D image of a ring (partial), a connection arm and two main anchorages**

3) As the wing-ring ropes have a certain elasticity, each row is connected to the corresponding ring by a “connection arm” that allows a limited rotating movement of the wing on a horizontal plane. In addition, as the thermal expansion of the steel ropes supporting the rings determines minor changes in the vertical position of the rings, there are, in the same connection arms, two points of limited rotation on a vertical plane, and a slight shift in the centrifugal-centripetal directions is possible. Finally, given the possibility of limited twisting movements of the rings, a line of horizontal movement is also taken into account in the connection arms (figs. 11-12).

4) Each wing element is connected to the corresponding element of the subsequent wing by a rope made of synthetic fibres (“wing-wing rope”, fig. 3). As there are 400 elements for each wing, the number of wing-wing ropes is  $3 \cdot 400 = 1,200$ .

5) 63 “rings”. The rings, all the same size (diameter of the entire ring = 10.6 m; diameter of a section of the ring = 9 cm), are made up of 16 rounds of a single synthetic fibre rope (“brown rope”), held together by other synthetic fibre ropes (“red ropes”), which fasten the brown ropes in 180 regularly spaced points and provide transverse stiffening of the ring. Moreover, the red ropes hold in place 180 anchorage supports (90 “anchorage for yellow transverse ropes” and 90 “anchorage for cyan transverse ropes”) for two alternate sets of synthetic fibre ropes (10 “yellow transverse reinforcement ropes” / “yellow ropes” and 10 “cyan transverse reinforcement ropes” / “cyan ropes”), which make the ring highly resistant to any deformation of the ring on the horizontal plane. Each of the yellow transverse ropes is made up of 9 segments forming a circle. Each of the cyan transverse ropes is made up of 9 segments which form two double circles. Yellow and cyan transverse ropes are anchored to even and odd anchorage supports respectively (figs. 13-14). Each yellow / cyan rope has a “transverse-rope-stretching junction”, which regulates rope tension.

Each ring has three pairs of anchorages for the connection arms (“connection arms anchorages”), which are fastened to the ring by an array of chamfer nails and by two blocking ropes (fig. 14).

Moreover, each ring has six “main anchorages” (figs. 15 and 16) for: a) the steel ropes that support the rings (“ring-supporting ropes”); b) the “blue ropes” or “internal ropes” (see below); c) the “yellow ropes” or “external ropes” (see below). The main anchorages that are not between the branches of a “connection arm” are also points of anchorage for the wing-ring ropes. Each main anchorage is fastened to the ring by an array of chamfer nails and by three pairs of synthetic fibre ropes (fig. 15).

Each of the 50 higher rings receives its rotary power from the corresponding rows of the three wings, while the lower 13 rings are not connected to the wings (fig. 2). Each ring transmits its rotary force to the rings above and below through 6+6 systems for the transmission of the rotary power (see below), while the last ring, via the same systems, transmits its force to the rotor at the base of the plant.

6) The elements of each row are connected to the “main anchorages” of the ring at the same height, through two sets of 8 synthetic fibre ropes (right and left “wing-ring ropes”, fig. 3). These ropes transmit the rotary power originated by the wind to the aforementioned ring. As there are 3 wings, each with 50 rows, the number of wing-ring ropes is  $3 \cdot 50 \cdot 2 \cdot 8 = 2,400$ . Each group of 8 ropes, before reaching the main anchorage, is grouped into a single cable, which is hooked following a precise path using the appropriate grooves on the anchorage (figs. 15-16).

A general view of a ring and its connections in a horizontal section is given in fig. 17.

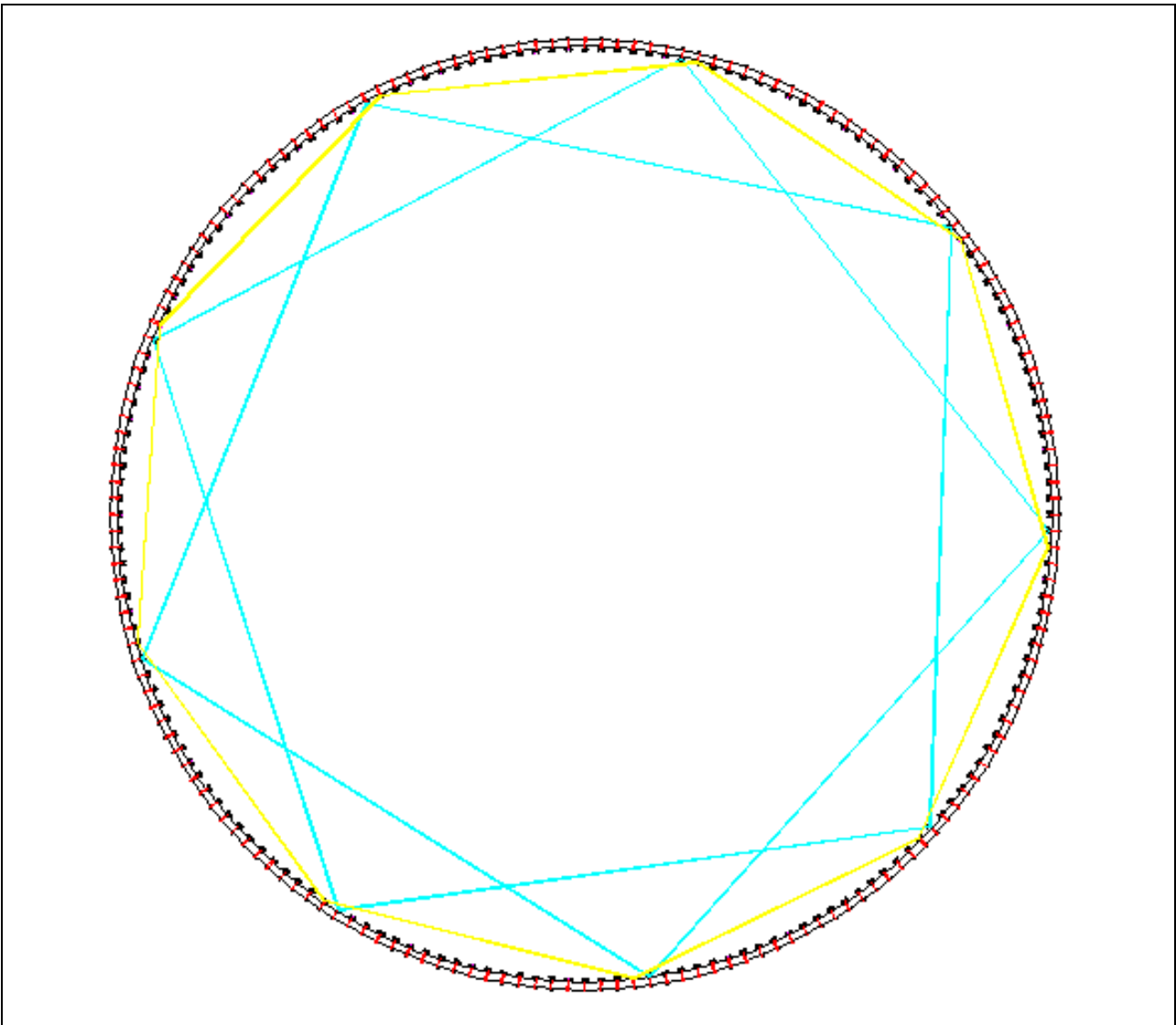


Figure 13 – A yellow transverse rope (single round) and a cyan transverse rope (double round) (detail of "ring.dwg")

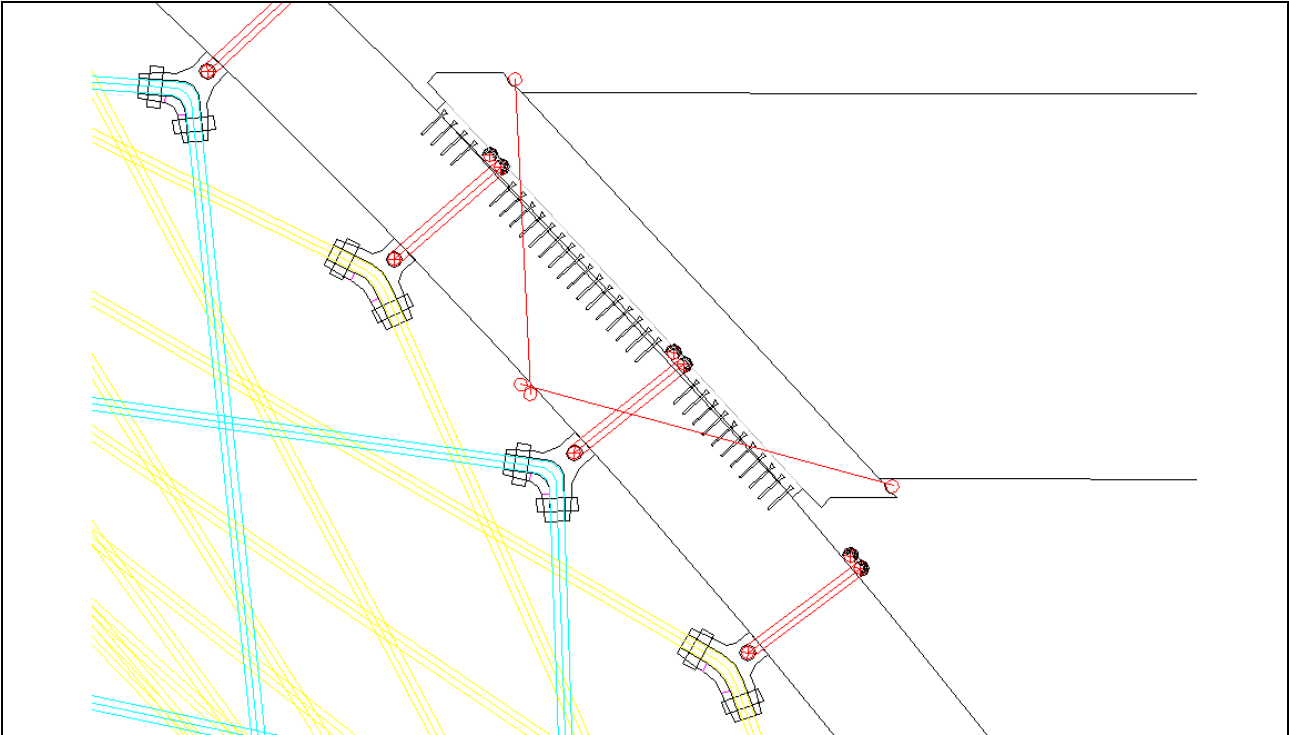


Figure 14 – One of the two connection arm anchorages and yellow and cyan ring transverse ropes anchorages (detail of "ring.dwg")

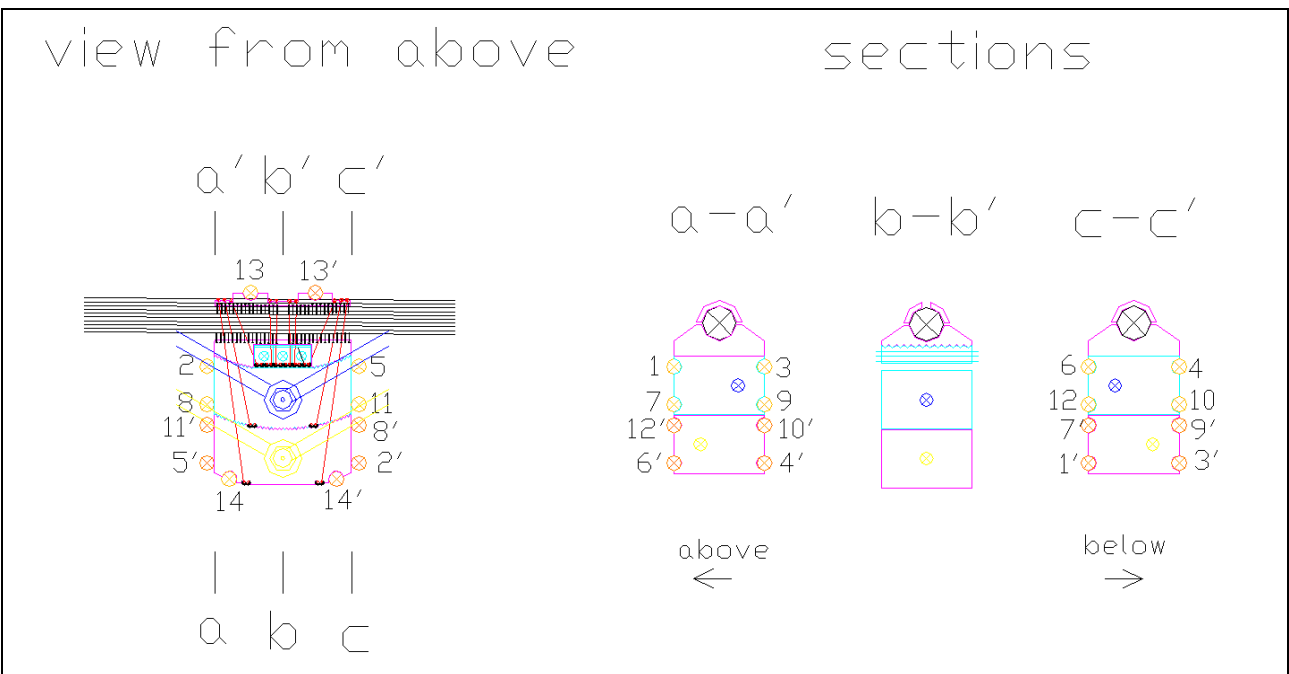
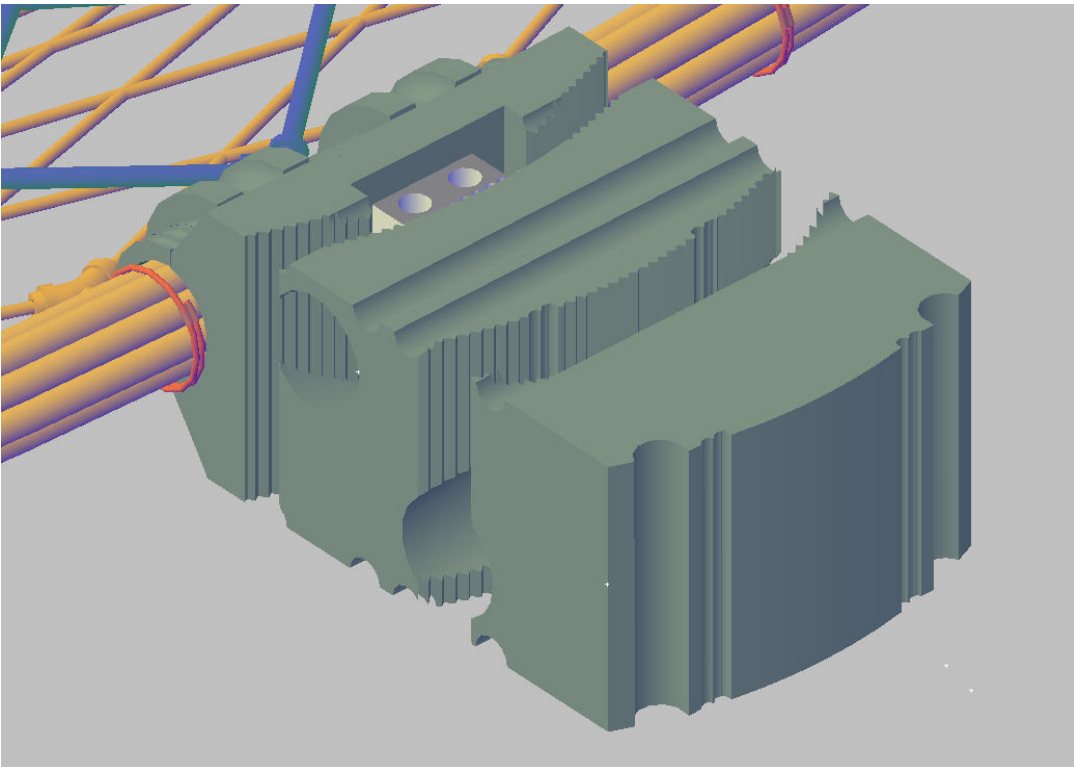
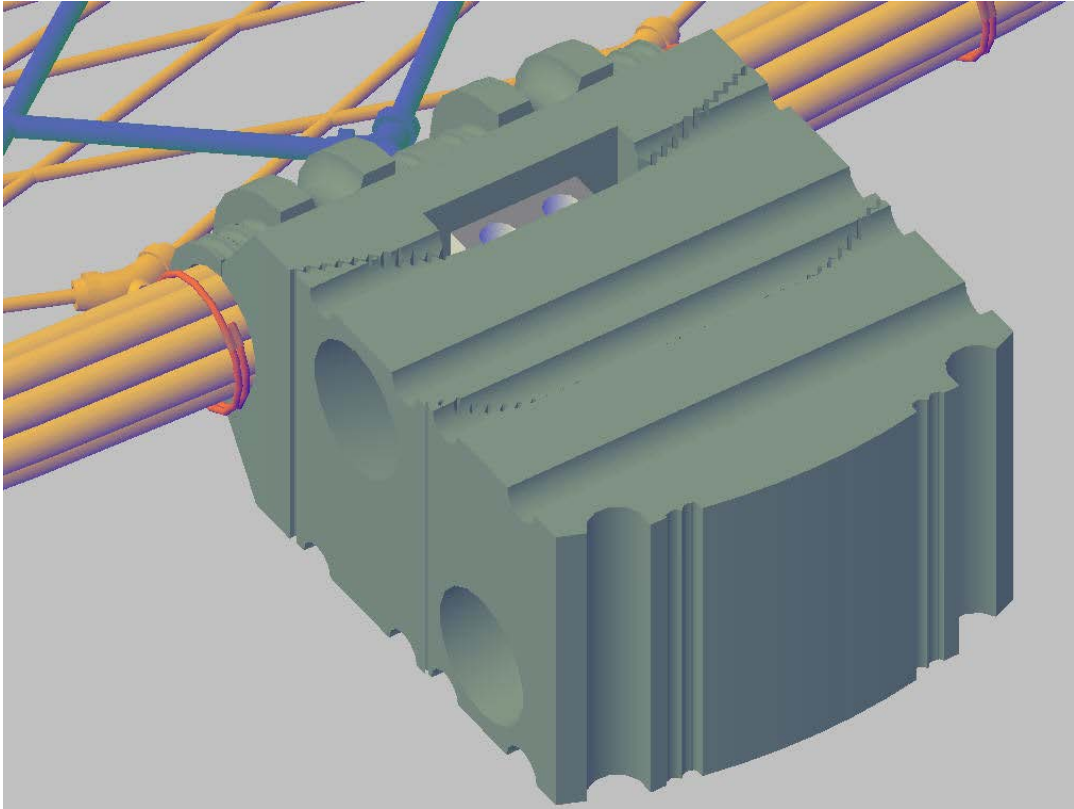
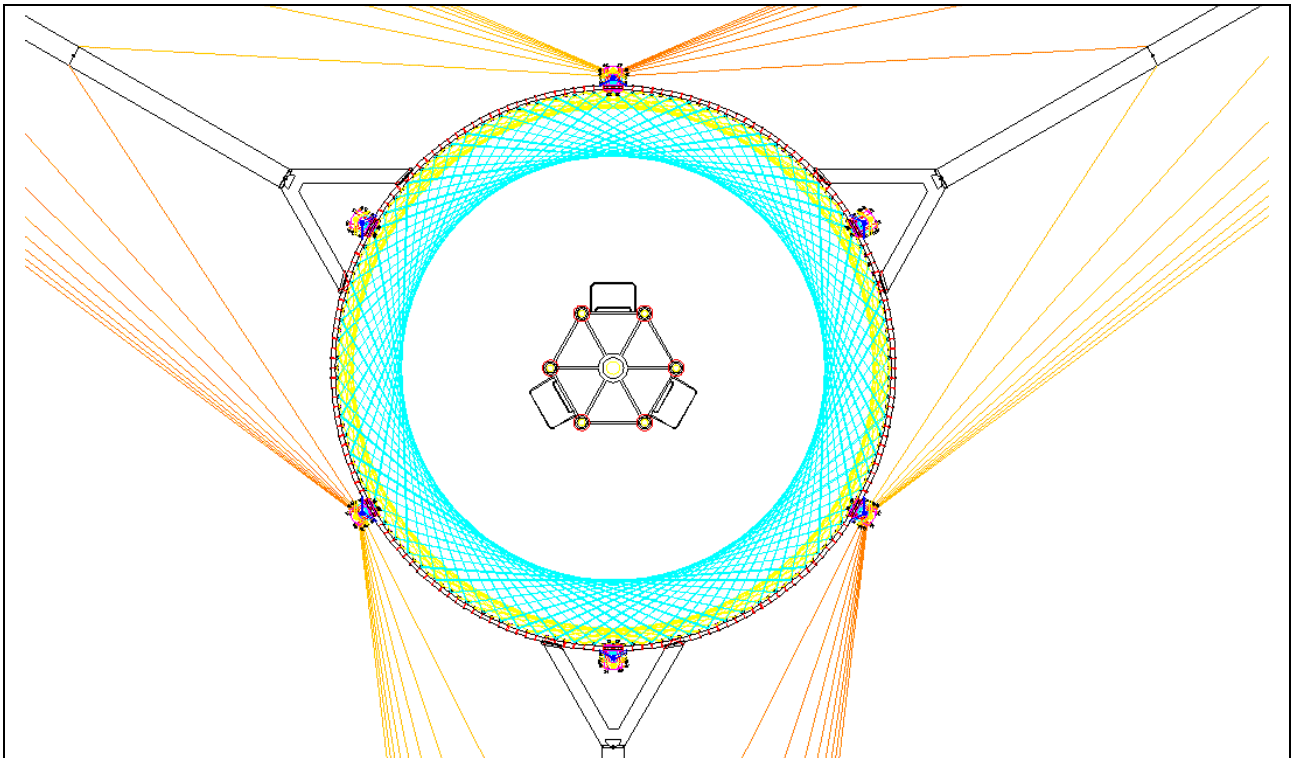


Figure 15 – A main anchorage (detail of "ring.dwg")



**Figure 16 – A main anchorage in two 3D-images**



**Figure 17 – A ring in a horizontal section (detail of "ring.dwg")**

7) The rings are interconnected by:

-- 6 groups of steel ropes (“ring-supporting ropes”) with vertical development and with overall capacity of loading and breaking load decreasing from top to bottom. These ring-supporting ropes are connected to the hanger ring above, to which the wing-supporting ropes are also anchored (fig. 7) and to the main ring anchorages below. For the higher rings, each group of ropes is composed of 3 ropes, which for the intermediate and the lower rings are reduced to 2 and 1, respectively;

-- 6 systems with downward clockwise path for the transmission of the rotary power (“internal systems for rotary force transmission” or “blue systems”). The systems must be rigid to avoid rotations between rings and thus torsional forces that would be unsustainable for the wings. Therefore, each system consists of steel axes, with junctions flexible on a horizontal plane in the main anchorages points (fig. 15). The flexibility of these junctions, as well as that of the rings, leads to small centripetal/centrifugal deformations caused by the centripetal/centrifugal forces determined by the wing movements. Each system makes a complete circle every 6 rings and each round consists of 6 segments with a length of about 6 meters, each at an angle of  $60^\circ$  to the previous segment.

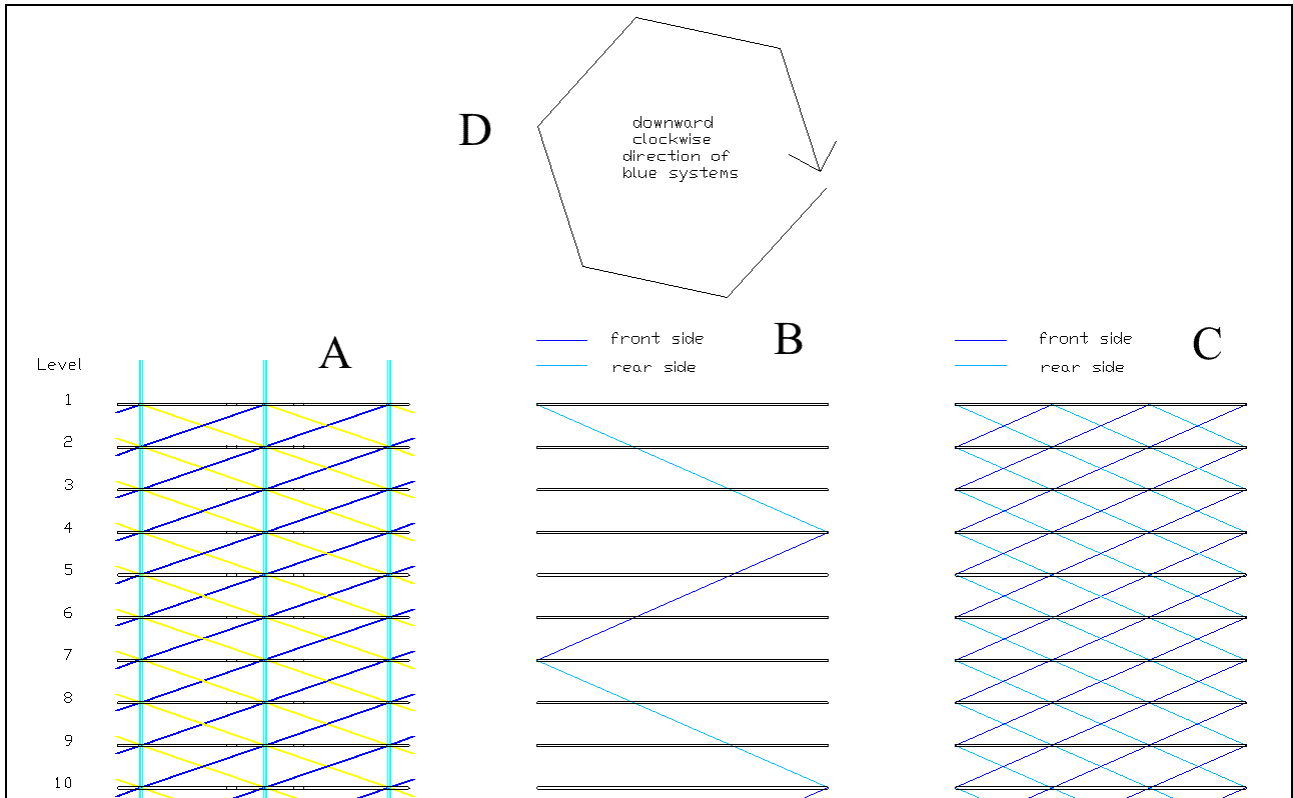
-- the same for 6 systems with downward anticlockwise path (“external systems for rotary force transmission” or “yellow systems”) (fig. 18). The definitions “blue system” and “yellow system” are not descriptive but concise and useful for graphic display.

The attributes “internal” / “external” mean that the two types of system are nearer to / further from the centre of the ring. The 6+6 systems cross at the main anchorages on the rings and form a sound net structure. Blue and yellow ropes never cross ropes with the same colour but only with ropes of the other colour (fig. 18).

Level with the lower flexing module, the segments of yellow and blue systems have in the middle a bending junction to allow the flexion of the vertical axis.

8) Some rings (11 in the project), for blocking possible oscillations on a horizontal plane, are connected by “anti-swing ropes” to a system that rotates around the vertical axis, thus forming an “anti-swing system” (fig. 19).





**Figure 18 – Scheme of the rotary systems (detail of "rotary\_systems.dwg"). A) General scheme of: 3 groups of supporting-ring ropes, the 6 blue systems, the 6 yellow systems (only that which is visible on one side is shown); B) Schematic view of a single blue system (both front and rear view), C) Scheme of all 6 blue system (both front and posterior view), D) diagram of the path of a blue system as seen from above.**

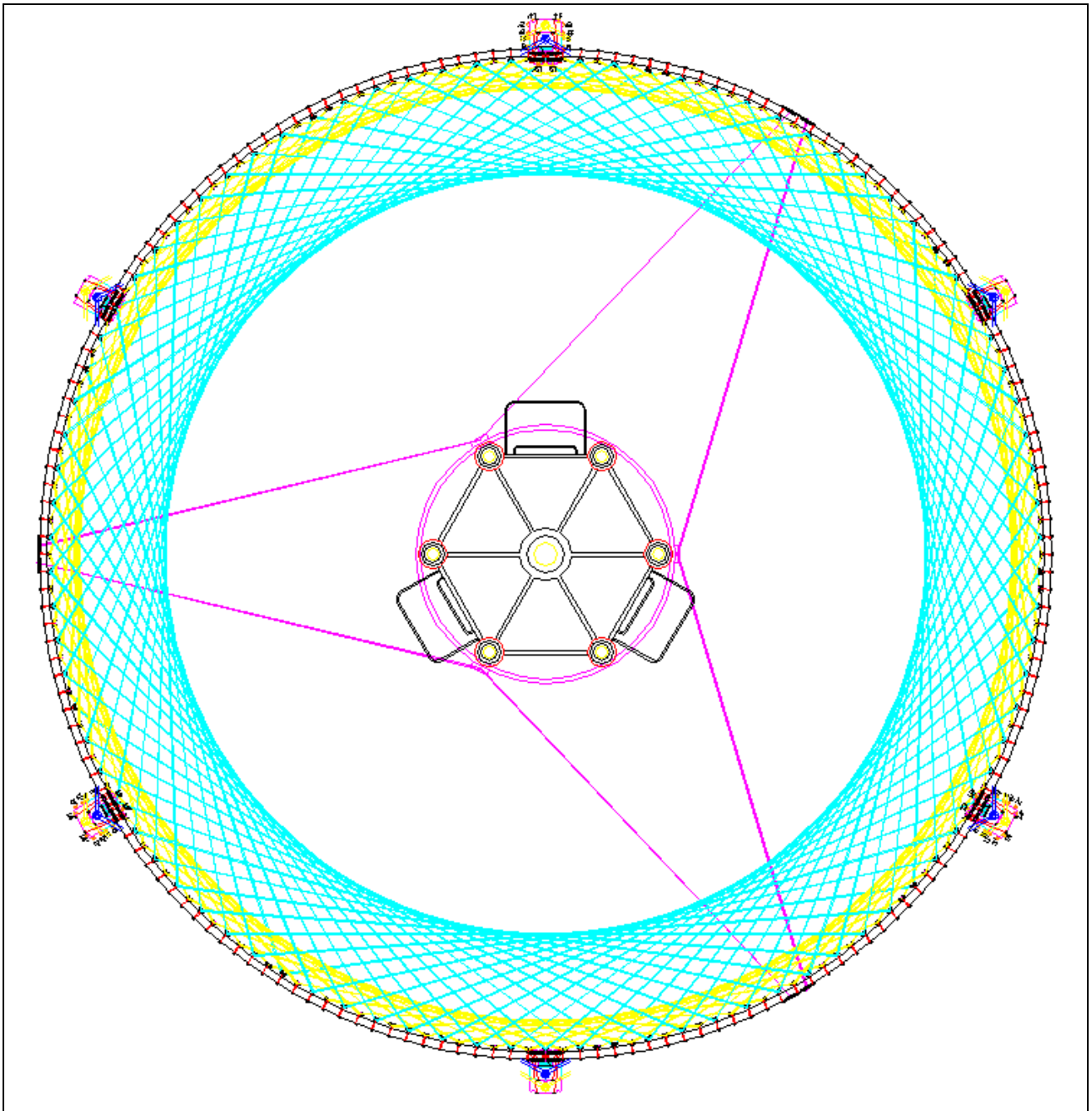


Figure 19 – An anti-swing system with its anti-swing ropes (detail of "ring.dwg")

#### **(4-C) Some technical details**

In the drawing up of this draft project, I have hypothesized, for the ropes, the use of materials readily available on the market with familiar characteristics. Of course this does not preclude the use of different materials.

Details of the materials used and the related raw calculations and references are given in the appendix material ("technical\_calculations.wls" file).

The fixed parts of the system are largely of steel with the characteristics and the qualities required for each part to be defined.

The moving parts are otherwise largely made of synthetic fibres with great resistance and low weight (Viper 78©, Dyneforce 78©) and of plastic materials in order to alleviate the structure weight considerably. The main steel components of the movable part are the wing-supporting ropes and the ring-supporting ropes (galvanized steel wire ropes W.S. 6 x 36 + IWRC WS).

Each wing is connected to the next wing by 400 wing-wing ropes, 8 mm in diameter, with a protective coating (if they are Dyneforce 78©, the breaking load of each rope is 7.1 T and the total breaking load =  $400 \cdot 8 = 3,200$  T). Moreover, each wing is connected to the rings by 400 wing-ring ropes on each side. The size of these ropes is calculated so that their total breaking load is equivalent to that of the wing-wing ropes.

The estimated weight of a single wing element is 44.76 kg and the total weight of a wing (elements + external and internal reinforcement elements + 50% of the weight of connection arms + wing-wing ropes + wing-ring ropes) is 24.4 T. Thus, the total weight of the 3 wings, horizontal axes excluded, is 73.21 T.

Each ring is made up of a rope 20 mm in diameter (Dyneforce 78 ©) which, overlapping on itself, rotates 16 times and has a breaking load equal to  $33.6 \text{ T} \cdot 16 = 537.6$  T. This main part is reinforced by 180 red ropes and 9+9 transverse ropes (8 mm in diameter plus a protective coating) with 180 anchorage points.

The estimated weight of each ring, anchorages for connection arms and main anchorages included, is 0.4098 T. The total weight of the 63 rings is 25.81 T. The 50% weight of  $3 \cdot 50$  connection arms is 7.75 T.

Blue and yellow systems (internal/external systems for the transmission of the rotary force) are made up of steel ropes and have an estimated total weight of 40.15 T.

The rough estimated weights of the wing-supporting ropes and of the ring-supporting ropes are 5.048 T and 1.2735 T, respectively.

The total weight of the rotating part is, therefore, approximately  $73.21 + 25.81 + 7.75 + 40.15 + 5.048 + 1.2735 = 153.24$  T plus the weight of the three horizontal axes. It is easy to plan the diameters of the wing-supporting ropes and of the ring-supporting ropes so that the aforesaid constant load does not exceed a small percentage of their breaking load (less than 5% in the calculations).

It is also possible to plan the rotary force transmission systems so that they are able to withstand up loads up to the breaking load of the wing-wing ropes.

The decision to use synthetic fibre ropes and plastic material is intended to lighten the structure so as to allow much larger and higher plants to be built without weights and costs reaching excessive or unfeasible levels.

## **(5) Construction of the plant**

The project is designed to facilitate plant construction and to minimize construction and maintenance costs.

In particular:

- 1) the plant consists of repetitive series of modules that can be manufactured on a large scale with resulting economies of scale (e.g.: standard modules of vertical axis, wing elements, rings, etc.);
- 2) for the construction, standardized and repetitive operations are planned; these are facilitated through the use of specialized equipment;
- 3) the project can be easily copied in various locations, thus reducing costs and construction times;
- 4) the plant is built using a top-down method of construction (see below), so as to limit necessary crane height drastically. While current plants require a powerful and expensive crane able to lift the heavy weight of propellers and electric generator to the top of the tower, it is possible, using the top-down method of construction, to use cranes of limited power, to lift loads to a height slightly greater than that of the scaffoldings, i.e. about 20 m for VertEolo 1:1. Moreover, the electric generator is on the ground and this eliminates the problems of having to lift a heavy load to the top of the tower and reduces the maintenance costs.
- 5) the plant has no very large or heavy parts (such as the propellers and the electric generator parts of current plants) with consequent transportation problems.

The construction phases can be schematized into the following steps.

1) Construction of:

- foundations of the vertical axis (see Documentary Appendix: “installation\_step\_01.dwg”);
- sockets for the “lifting worms” of the “circular support for the rings” and for the lifting worms of the “upper” and “lower circular platform” (“installation\_step\_01.dwg”);
- sockets for the moving chains of the lifting worms;
- foundations of the six ground anchorages.

2) Positioning of the first four modules of the vertical axis (“installation\_step\_02.dwg”).

3) On the ground, the head of the vertical axis (pivot part + superior flexing module + upper module + hanger ring support + hanger ring), plus anemometer and lightning conductor, is assembled with six groups of 2 anchorage ropes, six groups of 3 ring-supporting ropes, and three groups of 10 wing-supporting ropes, all starting from the hanger ring and rolled up separately. The head is then lifted, by a small crane, to the top of the vertical axis and connected to it.

4) Installation of:

- three powerful hoists with hydraulic pistons (“hoists”). These hoists are arranged in a circle and firmly interconnected (fig. 20). Each hoist can be clasped to three contiguous modules of the vertical axis through three pairs of hookings (“installation\_step\_03.dwg” and “scaffoldings.dwg”);
- the circular support for the rings with the related lifting worms and their moving chains and motors (“installation\_step\_04.dwg” and “scaffoldings.dwg”).

5) Positioning of the rings heap on the circular support for the rings (“installation\_step\_04.dwg”). Each ring is assembled in the plant construction area via the following steps: I) laying of 16 rounds of the continuous rope (“brown rope”) constituting the body of the ring; II) installation of 180 transverse stiffening ropes (“red ropes”) with an equal number of anchorages for transverse reinforcement ropes; III) installation of these reinforcement ropes (10 “yellow ropes” and 10 “cyan ropes”); IV) installation of three pairs of anchorages for each wing connection arm; V) installation of six main anchorages for ring-supporting ropes, wing-ring ropes, yellow systems and blue systems for the transmission of rotary force; VI) where necessary, installation of the coupler points for the anti-swing ropes.

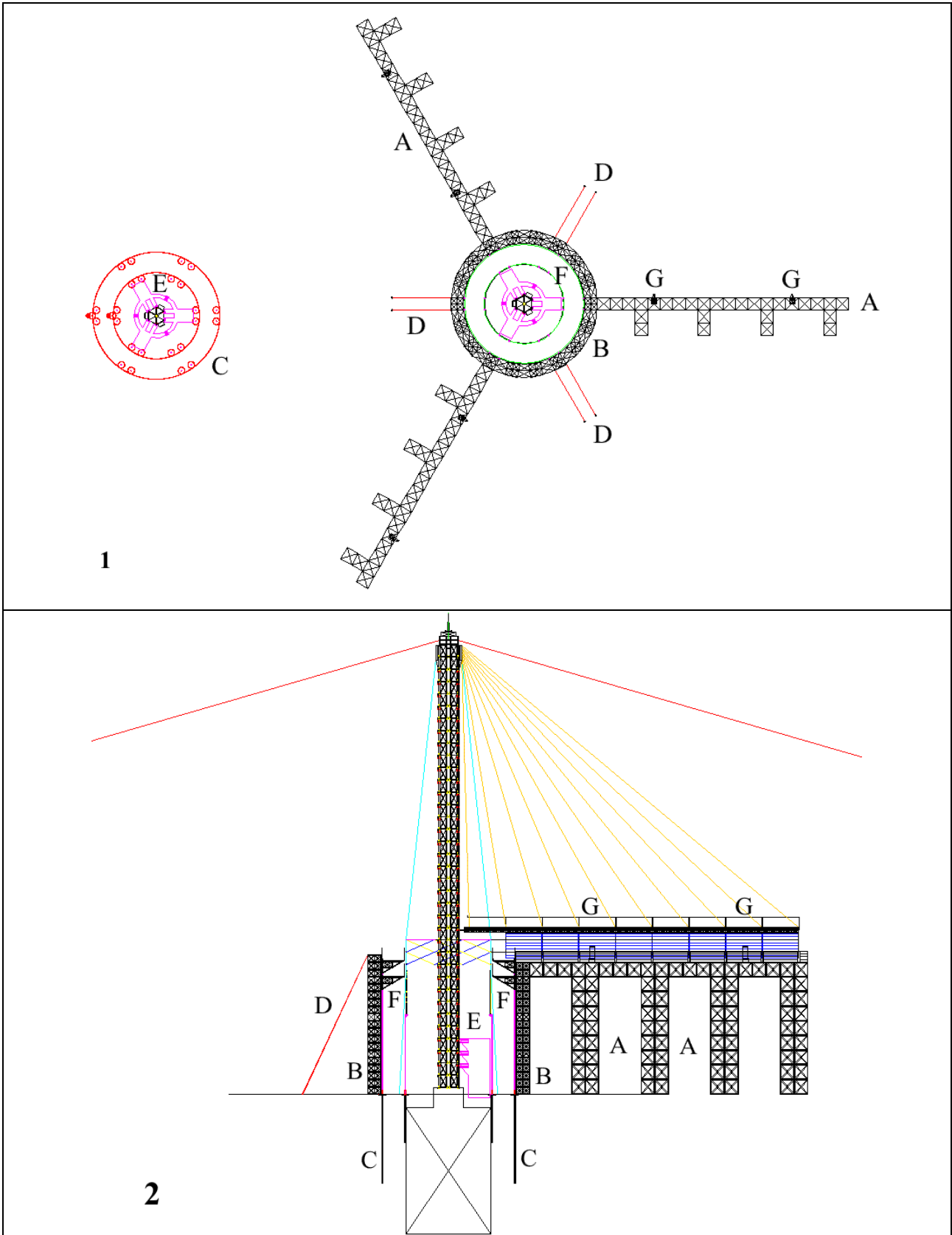


Figure 20 – Scaffoldings and lifting worms, view from above (1; particular of scaffoldings.dwg) and in a frontal section (2; particular of installation\_step\_15.dwg). A: linear scaffoldings; B: circular scaffolding; C: moving chain and motors for the lifting worms + lifting worms; D: circular scaffolding tension ropes; E: hoists; F: circular platforms; G: pulley.

- 6) Installation of (“installation\_step\_05.dwg”, “scaffoldings.dwg”):
- the circular scaffolding;
  - the upper circular platform and the lower circular platform with the related lifting worms and their moving chains and motors;
  - the three linear scaffoldings with a pair of pulleys for each scaffolding on the top.
- 7) Below the 4 upper modules and above the lower module (“base module”), a module is inserted via the following steps:
- a) the three hoists have their hookings in the low position and clasped to the three modules that are immediately above the base module (“installation\_step\_05.dwg”);
  - b) the three hoists pass their hookings to the high position raising the modules by about 2 metres above the base module (“installation\_step\_06.dwg”);
  - b) a module is placed on the base module (“installation\_step\_07.dwg”);
  - c) the three hoists pass to the intermediate position lowering the upper modules until they touch the inserted module (“installation\_step\_08.dwg”);
  - d) the inserted module and the module immediately above it are connected with nuts and bolts;
  - e) the three hoists are unhooked from the modules and return the hookings to the low position where they are clasped to the three modules above the base module. (“installation\_step\_09.dwg”).
- 8) This series of operations (called “insertion of a module”) is repeated seven times so that an equal number of modules is inserted and the vertical axis is now high 11 modules, excluding the head (“installation\_step\_10.dwg”).
- 9) The six ground anchorages are assembled.
- 10) The anchorage ropes are loosened and connected to the ground anchorages and tightened (“installation\_step\_11.dwg”). The ring-supporting ropes and the wing-supporting ropes are loosened and temporarily fastened to the ground and to the tops of the linear scaffoldings, respectively.
- 11) Another 22 modules are added to the base module through repetition of the “insertion of a module” operation. For each insertion, the anchorage ropes are lengthened or shortened, when necessary, by the synchronized action of the ground anchorages motors, so that the anchorage ropes are always appropriately tightened. After these insertions, the vertical axis is 32 modules high, excluding the head (“installation\_step\_12.dwg”).
- 12) Each of the three horizontal axes, after being assembled on the ground along with the couplers for the wing elements of the first row, is lifted by a pair of pulleys to the top of the corresponding linear scaffolding. Each horizontal axis is then connected to the hanger ring by the ten wing-supporting ropes and to the vertical axis by a circular system with low friction (“installation\_step\_13.dwg”).
- 13) Assembly operation of the first two rings and of the first wing row:
- a) another module is inserted into the lower part of the vertical axis;
  - b) the first two rings are connected to the hanger ring using the two circular platforms; that is, the ring-supporting ropes are hooked to the six main anchorages of each ring;
  - c) the upper and lower ends of each segment of the blue systems are hooked to the main anchorages of the upper and lower ring, respectively;
  - d) the upper and lower ends of each segment of the yellow systems are hooked to the main anchorages of the upper and lower ring, respectively;
  - e) For each wing, the first wing row, made up of 8 wing elements, an external reinforcement element, an internal reinforcement, and a connection arm, is assembled on the ground. In addition, the wing row is completed with 8 wing-wing ropes, 8 right wing-ring ropes, and 8 left wing-ring ropes. Each wing row is lifted by the pair of pulleys on the top of the corresponding linear scaffolding and hooked to the couplers below the horizontal axis. The connection arms are

clasped to the ring, each wing-wing rope is linked to the corresponding element of an adjacent wing, the right and left wing-ring ropes, grouped in two distinct bundles, are connected to the two main anchorages that, on the ring, are immediately to the right and the left of the connection arm.

14) The series of operations described in the preceding paragraph is repeated 49 times (see from “installation\_step\_15.dwg” to “installation\_step\_19.dwg”) with the following differences:

-- each wing row is hooked to the corresponding overlooking wing row and not to the couplers of a horizontal axis;

-- with the exception of the final repetition, the winglet-rotating ropes of the new wing row are hooked to the corresponding winglet-rotating ropes of the upper wing row.

15) The winglet-rotating motors, each moving the winglets of all the elements of a wing column, are hooked to the last wing row of the corresponding wing (“installation\_step\_20.dwg”).

16) Every six rings, there is a ring that has part of an anti-swing system. This part is connected to the corresponding part of the anti-swing system on a differentiated module of the vertical axis, which is inserted in an appropriate phase.

17) Meanwhile, immediately below the module corresponding to the last ring, the lower flexing module, instead of a standard module, has been inserted. Below the lower flexing module, at the end of the assembly, there are 15 standard modules.

18) Below the 50+1 rings already assembled, another 12 rings are added and connected to: a) the ring-supporting ropes; b) the "blue systems"; c) the "yellow systems" (“installation\_step\_21.dwg”).

19) Disassembly and removal of: a) the three linear scaffoldings with their pulleys; c) the circular scaffolding; b) the two circular platforms; d) the circular support for the rings; e) the lifting worms and the related moving chains and motors; (“installation\_step\_22.dwg”).

20) The stator and the rotor of the electric generator are assembled around the lower modules of the vertical axis,. The rotor is connected to the lower ends of the “yellow” and “blue” systems” (“installation\_step\_22.dwg”).

## **(6) Short description of VertEolo 2:3 and VertEolo 3:6**

The plant named VertEolo 2:3, as the name suggests, has sails with the following dimensions: width = 2 unities of wing width (=  $2 \cdot 8$  elements = 16 elements = 80 m), height = 3 unities of wing height (=  $3 \cdot 50$  rows = 150 rows = 252 m). The main differences between VertEolo 2:3 and VertEolo 1:1 are:

The rings have a diameter that is doubled (23.2 m), so that the angles between wing-ring ropes and wing are the same. The diameter of a ring section is increased from 9 to 12 cm. The number of rounds of the 20 mm rope changes from 16 to 31 and the breaking load from 538 to 1042 T. The diameter of vertical axis modules is increased by 50% so that the area is increased by  $1.5^2 = 2.25$ . The number of yellow and blue systems is doubled from 6+6 to 12+12 and each of these systems makes a turn in not 6 but 12 steps, each going from one ring to the one below.

As the hoists clasp six rather than three modules, and are, therefore, higher, and the ring heap is higher ( $[12+1] \text{ cm} \cdot 163 = 21.19 \text{ m}$  instead of  $[9+1] \text{ cm} \cdot 63 = 6.3 \text{ m}$ ), the part of the vertical axis below the wings is higher, that is, it must have another 10 modules ( $10 \cdot 1.68 = 16.8 \text{ m}$ ) and the scaffoldings are correspondingly higher. The total height of the plant increases from about 157 m to 372 m. The distance between opposed anchorage systems increases from 420 to 936 m (fig. 21).

As the surface of the sails is 6 times that of VertEolo 1:1, plant power is increased proportionally. Furthermore, since given that the plant is of a height at which winds are stringer and more constant, a greater increase of plant power, a lower cut-in and a higher capacity factor can be expected.

The VertEolo 3:6 plant, as the name suggests, has sails with the following dimensions: width = 3 unities of wing width (=  $3 \cdot 8$  elements = 24 elements = 120 m), height = 6 unities of wing height (=  $6 \cdot 50$  rows = 300 rows = 504 m).

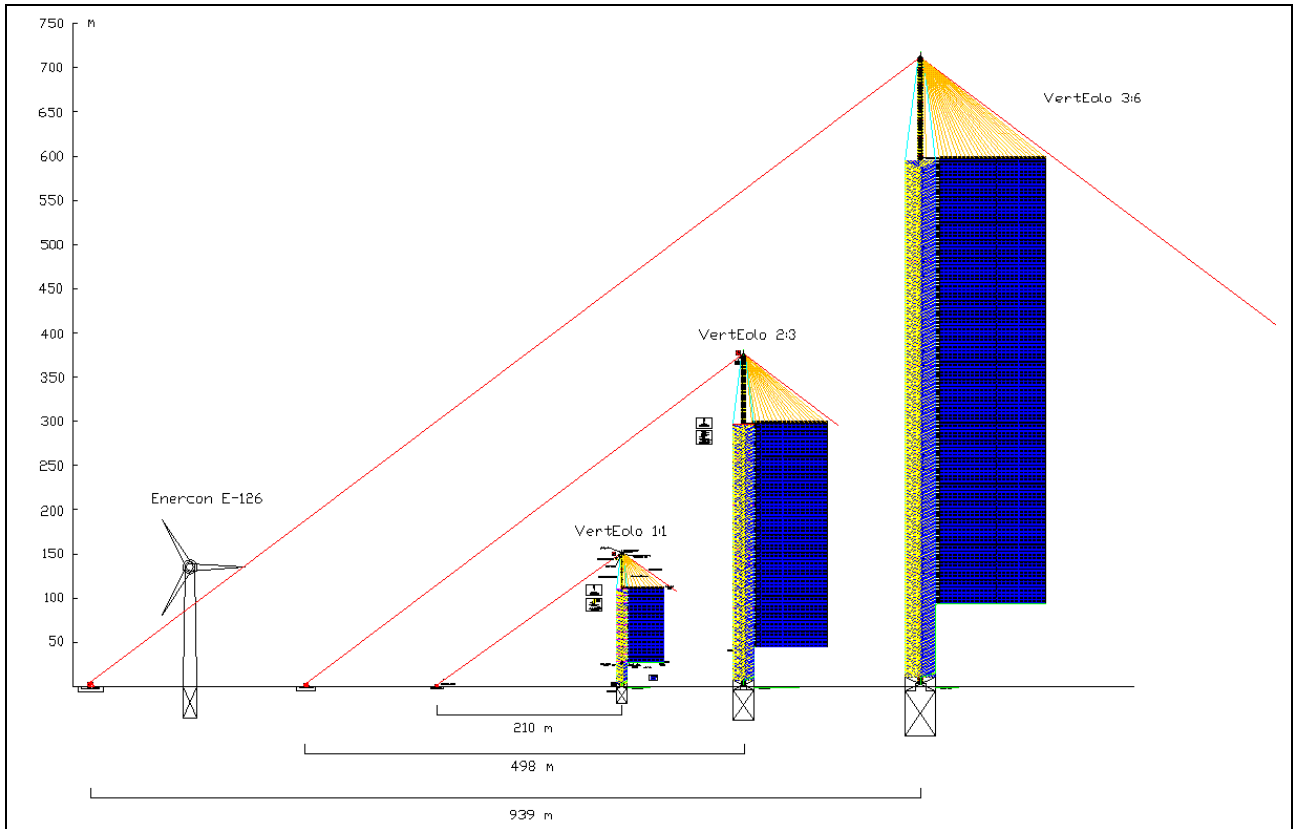
The changes in dimensions are proportional to this increased surface. In particular, in the comparison with VertEolo 1:1: a) the diameter of the rings is tripled, increasing from 11.6 to 34.8 m; b) the diameter of a ring section increases to 15 cm, with 45 rounds of the brown rope and a breaking load of 1512 T.

Both the height and the diameter of vertical axis modules are doubled. The number of blue and yellow systems is tripled, increasing from 6+6 to 18+18 and each of this system makes a turn in 18 steps.

As the hoists clasp nine and not three modules, with the modules having double height, and a higher ring heap ( $[15+1] \text{ cm} \cdot 313 = 50.08 \text{ m}$  instead of  $[9+1] \text{ cm} \cdot 63 = 6.3 \text{ m}$ ), the part of the vertical axis below the wings must be higher; that is, it must have about 15 other modules ( $15 \cdot 3.36 = 50.4 \text{ m}$ ) and the scaffoldings must be equally higher. The total height of the plant increases to about 712 m and the distance between opposed anchorage systems increases to 1878 m (fig. 21).

The power grows to 18 times that of VertEolo 1:1, and plant power and capacity factor also increase, due to the increased height.





**Figure 21 – VertEolo 1:1, VertEolo 2:3, VertEolo 3:6 + a scheme of an Enercon E-126 (“VertEolo\_plants.dwg”)**

## (7) Power of the hypothesized plants

The kinetic energy ( $E$ ) of a body with mass  $m$  and moving with velocity  $v$  is given by the formula:  

$$E = \frac{1}{2} m v^2 \quad (1)$$

For a wind power plant, in the calculation of the kinetic energy for a fluid such as the air, the mass is given by the air density ( $\rho$ ) multiplied for the wind speed ( $v$ ) and for the area intercepted by the plant ( $S$ ). For the type of plant currently in use,  $S$  is given by the area of the circle of radius  $r$  defined by the propellers, i.e.:

$$S = \pi r^2 \quad (2)$$

A wind power plant can extract only a part  $C$  of the kinetic energy of the air that passes through  $S$ . Therefore the power ( $P$ ) that the plant can extract is equal to:

$$P = C \frac{1}{2} S \rho v^3 \quad (3)$$

Betz developed this formula and, among other things, showed that the maximum value of  $C$  is equal to 0.593 [20].

For installations with vertical axis of rotation of the type proposed in this work, the formula of Betz is not easily and immediately applicable. A precise definition of the power obtainable by these plants will be possible only after their construction and verification.

The first obstacle is the calculation of  $S$ . In the continuous rotation of the sails, their surfaces are exposed to the wind with continuously varying angles. In the hemicycle where the wind is favorable, for two-thirds of the rotation, two sails have a favorable wind at the same time while, for the other third, only one sail has favorable wind (fig. 22). Moreover, in the calculation of  $S$ , as for plants with horizontal axis, we consider both the relatively small areas of the propeller sections and the greater interposed areas; as in the case of the proposed plants with vertical axis of rotation, we should consider both the areas of the sails and some of the adjacent areas involved in the air flows. Furthermore, there is no certain data that would allow us to indicate a reliable value for  $C$ .

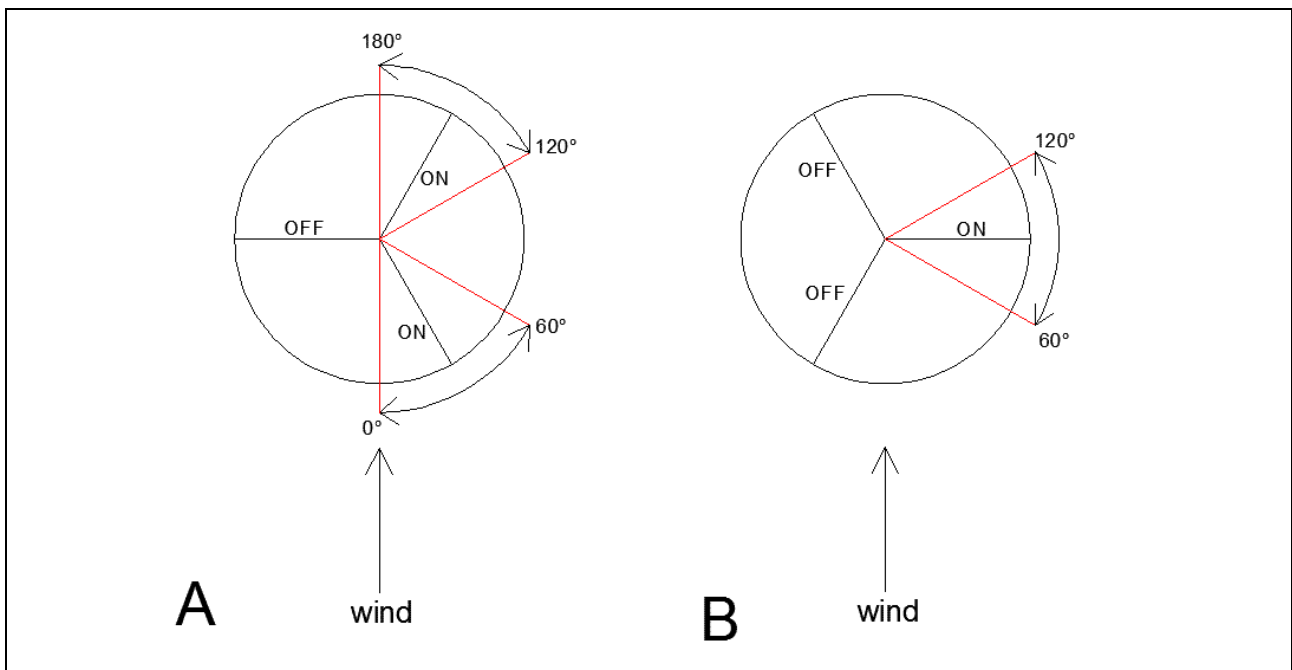


Figure 22 – Exposition of the sails to the wind. A) In its rotation, from angle 0° to 60° and from angle 120° to 180°, a sail is exposed to a favorable wind at the same time as with another sail; B) From angle 60° to 120°, a single sail is exposed to favorable wind.

For now, it is, then, only possible to use hypothetical and approximate formulas to estimate the power of the proposed plants. With the prudent assumptions:  $S = 2s$  ( $s$  = surface of a wing);  $C = 0.5$  and, moreover, assuming that cut-off values are greater for plants with vertical axis of rotation, as a consequence of their greater stability compared to that of those currently in use, I have drawn the wind speed/power curves for the plants VertEolo 1:1 (cut-off = 8 MW), VertEolo 2:3 (cut-off = 50 MW) and VertEolo 3:6 (cut-off = 150 MW) and compared them with that of the Enercon E-126 plant (cut-off = 7.8 MW) (fig. 23).

These curves are certainly of little value until they can be confirmed by actual plants, but there are certain aspects that deserve our attention:

- 1) With VertEolo plants of dimensions similar to those of the major plants with horizontal axis of rotation built to date, similar levels of powers are reached, but with greatly reduced use of materials and with a type of construction that is inherently much less expensive.
- 2) It is possible to envisage plants with vertical axis of rotation that will be much larger than VertEolo 1:1, which, despite being similar in size to the largest traditional wind turbines, should be considered, if realized, a relatively small prototype. The feasibility of much larger plants, such as VertEolo 2:3 and VertEolo 3:6, would allow a single plant to achieve levels of power comparable to those of average power plants that use non-renewable fuels.
- 3) For current plants with horizontal axis of rotation, plants much larger than those currently used cannot be hypothesized, because as size, and therefore power increase, costs and other obstacles grow exponentially.

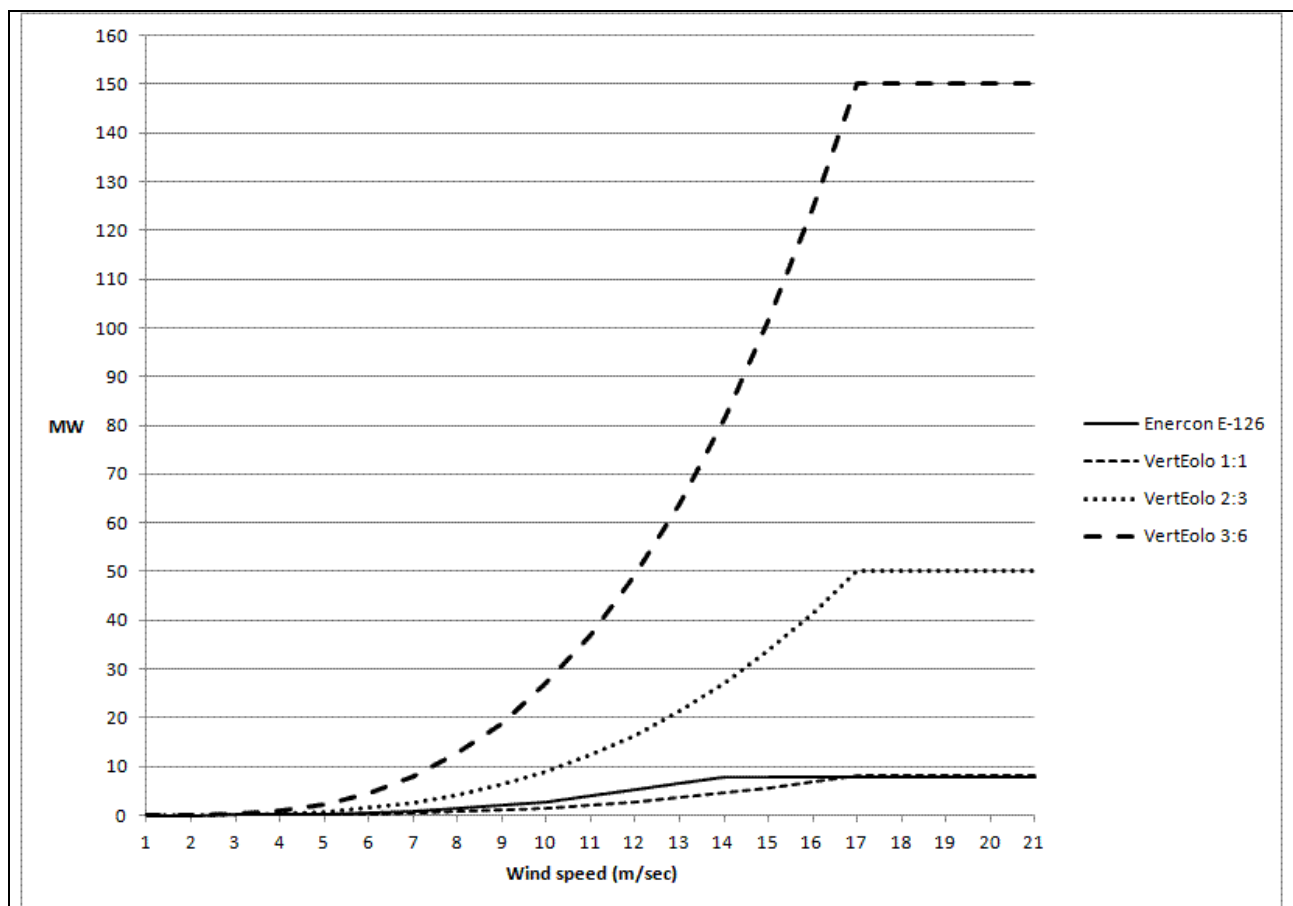


Figure 23 – Wind speed/power curves for the three hypothesized wind power plants with vertical axis of rotation compared with that of the most powerful existing plant with horizontal axis of rotation.

## (8) Conclusion

In the introduction, the serious problem of global energy demand and the possible catastrophic consequences of current massive use of CO<sub>2</sub> producing fuels were briefly expounded. It is theoretically possible that current wind power plants can resolve these problems, but the number of facilities required is very high, even if we use the largest available power plants (Table 4), i.e., by using 7.8 MW, capacity factor=0.45 plants, the necessary number of them would be around 3.88 million, and the density relevant (n/ M km<sup>2</sup> about 29,880; n/ M inhab. 388.44), and the costs proportionally high.

By employing very large plants with vertical axis of rotation, it would be possible to reduce drastically the number of necessary facilities and lower the costs to levels that would make all existing plants for energy production non-competitive, be they wind power plants or any other type of power plant.

If my assumptions and the calculations are correct, about 165,000 plants of the type VertEolo 3:6 (150 MW, capacity factor=0.55), i.e. about 1,271 plants per million km<sup>2</sup> or 16.53 plants per million of inhabitants (Table 4), would be enough to cover all the energy needs of any type now covered by non-renewable sources, for a world population increased according to demographic forecasts and with levels of consumption comparable to those of present industrially developed countries.

**Table 4 – Required plants to satisfy world Energy needs**

		<b>Enercon E-126</b>			<b>VertEolo 1:1</b>		
<b>Nameplate power*</b>		0.0078 GW			0.008 GW		
<b>Capacity factor*</b>		0.45			0.45		
<b>Effective power*</b>		0.00351 GW			0.0036 GW		
	<b>GW</b>	<b>n</b>	<b>n / M km<sup>2</sup></b>	<b>n / M inhab.</b>	<b>n / M km<sup>2</sup></b>	<b>n / M inhab.</b>	<b>n / M km<sup>2</sup></b>
<b>A</b>	1,870	532,844	4,099	53.28	519,523	3,996	51.95
<b>B</b>	3,741	1,065,689	8,198	106.57	1,039,047	7,993	103.90
<b>A+C</b>	5,611	1,598,533	12,296	159.85	1,558,570	11,989	155.86
<b>C</b>	4,545	1,294,812	9,960	129.48	1,262,442	9,711	126.24
<b>D</b>	9,090	2,589,624	19,920	258.96	2,524,883	19,422	252.49
<b>C+D</b>	13,634	3,884,436	29,880	388.44	3,787,325	29,133	378.73

		<b>VertEolo 2:3</b>			<b>VertEolo 3:6</b>		
<b>Nameplate power*</b>		0.05 GW			0.15 GW		
<b>Capacity factor*</b>		0.5			0.55		
<b>Effective power*</b>		0.025 GW			0.0825 GW		
	<b>GW</b>	<b>n</b>	<b>n / M km<sup>2</sup></b>	<b>n / M inhab.</b>	<b>n</b>	<b>n / M km<sup>2</sup></b>	<b>n / M inhab.</b>
<b>A</b>	1,870	74,811	575	7.48	22,670	174	2.27
<b>B</b>	3,741	149,623	1,151	14.96	45,340	349	4.53
<b>A+C</b>	5,611	224,434	1,726	22.44	68,010	523	6.80
<b>C</b>	4,545	181,792	1,398	18.18	55,088	424	5.51
<b>D</b>	9,090	363,583	2,797	36.36	110,177	848	11.02
<b>C+D</b>	13,634	545,375	4,195	54.54	165,265	1,271	16.53

Notes:

\*: Actual or hypothesized values;

n: Number of plants to produce the required GW;

n / M km<sup>2</sup>: no. per millions of square kilometers, using the parameter of 130 M km<sup>2</sup> of world usable surface;

n / M inhab.: no. per million of inhabitants (considering a future world population of 10,000 millions);

A: In 2008, the electric energy obtained by non-renewable sources was 16,406 TWh. If 1 TWh is produced by 0.114 GW in a year, a power of 1,870 GW is necessary to produce this amount of energy.

B: Energy produced for other necessities by non-renewable sources, roughly estimated as the double of A.

C: Electric energy that will be produced with a mean global usage equal to that of the more industrialized countries (i.e. increasing from 70 to 170 GJ per capita consumption), plus an increase in the population from 7 to 10 billions, minus a saving of 30%. Estimated multiplying A by 2.43.

D: As for C but concerning the energy produced for other necessities. Roughly estimated as the double of C.

The availability of energy would allow the production of synthetic fuels with CO<sub>2</sub> absorption in the phase of synthesis and the release of an equal amount of CO<sub>2</sub> when they are burned. For many industrial plants, such as foundries, the combustion of large quantities of fossil fuels would no longer be necessary, but electricity or synthetic fuels could be used. Overproduction of energy at certain times or in some areas would be used for the production of synthetic fuels or energy-intensive materials.

This would be a contemporary solution for several serious problems such as the progressive depletion of fossil fuels, the increasing air levels of CO<sub>2</sub> with the resulting catastrophic effects on the global climate, the increasing costs of fuels, the political problems related to the unequal distribution of fossil fuels and the related disputes, the environmental problems and the human health problems related to the use of fossil and nuclear fuels, etc.

The economic aspect should be considered too.

If 4,467,314.86 ktoe are necessary to produce 20,262.40 TWh [1], i.e. 220,473.1355 toe/TWh, by considering that a toe is 6.841 barrels of oil equivalent or boe (value obtained from the ratio between the conventional definition of IEA/OECD for a toe = 41.868 GJ and the conventional definition of US Internal Revenue Service for a boe = 6.12 GJ), the above-mentioned value of necessary toe can be expressed as 1,508,256.72 boe/TWh.

If a wind power plant with nameplate power = 0.15 GW and capacity factor = 0.55, i.e. with an effective power = 0.0825 GW, produces, in one year, 0.0825 GW / 0.114 GW/TWh = 0.723684211 TWh, this means a saving of 0.723684211 TWh multiplied per 1,508,256.72 boe/TWh = 1,091,501.573 boe.

The cost of the saved fuel will be this number multiplied by the cost of a single boe, and so, assuming a cost of 70\$ per boe, the cost of the fuel saved in a year will be about 76,4 M\$.

This means that, if the cost for the construction of a single VertEolo 3:6 is 100 M\$, its cost would be recovered by fuel savings in less than 16 months, even disregarding the costs deriving from the use of fossil fuels on the environment and on human health.

As regards the environmental impact of the proposed plants, certain concepts must be underlined.

Wind power plants do not produce any harmful substances nor any radioactive waste, with their related problems and costs, and this is certainly an advantage over any plant that burns fossil or nuclear fuels.

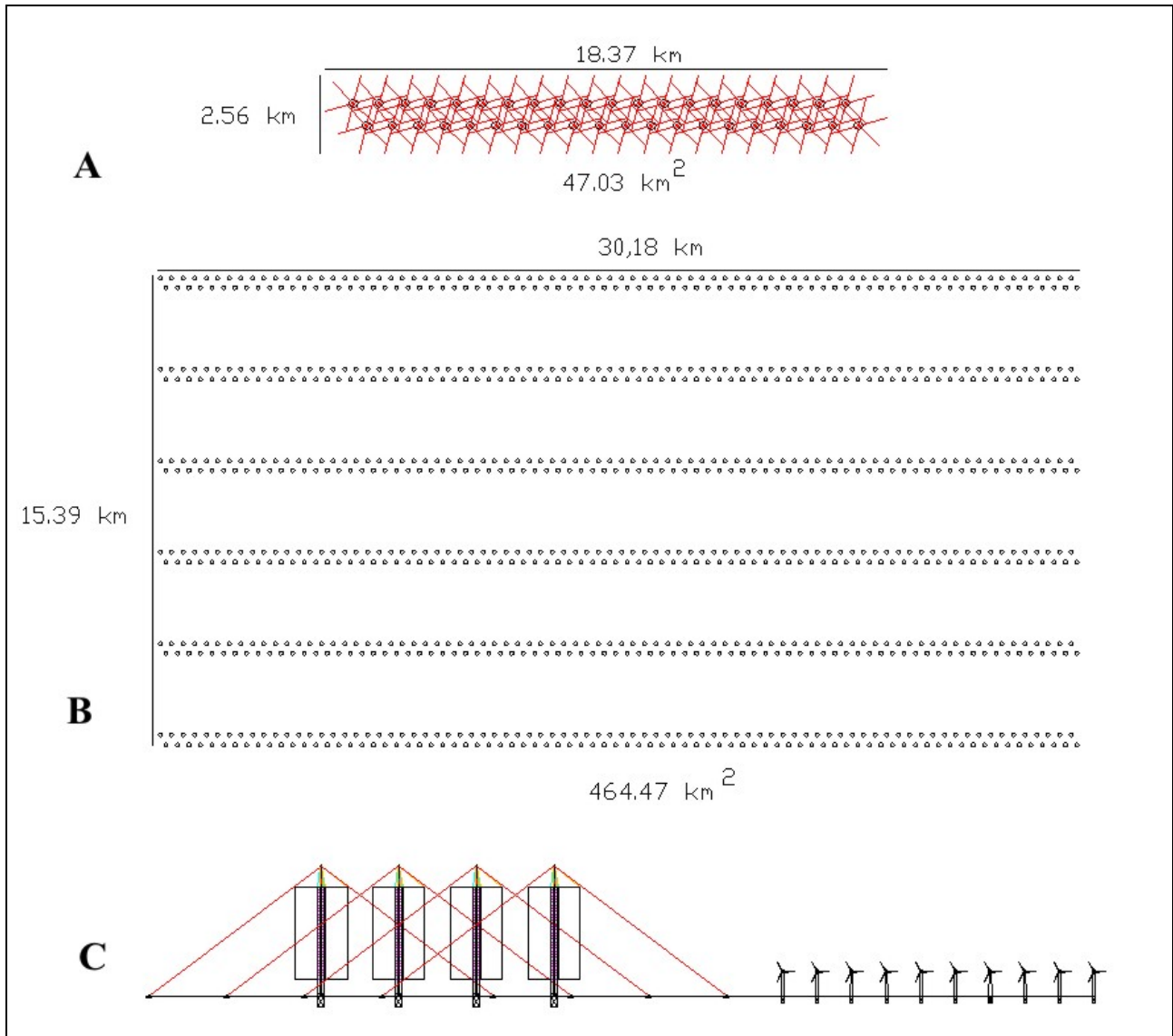
With regard to the indirect environmental impact deriving from the materials used in their construction, plants of the proposed type with vertical axis of rotation, are advantageous compared to the traditional ones, given that they use fewer raw materials.

As regards the possible harms for avian species, it is difficult to imagine how a bird could not see a sail of a plant with vertical axis of rotation and knock against it.

As far as the environmental impact due to their sheer physical presence is concerned, it is obvious that very high plants, such as VertEolo 3:6, will not go unnoticed and their impact will not be neutral. In many areas of environmental, historical or touristic value, their construction should certainly be prohibited. However, there are many other areas that could accommodate rows of plants of this type (e.g., two rows of plants, out of phase with each other, and each row consisting of 20 plants), thereby limiting the visual impact to few sites. In assessing the impact of such a group, we should also consider the impact of an equivalent group of 800 traditional wind power plants (fig. 24). However, the impact could be mitigated, or even rendered advantageous, by using different colors for neighboring plants, with artistic combinations, for the wings and other parts.

Electricity production of the United Kingdom, France or Italy by non-renewable resources (41.27, 56.32, and 28.84 GW, respectively, in 2008) would be covered by 12.5, 17, and 8.7 arrays, respectively. The average total future energy needs of a nation of 60 million inhabitants could be covered by about 25 arrays.

Moreover, it should be considered that part of the production of energy, in particular for the making of synthetic fuels or for materials and articles requiring a high use of energy, could be distributed on a global scale to areas that are sparsely populated and thus suitable for the installation of large arrays of wind power plants.



**Figure 24 – Comparison between an array of 40 VertEolo 3:6 (A) and an array of 800 current wind-power plants, each with 1/20 of the hypothesized power of a VertEolo 3:6 (B). The first group is arranged in two rows, each of 20 plants, while the second group is arranged in five groups of two rows, each row of 80 plants, appropriately spaced out (“VertEolo\_array.dwg”). C) Frontal views (partial).**

## (9) References

- [1] IEA (International Energy Agency) Statistics and Balances, 2011.
- [2] Observ'ER (L'Observatoire des énergies renouvelables) 2.2 Electricity Production From Wind Sources: Main Wind Power Producing Countries – 2010 (text & table), Worldwide Electricity Production From Renewable Energy Sources: Stats and Figures Series: Thirteenth Inventory – Edition 2011, Paris, Observ'ER.
- [3] REN21 (Renewable Energy Policy Network for the 21<sup>st</sup> century), Renewables 2011: Global Status Report. (<http://www.map.ren21.net/GSR/GSR2012.pdf>)
- [4] IEA, 2008 Energy Balance for World, 2011.
- [5] Murray, J., King D. (2012) Oil's tipping point has passed. *Nature* 481, 433-5.
- [6] Dr. Pieter Tans, NOAA/ESRL ([www.esrl.noaa.gov/gmd/ccgg/trends/](http://www.esrl.noaa.gov/gmd/ccgg/trends/)) and Dr. Ralph Keeling, Scripps Institution of Oceanography ([scrippsco2.ucsd.edu/](http://scrippsco2.ucsd.edu/)).
- [7] Etheridge, D.M.; Steele, L.P., Langenfelds, R.L., Francey, R.J., Barnola, J.-M., Morgan, V.I. (1996). "Natural and anthropogenic changes in atmospheric CO<sub>2</sub> over the last 1000 years from air in Antarctic ice and firn". *Journal of Geophysical Research* 101, 4115–28.
- [8] IPCC (Intergovernmental Panel on Climate Change) Fourth Assessment Report: Climate Change 2007.
- [9] IPCC Third Assessment Report - Climate Change 2001 – Chapter 11. Changes in sea level
- [10] BP Statistical Review of World Energy 2012.
- [11] International Atomic Energy Agency - Power Reactor Information System (IAEA - PRIS) <http://www.iaea.org/pris/>
- [12] Energy Information Administration, Annual Energy Outlook 2011, December 2010. DOE/EIA-0383(2010).
- [13] Zehner, O. (2012) *Green Illusions*, University of Nebraska Press, Lincoln and London.
- [14] Global Wind Energy Commission (GWEC), Global Wind Statistics 2011.
- [15] <http://www.reuk.co.uk/Burradale-Wind-Farm-Shetland-Islands.htm>.
- [16] BTM Forecasts 340-GW of Wind Energy by 2013. [renewableenergyworld.com](http://renewableenergyworld.com). 27 March 2009. Retrieved 29 August 2010.
- [17] BTM Consult (2009). International Wind Energy Development World Market Update 2009
- [18] [http://www.enercon.de/p/downloads/ENERCON\\_PU\\_en.pdf](http://www.enercon.de/p/downloads/ENERCON_PU_en.pdf)
- [19] <http://www.windfair.net/press/9167.html>].
- [20] Betz, A. (1966) *Introduction to the Theory of Flow Machines*. (D. G. Randall, Trans.) Oxford: Pergamon Press.

## **(10) Acknowledgments**

I thank strongly Eng. Gianfranco Dell'Aversana for his precious help with the elaboration of 3D images, and Eng. Vittorio Castaldo and Eng. Theodore Goldsmith for their encouragements.

I offer special thanks to Prof. Alan Russell, illustrious Editor-in-Chief of the journal *Disruptive Science and Technology*, and to others, for their nearsighted undervaluation about the importance of the topic of this book, because their undervaluation has been a strong stimulus for the preparation and publication of it.



# APPENDIX

## Section 1 – Images from the original files (available at [www.r-site.org/VertEolo](http://www.r-site.org/VertEolo))

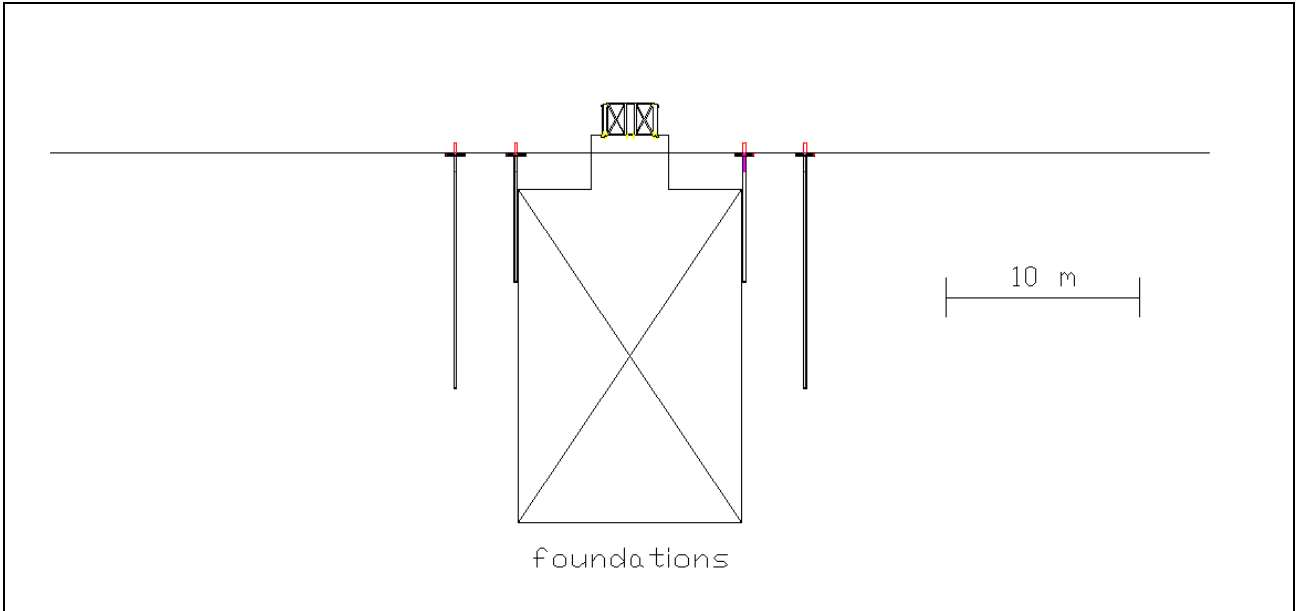


Figure A1 (from installation\_step\_01.dwg)

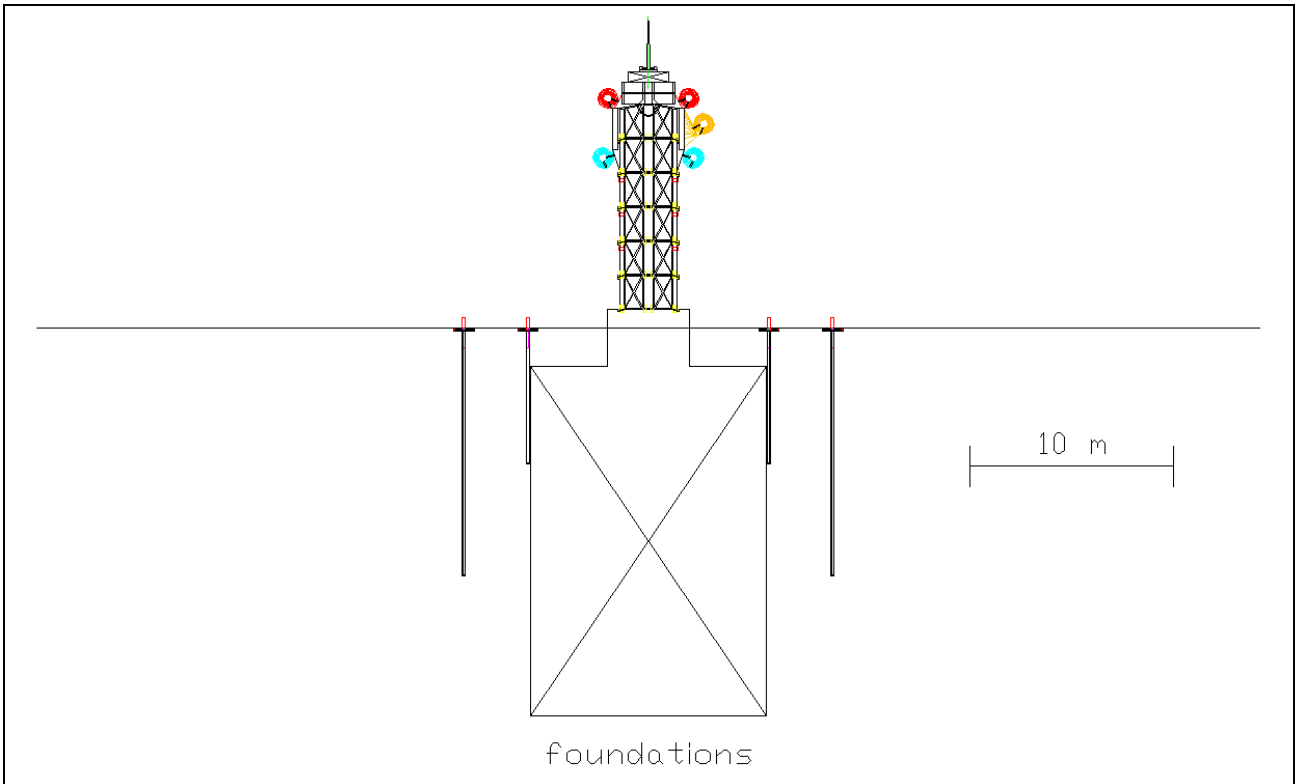


Figure A2 (from installation\_step\_02.dwg) - A

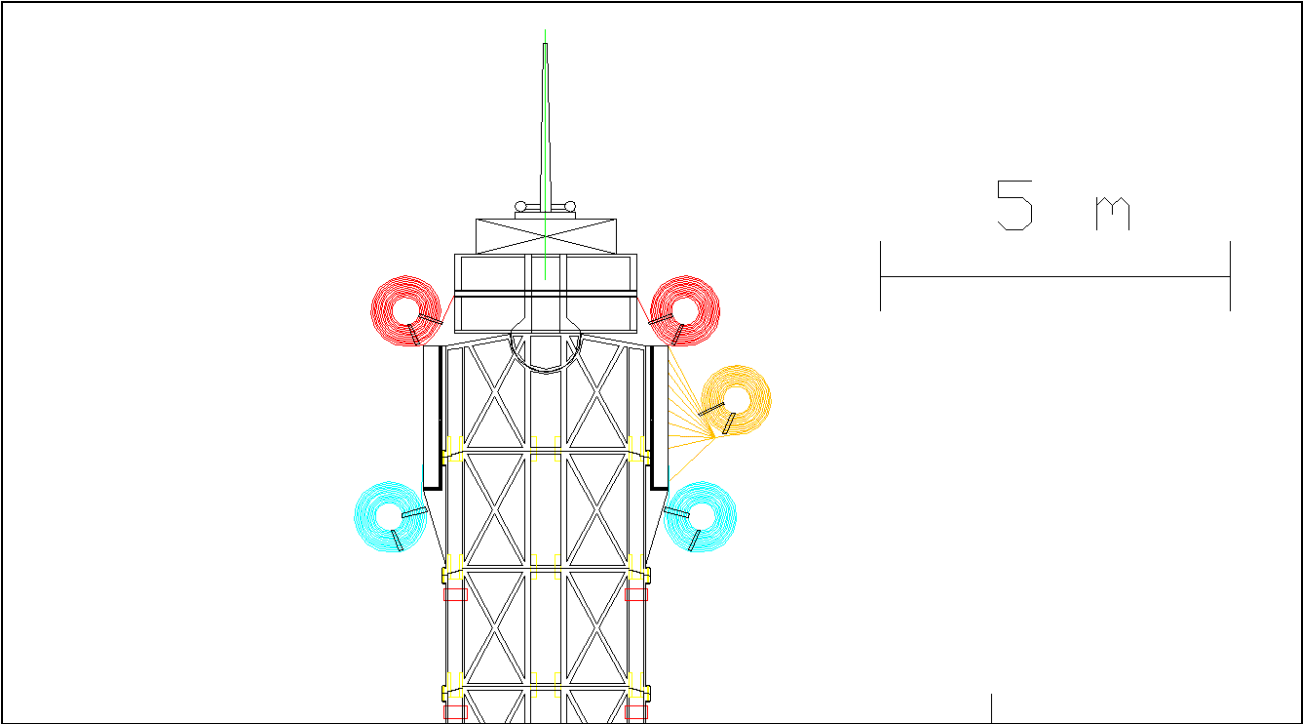


Figure A3 (from installation\_step\_02.dwg) - B

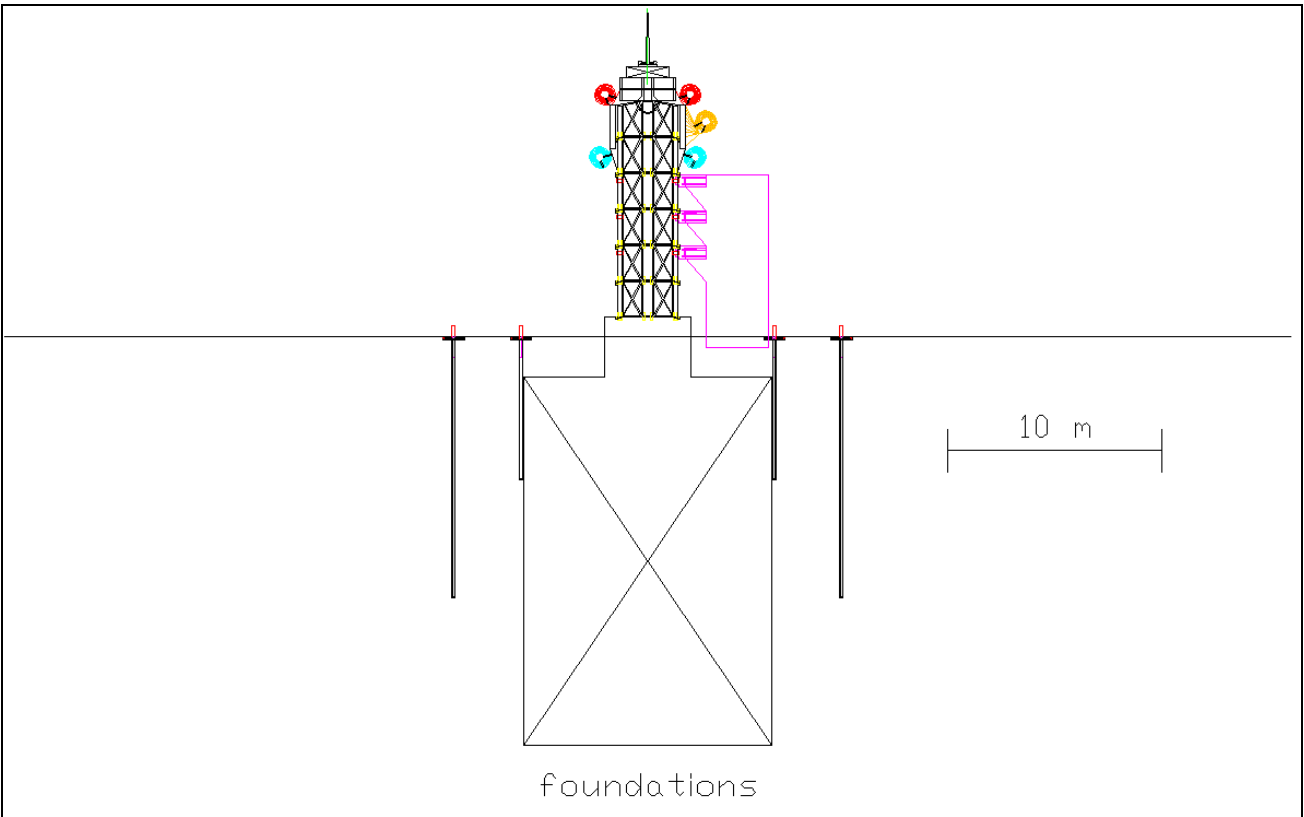


Figure A4 (from installation\_step\_03.dwg)

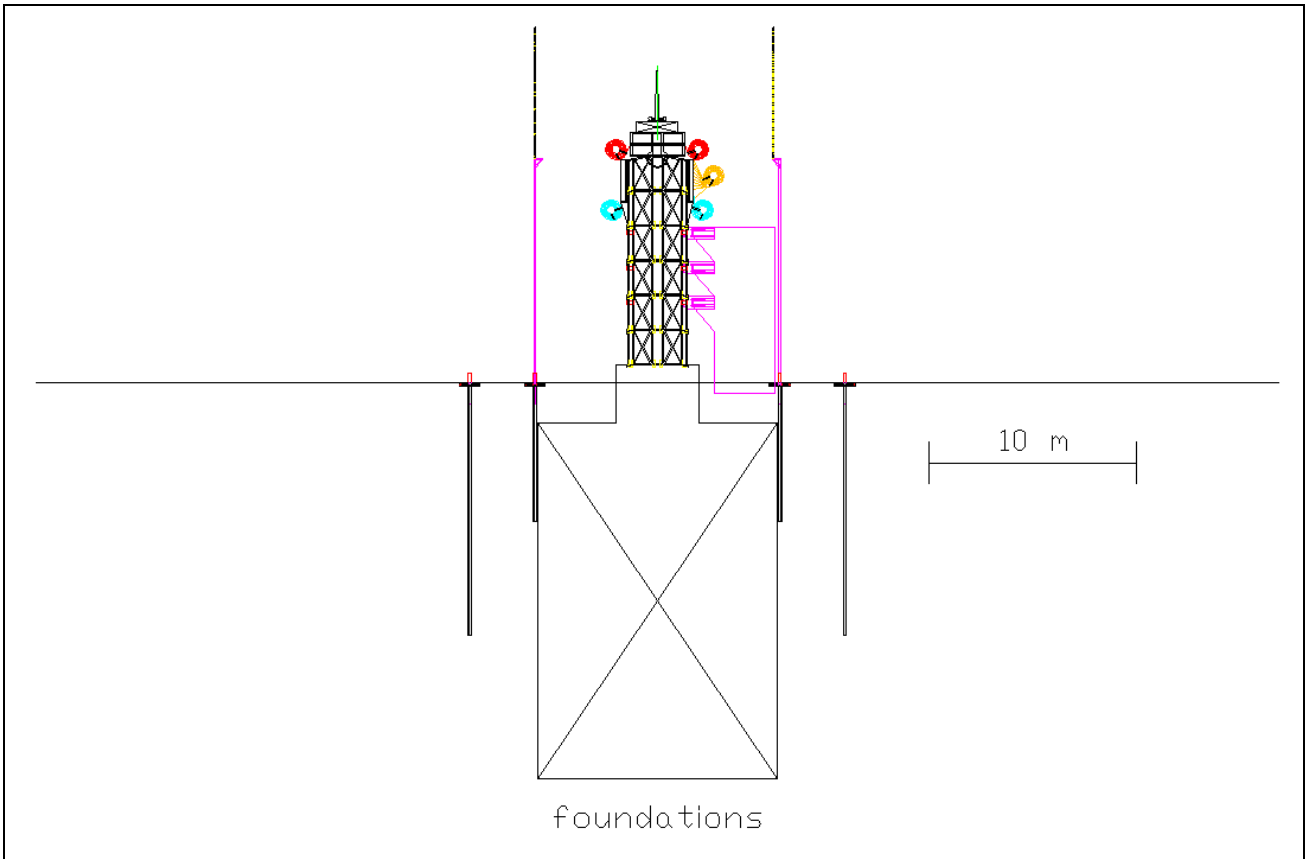


Figure A5 (from installation\_step\_04.dwg) - A

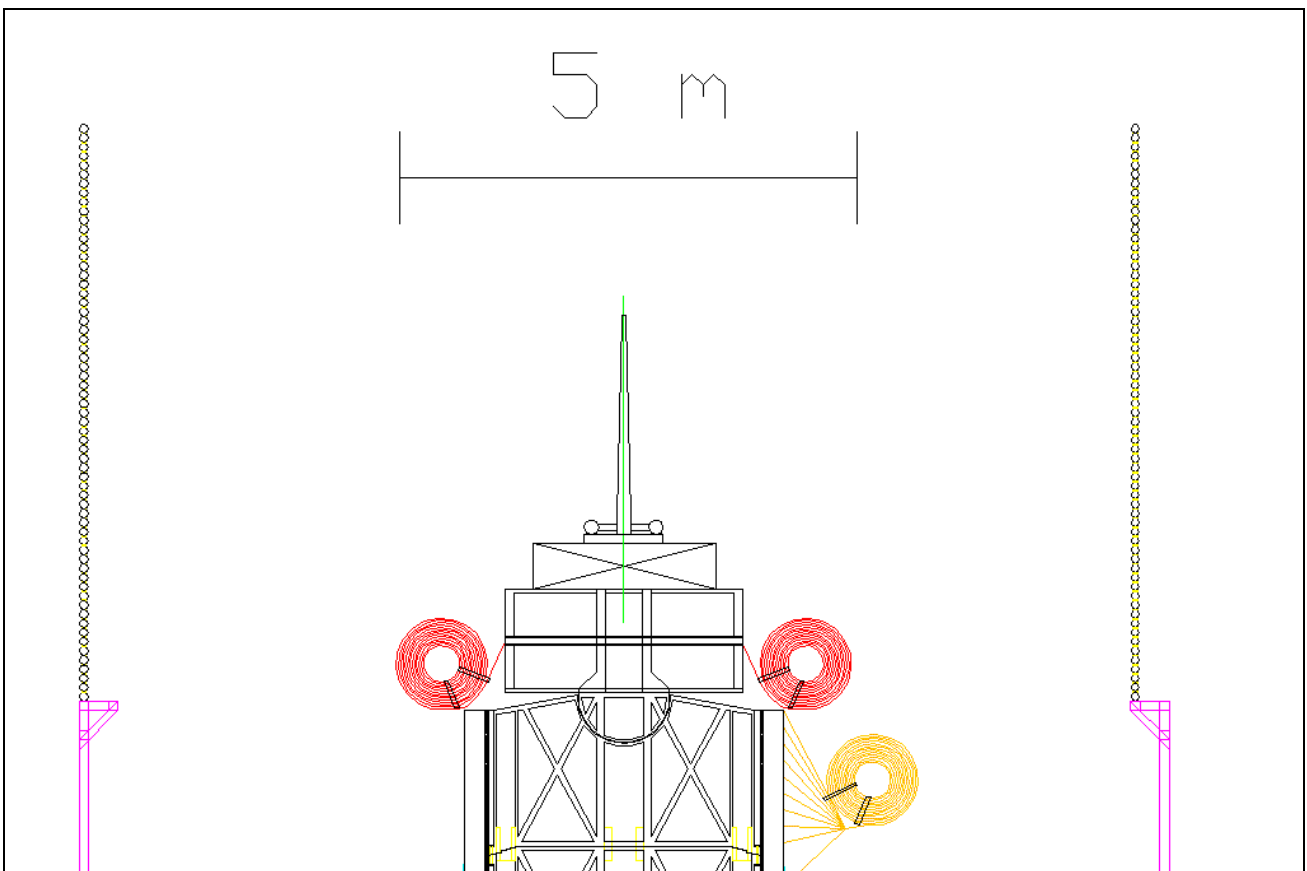


Figure A6 (from installation\_step\_04.dwg) - B

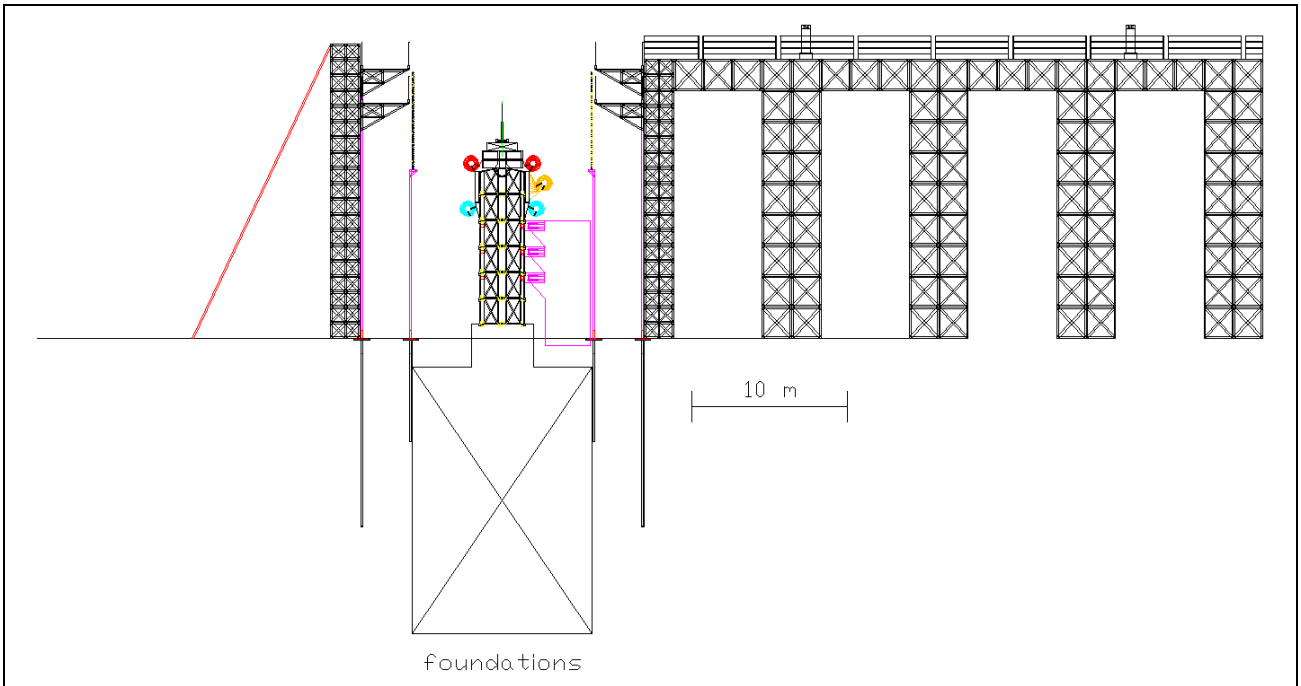


Figure A7 (from installation\_step\_05.dwg) - A

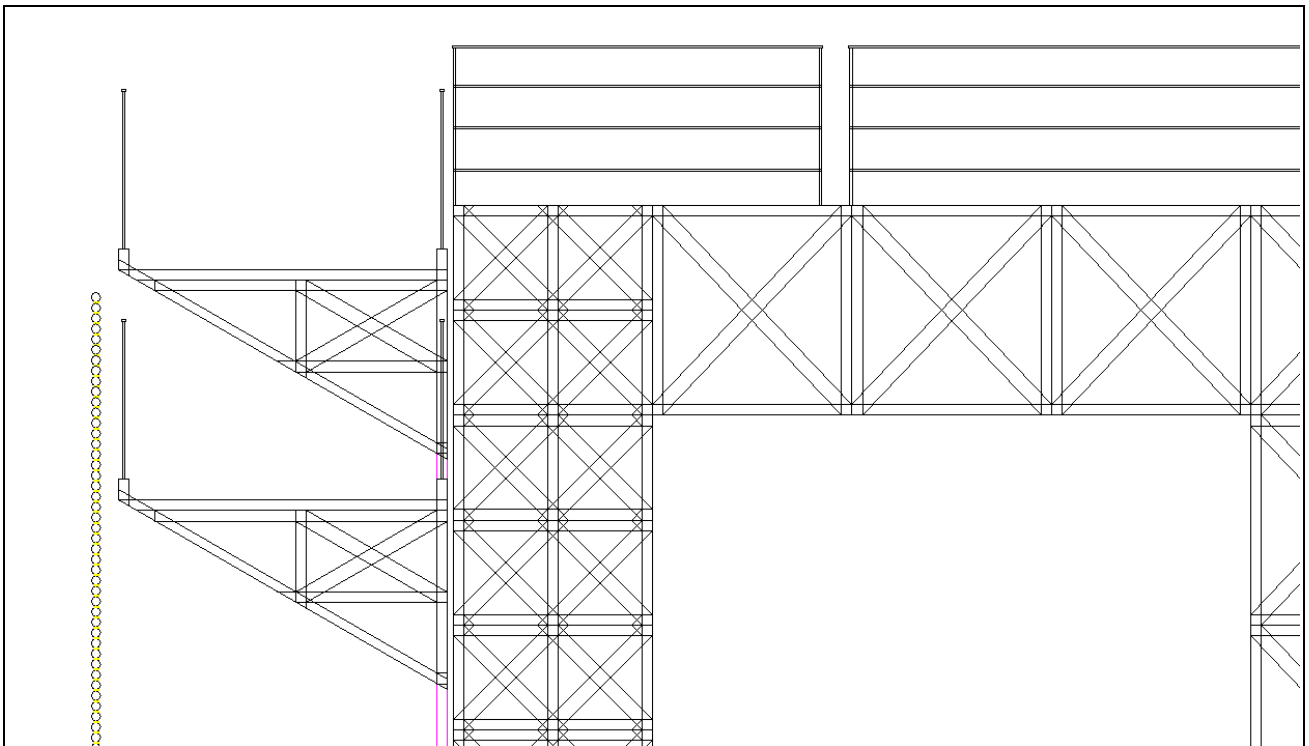


Figure A8 (from installation\_step\_05.dwg) - B

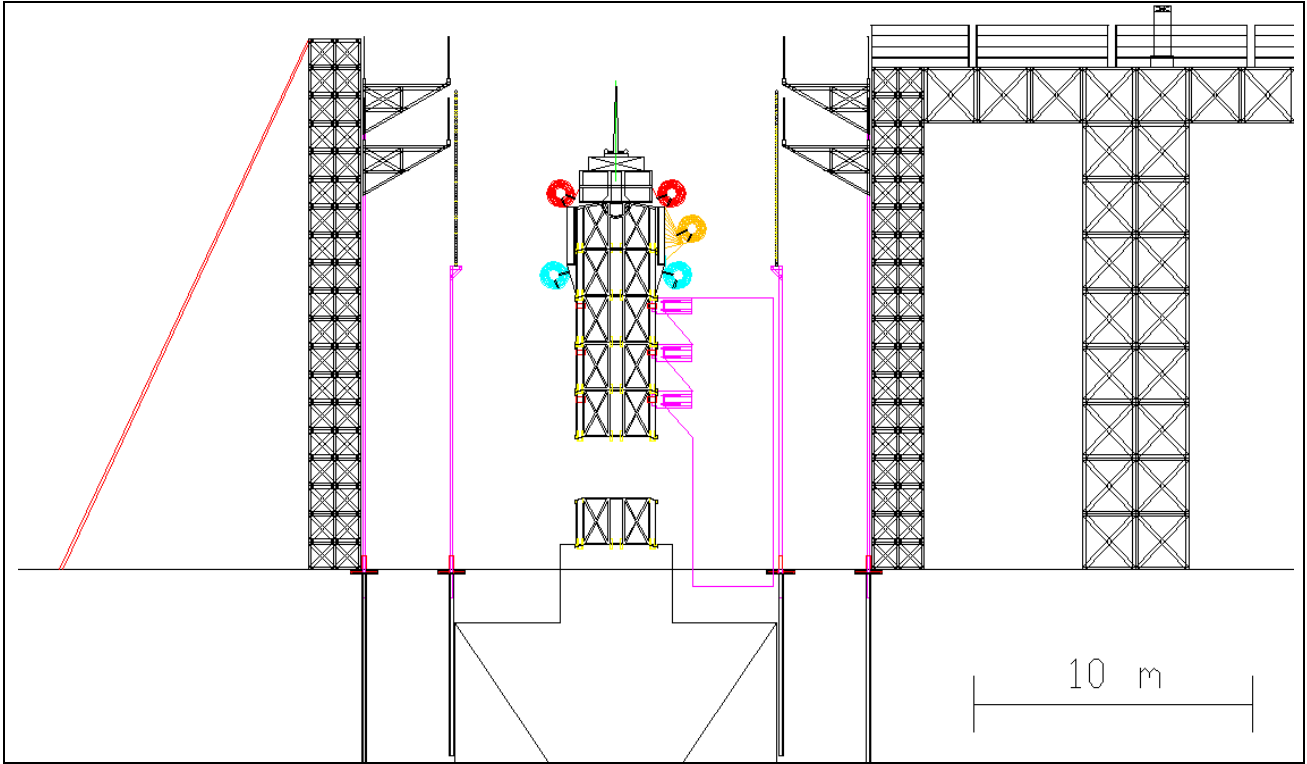


Figure A9 (from installation\_step\_06.dwg)

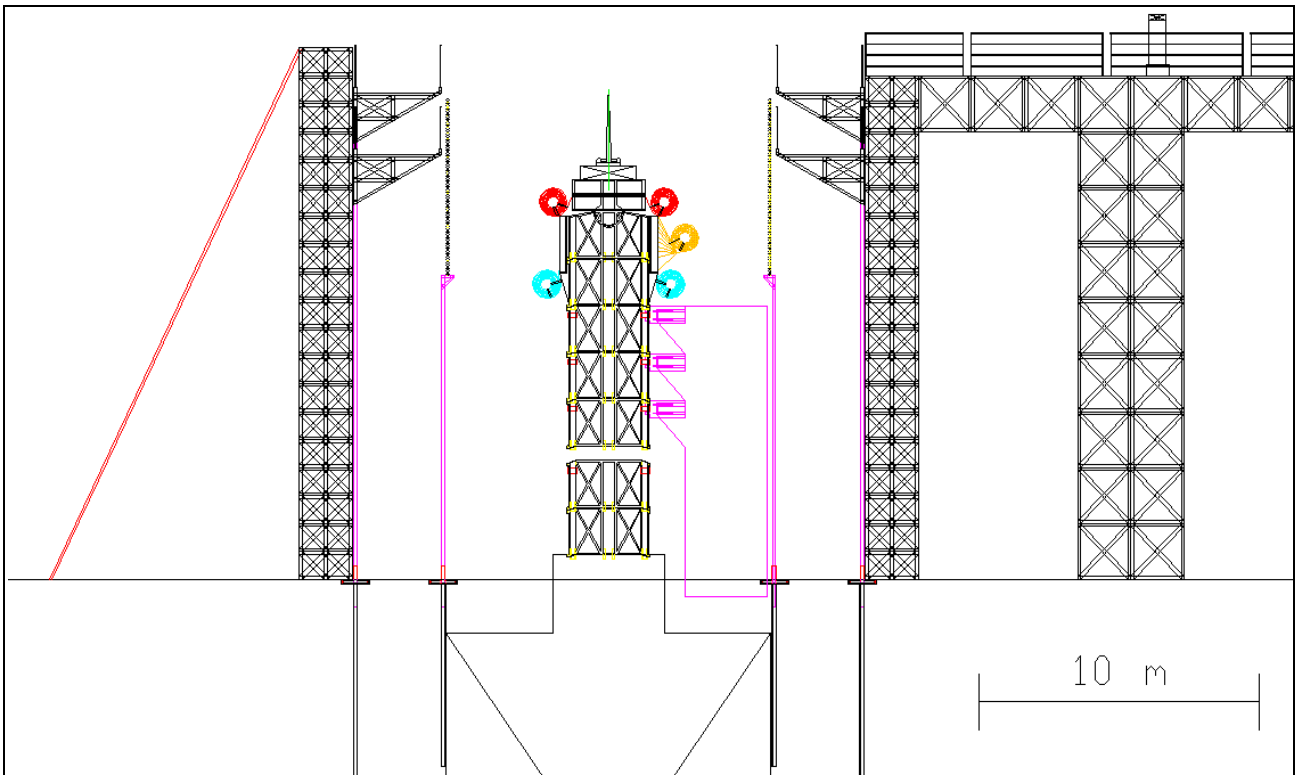


Figure A10 (from installation\_step\_07.dwg)



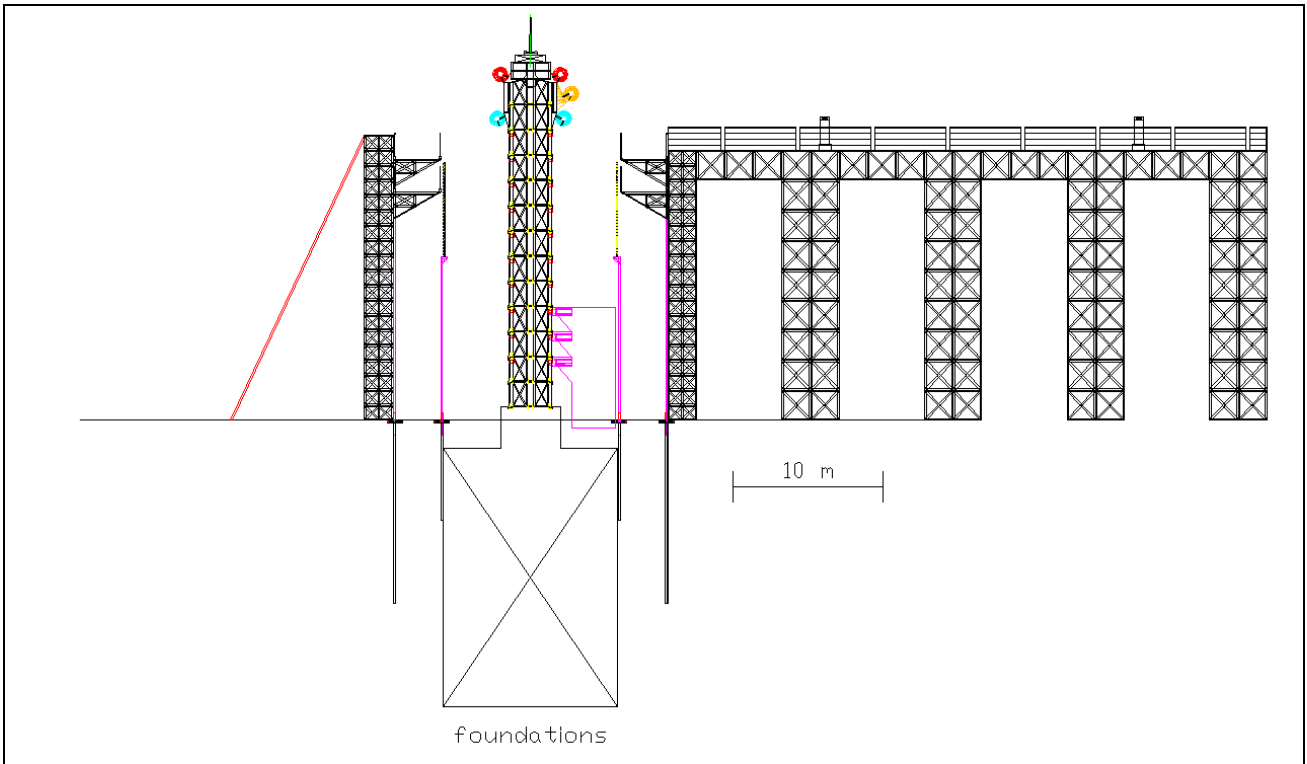


Figure A13 (from installation\_step\_10.dwg)

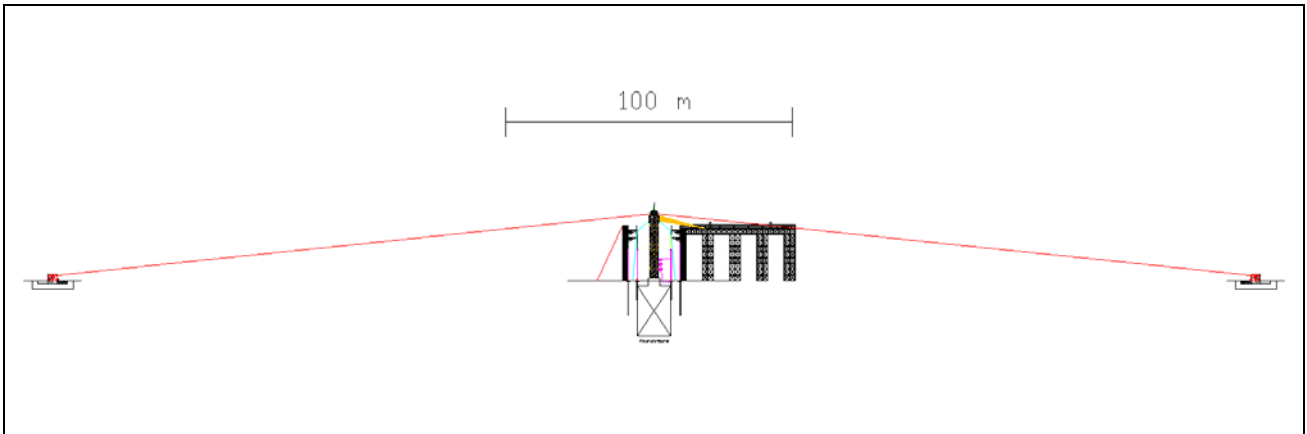


Figure A14 (from installation\_step\_11.dwg) - A

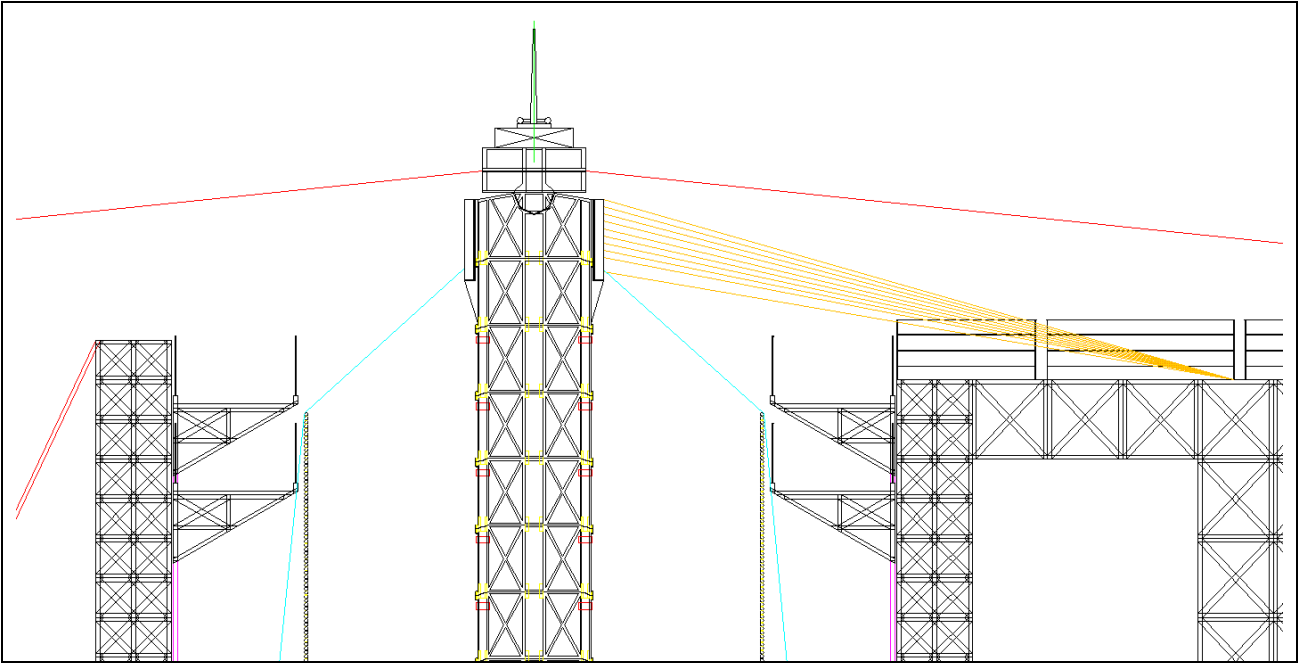


Figure A15 (from installation\_step\_11.dwg) - B

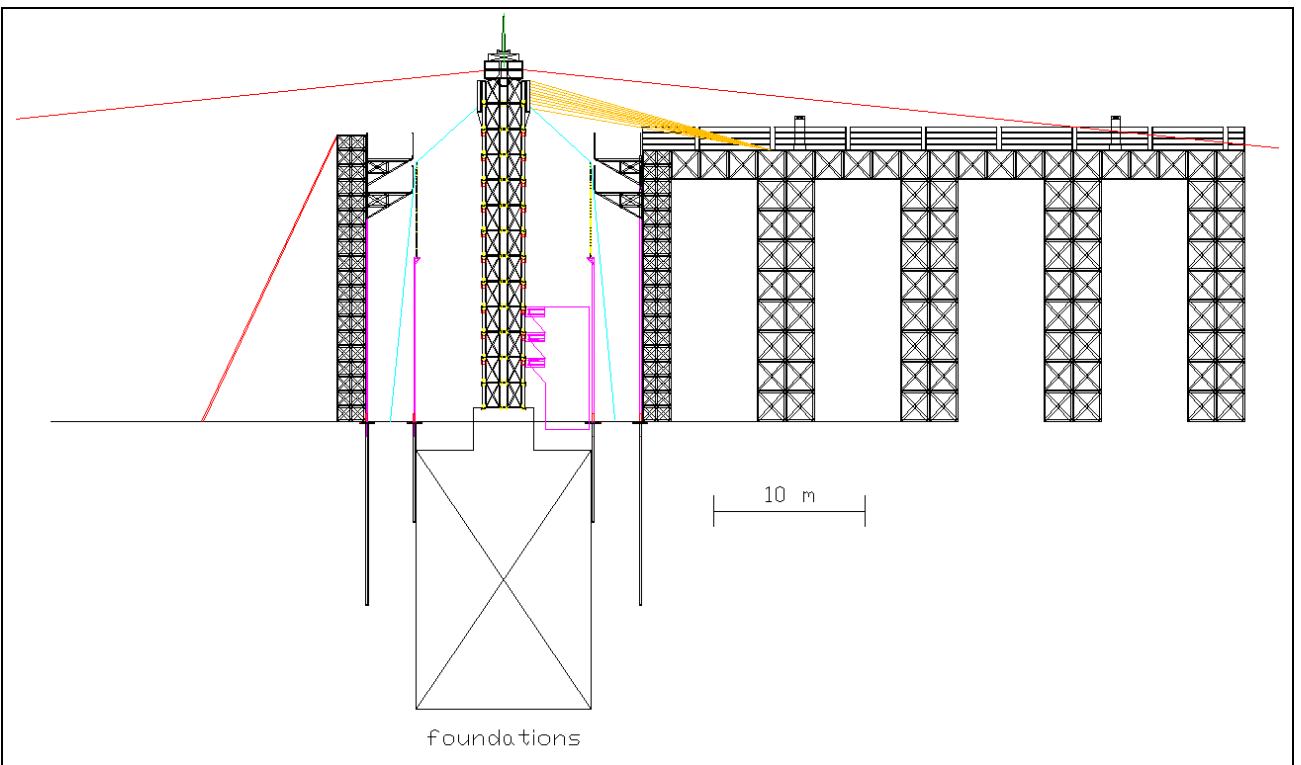


Figure A16 (from installation\_step\_11.dwg) - C



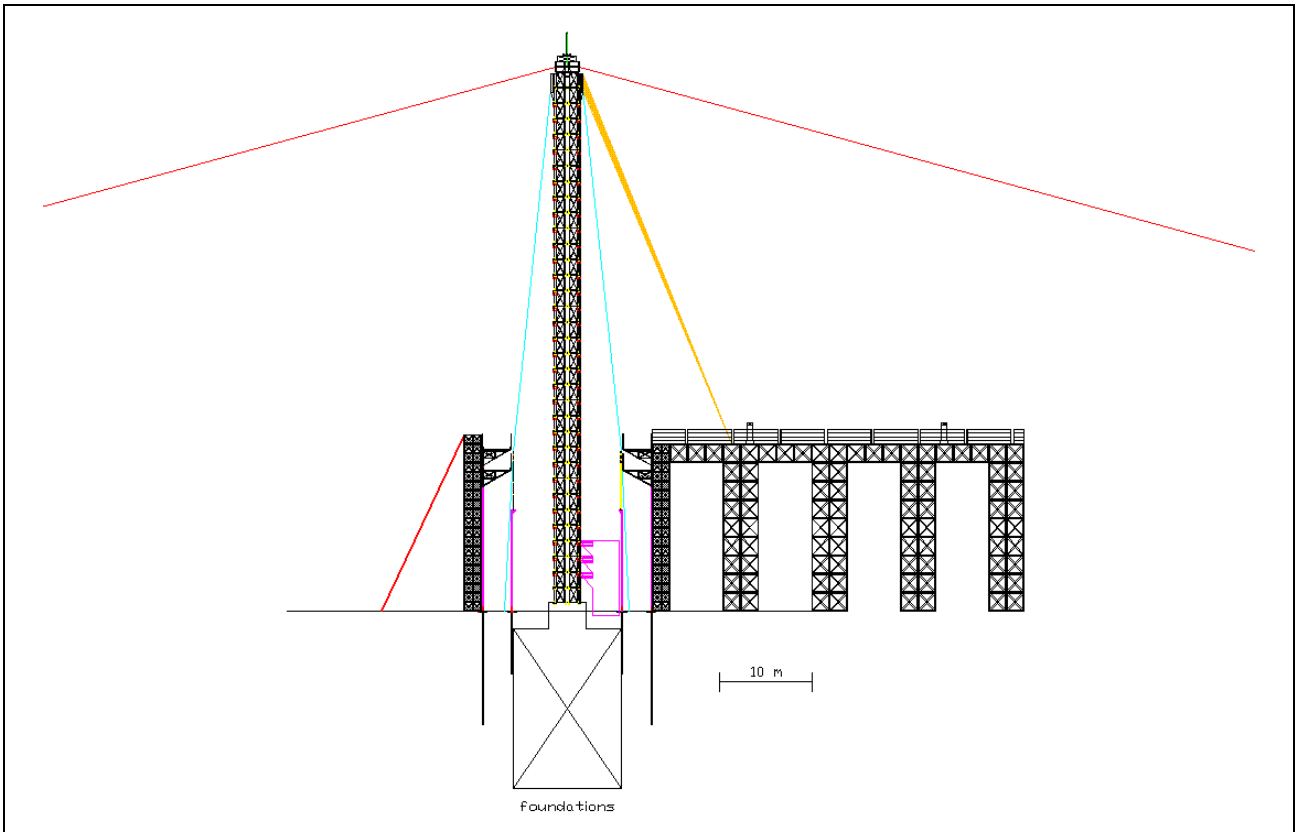


Figure A17 (from installation\_step\_12.dwg)

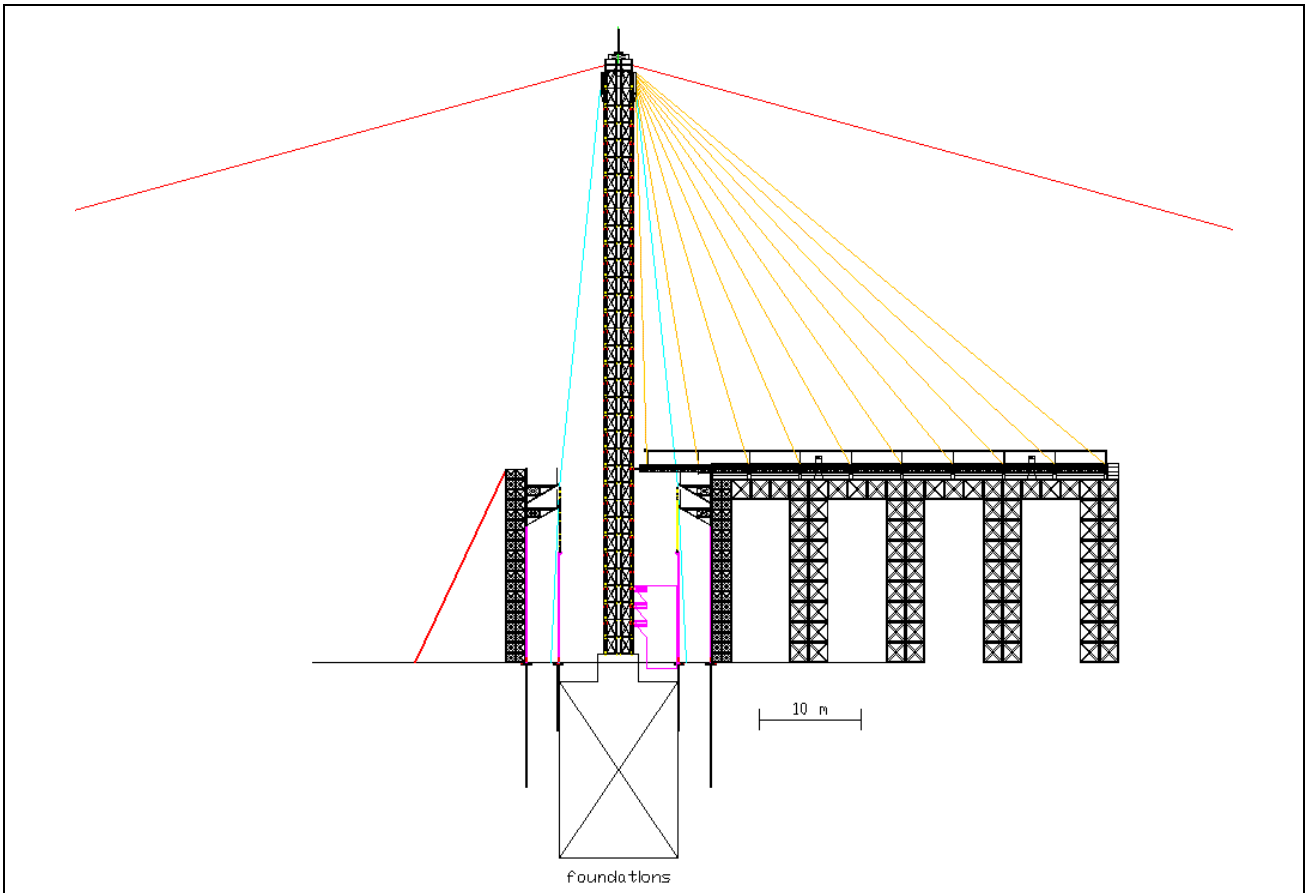


Figure A18 (from installation\_step\_13.dwg) – A

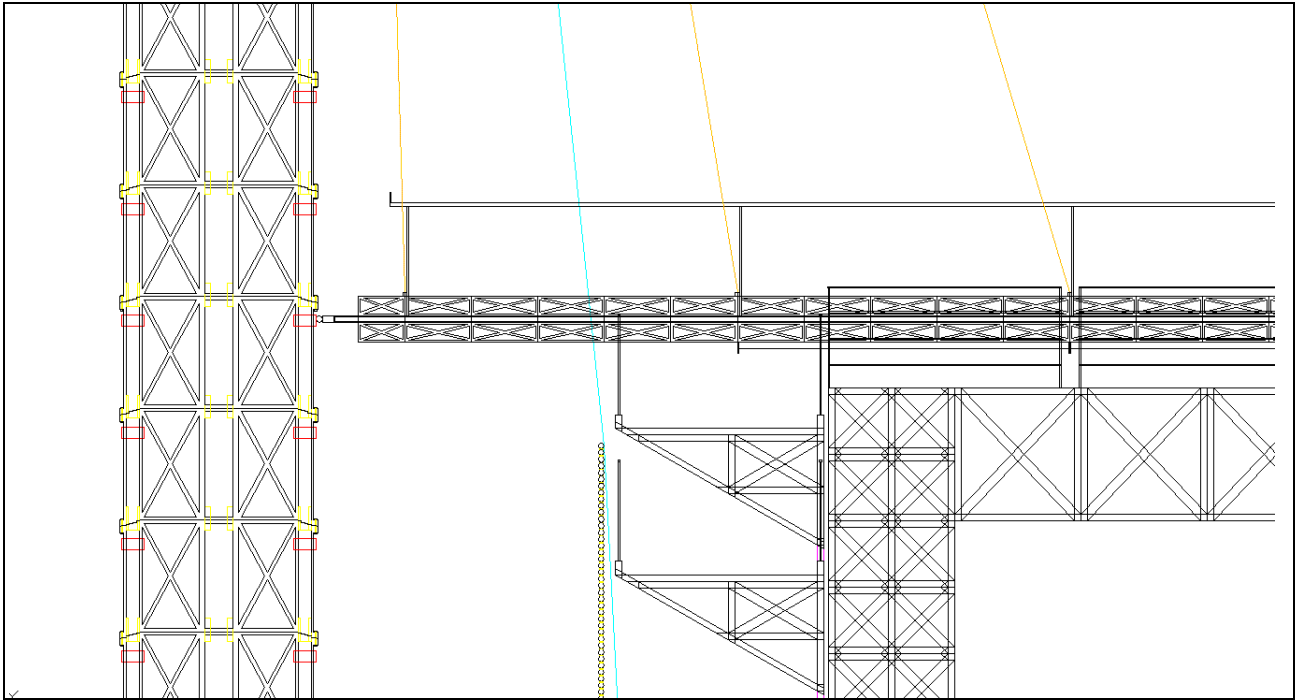


Figure A19 (from installation\_step\_13.dwg) - B

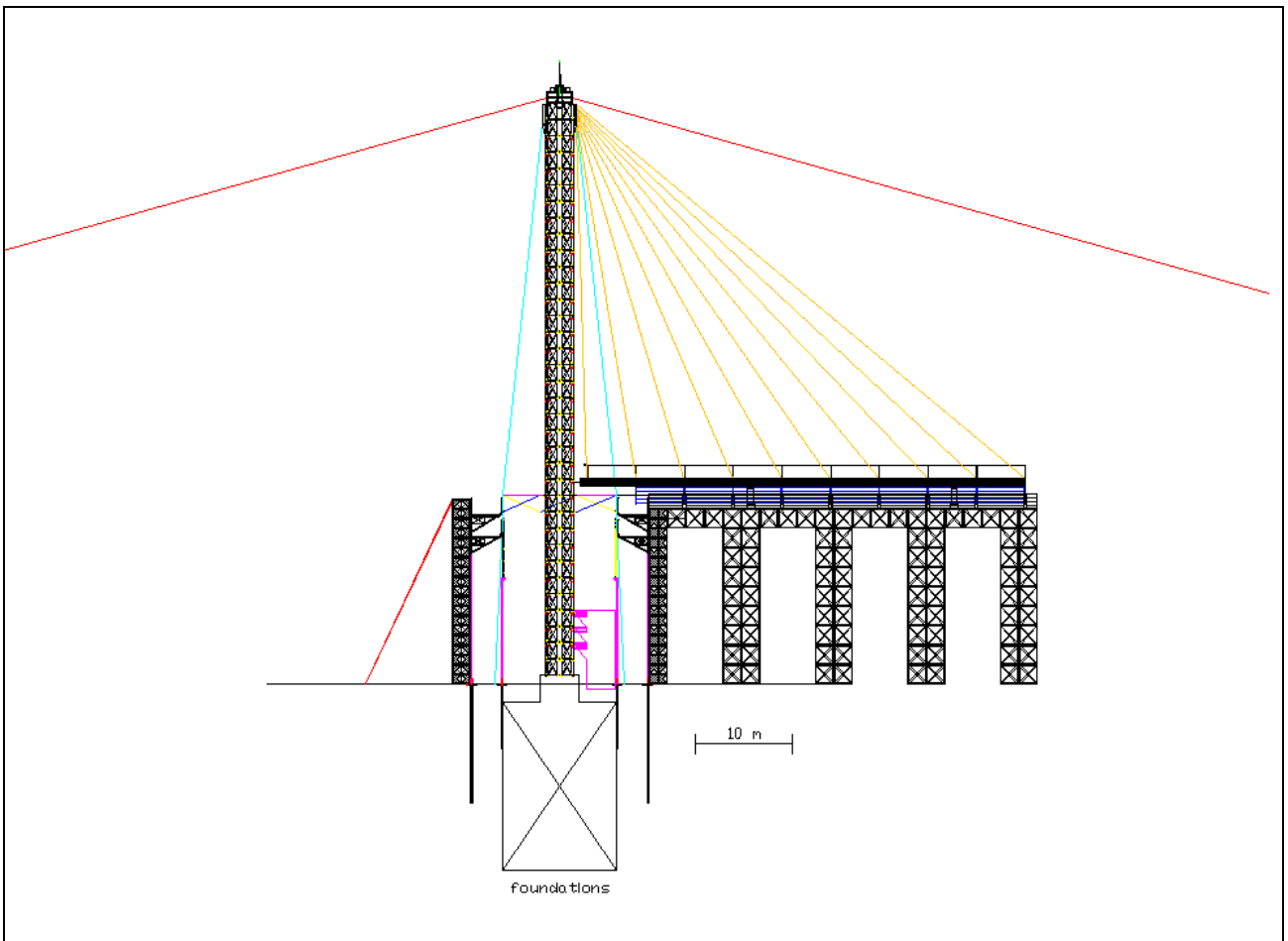


Figure A20 (from installation\_step\_14.dwg) - A

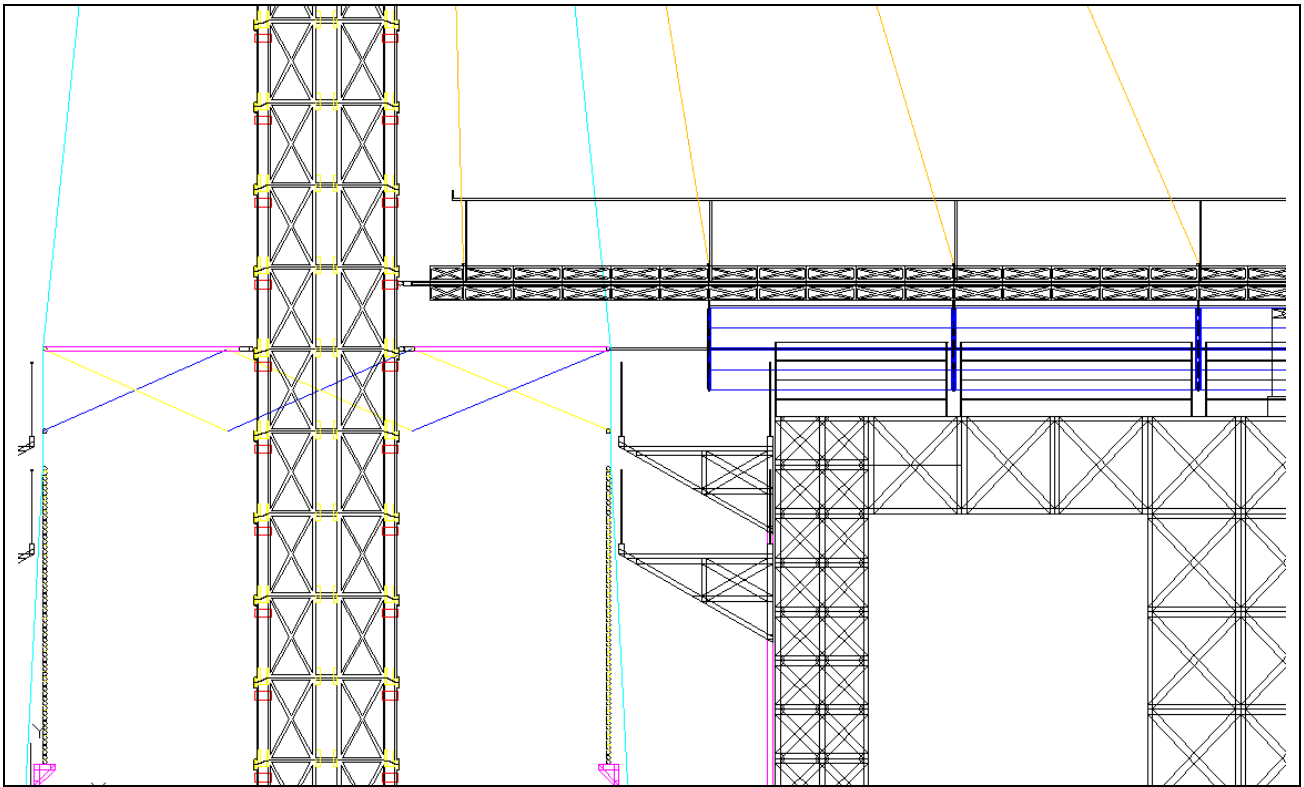


Figure A21 (from installation\_step\_14.dwg) - B

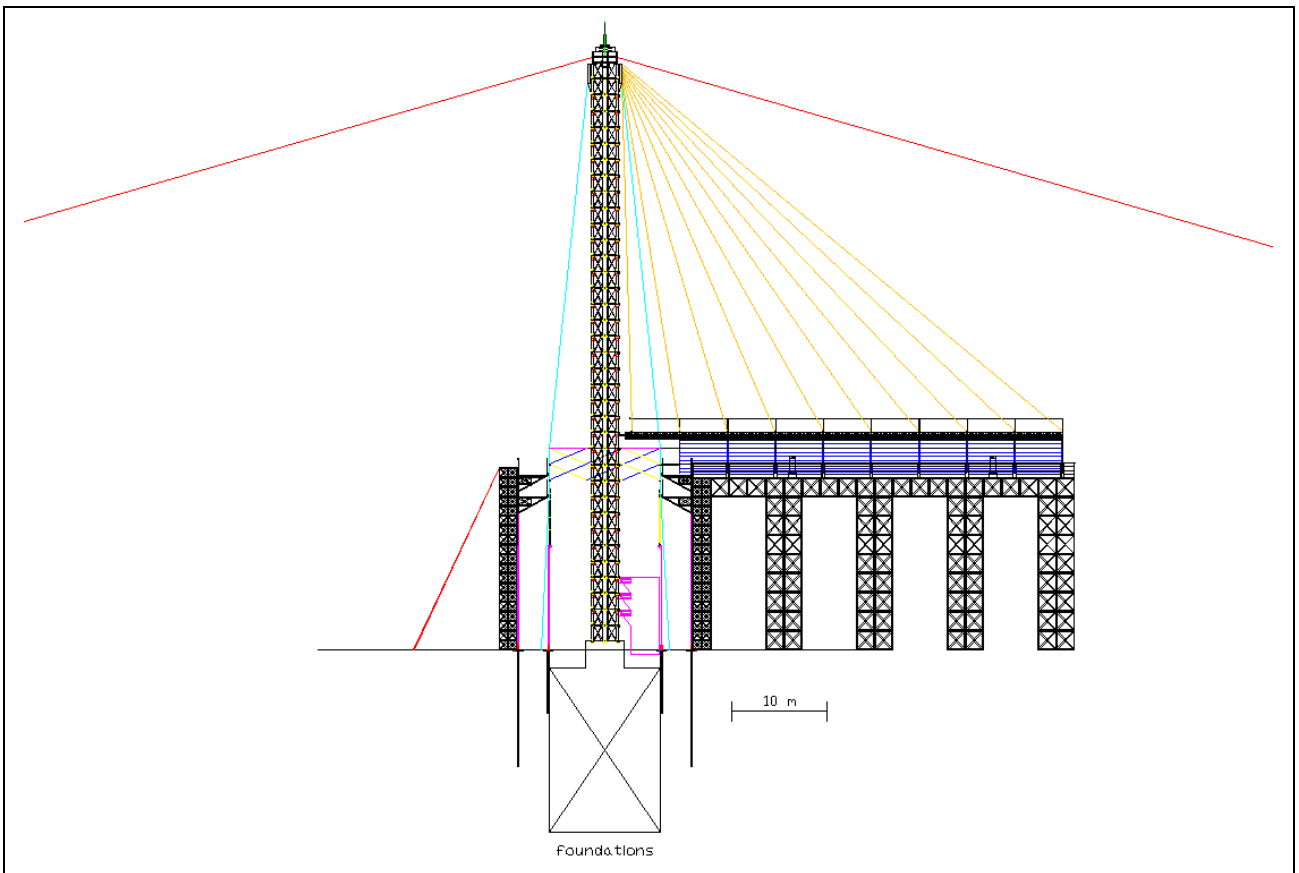


Figure A22 (from installation\_step\_15.dwg)

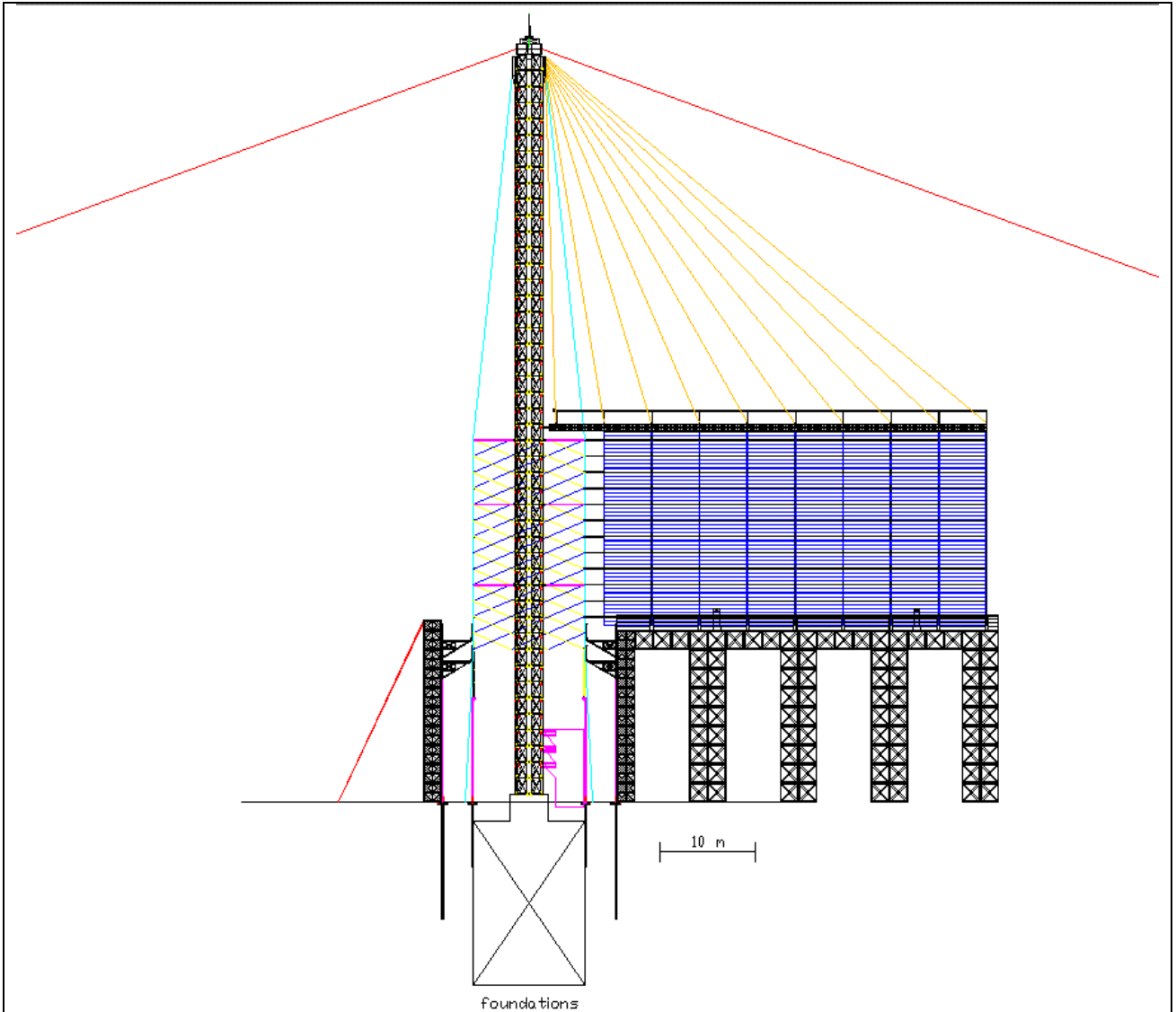


Figure A23 (from installation\_step\_16.dwg)

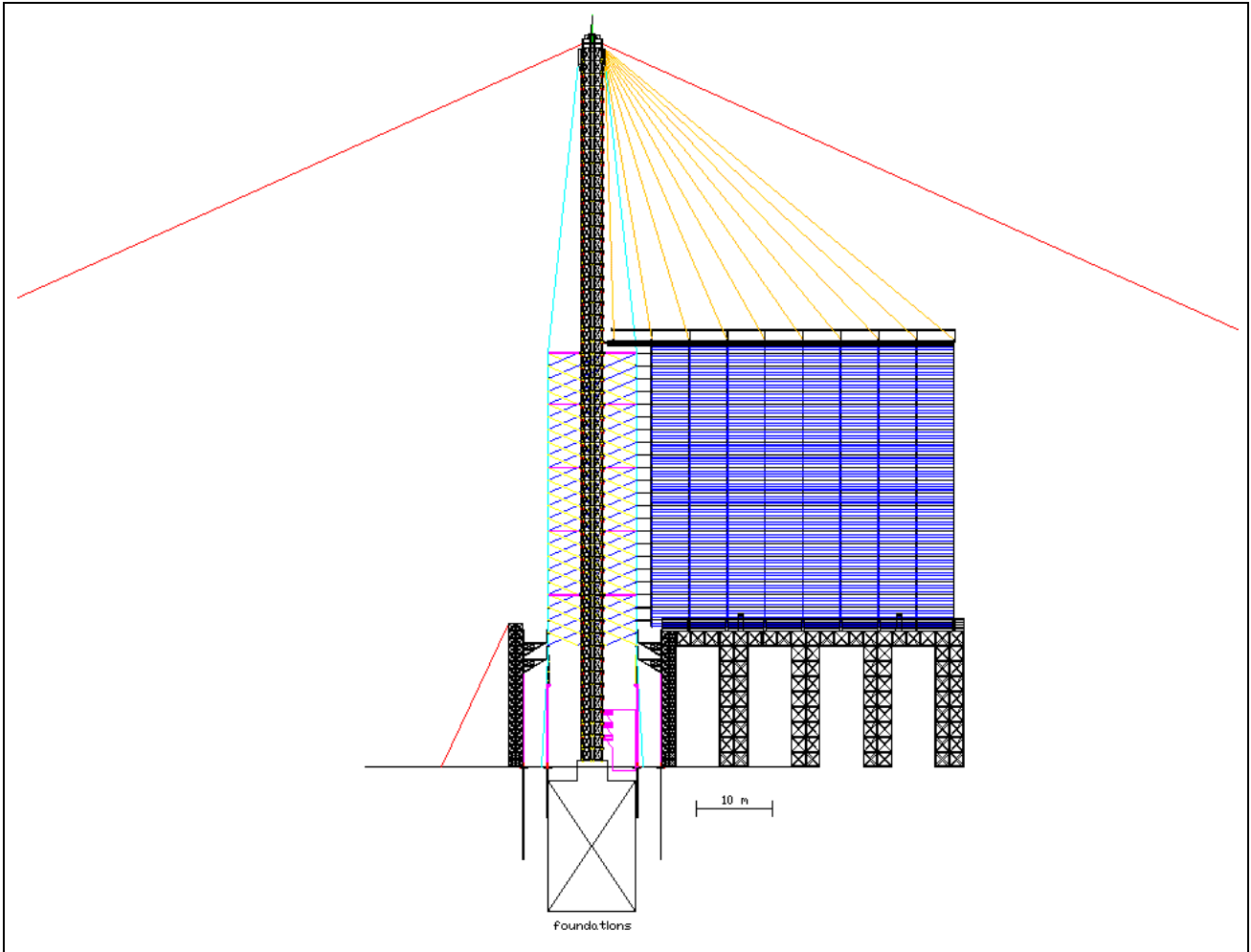


Figure A24 (from installation\_step\_17.dwg)

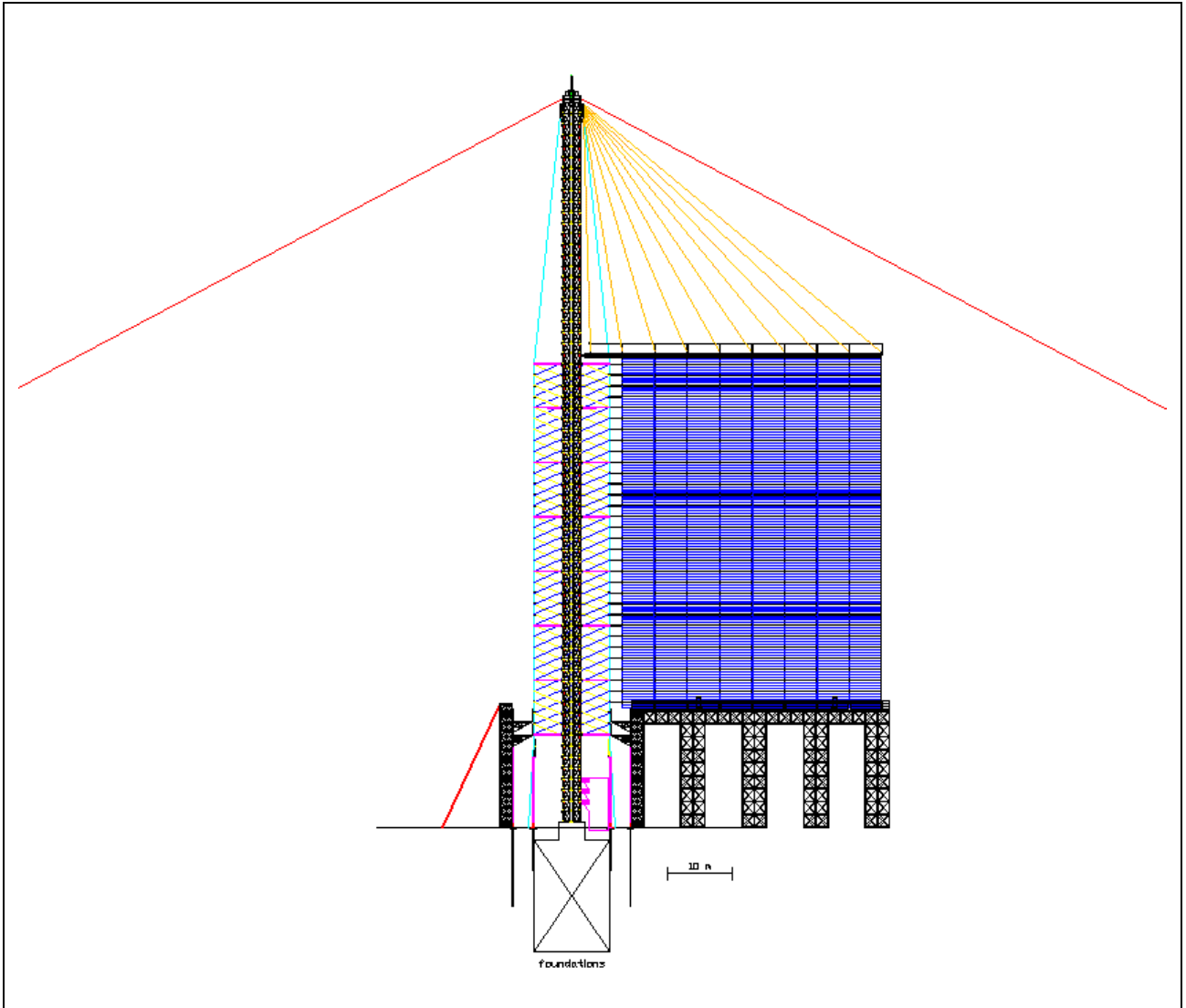


Figure A25 (from installation\_step\_18.dwg)

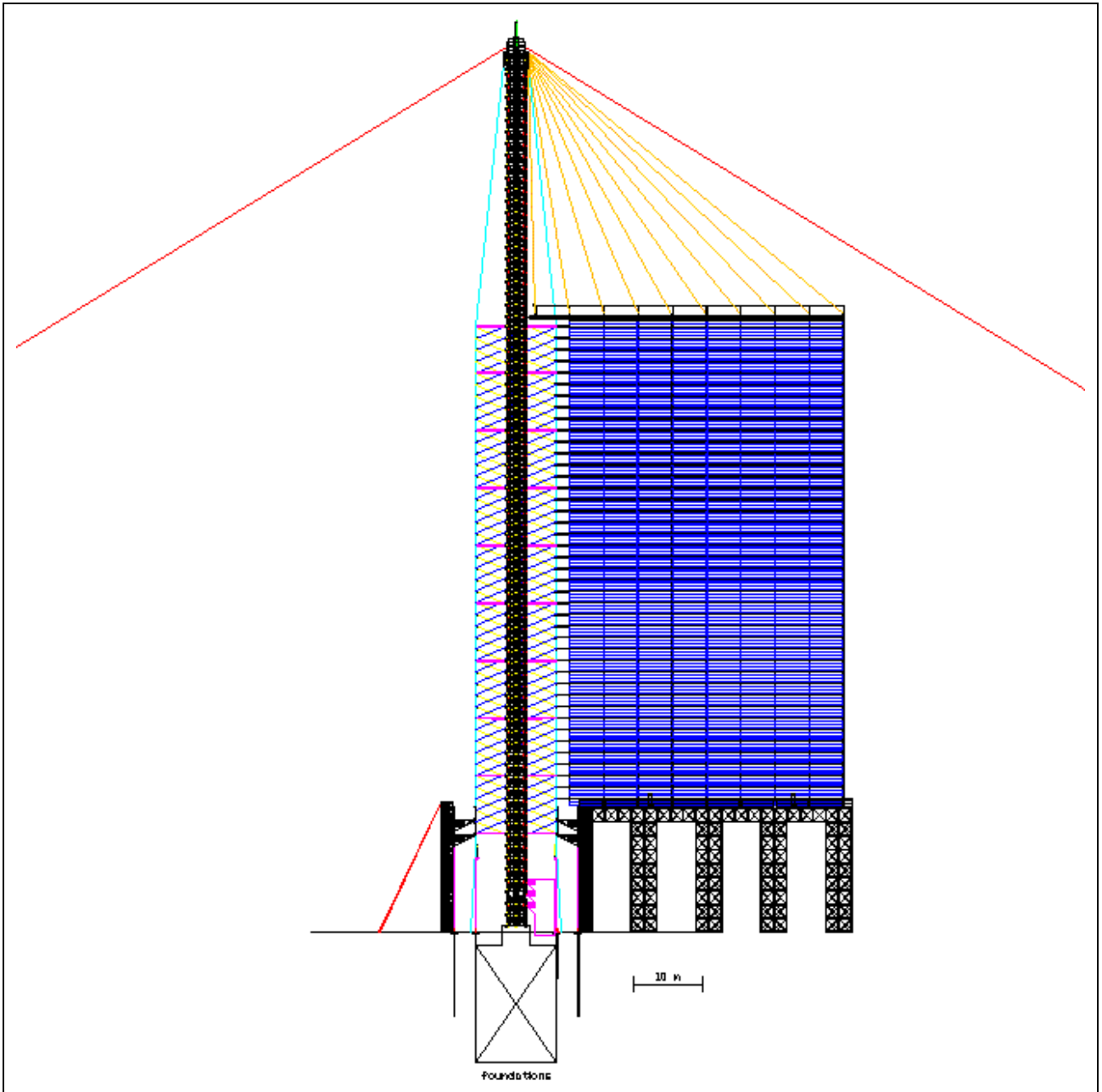


Figure A26 (from installation\_step\_19.dwg)

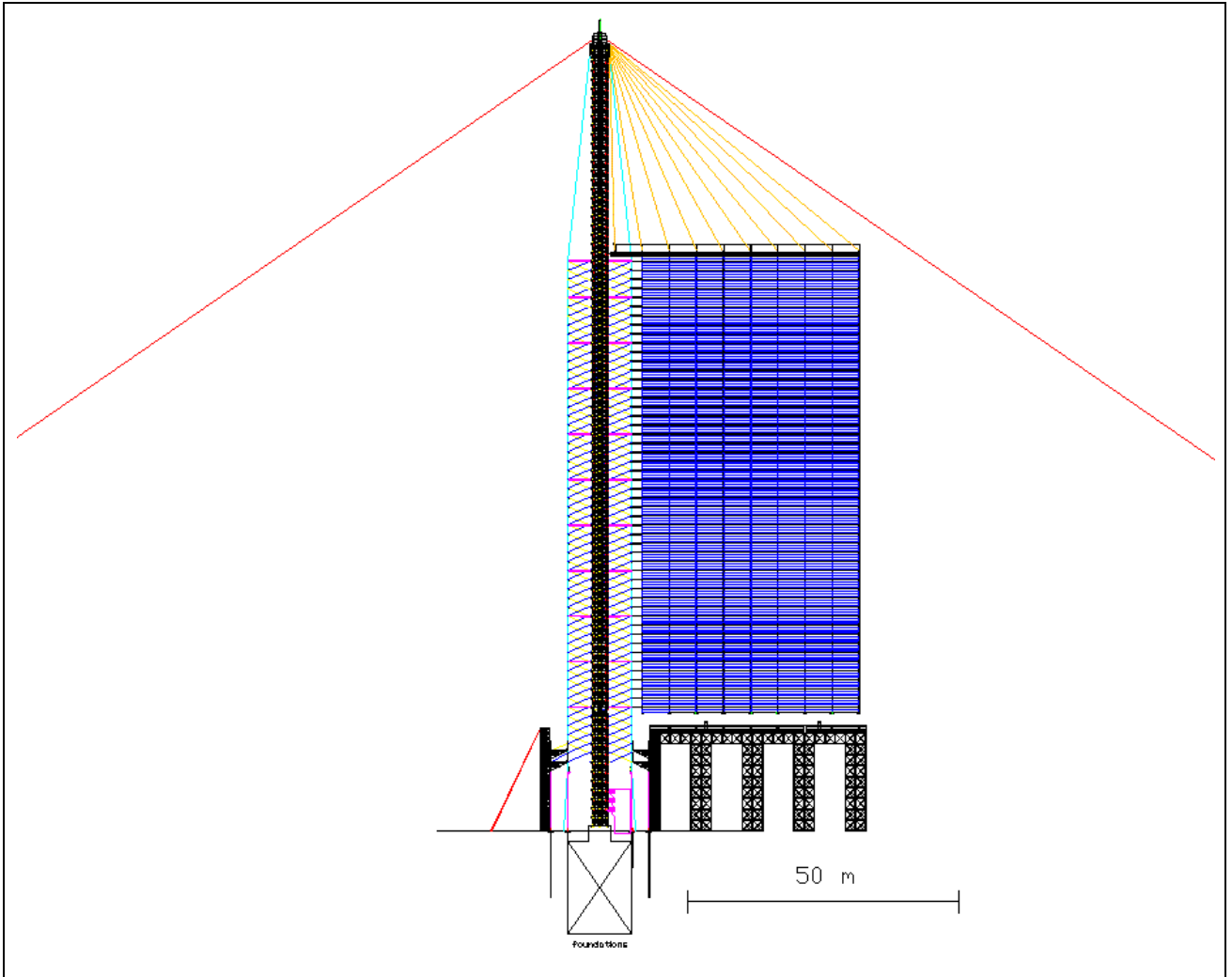


Figure A27 (from installation\_step\_20.dwg)



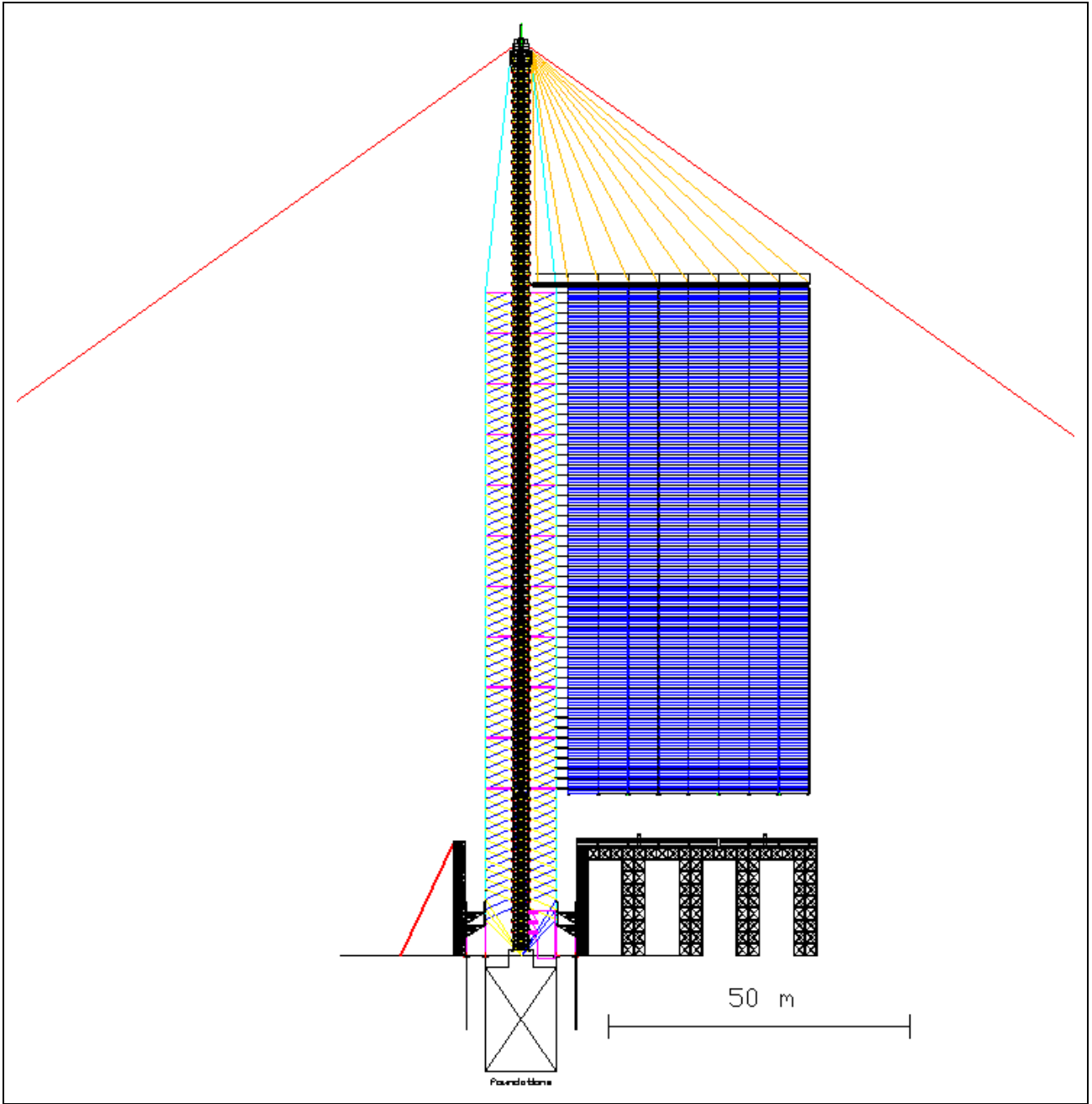


Figure A28 (from installation\_step\_21.dwg)

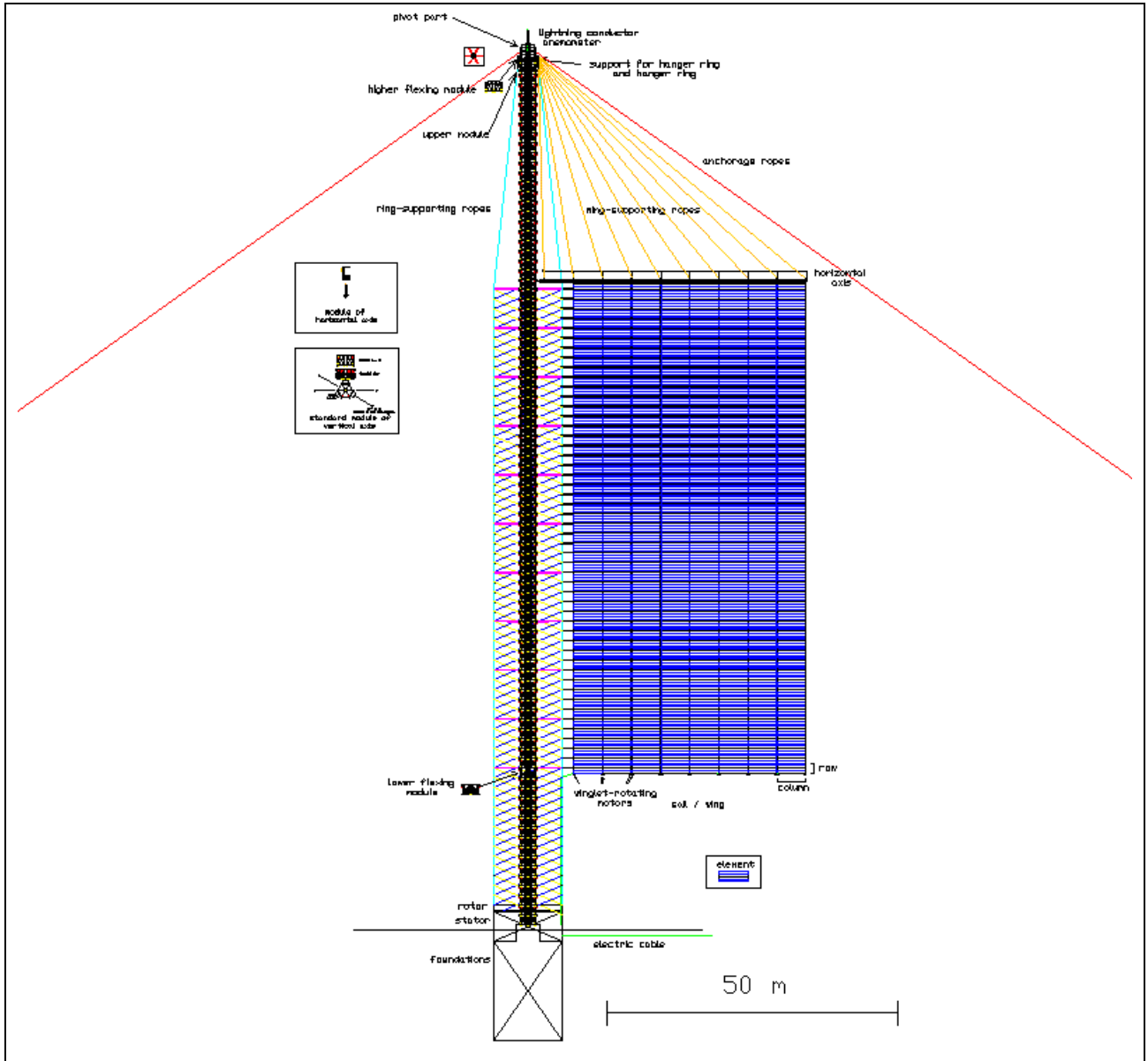


Figure A29 (from installation\_step\_22.dwg; the same of general\_scheme\_frontal\_section.dwg) - A

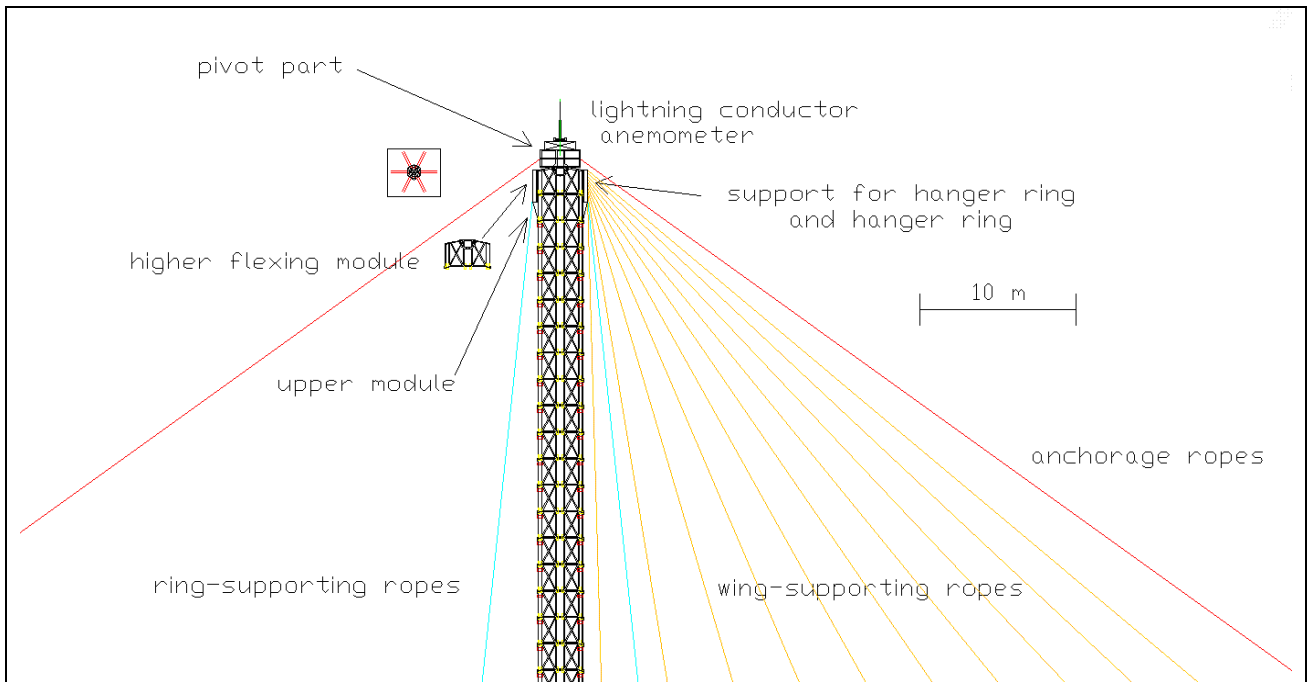


Figure A30 (from installation\_step\_22.dwg) - B

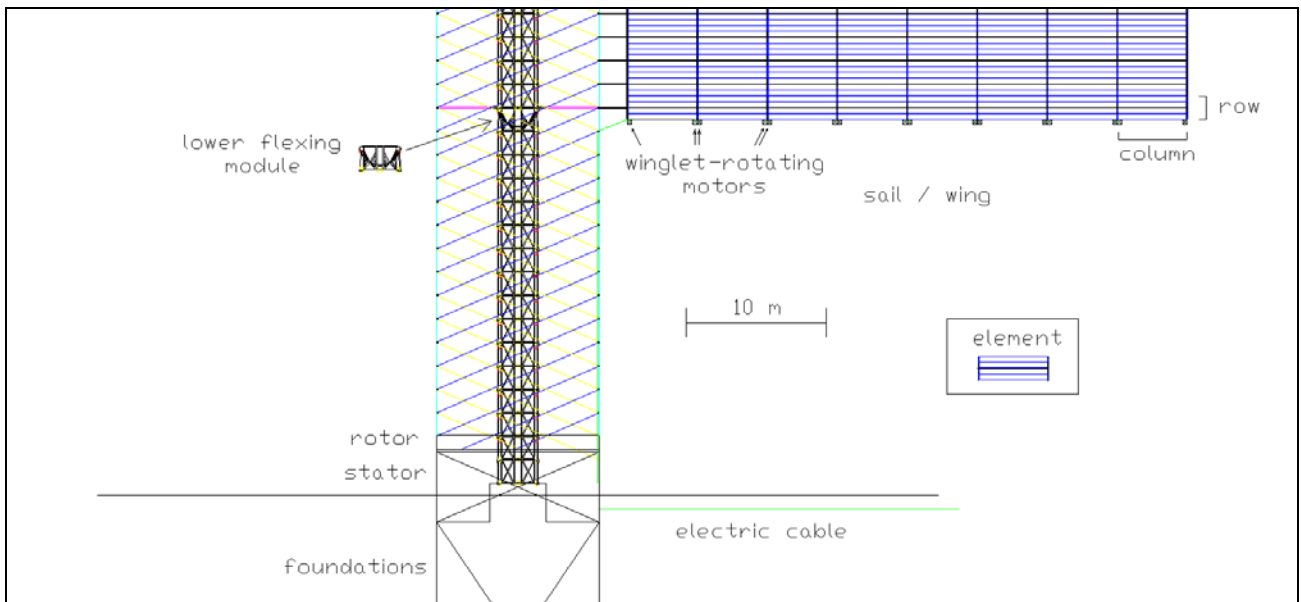


Figure A31 (from installation\_step\_22.dwg) - C

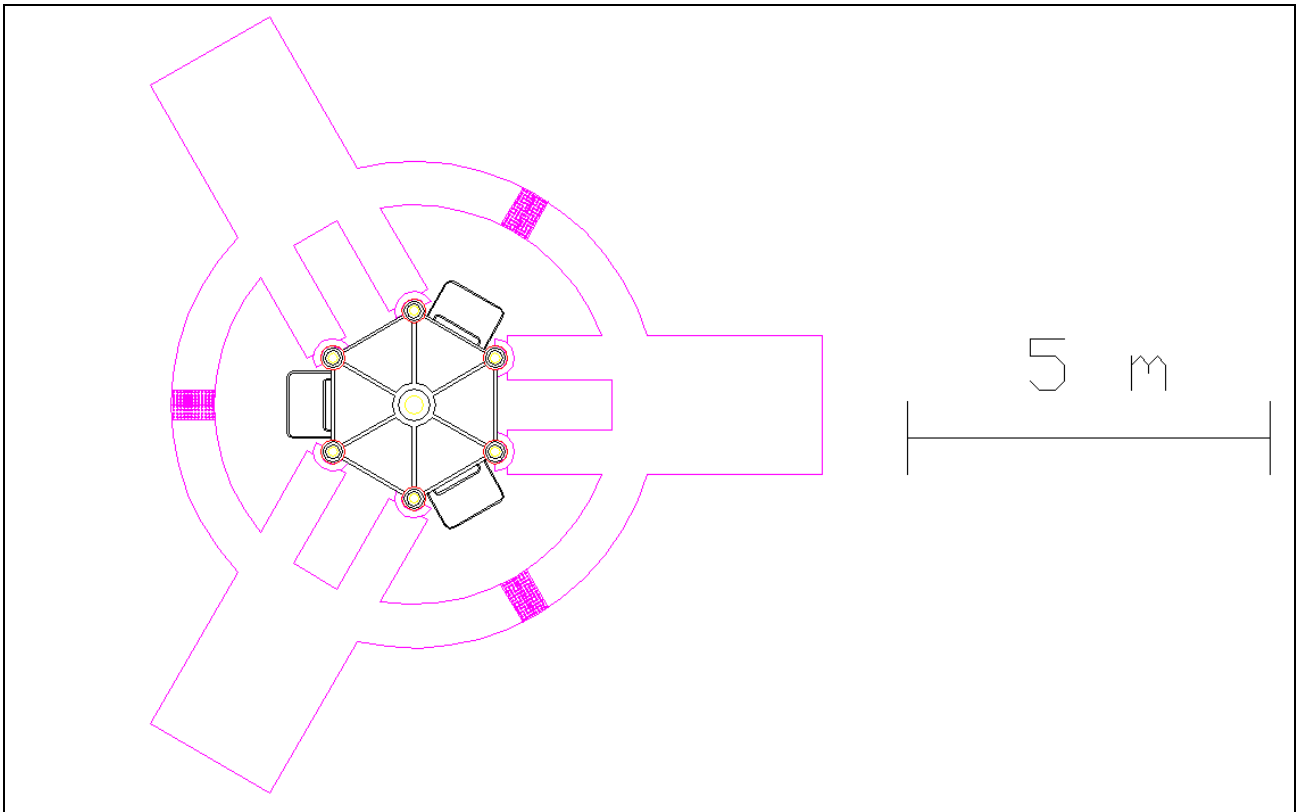


Figure A32 (from scaffoldings.dwg) – A: The three hydraulic hoists (seen from above)

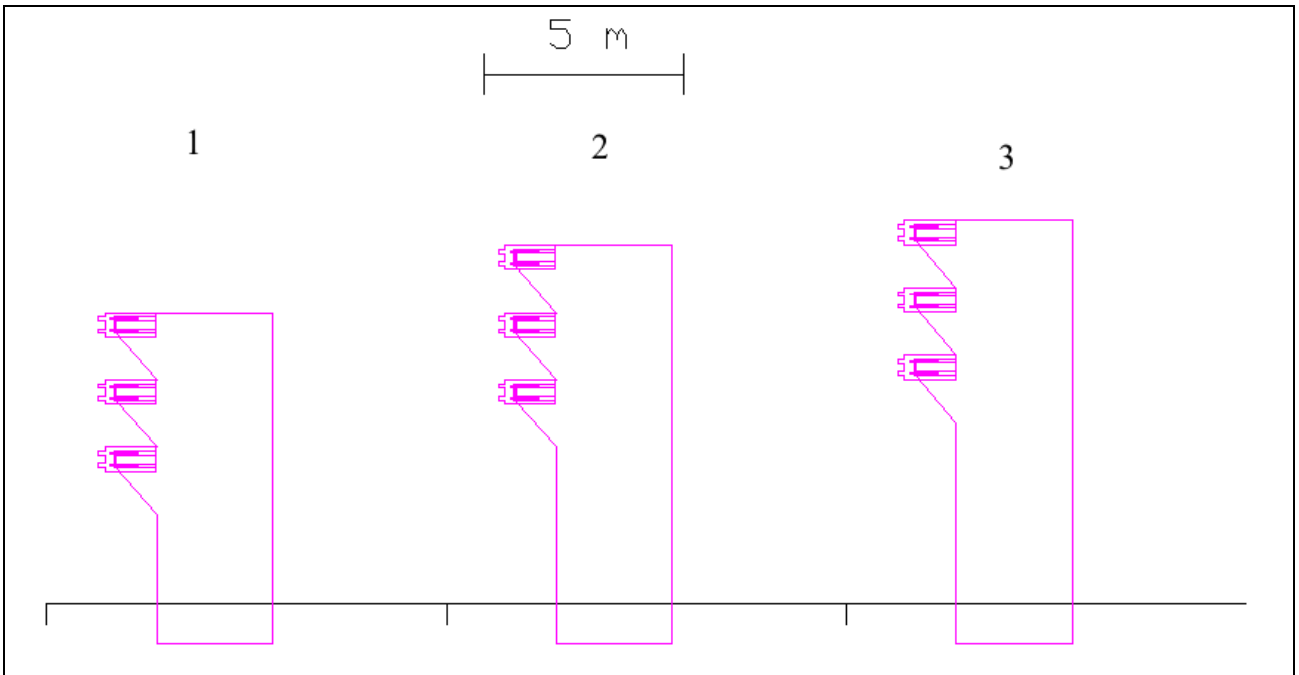


Figure A33 (from scaffoldings.dwg) – B: A hoist in the lower position (1), in the intermediate position (2), in the higher position (3)

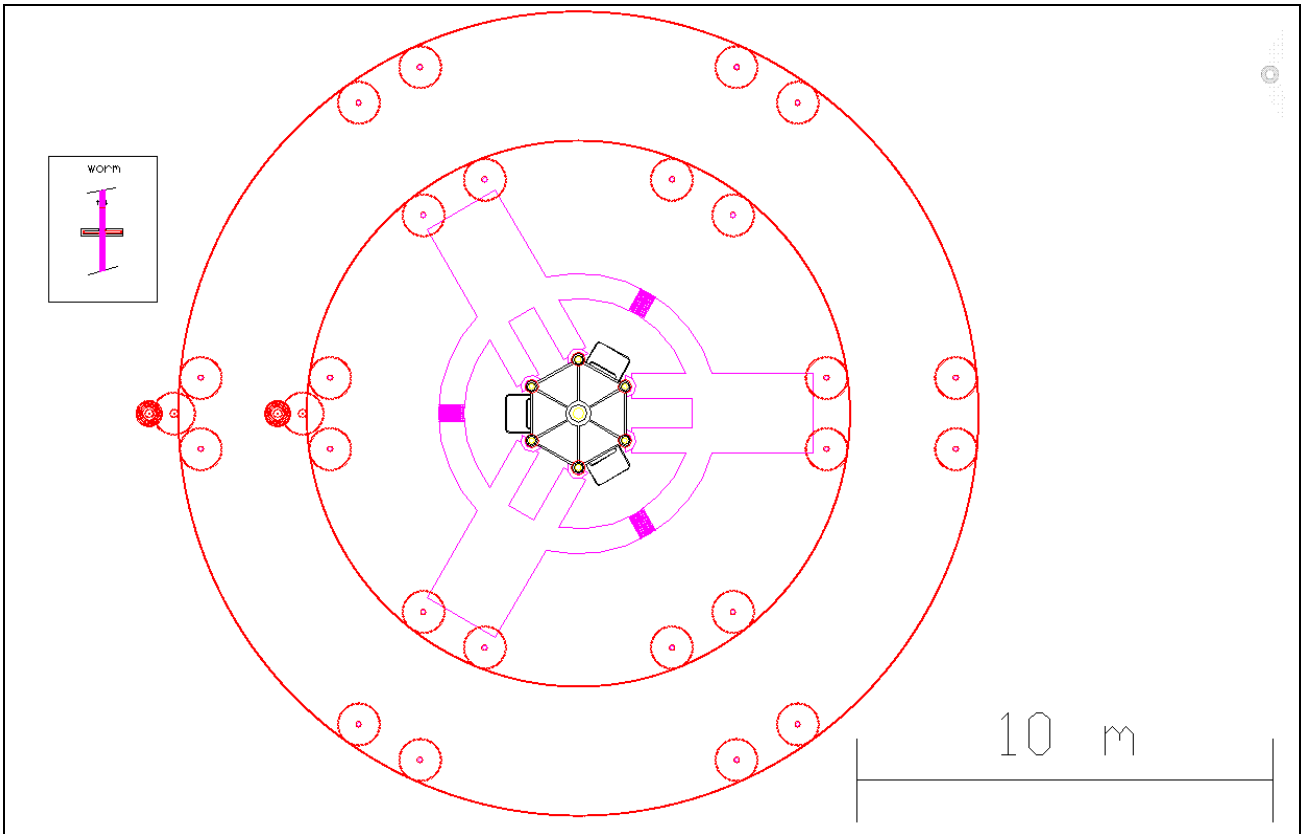


Figure A34 (from scaffoldings.dwg) – C

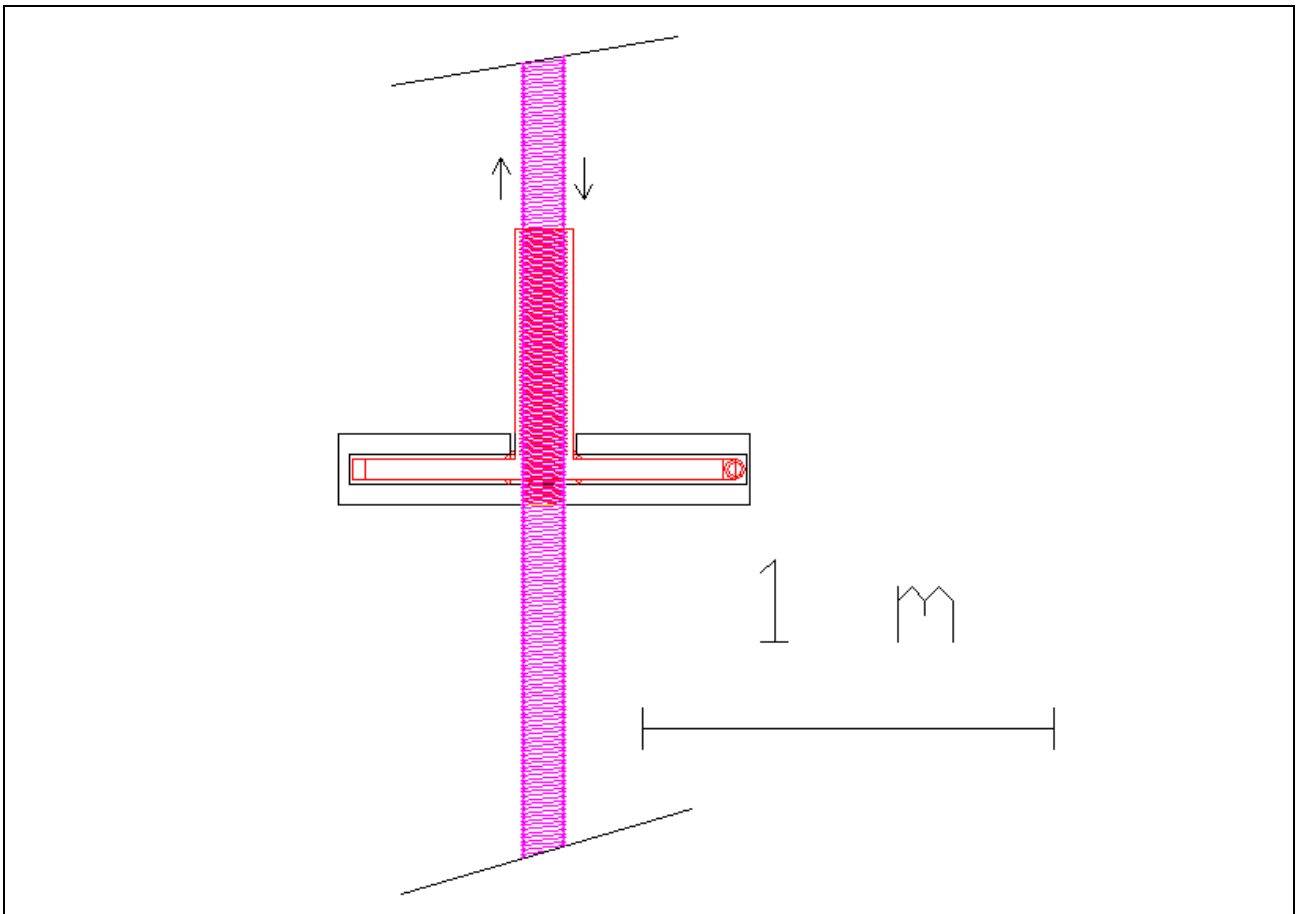


Figure A35 (from scaffoldings.dwg) – D

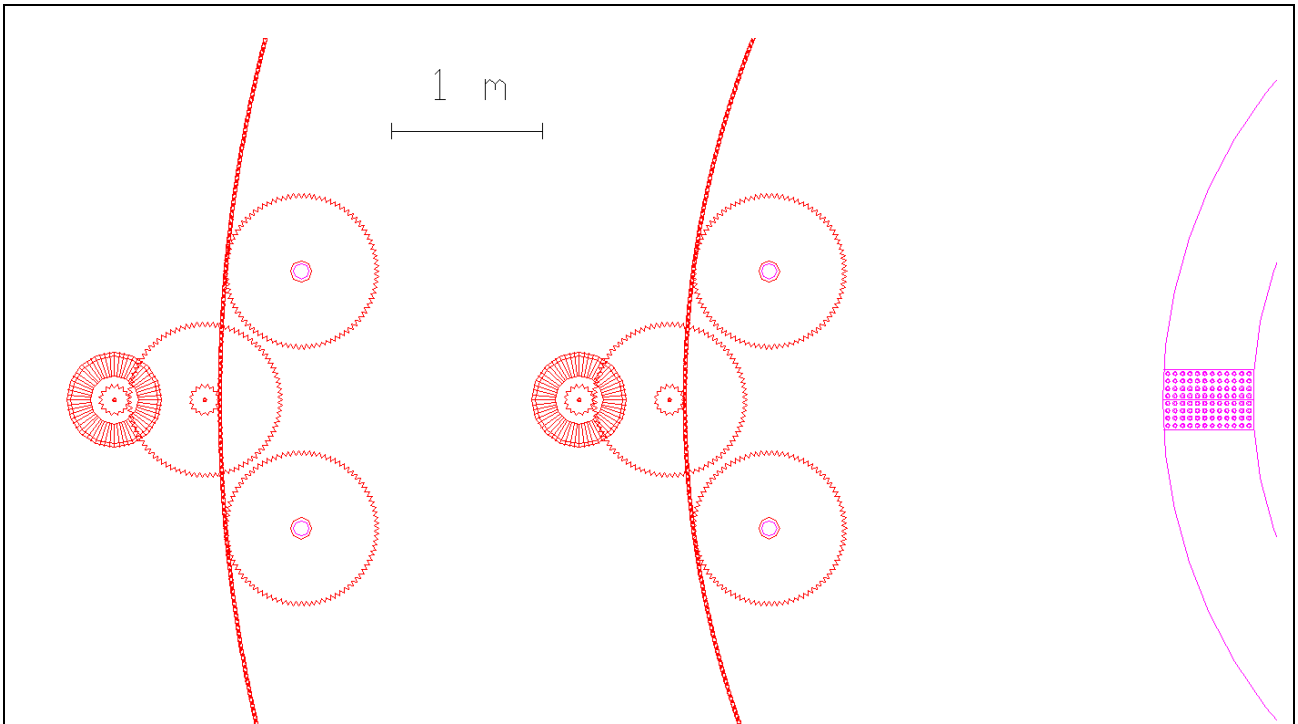


Figure A36 (from scaffoldings.dwg) - E

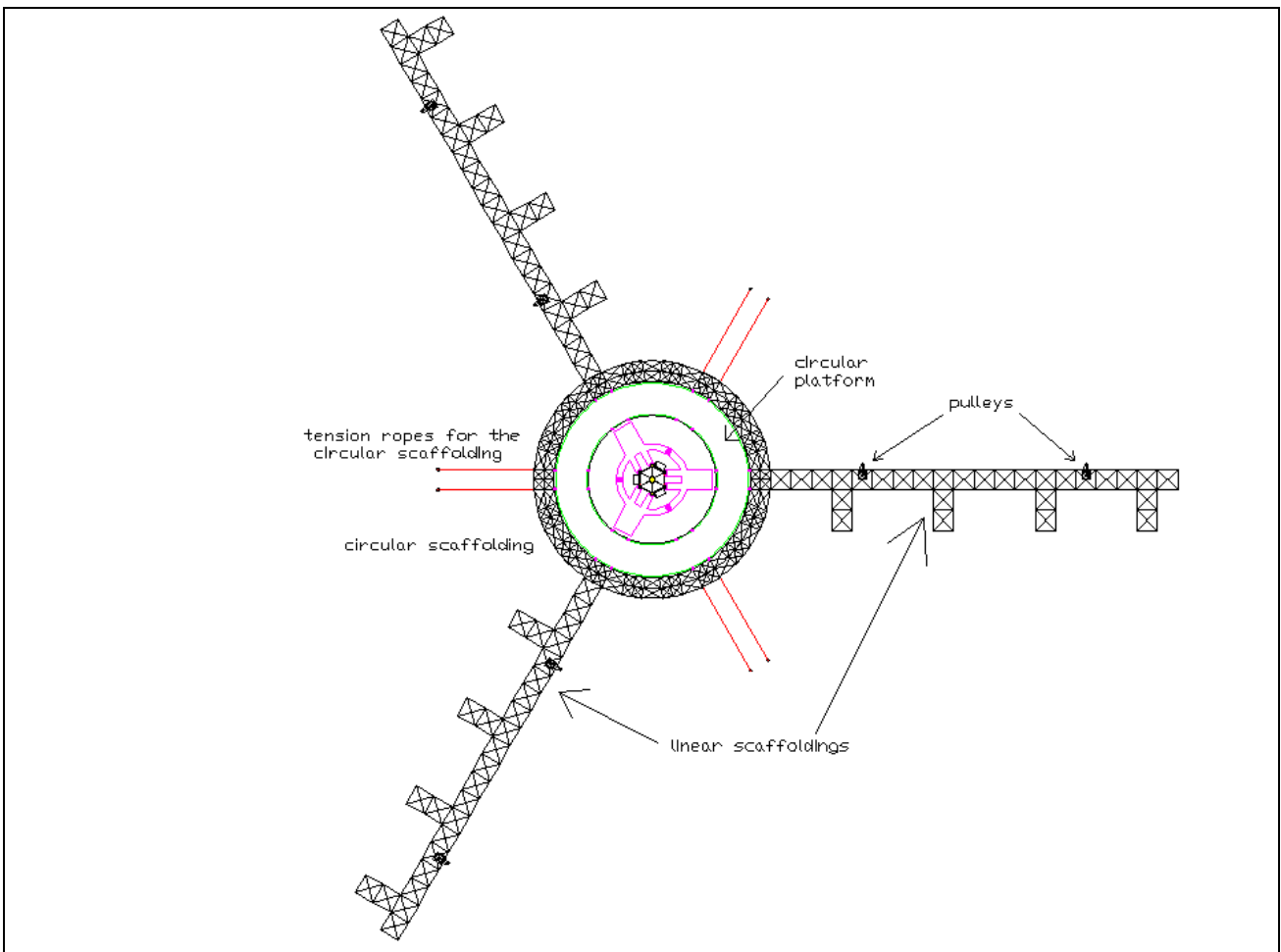


Figure A37 (from scaffoldings.dwg) – F

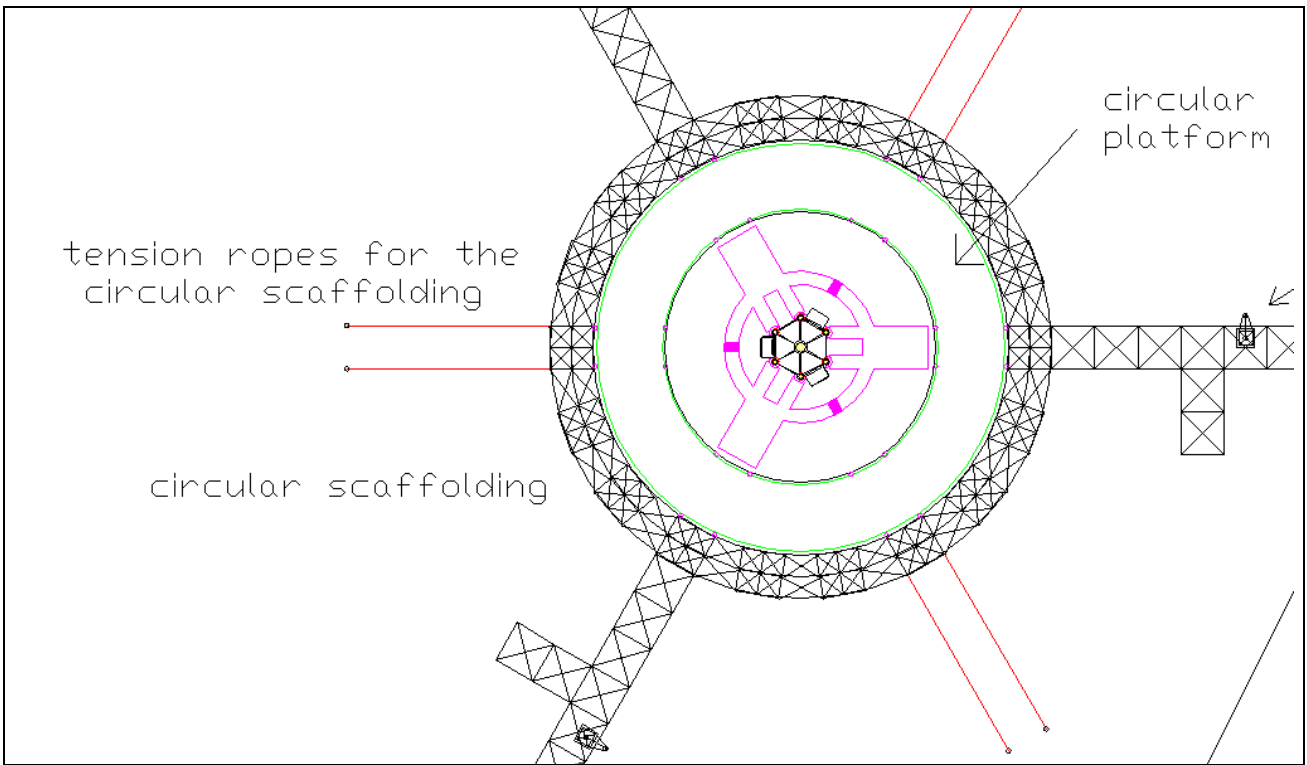


Figure A38 (from scaffoldings.dwg) – G

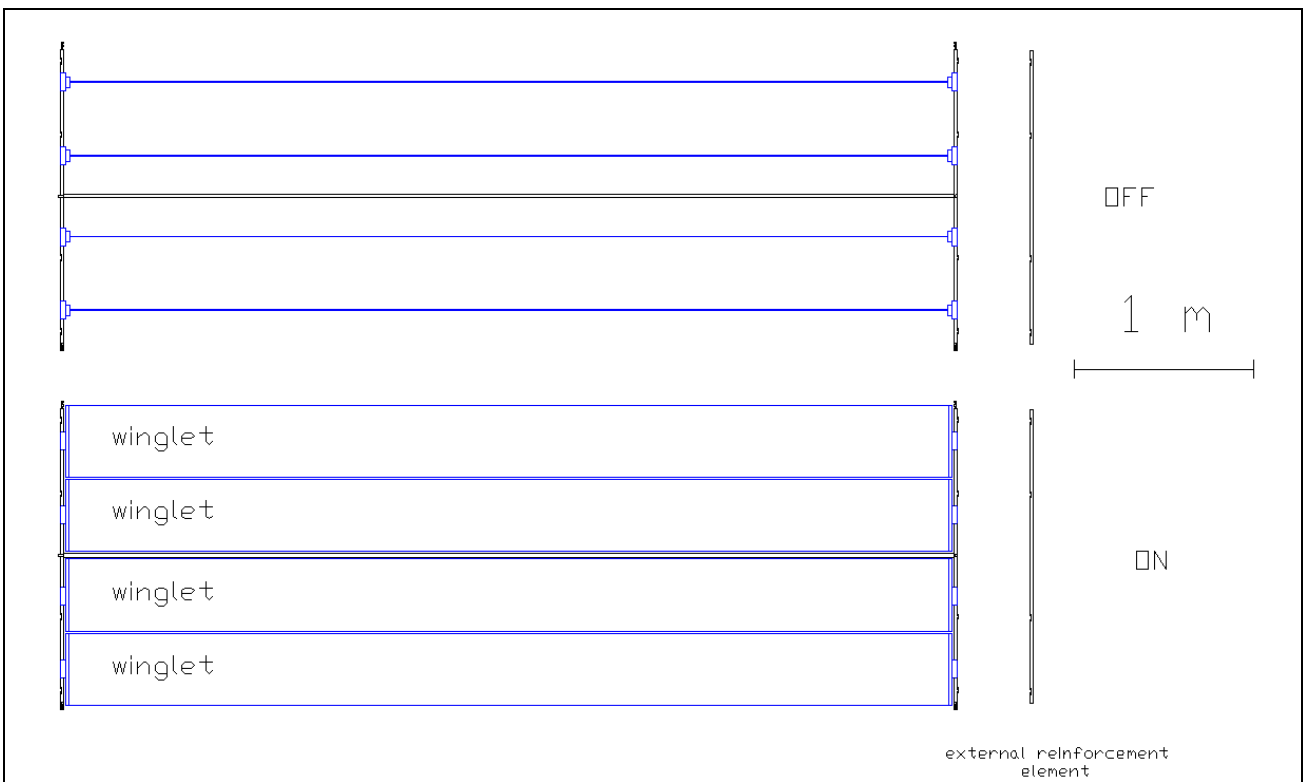
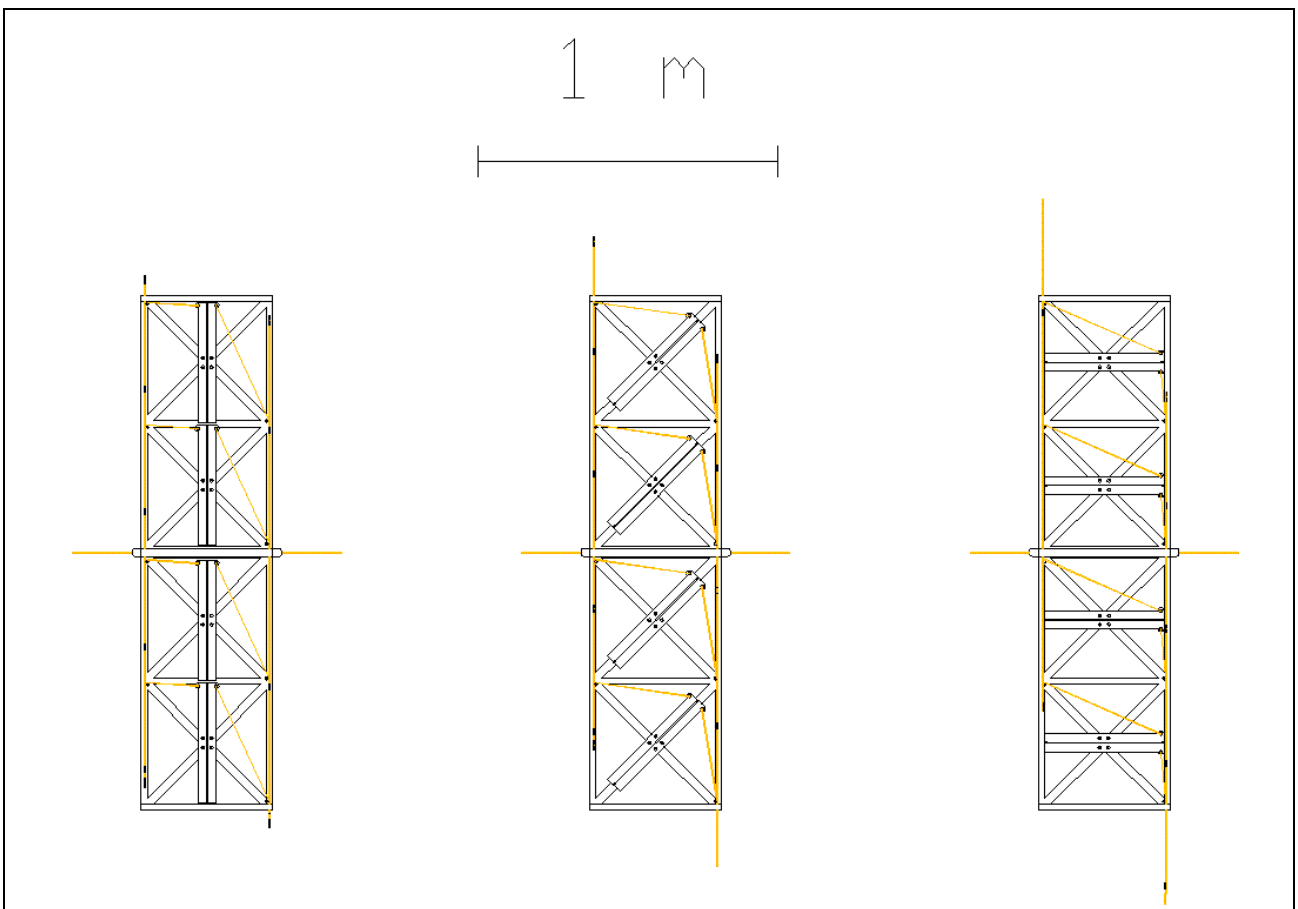
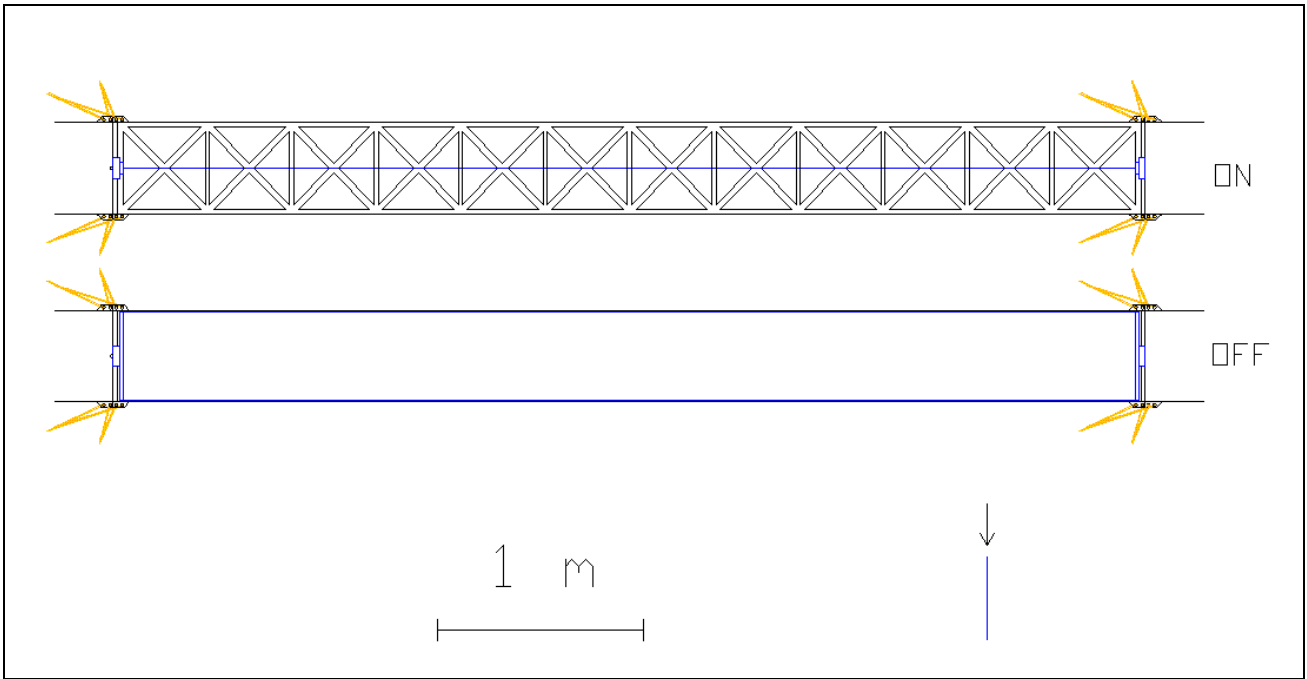


Figure A39 (from wing\_element.dwg) – A: A wing element, frontal view (ropes left out)





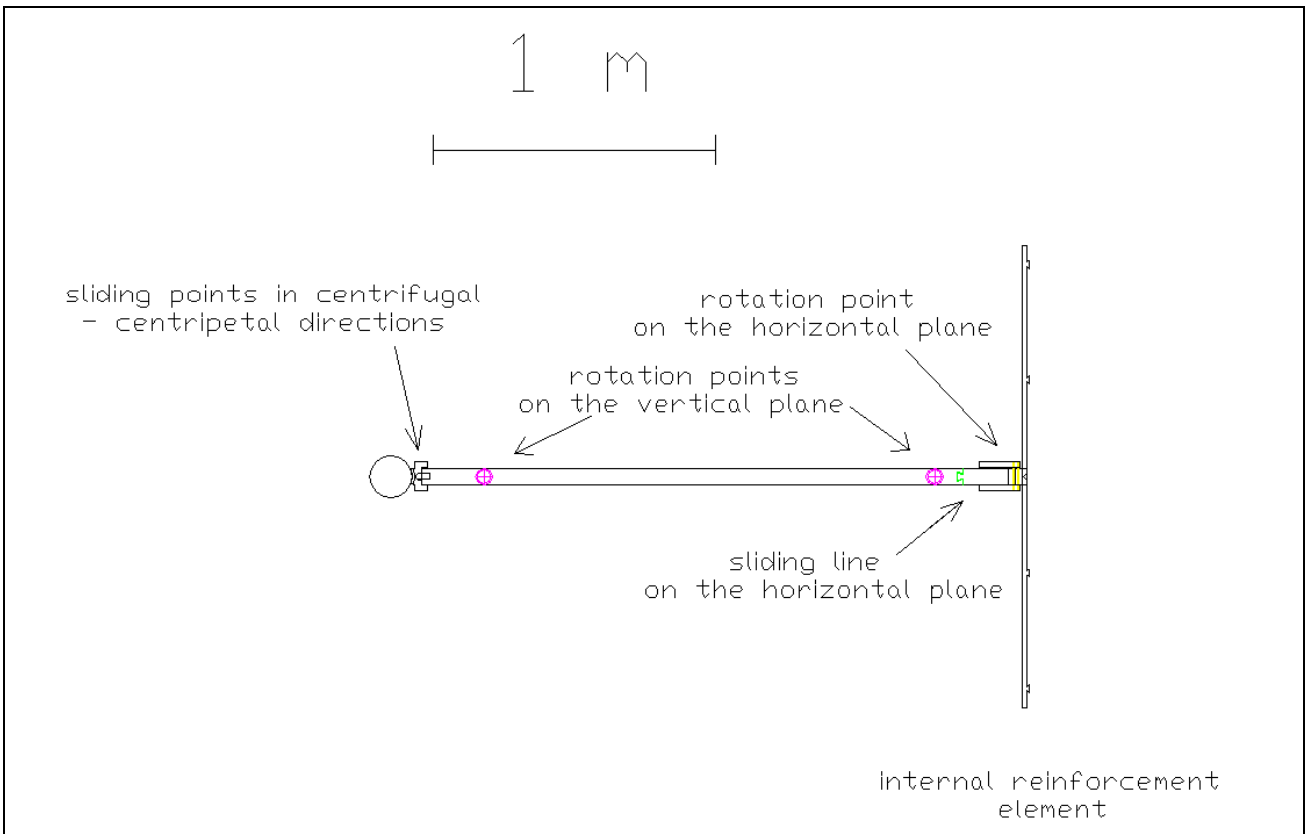


Figure A42 (from wing\_element.dwg) - D

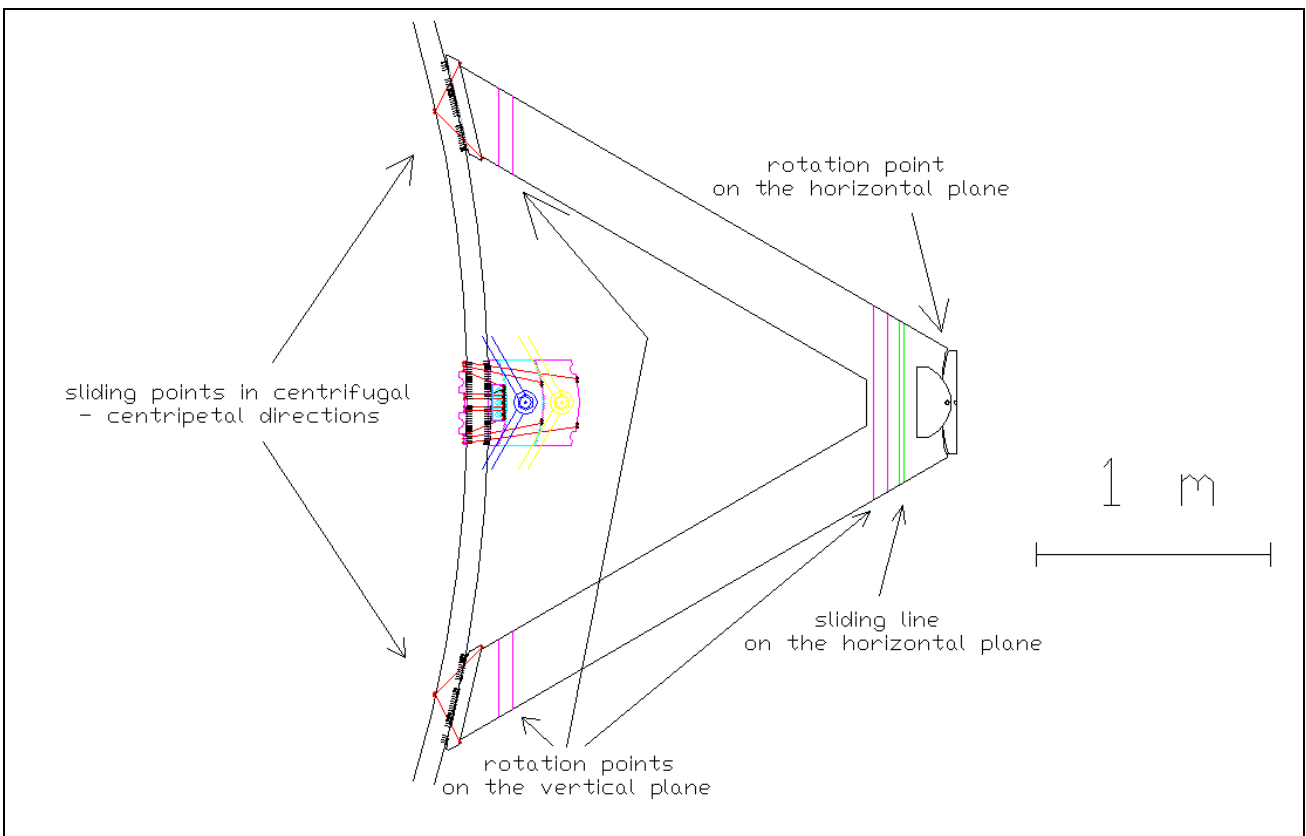


Figure A43 (from wing\_element.dwg) - E

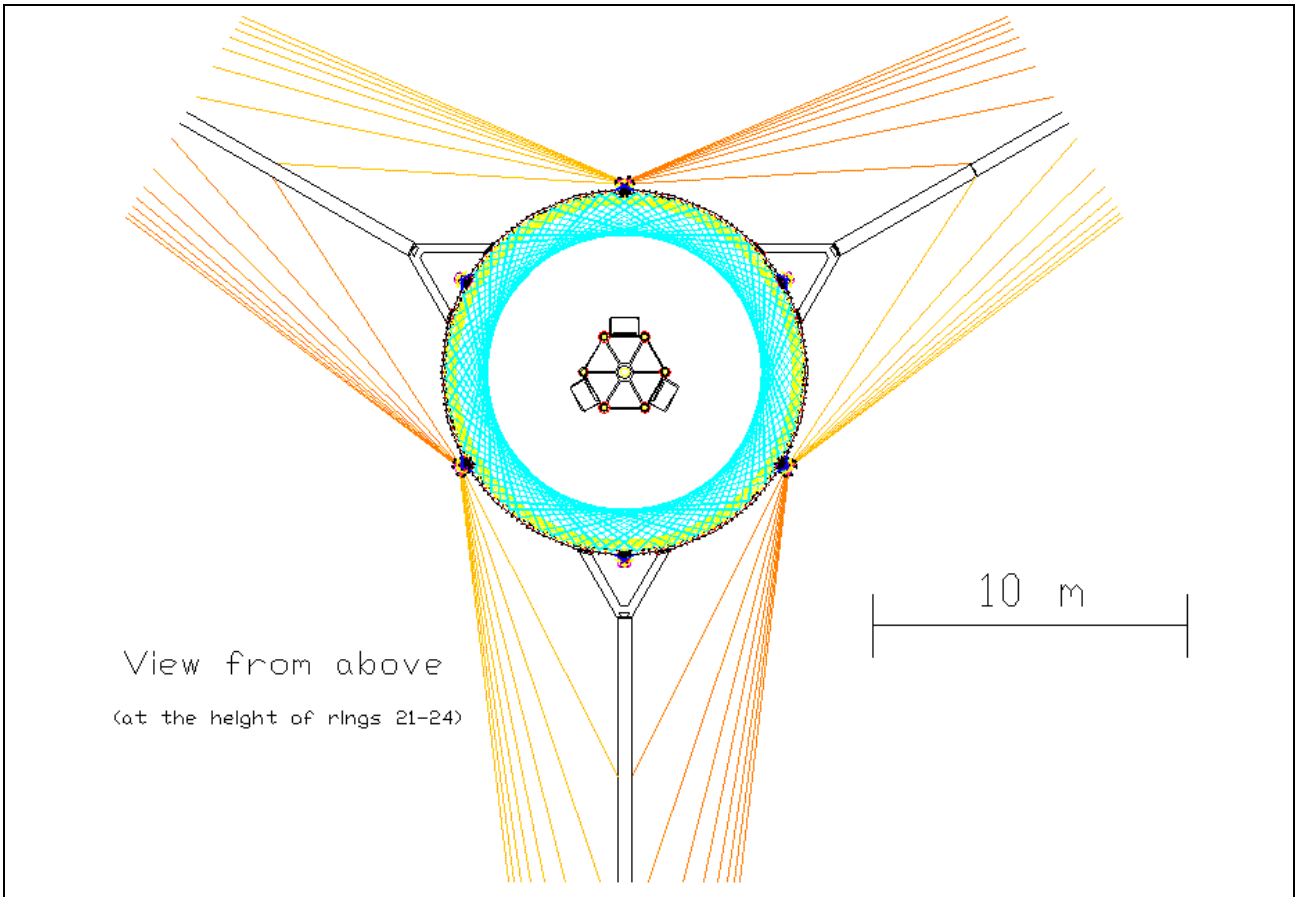


Figure A44 (from ring.dwg) - A

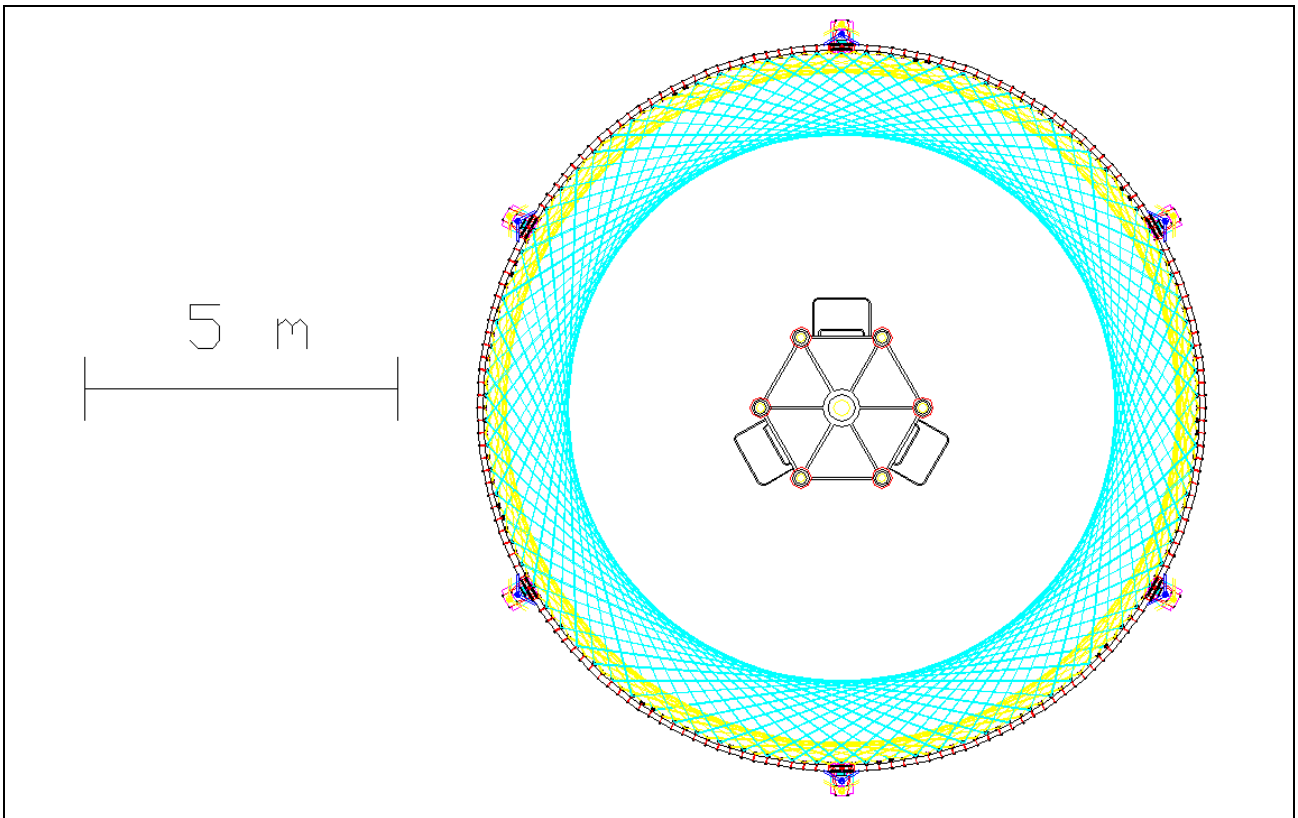


Figure A45 (from ring.dwg) – B: View of a ring, from above (at the height of rings 51-63)

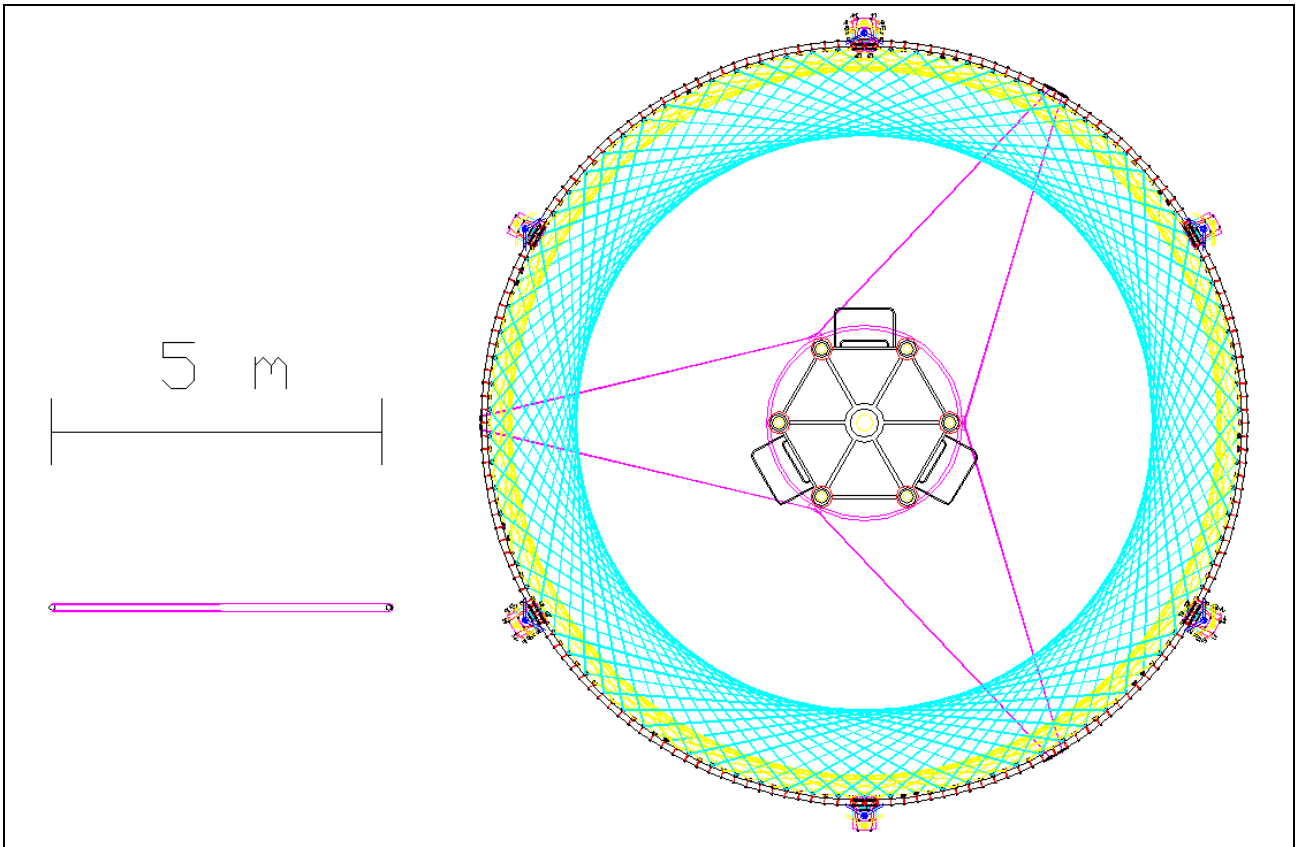


Figura A46 (from ring.dwg) – C: An anti-oscillation system

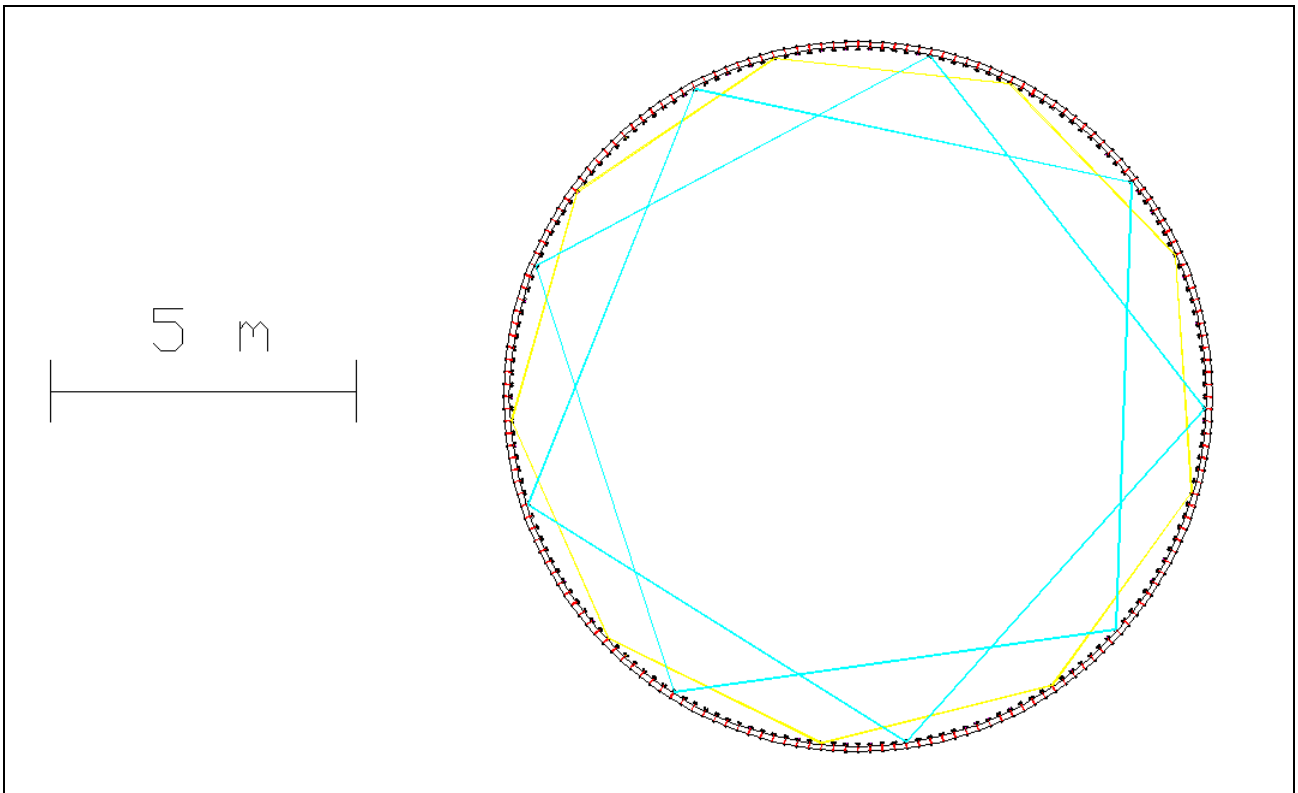


Figure A47 (from ring.dwg) – D: Scheme of a single cyan transverse rope and of a single yellow transverse rope

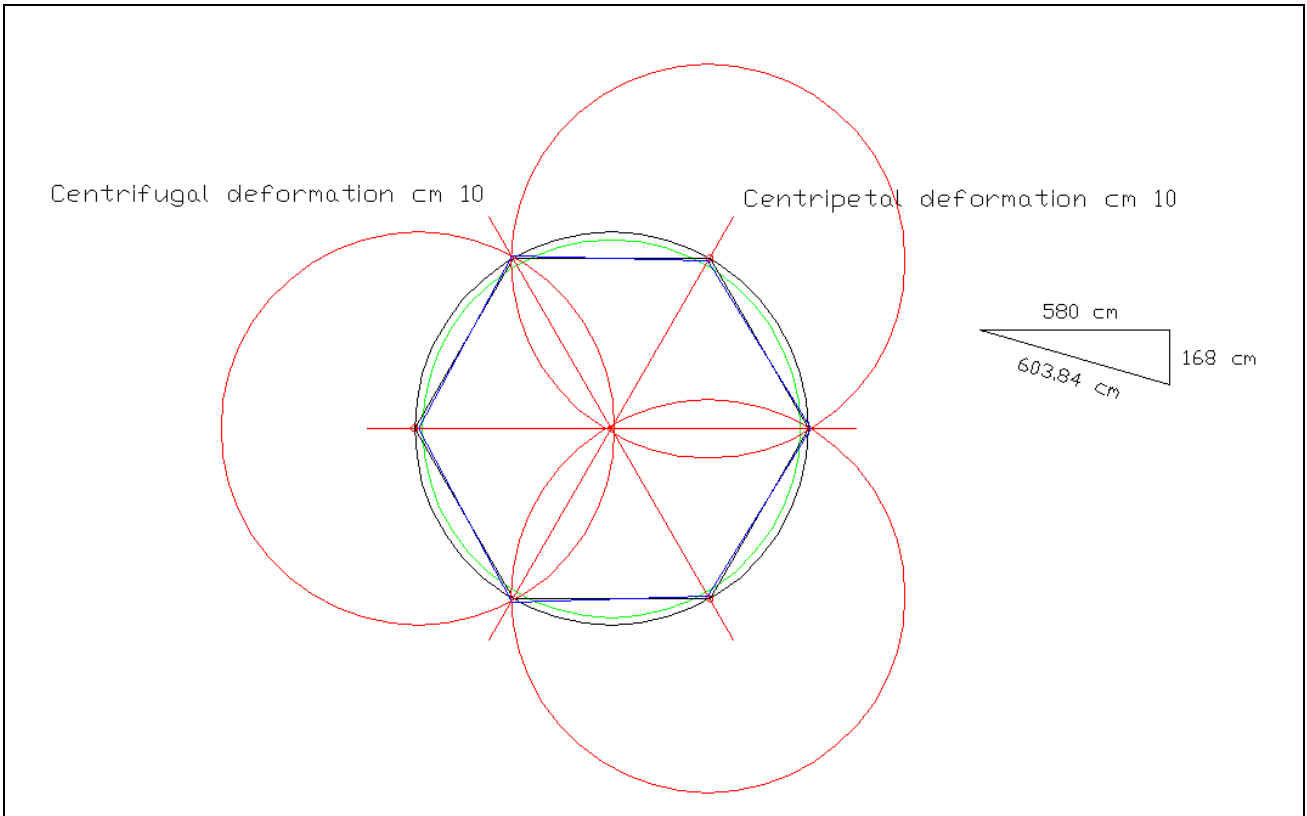


Figure A48 (from ring.dwg) – E: Deformations of a ring on the horizontal plane

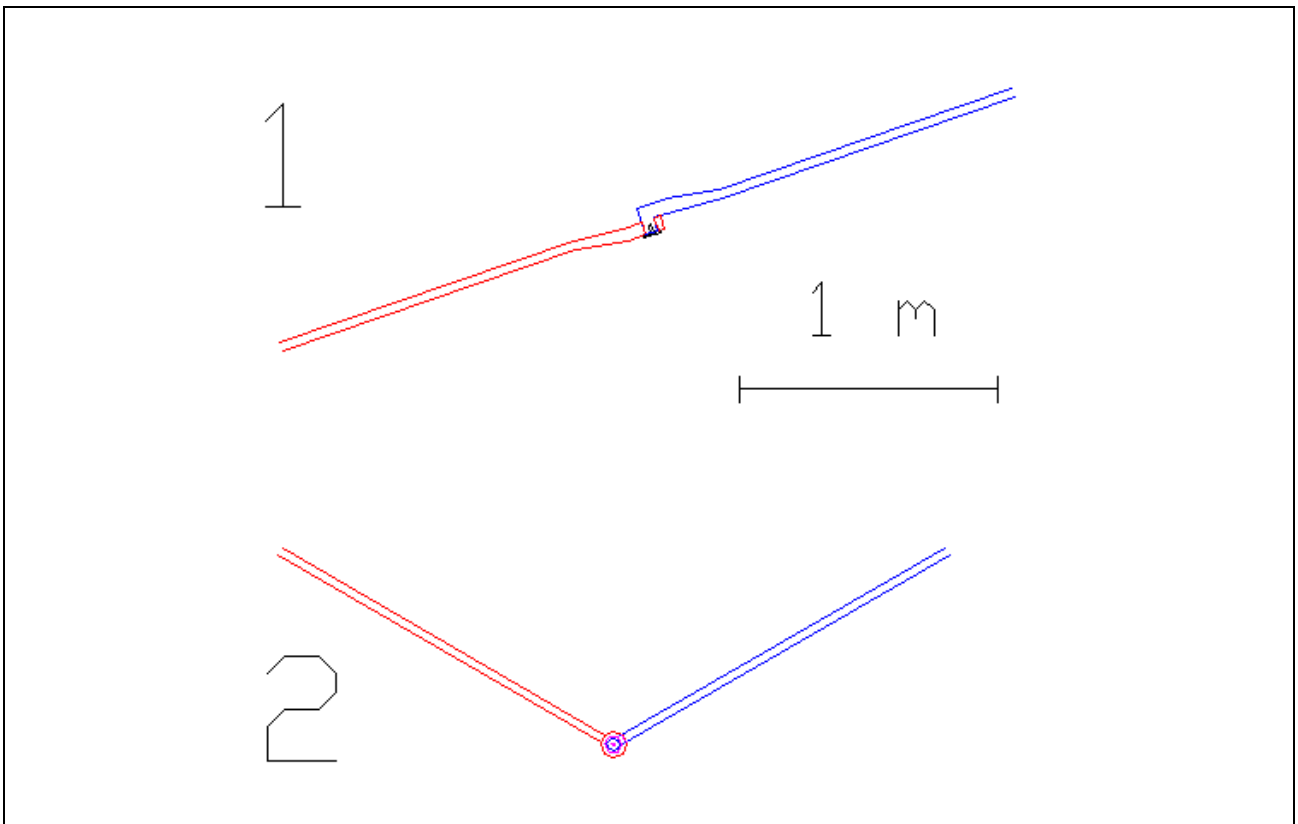


Figure A49 (from ring.dwg) – F: Details of the system of transmission of the rotary force (blue and yellow systems), frontal view (1), view from above (2)

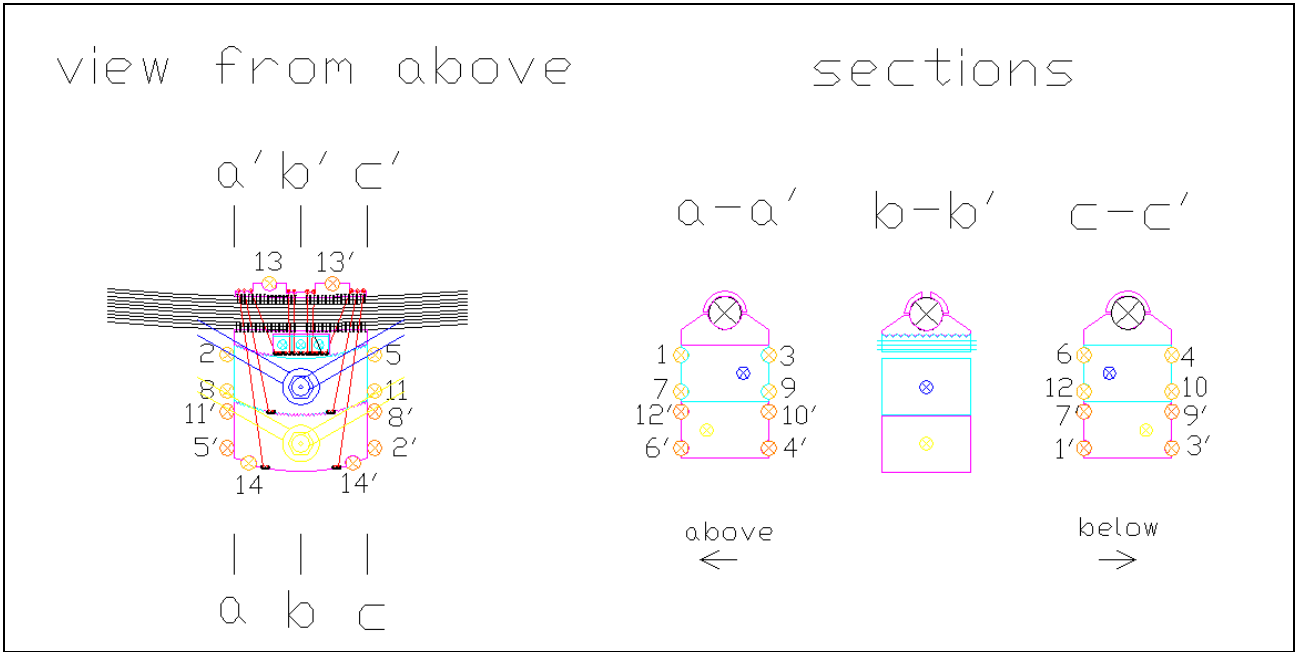


Figure A50 (from ring.dwg) – G: Details of main anchorages (with wing-ring ropes anchorage; views in projection and not in section)

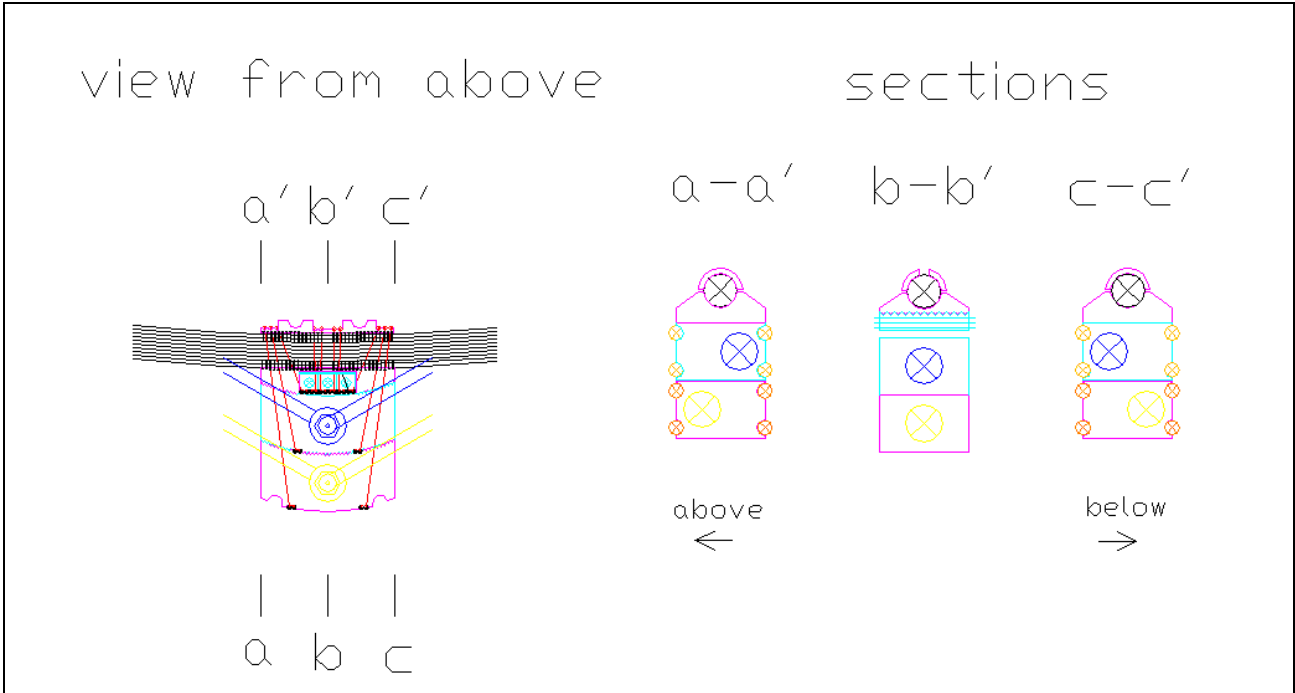


Figure A51 (from ring.dwg) – H: Details of main anchorages (without wing-ring ropes anchorage; views in projection and not in section)

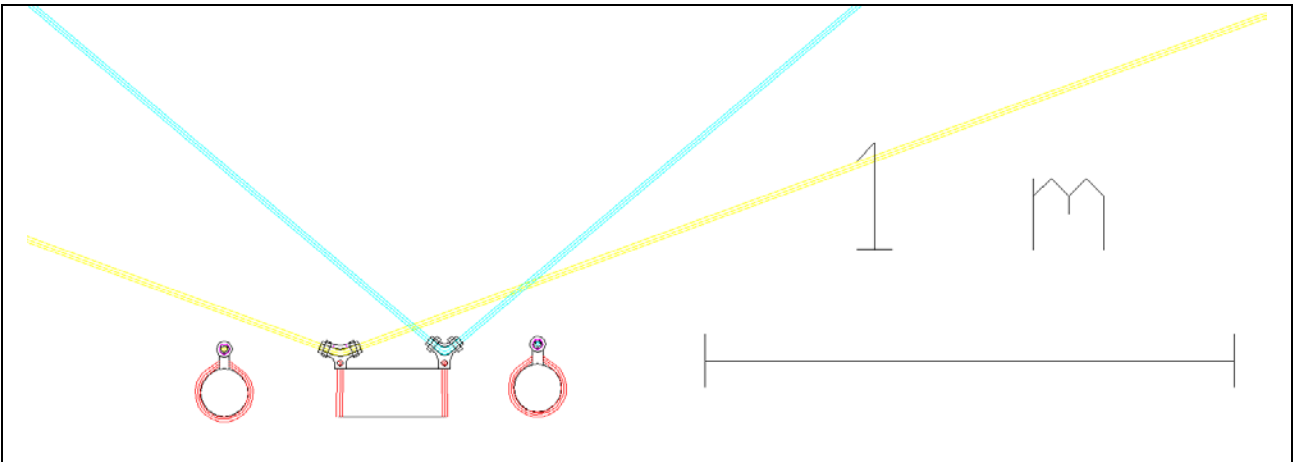


Figure A52 (from ring.dwg) – I: Details of the anchorage for yellow and cyan ring transverse ropes

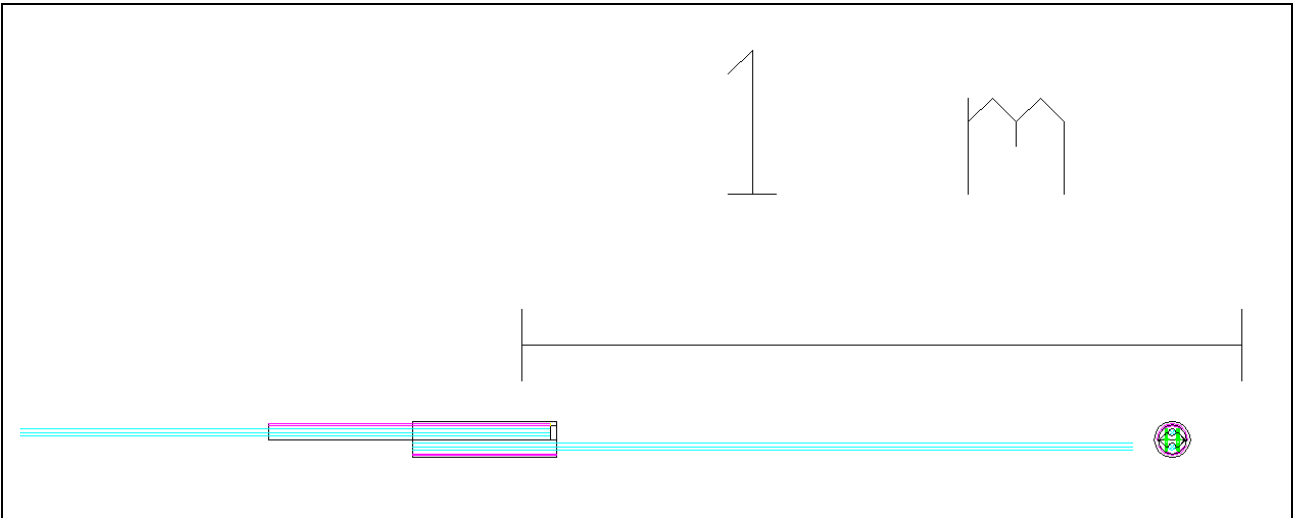


Figure A53 (from ring.dwg) – J: Details of rope-stretching junction

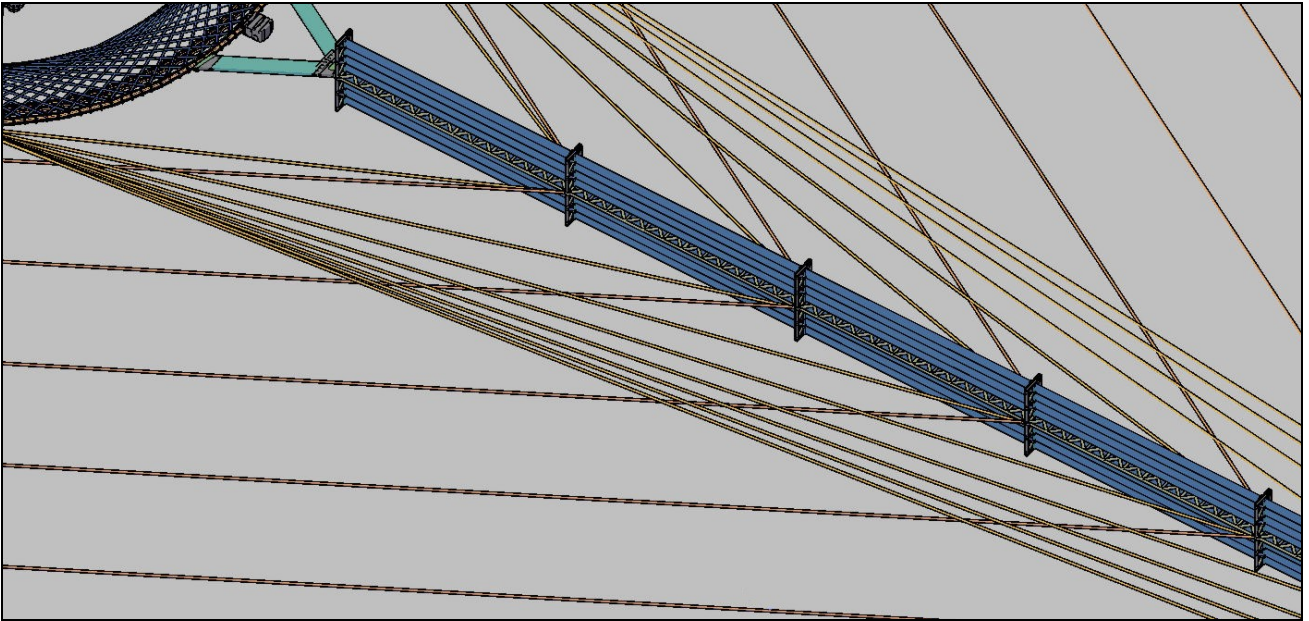


Figure A54 – A 3D (partial) image of a row and its ropes

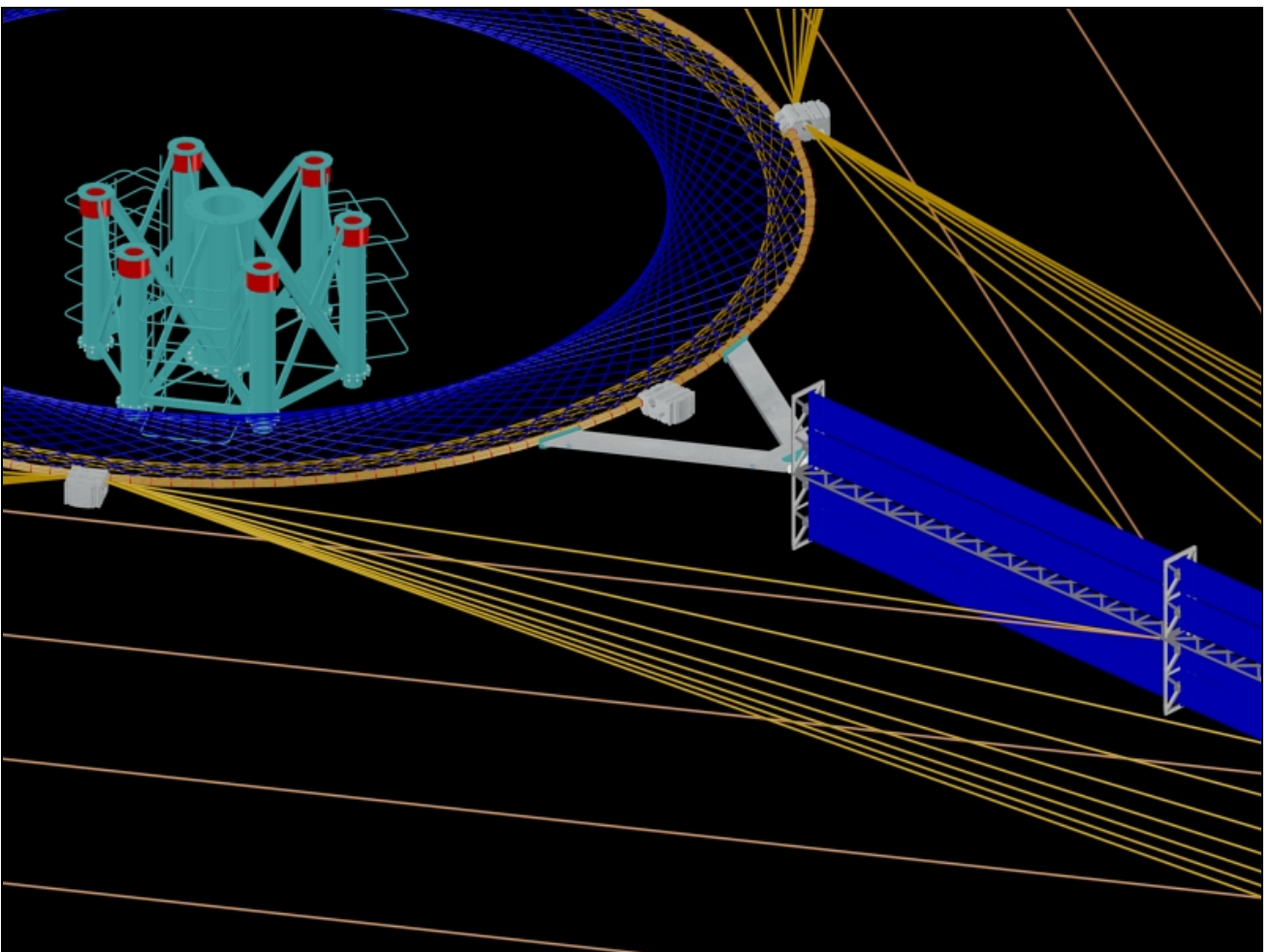


Figure A55 – A 3D (partial) image of a row, a ring and an element of the vertical axis

## Section 2 – Technical calculations

(from the file technical\_calculations.xls, available at [www.r-site.org/VertEolo](http://www.r-site.org/VertEolo))

### (1) Characteristics of the ropes used in the draft project

These rope types are not necessarily the best solution, but they have been useful to elaborate the draft project

#### Viper 78 ropes

[http://www.armare.it/media/43\\_1\\_extra2.pdf](http://www.armare.it/media/43_1_extra2.pdf)

Diameter (mm)	Breaking load (T)	Weight (kg/m)
4	-	-
6	1.9	27
8	4.48	50
10	6.7	71
12	9.74	99
14	12.21	137
16	16.69	178
18	20.16	211
20	24.8	247
22	28	297
24	33.6	350
26	37.2	397
28	42	465
30	46	545

#### Dyneforce 78 ropes

[http://www.armare.it/media/43\\_1\\_extra2.pdf](http://www.armare.it/media/43_1_extra2.pdf)

Diameter (mm)	Breaking load (T)	Weight (kg/m)
4	1.90	8
5	3.14	14
8	8.00	35
10	12.21	55
12	16.69	76
14	20.16	105
16	24.80	130
18	28.00	157
20	33.60	191
22	37.20	228
24	-	-
26	-	-
28	-	-
30	-	-



**Galvanized steel wire ropes W.S. 6 x 36 + IWRC WS**

<http://www.eurosupply.it/download/steelwire.pdf>

Diameter (mm)	Breaking load (T)	Weight (kg/m)
-	-	-
-	-	-
-	-	-
10	7.12	0.418
12	10.26	0.602
14	14.0	0.82
16	18.3	1.07
18	23.1	1.35
20	28.5	1.67
22	34.5	2.02
24	41.0	2.41
26	48.1	2.83
28	55.9	3.28
30	64.2	3.76

**(2) Approximate dimensions and weight of a ring**

Specific weight of synthetic fiber ropes (W.fiber) =	1.1	kg/dm <sup>3</sup>
Specific weight of steel ropes (W.steel) =	7.9	kg/dm <sup>3</sup>

		Size 1	Size 2	Size 3	Size 4
Radius of the external perimeter	A (dm)	58.00	<b>58.00</b>	58.00	58.00
Radius of the section of the ring	B (dm)	0.3	<b>0.45</b>	0.6	0.75
Mean Perimeter = $2 * (A-B) * \pi$	P.ring (dm)	362.54	<b>361.60</b>	360.65	359.71

		Size 1	Size 2	Size 3	Size 4	
Section of the ring	Radius =	(dm)	0.3	<b>0.45</b>	0.6	0.75
	Perimeter =	P.sect (dm)	1.88	<b>2.83</b>	3.77	4.71
	Area =	A.sect (dm <sup>2</sup> )	0.28	<b>0.64</b>	1.13	1.77

A ring is made up of a main part (1 synthetic fiber rope) + reinforcement ropes (synthetic fiber ropes)

**Weight of the main part (synthetic fiber ropes)**

**Weight (Wa) =**

		Size 1	Size 2	Size 3	Size 4
= A.sect * P.ring	(dm <sup>2</sup> )	102.51	<b>230.04</b>	407.89	635.66
* W.fiber /1000	(T)	<b>0.11</b>	<b>0.25</b>	<b>0.45</b>	<b>0.70</b>

**Weight of the reinforcement ropes (synthetic fiber ropes)**

Weight (Wb) =	Number of segments	Length of segm. (m)	Number (units)	Total (m)	Weight (kg/m)	Total weight (kg)
	A	B	C	D (=A*B*C)	E	D*E
Red ropes (d = 10 mm)	1	0.5	180	90.0	0.071	6.39
Yellow ropes (d = 10 mm)	18	3.9	5	351.0	0.071	24.921
Cyan ropes (d = 10 mm)	18	7.2	5	648.0	0.071	46.008
Anchorage for yellow / cyan ropes	-	-	180	-	0.100	18
Rope-stretching junction	-	-	10	-	0.500	5
Total:					(T)	<b>0.100319</b>

**Weight of anchorages for connection arms and of main anchorages (plastic material + chamfer steel nails)**

Weight (Wc) =		Number	
Anchorage for connection arms (40 cm * 0.6)	dm <sup>2</sup>	2.4	6
Main anchorages (30 cm * 0.6)	dm <sup>2</sup>	1.8	6
		Tot. surfaces:	25.2
		*0.1*W.fiber	(kg)
			2.772
Chamfer steel nails (r=0.75mm; l=2.5cm; 100/dm <sup>2</sup> )		0.034901	
		Total:	(T)
			<b>0.0037</b>

**Weight of connection arms (plastic material for the most part)**

Weight (Wd) =	Thickness (cm)	Length of segm. (cm)	Perimeter (cm)	Volume (dm <sup>3</sup> )	Weight (kg)
Branches	2	500	84	84	92,4
Other					10
Junction					3.14
Total:					(T)
50%					(T)
* 3					(T)
					<b>0.1583</b>

Total Weight (Wt = Wa + Wb + Wc + Wd/2)		Size 1	Size 2	Size 3	Size 4
Wa =	(T)	0.1128	<b>0.2530</b>	0.4487	0.6992
+ Wb =	(T)	0.1003	<b>0.1003</b>	0.1003	0.1003
+ Wc =	(T)	0.0037	<b>0.0037</b>	0.0037	0.0037
+ Wd/2 =	(T)	0.0528	<b>0.0528</b>	0.0528	0.0528
Wt =	(T)	<b>0.2695</b>	<b>0.4098</b>	<b>0.6054</b>	<b>0.8560</b>

### (3) Breaking load of the ring

((area of a section of the ring - 20%) / (area of a section of rope X) ) \* breaking load of rope X

Rope type (denomination)	Rope diameter (mm)	Weight (g/m)	Breaking load (=Bl) (T)	Area of section (A.sectRope) (dm <sup>2</sup> )				
Dyneforce 78	20	191	33.6	0.0314				
Viper 78	30	545	46	0.0707				
					Size 1	<b>Size 2</b>	Size 3	Size 4
		A.sect - 20% =	A (dm <sup>2</sup> )		0,2262	<b>0.5089</b>	0.9613	1.4137
with 20 mm ropes		A.sectRope =	B1 (dm <sup>2</sup> )		0,0314	<b>0.0314</b>	0.0314	0.0314
		no. of ropes (rounded) =	C=int(A/B1+0,5)		7	<b>16</b>	31	45
		breaking load (rounded) =	C * Bl (T)		235	<b>538</b>	1042	1512
with 30 mm ropes		A.sectRope =	B2 (dm <sup>2</sup> )		0,0707	<b>0.0707</b>	0.0707	0.0707
		no. of ropes (rounded) =	C= int(A/B2+0,5)		3	<b>7</b>	14	20
		breaking load (rounded) =	C * B1 (T)		138	<b>322</b>	644	920

**(4) Breaking load for each blue / yellow system at each ring (= 21,33 T \* Level / 6)**

Blue and yellow systems composed of steel axes (from the 1st to the 63rd ring; estimation of weight and breaking load)

Level (from the ring 1 to the ring 63)	Breaking load (A) (T)	Diameter of axes (mm)	Breaking load (T)	Number (for each group) (units)	Total load (B) (T)	Safety margin (B-A) (T)	Length (m)	Weight (kg/m)	Weight (for each group) (kg)	Weight (x 6 groups *2) (T)
1	3.56	15	15.99	1	15.99	12.44	6	1.237	7.422	0.0891
2	7.11	15	15.99	1	15.99	8.88	6	1.237	7.422	0.0891
3	10.67	15	15.99	1	15.99	5.33	6	1.237	7.422	0.0891
4	14.22	15	15.99	1	15.99	1.77	6	1.237	7.422	0.0891
5	17.78	21	31.34	1	31.34	13.57	6	2.424	14.544	0.1745
6	21.33	21	31.34	1	31.34	10.01	6	2.424	14.544	0.1745
7	24.89	21	31.34	1	31.34	6.46	6	2.424	14.544	0.1745
8	28.44	21	31.34	1	31.34	2.90	6	2.424	14.544	0.1745
9	32.00	25	44.42	1	44.42	12.43	6	3.426	20.556	0.2467
10	35.55	25	44.42	1	44.42	8.87	6	3.426	20.556	0.2467
11	39.11	25	44.42	1	44.42	5.32	6	3.426	20.556	0.2467
12	42.66	25	44.42	1	44.42	1.76	6	3.426	20.556	0.2467
13	46.22	29	59.78	1	59.78	13.57	6	4.623	27.738	0.3329
14	49.77	29	59.78	1	59.78	10.01	6	4.623	27.738	0.3329
15	53.33	29	59.78	1	59.78	6.46	6	4.623	27.738	0.3329
16	56.88	29	59.78	1	59.78	2.90	6	4.623	27.738	0.3329
17	60.44	32	72.78	1	72.78	12.35	6	5.629	33.774	0.4053
18	63.99	32	72.78	1	72.78	8.79	6	5.629	33.774	0.4053
19	67.55	32	72.78	1	72.78	5.24	6	5.629	33.774	0.4053
20	71.10	32	72.78	1	72.78	1.68	6	5.629	33.774	0.4053
21	74.66	35	87.07	1	87.07	12.42	6	6.734	40.404	0.4848
22	78.21	35	87.07	1	87.07	8.86	6	6.734	40.404	0.4848
23	81.77	35	87.07	1	87.07	5.30	6	6.734	40.404	0.4848
24	85.32	35	87.07	1	87.07	1.75	6	6.734	40.404	0.4848
25	88.88	38	102.63	1	102.63	13.76	6	7.939	47.634	0.5716
26	92.43	38	102.63	1	102.63	10.20	6	7.939	47.634	0.5716
27	95.99	38	102.63	1	102.63	6.65	6	7.939	47.634	0.5716
28	99.54	38	102.63	1	102.63	3.09	6	7.939	47.634	0.5716
29	103.10	41	119.48	1	119.48	16.39	6	9.241	55.446	0.6654
30	106.65	41	119.48	1	119.48	12.83	6	9.241	55.446	0.6654
31	110.21	41	119.48	1	119.48	9.28	6	9.241	55.446	0.6654
32	113.76	41	119.48	1	119.48	5.72	6	9.241	55.446	0.6654
33	117.32	43	131.42	1	131.42	14.11	6	10.165	60.990	0.7319
34	120.87	43	131.42	1	131.42	10.55	6	10.165	60.990	0.7319
35	124.43	43	131.42	1	131.42	6.99	6	10.165	60.990	0.7319
36	127.98	43	131.42	1	131.42	3.44	6	10.165	60.990	0.7319
37	131.54	45	143.93	1	143.93	12.40	6	11.133	66.798	0.8016
38	135.09	45	143.93	1	143.93	8.84	6	11.133	66.798	0.8016

39	138.65	45	143.93	1	143.93	5.29	6	11.133	66.798	0.8016
40	142.20	45	143.93	1	143.93	1.73	6	11.133	66.798	0.8016
41	145.76	47	157.01	1	157.01	11.26	6	12.144	72.864	0.8744
42	149.31	47	157.01	1	157.01	7.70	6	12.144	72.864	0.8744
43	152.87	47	157.01	1	157.01	4.15	6	12.144	72.864	0.8744
44	156.42	47	157.01	1	157.01	0.59	6	12.144	72.864	0.8744
45	159.98	49	170.65	1	170.65	10.68	6	13.200	79.200	0.9504
46	163.53	49	170.65	1	170.65	7.12	6	13.200	79.200	0.9504
47	167.09	49	170.65	1	170.65	3.57	6	13.200	79.200	0.9504
48	170.64	49	170.65	1	170.65	0.01	6	13.200	79.200	0.9504
49	174.20	50	177.69	1	177.69	3.50	6	13.744	82.464	0.9896
Next 14 (50-63)	174.20	50	177.69	1	177.69	3.50	6	13.744	82.464	13.8540
									Total:	40.1573

**(5) Weight of rings + blue & yellow systems + 1/2 connection arms**

Level (from top to bottom)	Weight of the ring (T)	Weight of blue & yellow s. (T)	1/2 weight of connexion arms (T)	Total (T)
1	0.4098	0.0891	0.1583	0.6572
2	0.4098	0.0891	0.1583	0.6572
3	0.4098	0.0891	0.1583	0.6572
4	0.4098	0.0891	0.1583	0.6572
5	0.4098	0.1745	0.1583	0.7426
6	0.4098	0.1745	0.1583	0.7426
7	0.4098	0.1745	0.1583	0.7426
8	0.4098	0.1745	0.1583	0.7426
9	0.4098	0.2467	0.1583	0.8148
10	0.4098	0.2467	0.1583	0.8148
11	0.4098	0.2467	0.1583	0.8148
12	0.4098	0.2467	0.1583	0.8148
13	0.4098	0.3329	0.1583	0.9009
14	0.4098	0.3329	0.1583	0.9009
15	0.4098	0.3329	0.1583	0.9009
16	0.4098	0.3329	0.1583	0.9009
17	0.4098	0.4053	0.1583	0.9734
18	0.4098	0.4053	0.1583	0.9734
19	0.4098	0.4053	0.1583	0.9734
20	0.4098	0.4053	0.1583	0.9734
21	0.4098	0.4848	0.1583	1.0529
22	0.4098	0.4848	0.1583	1.0529
23	0.4098	0.4848	0.1583	1.0529
24	0.4098	0.4848	0.1583	1.0529
25	0.4098	0.5716	0.1583	1.1397
26	0.4098	0.5716	0.1583	1.1397
27	0.4098	0.5716	0.1583	1.1397
28	0.4098	0.5716	0.1583	1.1397
29	0.4098	0.6654	0.1583	1.2334
30	0.4098	0.6654	0.1583	1.2334
31	0.4098	0.6654	0.1583	1.2334
32	0.4098	0.6654	0.1583	1.2334
33	0.4098	0.7319	0.1583	1.3000
34	0.4098	0.7319	0.1583	1.3000
35	0.4098	0.7319	0.1583	1.3000
36	0.4098	0.7319	0.1583	1.3000
37	0.4098	0.8016	0.1583	1.3697
38	0.4098	0.8016	0.1583	1.3697
39	0.4098	0.8016	0.1583	1.3697
40	0.4098	0.8016	0.1583	1.3697
41	0.4098	0.8744	0.1583	1.4425

42	0.4098	0.8744	0.1583	1.4425
43	0.4098	0.8744	0.1583	1.4425
44	0.4098	0.8744	0.1583	1.4425
45	0.4098	0.9504	0.1583	1.5185
46	0.4098	0.9504	0.1583	1.5185
47	0.4098	0.9504	0.1583	1.5185
48	0.4098	0.9504	0.1583	1.5185
49	0.4098	0.9896	0.1583	1.5577
50	0.4098	0.9896	-	1.3994
51	0.4098	0.9896	-	1.3994
52	0.4098	0.9896	-	1.3994
53	0.4098	0.9896	-	1.3994
54	0.4098	0.9896	-	1.3994
55	0.4098	0.9896	-	1.3994
56	0.4098	0.9896	-	1.3994
57	0.4098	0.9896	-	1.3994
58	0.4098	0.9896	-	1.3994
59	0.4098	0.9896	-	1.3994
60	0.4098	0.9896	-	1.3994
61	0.4098	0.9896	-	1.3994
62	0.4098	0.9896	-	1.3994
63	0.4098	0.9896	-	1.3994
Totals:	25.8163	40.1573	7.7572	73.7308

## (6) Ring-supporting ropes

Galvanized steel wire ropes W.S. 6 x 36 + IWRC WS

Diameter (mm)	Weight (kg/m)	Breaking load (T)
30	3.76	64.20

Load for each level (constant)

Level (from top to bottom)	Load (A) (T)	Diameter of steel ropes (mm)	Breaking load (T)	Number of ropes (units)	Total breaking load (B) (T)	% of breaking load (=A/B*100)	Length (m)	Weight (Kg/m)	Weight (T)
1	73.7308	30	64.2	18	1155.6	6.38	1.68	3.76	0.1137
2	73.0736	30	64.2	18	1155.6	6.32	1.68	3.76	0.1137
3	72.4165	30	64.2	18	1155.6	6.27	1.68	3.76	0.1137
4	71.7593	30	64.2	18	1155.6	6.21	1.68	3.76	0.1137
5	71.1021	30	64.2	18	1155.6	6.15	1.68	3.76	0.1137
6	70.3595	30	64.2	18	1155.6	6.09	1.68	3.76	0.1137
7	69.6169	30	64.2	18	1155.6	6.02	1.68	3.76	0.1137
8	68.8743	30	64.2	18	1155.6	5.96	1.68	3.76	0.1137
9	68.1317	30	64.2	18	1155.6	5.90	1.68	3.76	0.1137
10	67.3169	30	64.2	18	1155.6	5.83	1.68	3.76	0.1137
11	66.5021	30	64.2	18	1155.6	5.75	1.68	3.76	0.1137
12	65.6874	30	64.2	18	1155.6	5.68	1.68	3.76	0.1137
13	64.8726	30	64.2	18	1155.6	5.61	1.68	3.76	0.1137
14	63.9717	30	64.2	18	1155.6	5.54	1.68	3.76	0.1137
15	63.0707	30	64.2	18	1155.6	5.46	1.68	3.76	0.1137
16	62.1698	30	64.2	18	1155.6	5.38	1.68	3.76	0.1137
17	61.2688	30	64.2	18	1155.6	5.30	1.68	3.76	0.1137
18	60.2954	30	64.2	18	1155.6	5.22	1.68	3.76	0.1137
19	59.3221	30	64.2	18	1155.6	5.13	1.68	3.76	0.1137
20	58.3487	30	64.2	18	1155.6	5.05	1.68	3.76	0.1137
21	57.3753	30	64.2	18	1155.6	4.96	1.68	3.76	0.1137
22	56.3223	30	64.2	18	1155.6	4.87	1.68	3.76	0.1137
23	55.2694	30	64.2	18	1155.6	4.78	1.68	3.76	0.1137
24	54.2165	30	64.2	18	1155.6	4.69	1.68	3.76	0.1137
25	53.1635	30	64.2	18	1155.6	4.60	1.68	3.76	0.1137
26	52.0238	30	64.2	12	770.4	6.75	1.68	3.76	0.0758
27	50.8841	30	64.2	12	770.4	6.60	1.68	3.76	0.0758
28	49.7444	30	64.2	12	770.4	6.46	1.68	3.76	0.0758
29	48.6047	30	64.2	12	770.4	6.31	1.68	3.76	0.0758
30	47.3713	30	64.2	12	770.4	6.15	1.68	3.76	0.0758
31	46.1378	30	64.2	12	770.4	5.99	1.68	3.76	0.0758
32	44.9044	30	64.2	12	770.4	5.83	1.68	3.76	0.0758
33	43.6709	30	64.2	12	770.4	5.67	1.68	3.76	0.0758
34	42.3710	30	64.2	12	770.4	5.50	1.68	3.76	0.0758
35	41.0710	30	64.2	12	770.4	5.33	1.68	3.76	0.0758
36	39.7710	30	64.2	12	770.4	5.16	1.68	3.76	0.0758



37	38.4711	30	64.2	12	770.4	4.99	1.68	3.76	0.0758
38	37.1014	30	64.2	12	770.4	4.82	1.68	3.76	0.0758
39	35.7317	30	64.2	12	770.4	4.64	1.68	3.76	0.0758
40	34.3621	30	64.2	12	770.4	4.46	1.68	3.76	0.0758
41	32.9924	30	64.2	12	770.4	4.28	1.68	3.76	0.0758
42	31.5499	30	64.2	12	770.4	4.10	1.68	3.76	0.0758
43	30.1075	30	64.2	12	770.4	3.91	1.68	3.76	0.0758
44	28.6650	30	64.2	12	770.4	3.72	1.68	3.76	0.0758
45	27.2225	30	64.2	12	770.4	3.53	1.68	3.76	0.0758
46	25.7040	30	64.2	6	385.2	6.67	1.68	3.76	0.0379
47	24.1856	30	64.2	6	385.2	6.28	1.68	3.76	0.0379
48	22.6671	30	64.2	6	385.2	5.88	1.68	3.76	0.0379
49	21.1486	30	64.2	6	385.2	5.49	1.68	3.76	0.0379
50	19.5909	30	64.2	6	385.2	5.09	1.68	3.76	0.0379
51	18.1916	30	64.2	6	385.2	4.72	1.68	3.76	0.0379
52	16.7922	30	64.2	6	385.2	4.36	1.68	3.76	0.0379
53	15.3929	30	64.2	6	385.2	4.00	1.68	3.76	0.0379
54	13.9935	30	64.2	6	385.2	3.63	1.68	3.76	0.0379
55	12.5942	30	64.2	6	385.2	3.27	1.68	3.76	0.0379
56	11.1948	30	64.2	6	385.2	2.91	1.68	3.76	0.0379
57	9.7955	30	64.2	6	385.2	2.54	1.68	3.76	0.0379
58	8.3961	30	64.2	6	385.2	2.18	1.68	3.76	0.0379
59	6.9968	30	64.2	6	385.2	1.82	1.68	3.76	0.0379
60	5.5974	30	64.2	6	385.2	1.45	1.68	3.76	0.0379
61	4.1981	30	64.2	6	385.2	1.09	1.68	3.76	0.0379
62	2.7987	30	64.2	6	385.2	0.73	1.68	3.76	0.0379
63	1.3994	30	64.2	6	385.2	0.36	1.68	3.76	0.0379
Totale (T)									5.0408

**Ring-supporting ropes (divided in three groups; galvanized steel wire ropes W.S. 6 x 36 + IWRC WS)**

Total load =	(T)	A	78.77
Cos(10°) =	number	B	0.98
Effective load =	(T)	C (=A*B)	77.57
Rope diameter =	(mm)		30
Breaking load for each rope =	(T)		64.2
Number of ropes	(units)		18
Total breaking load =	(T)	D	1155.6
Ratio C/D =	(%)	(=C/D*100)	6.71

## (7) Weights of the wings

Weight of a wing element

	(dm)	(dm)	(dm)	(dm <sup>3</sup> )	Weight
<b>Winglet</b>	50	0.02	4	4.00	4.40
<b>Reinforcement</b>	50	0.04	0.08	0.16	0.176
<b>Circle behind the support (in dm<sup>2</sup>)</b>		0.79	0.1	0.08	0.09
<b>Support of a winglet (right side)</b>	5	0.6	0.2	0.6	0.66
<b>Support of a winglet (left side)</b>	5	0.6	0.2	0.6	0.66
<b>Totale:</b>					<b>5.98</b>

<b>Horizontal part</b>	(dm)	(dm)	(dm)	(dm <sup>3</sup> )	Weight	Number	Total
	50	0.3	0.2	3	3.3	2	6.6000
	5.3	0.3	0.1	0.159	0.1749		
	5	0.3	0.1	0.15	0.165		
	3.8	0.3	0.1	0.114	0.1254		
	<b>Tot.:</b>				0.4653	12	5.5836
<b>Total:</b>							<b>12.1836</b>

<b>Vertical part</b>	(dm)	(dm)	(dm)	(dm <sup>3</sup> )	Weight	Number	Total
	16.8	0.3	0.2	1.008	1.1088	2	2.2176
	5.3	0.3	0.1	0.159	0.1749		
	5	0.3	0.1	0.15	0.165		
	3.8	0.3	0.1	0.114	0.1254		
	<b>Tot.:</b>				0.4653	4	1.8612
<b>Total:</b>							<b>4.0788</b>

<b>Internal ropes</b>	(dm)	Number	Tot. dm	Weight
(Dyneforce 78. 4 mm. 8 g/m)	16.8	2	33.6	
	3.1	8	24.8	
<b>Tot.:</b>			58.4	<b>0.04672</b>

**Weight of a single element**

Winglet	5.98	4	23.93	kg
Horizontal part	12.1836	1	12.18	kg
Vertical parts	4.0788	2	8.16	kg
Internal ropes	0.04672	2	0.09	kg
Nails, connections	0.2	2	0.40	kg
<b>44.76</b>			<b>kg</b>	

<b>Total weights (in T)</b>	Wing without external ropes	wing-wing ropes	wing-ring ropes	Total		External reinforcements	50% conn. arms	Total
Weight of a single row	0.3581	0.0149	0.0591	0.4322		0.0031	0.0528	
Weight of a single col.	2.2382	0.0932	0.3697	2.7011	for columns 2-7	-	-	2.7011
					for column 1	-	2.6385	5.3396
					for column 8	0.1570	-	2.8581
Weight of a wing	17.9057	0.7455	2.9573	21.6086		0.1570	2.6385	24.4041
Weight of the 3 wings	53.7171	2.2366	8.8720	64.8257		0.4710	7.9155	73.2122

### Wing-wing ropes

(Dyneforce 78; diametro 8 mm)

Breaking load (T) =	8.00	Weight (g/m) =	35
---------------------	------	----------------	----

Breaking load for:	(T)
1 rope (=y)	8.00
1 row of 3 wings (= 8 y)	64.00
1 wing (= 8 y 50)	3.200.00

### Length of wing-wing ropes

	Length (+ 1 m) (m)	Weight (T)
Rope 1	83.57	0.002925
Rope 2	74.9	0.002622
Rope 3	66.24	0.002318
Rope 4	57.58	0.002015
Rope 5	48.93	0.001713
Rope 6	40.26	0.001409
Rope 7	31.6	0.001106
Rope 8	22.94	0.000803
Total:	426.02	0.014911
x 50 rows	21.301	0.745535
x 3 wings	63.903	2.236605

**(8) Breaking load for each wing-wing rope (the rope 1 is the most internal)**

(Cavi Dyneforce 78)

	(T)
Breaking load for 1 row of a single wing / 3	21.33
Breaking load for a wing / 3	1.066.67

**Abbreviations**

Z = breaking load of 1 row of a single wing / 8

a = Z/2 ;      b = Z/2 + Z/2;      c. a. = connection arm; w-w = wing-wing

	A		angle (B) (degrees)	sin(rad(B)) (C) (number)	Load (E) (=A/C)	Rope diameter (mm)	Weight (P) (g/m)	Breaking Load (F) (T)	% (E/F * 100) (%)	Length (+ 1m) G (m)	Weight (P*G /1000) (kg)	Weight (T)
= a	1.3333	c. a.	-	-	-	-	-	-	-	-	-	
= b	2.6667	w-w r. 1	26	0.43837	6.08313	10	(number)	(degrees)	49.82	11.94	0.66	
= b	2.6667	w-w r. 2	18	0.30902	8.62951	10	(number)	(degrees)	70.68	16.58	0.91	
= b	2.6667	w-w r. 3	14	0.24192	11.02284	12	-	-	66.04	21.49	1.63	
= b	2.6667	w-w r. 4	11	0.19081	13.97558	14	0.43837	26	69.32	26.37	2.77	
= b	2.6667	w-w r. 5	9	0.15643	17.04654	16	0.30902	18	68.74	31.24	4.06	
= b	2.6667	w-w r. 6	8	0.13917	19.16079	18	0.24192	14	68.43	36.18	5.68	
= b	2.6667	w-w r. 7	7	0.12187	21.88136	20	0.19081	11	65.12	41.14	7.86	
= a	1.3333	w-w r. 8	6	0.10453	12.75570	16	0.30902	18	51.43	46.18	6.00	
Tot.:	21.3333								Total	231.12	29.57	0.0296
											* 2	0.0591

**(9) Wing-supporting ropes**

(galvanized steel wire ropes W.S. 6 x 36 + IWRC WS)

	Diameter (mm) 26		Breaking lo. (T)=48.10		Weight (kg/m) = 2.83			
Weight of 1 wing. ropes incl.	(k1) =21.6086		Weight ext. reinf. (k3) = 0.1570		Total:		24.4041	
Weight of 1 column of wing	(k1/8) (k2) =2.7011		Weight 50% int. reinf. (k4) = 2.6385					
	Constant load (A) (T)	Rope Diameter (mm)	Breaking load (B) (T)	No. Of ropes (C) (units)	Angle (D) (degrees)	Cos(rad(D)) (E) (number)	Tot. Breaking lo. = B*C*E (F) (T)	% (=A/F*100) (%)
Rope 1 (=k2/2 + k4)	3.9890	26	48.1	2	9	0.987688	95.02	4.20
Rope 2 (=k2)	2.7011	26	48.1	2	17	0.956305	92.00	2.94
Rope 3 (=k2)	2.7011	26	48.1	2	23	0.920505	88.55	3.05
Rope 4 (=k2)	2.7011	26	48.1	2	29	0.874620	84.14	3.21
Rope 5 (=k2)	2.7011	26	48.1	2	35	0.819152	78.80	3.43
Rope 6 (=k2)	2.7011	26	48.1	2	39	0.777146	74.76	3.61
Rope 7 (=k2)	2.7011	26	48.1	2	43	0.731354	70.36	3.84
Rope 8 (=k2)	2.7011	26	48.1	2	47	0.681998	65.61	4.12
Rope 9 (=k2/2+k3)	1.5075	26	48.1	2	50	0.642788	61.84	2.44
Total:	24.4041							

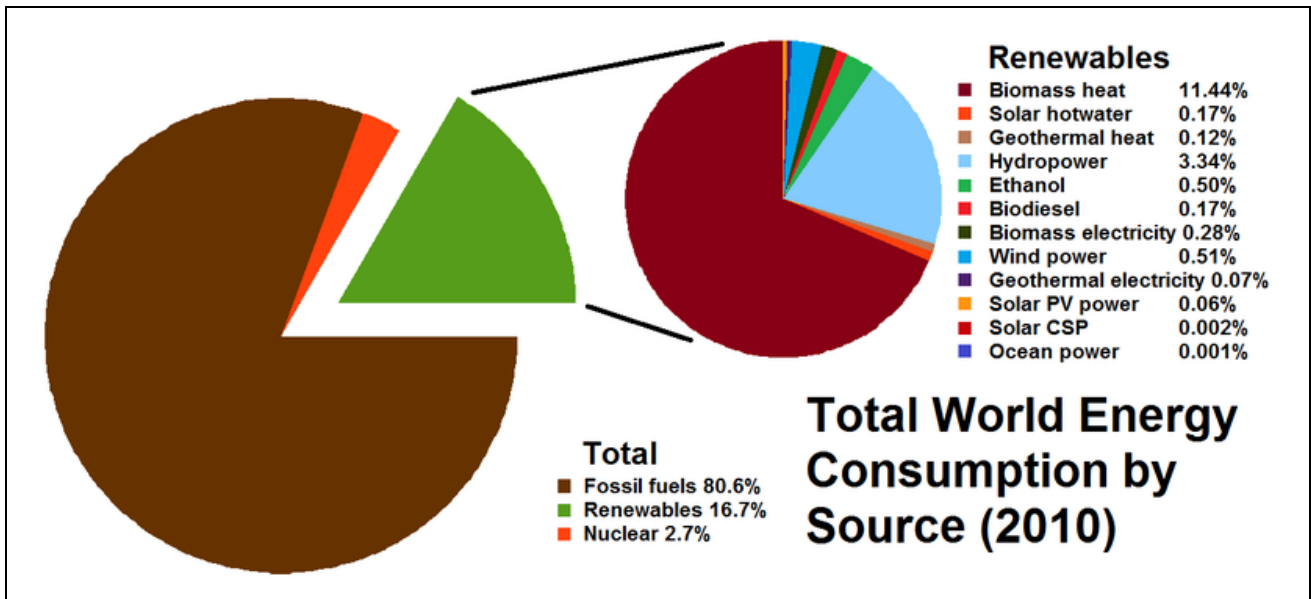
**(10) Pressure in centripetal direction for each wing**

	Constant load (A) (T)	Angle (B) (degrees)	sin(rad(B)) (C) (number)	Pressure (=A*C) (T)
Rope 1 (=k2/2 + k4)	3.9890	9	0.1564	0.6240
Rope 2 (=k2)	2.7011	17	0.2924	0.7897
Rope 3 (=k2)	2.7011	23	0.3907	1.0554
Rope 4 (=k2)	2.7011	29	0.4848	1.3095
Rope 5 (=k2)	2.7011	35	0.5736	1.5493
Rope 6 (=k2)	2.7011	39	0.6293	1.6998
Rope 7 (=k2)	2.7011	43	0.6820	1.8421
Rope 8 (=k2)	2.7011	47	0.7314	1.9754
Rope 9 (=k2/2+k3)	1.5075	50	0.7660	1.1548
Total:	24.4041		Totale:	12.0001

Rough mean length of each rope = 50 m; total length = 450 m; total weight = 1.2735 T

**Section 3 – Energy production, consumption, and cost**  
 (From Wikipedia, 20 January 2013)

**(1) Total world energy consumption by source 2010**



**Page:** Energy Development

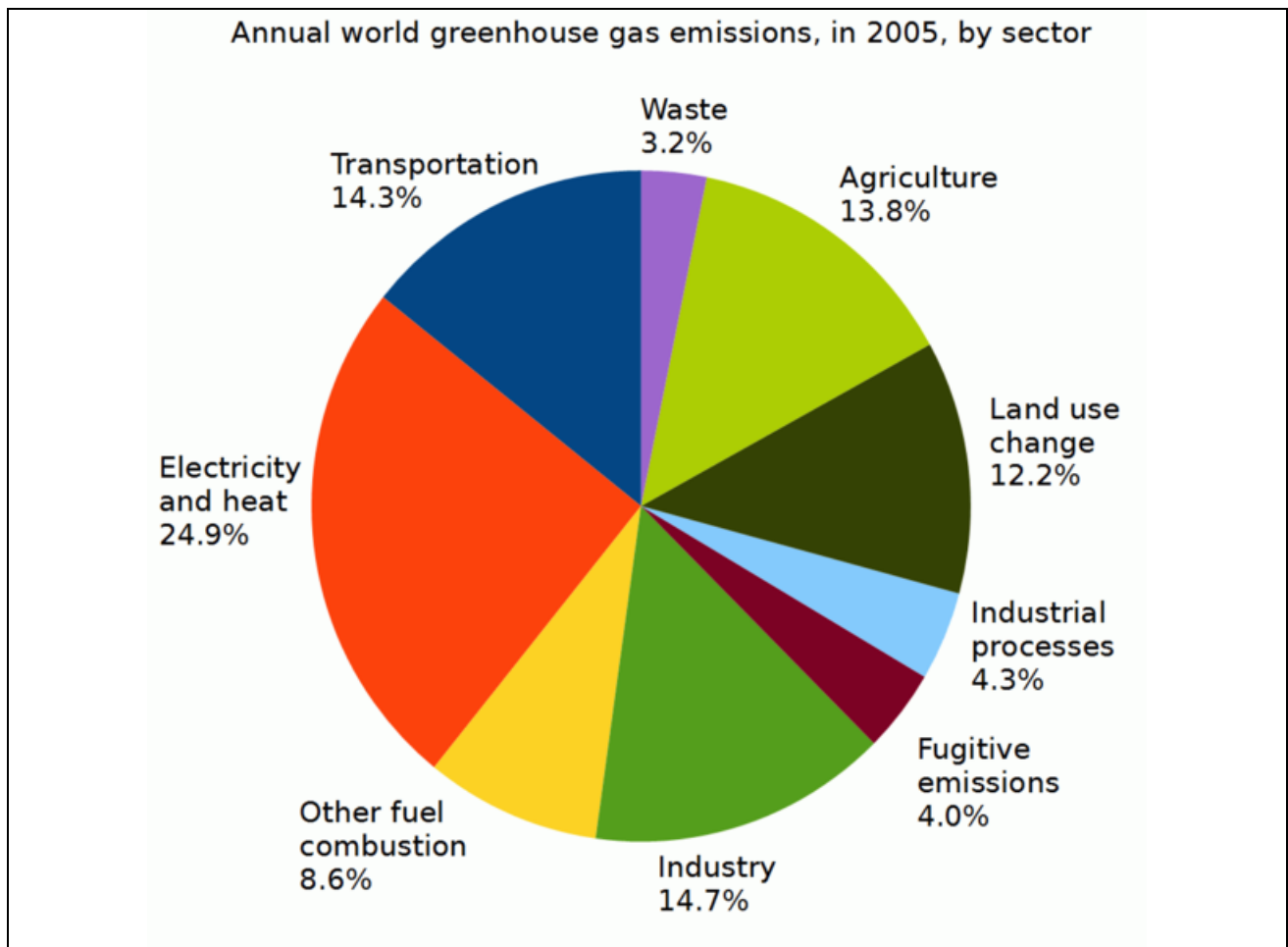
**Description:** Total world energy consumption by source 2010, from REN21 Renewables 2012 Global Status Report.

**Date:** 25 June 2012

**Source:** Own work

**Author:** Delphi234

## (2) Annual world greenhouse gas emissions, in 2005



### Page: Global Warming

**Description:** This pie chart shows annual world greenhouse gas emissions, in 2005, by sector. Emissions are measured as a percentage of total world carbon dioxide equivalent emissions.

Emissions due to land-use change include both emissions and absorptions (i.e., processes that both add to and remove carbon from the atmosphere). Emissions due to land-use change are highly uncertain.

**References:** Herzog, Timothy (July 2009), World Greenhouse Gas Emissions in 2005. WRI Working Paper, Washington, DC, USA: World Resources Institute (WRI), p.2.

**Date:** 23 November 2012

Source: Own work










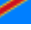








Author: Enescot

### (3) List of countries with source of electricity 2008

#### Page: Electricity Generation

Data source of values (electric power generated) is IEA/OECD [IEA Statistics and Balances, retrieved 2011-5-8]

Listed countries are top 20 by population or top 20 by GDP (PPP) and Saudi Arabia based on CIA World Factbook 2009 [CIA World Factbook 2009, retrieved 2011-5-8]

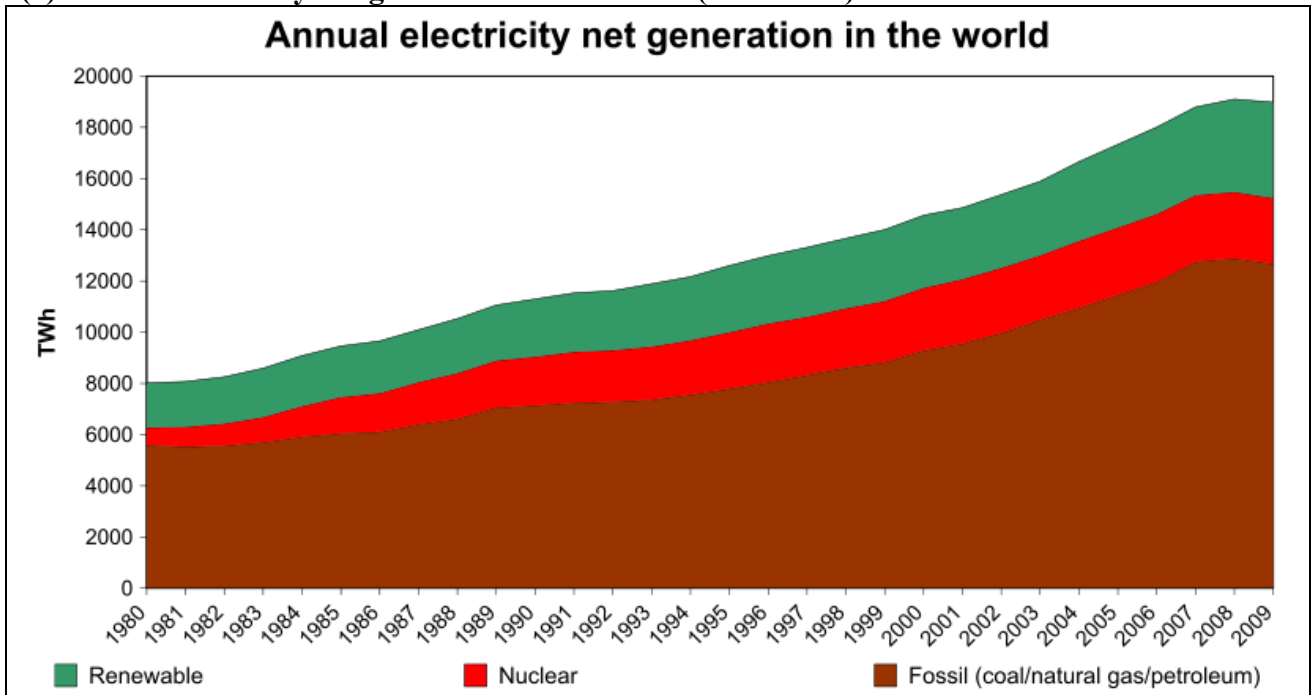
Composition of Electricity by Resource (TWh per year 2008)																		
Country	Fossil Fuel					Nuclear	rank	Renewable							Bio other*	total	rank	
	Coal	Oil	Gas	sub total	rank			Hydro	Geo Thermal	Solar PV*	Solar Thermal	Wind	Tide	sub total				rank
World total	8,263	1,111	4,301	13,675	-	2,731	-	3,288	65	12	0.9	219	0.5	3,584	-	271	20,261	-
Proportion	41%	5.5%	21%	67%	-	13%	-	16%	0.3%	0.06%	0.004%	1.1%	0.003%	18%	-	1.3%	100%	-
 China	2,733	23	31	2,788	2	68	8	585	-	0.2	-	13	-	598	1	2.4	3,457	2
 India	569	34	82	685	5	15	-6	114	-	0.02	-	14	-	128.02	6	2.0	830	-5
 USA	2,133	58	911	3,101	1	838	1	282	17	1.6	0.88	56	-	357	4	73	4,369	1
 Indonesia	61	43	25	130	19	-	-	12	8.3	-	-	-	-	20	17	-	149	20
 Brazil	13	18	29	59	23	14	13	370	-	-	-	0.6	-	370	3	20	463	9
 Pakistan	0.1	32	30	62	22	1.6	160	28	-	-	-	-	-	28	14	-	92	24
 Bangladesh	0.6	1.7	31	33	27	-	-	1.5	-	-	-	-	-	1.5	29	-	35	27
 Nigeria	-	3.1	12	15	28	-	-	5.7	-	-	-	-	-	5.7	25	-	21	28
 Russia	197	16	495	708	4	163	4	167	0.5	-	-	0.01	-	167	5	2.5	1,040	4
 Japan	288	139	283	711	3	258	3	83	2.8	2.3	-	2.6	-	91	7	22	1,082	3
 Mexico	21	49	131	202	13	9.8	14	39	7.1	0.01	-	0.3	-	47	12	0.8	259	14
 Philippines	16	4.9	20	40	26	-	-	9.8	11	0.001	-	0.1	-	21	16	-	61	26
 Vietnam	15	1.6	30	47	25	-	-	26	-	-	-	-	-	26	15	-	73	25
 Ethiopia	-	0.5	-	0.5	29	-	-	3.3	0.01	-	-	-	-	3.3	28	-	3.8	30
 Egypt	-	26	90	115	20	-	-	15	-	-	-	0.9	-	16	20	-	131	22
 Germany	291	9.2	88	388	6	148	5	27	0.02	4.4	-	41	-	72	9	29	637	7
 Turkey	58	7.5	99	164	16	-	-	33	0.16	-	-	0.85	-	34	13	0.22	198	19
 DR Congo	-	0.02	0.03	0.05	30	-	-	7.5	-	-	-	-	-	7.5	22	-	7.5	29
 Iran	0.4	36	173	209	11	-	-	5.0	-	-	-	0.20	-	5.2	26	-	215	17
 Thailand	32	1.7	102	135	18	-	-	7.1	0.002	0.003	-	-	-	7.1	23	4.8	147	21
 France	27	5.8	22	55	24	439	2	68	-	0.04	-	5.7	0.51	75	8	5.9	575	8
 UK	127	6.1	177	310	7	52	10	9.3	-	0.02	-	7.1	-	16	18	11	389	11
 Italy	49	31	173	253	9	-	-	47	5.5	0.2	-	4.9	-	58	11	8.6	319	12
 South Korea	192	15	81	288	8	151	5	5.6	-	0.3	-	0.4	-	6.3	24	0.7	446	10
 Spain	50	18	122	190	14	59	9	26	-	2.6	0.02	32	-	61	10	4.3	314	13
 Canada	112	9.8	41	162	17	94	7	383	-	0.03	-	3.8	0.03	386	2	8.5	651	6
 Saudi Arabia	-	116	88	204	12	-	-	-	-	-	-	-	-	-	-	-	204	18
 Taiwan	125	14	46	186	15	41	11	7.8	-	0.004	-	0.6	-	8.4	21	3.5	238	16
 Australia	198	2.8	39	239	10	-	-	12	-	0.2	0.004	3.9	-	16	19	2.2	257	15
 Netherlands	27	2.1	63	92	21	4.2	15	0.1	-	0.04	-	4.3	-	4.4	27	6.8	108	23

Solar PV\* is Photovoltaics

Bio other\* = 198TWh (Biomass) + 69TWh (Waste) + 4TWh (other)



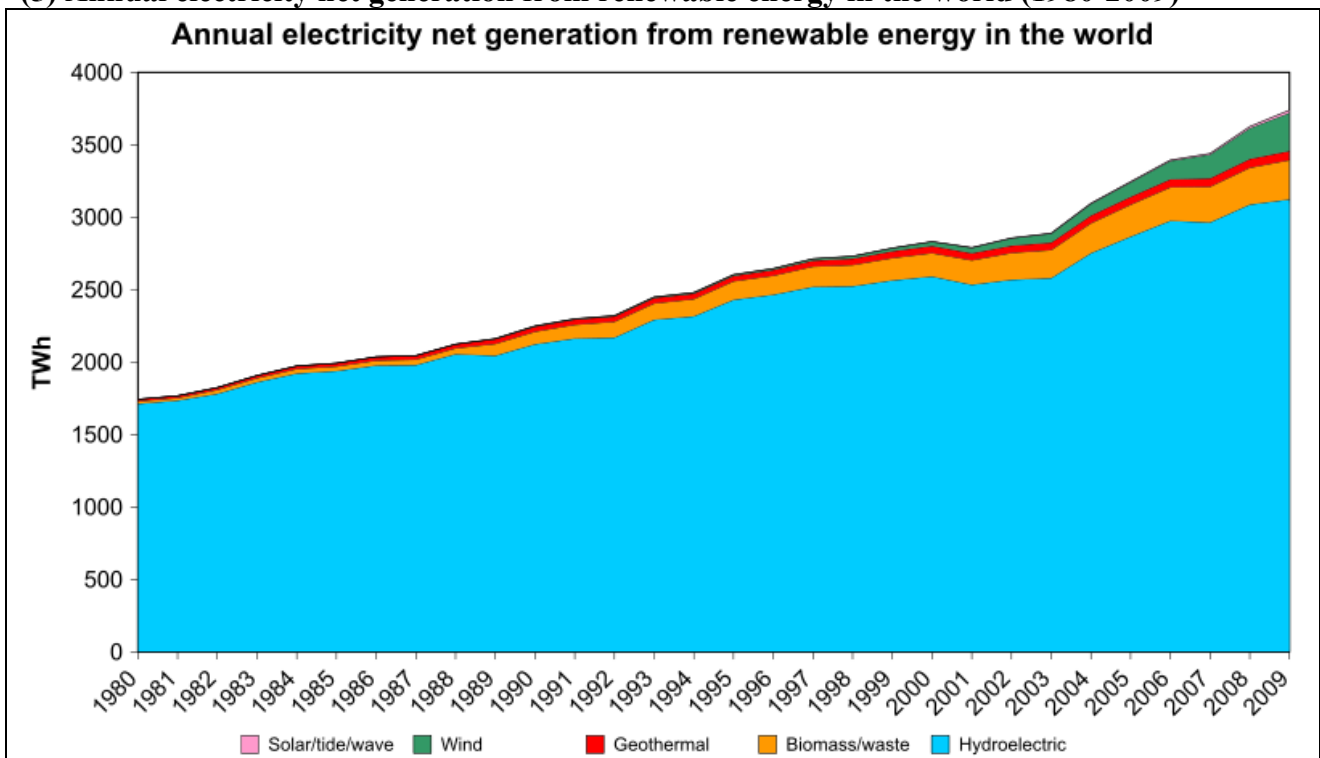
**(4) Annual electricity net generation in the world (1980-2009)**



Page: Electricity Generation

Date: 22 April 2012; Source: EIA; Author: Lery007

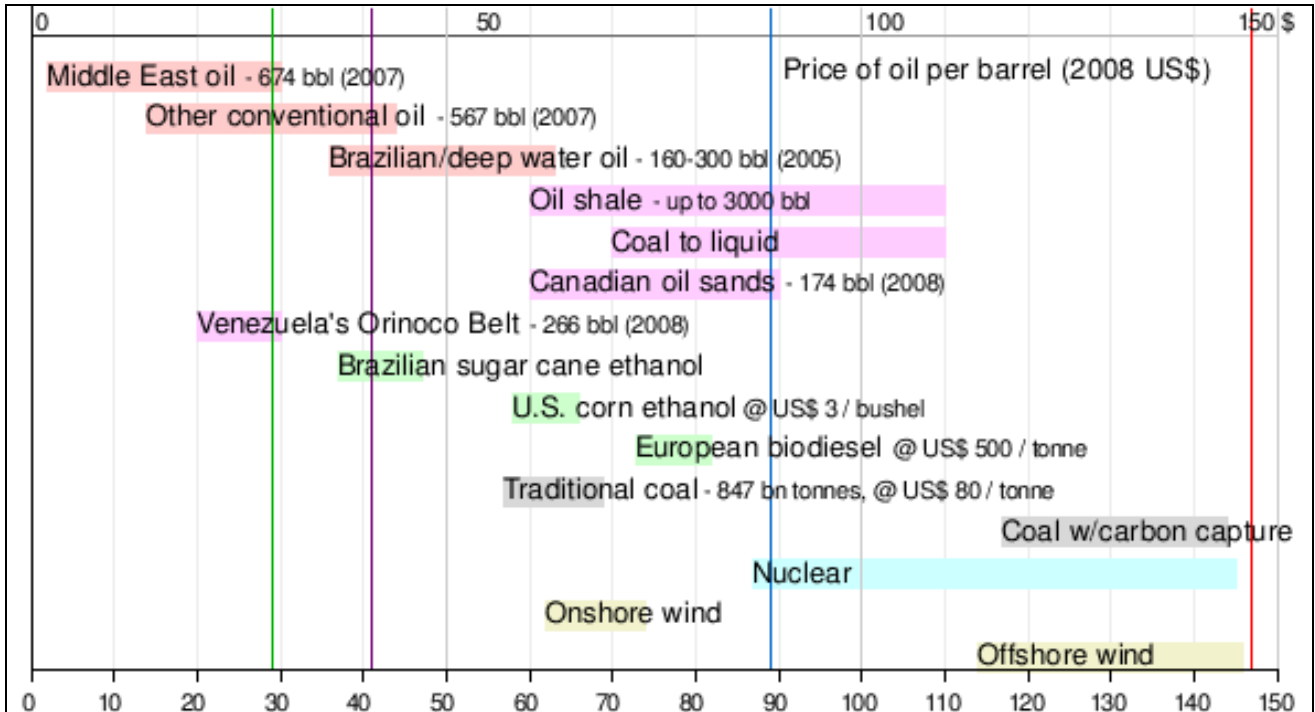
**(5) Annual electricity net generation from renewable energy in the world (1980-2009)**



Page: Electricity Generation

Date: 22 April 2012; Source: EIA; Author: Lery007

**(6) Price of oil per barrel (bbl) at which energy sources are competitive**



■ Conventional oil  
 ■ Unconventional oil  
 ■ Biofuels  
 ■ Coal  
 ■ Nuclear  
 ■ Wind

Colored vertical lines indicate various historical oil prices. From left to right:

— 1990s average  
 — January 2009  
 — 1979 peak  
 — 2008 peak

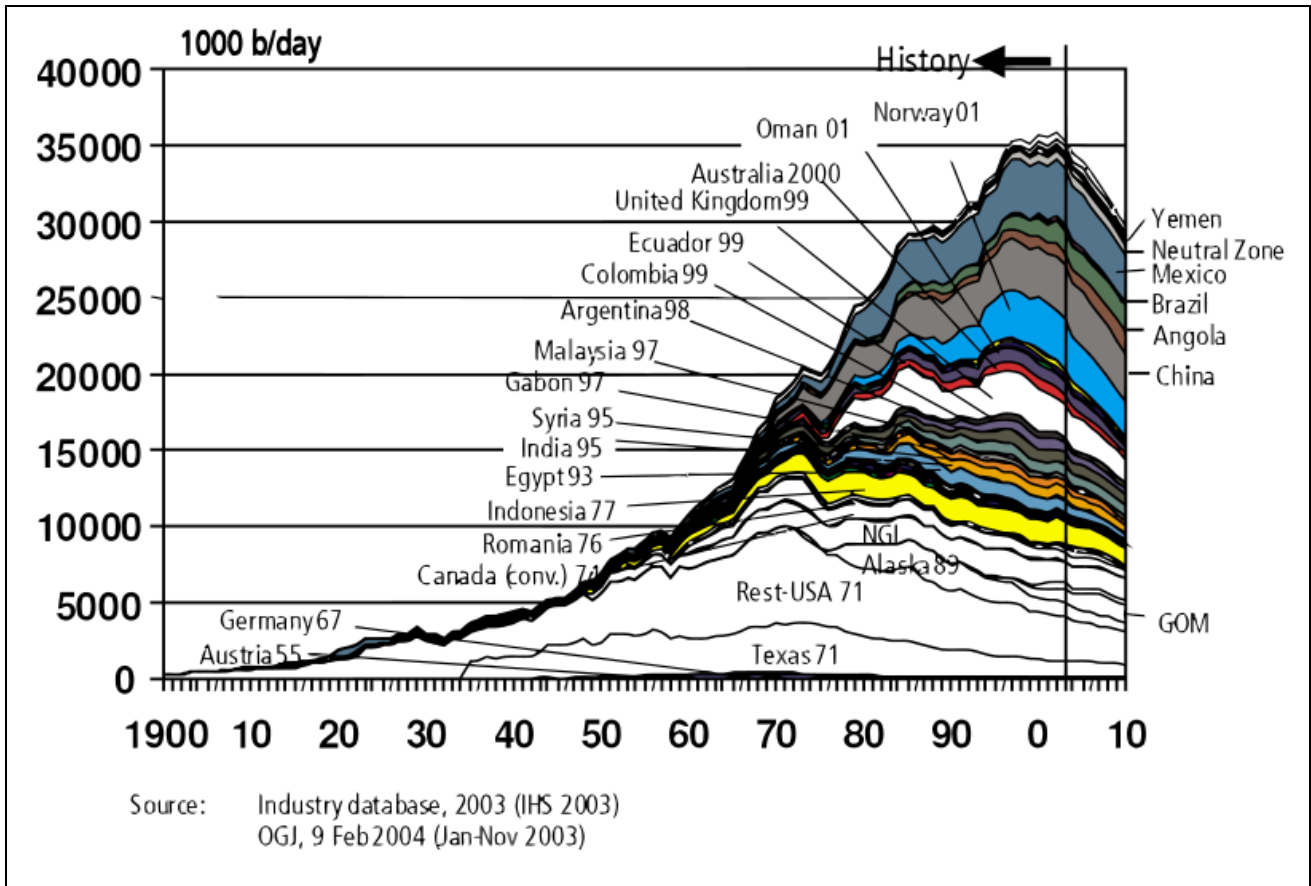
- **Right end of bar** is viability without subsidy.
- **Left end of bar** requires regulation or government subsidies.
- **Wider bars** indicate uncertainty.

**Page: Energy Development**

**Source: Financial Times**

The chart does not include the external costs of using fossil fuels

(7) Hubbert peak graph showing the world's oil production peak



**Page: Hubbert peak theory**

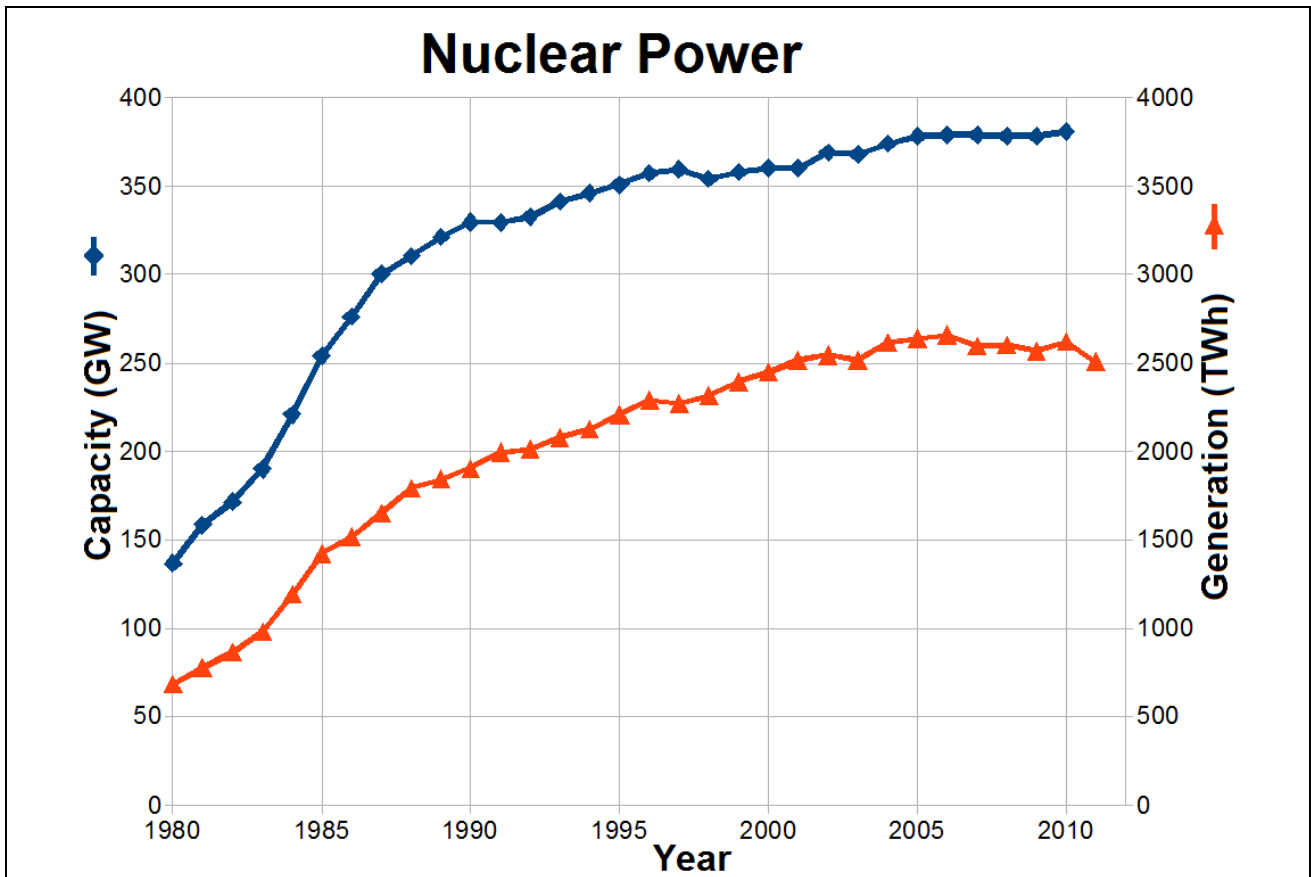
**Date:** 21 January 2012 (original upload date)

**Source:** Transferred from it.wikipedia; transfer was stated to be made by User:Rronny.

(Original text: Strategic Significance of America s Oil Shale Resource, Volume I Assessment of Strategic Issues)

**Author:** USA Government. Original uploader was Rronny at it.wikipedia

(8) Total world nuclear power capacity, in GW, and generation, in TWh, for the years 1980 to 2007



**Page: Nuclear power**

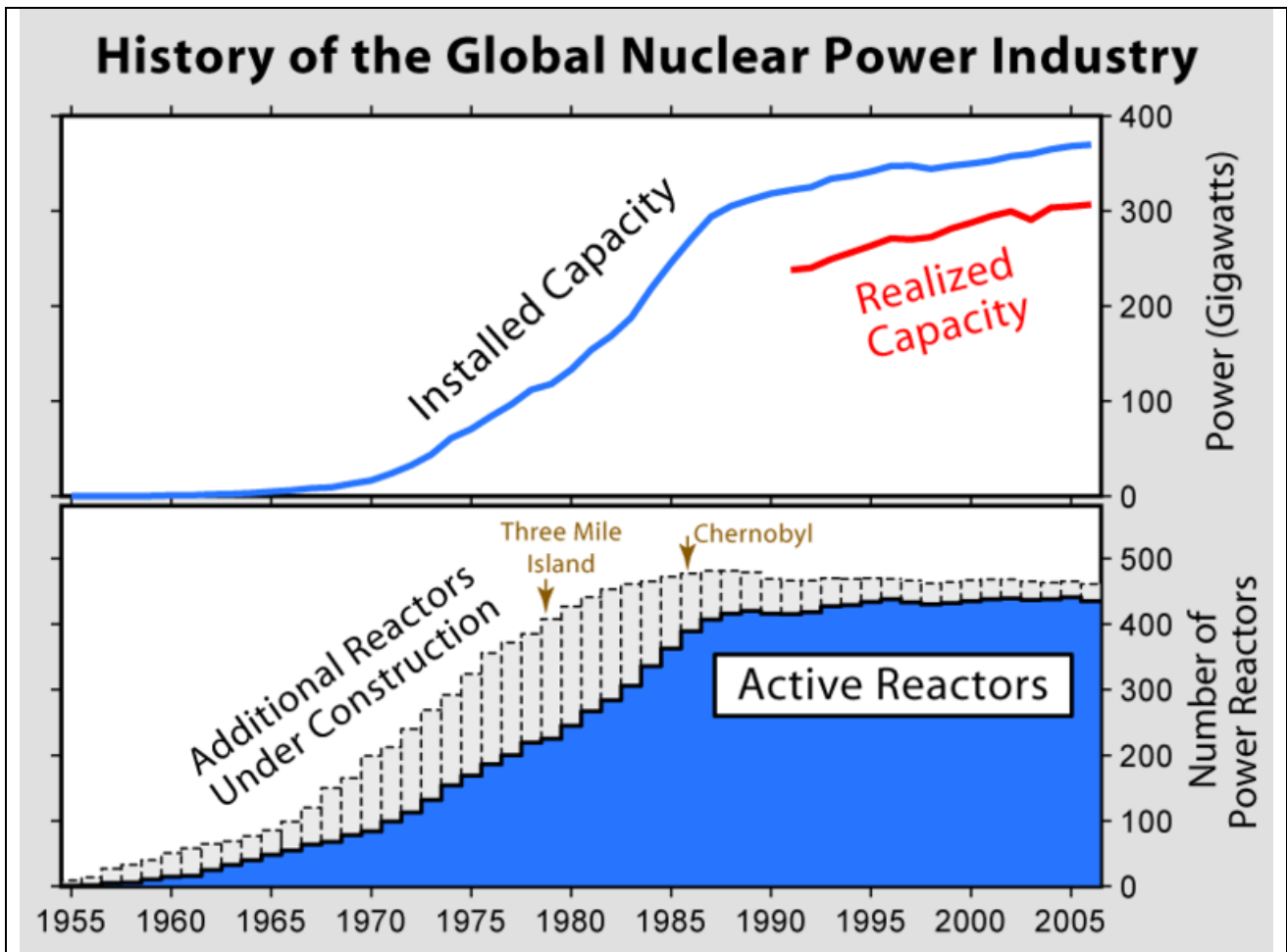
**Description:** Total world nuclear power capacity, in GW, and generation, in TWh, for the years 1980 to 2007. Capacity increased by 12.3% per year from 1981 to 1987, and by 1.3% per year from 1987 to 2007, post Chernobyl.

**Date:** 20 April 2009

**Source:** Own work by uploader, data from EIA  
 [<http://www.eia.gov/cfapps/ipdbproject/IEDIndex3.cfm>]

**Author:** Delphi234

(9) History of nuclear power generation



**Page: Nuclear power**

**Description:** This figure shows the history of nuclear power generation.

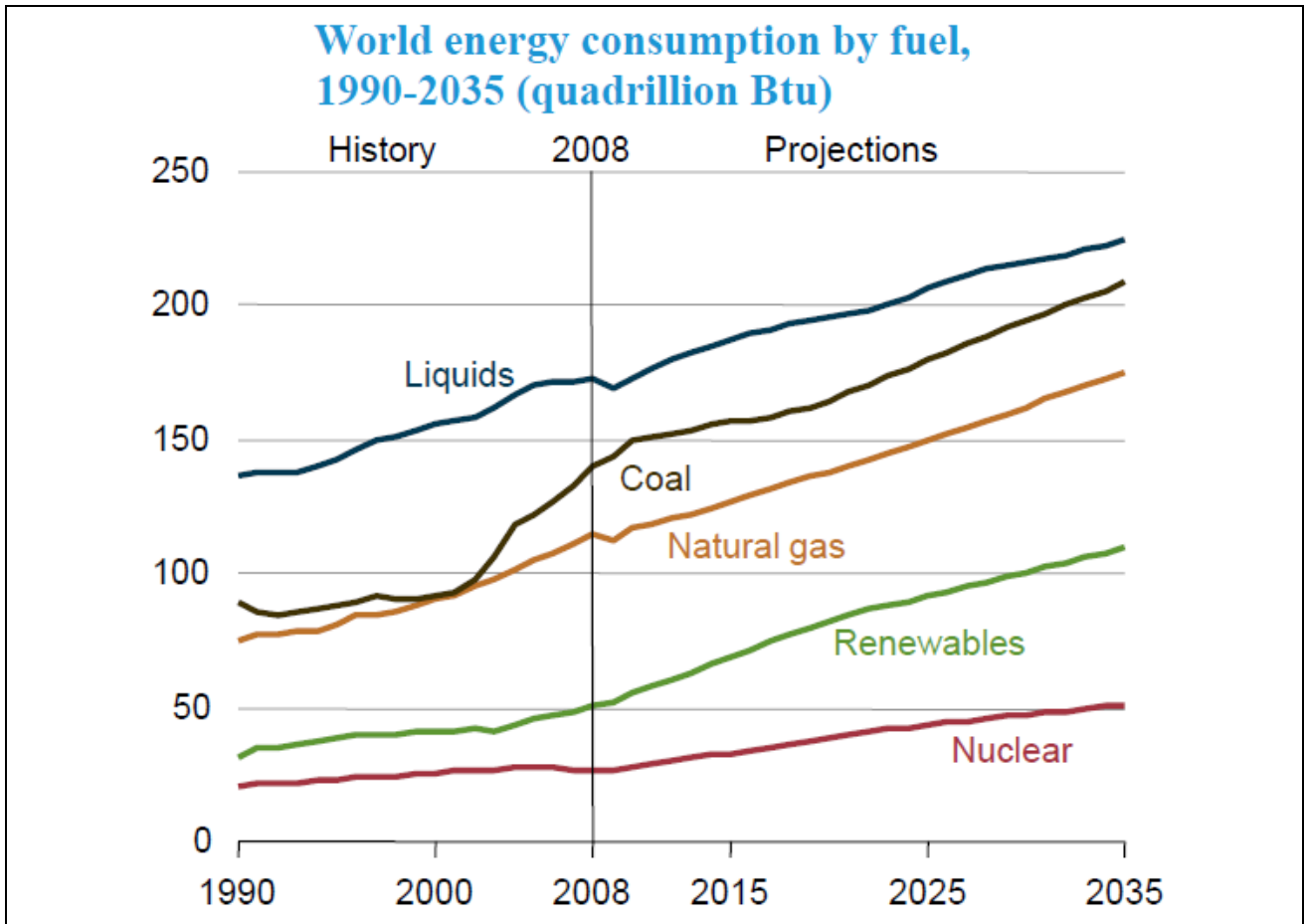
The top panel shows the installed global nuclear capacity (in gigawatts), and since 1991, the fraction of that power which was actually available after accounting for planned and unplanned outages. The bottom panel shows the number of active nuclear reactors by year (in blue) and dashed extensions indicating the number of additional reactors that were under construction during each year. The average construction time was slightly more than 7 years.

Also indicated are the times of the Three Mile Island (1979) and Chernobyl (1986) nuclear accidents.

Data presented is from the International Atomic Energy Agency, principally "Nuclear Power Reactors in the World" [[http://www-pub.iaea.org/MTCD/publications/PDF/RDS2-26\\_web.pdf](http://www-pub.iaea.org/MTCD/publications/PDF/RDS2-26_web.pdf)] with additions received by direct communication.

**Author:** Robert A. Rohde for the Global Warming Art project.

(10) World energy consumption outlook from the International Energy Outlook



**Page:** Nuclear power

**Description:** World energy consumption outlook from the International Energy Outlook, published by the U.S. DOE Energy Information Administration 2011

**Date:** 19 September 2011

**Source:** International Energy Outlook [[www.eia.gov](http://www.eia.gov)]

**Author:** EIA

## **(11) Cost of electricity by source**

### **Page: Cost of electricity by source**

#### **(11-A) US Department of Energy estimates**

The tables below list the estimated cost of electricity by source for plants entering service in 2017. The tables are from a January 23, 2012 report of the Energy Information Administration (EIA) of the U.S. Department of Energy (DOE) called "Levelized Cost of New Generation Resources in the Annual Energy Outlook 2012"<sup>[10]</sup>.

- **Total System Levelized Cost** (the rightmost column) gives the dollar cost per megawatt-hour that must be charged over time in order to pay for the total cost. Divide by 1000 to get the cost per kilowatt-hour (move the decimal point 1 place to the left to get the cost in cents/kWh).

These calculations reflect an adjustment to account for the high level of carbon dioxide produced by coal plants. From the EIA report:

"a 3-percentage point increase in the cost of capital is added when evaluating investments in greenhouse gas (GHG) intensive technologies like coal-fired power and coal-to-liquids (CTL) plants without carbon control and sequestration (CCS). While the 3-percentage point adjustment is somewhat arbitrary, in levelized cost terms its impact is similar to that of a \$15 per metric ton of carbon dioxide (CO<sub>2</sub>) emissions fee. ... As a result, the levelized capital costs of coal-fired plants without CCS are higher than would otherwise be expected."<sup>[10]</sup>

No tax credits or incentives are incorporated in the tables. From the EIA report (emphasis added):

"Levelized cost represents the present value of the total cost of building and operating a generating plant over an assumed financial life and duty cycle, converted to equal annual payments and expressed in terms of real dollars to remove the impact of inflation. Levelized cost reflects overnight capital cost, fuel cost, fixed and variable O&M cost, financing costs, and an assumed utilization rate for each plant type. The availability of various incentives including state or federal tax credits can also impact the calculation of levelized cost. The values shown in the tables below do not incorporate any such incentives."<sup>[10]</sup>

Incentives, tax credits, production mandates, etc. are discussed in the overall comprehensive EIA report: "Annual Energy Outlook 2012"<sup>[11-13]</sup>.

Photovoltaics (solar PV) can be used both by distributed residential or commercial users and utility scale power plants. The costs shown are for utility scale photovoltaic power plants<sup>[10]</sup>.

**Estimated Levelized Cost of New Generation Resources, 2017<sup>[10]</sup>**

**U.S. Average Levelized Cost for Plants Entering Service in 2017 (2010 USD/MWh)**

<b>Plant Type</b>	<b>Capacity Factor (%)</b>	<b>Levelized Capital Cost</b>	<b>Fixed O&amp;M</b>	<b>Variable O&amp;M (including fuel)</b>	<b>Transmission Investment</b>	<b>Total System Levelized Cost</b>
Conventional Coal	85	65.8	4.0	28.6	1.2	99.6
Advanced Coal	85	75.2	6.6	29.2	1.2	112.2
Advanced Coal with CCS	85	93.3	9.3	36.8	1.2	140.7
Natural Gas Fired						
Conventional Combined Cycle	87	17.5	1.9	48.0	1.2	68.6
Advanced Combined Cycle	87	17.9	1.9	44.4	1.2	65.5
Advanced CC with CCS	87	34.9	4.0	52.7	1.2	92.8
Conventional Combustion Turbine	30	46.0	2.7	79.9	3.6	132.0
Advanced Combustion Turbine	30	31.7	2.6	67.5	3.6	105.3
Advanced Nuclear	90	88.8	11.3	11.6	1.1	112.7
Geothermal	92	76.6	11.9	9.6	1.5	99.6
Biomass	83	56.8(MC (Yi=0)=*26.5)	13.8	48.3	1.3	120.2
Wind <sup>1</sup>	34	83.3	9.7	0.0	3.7	96.8
Wind — Offshore <sup>a</sup>	27	300.6	22.4	0.0	7.7	330.6
Solar PV <sup>a,b</sup>	25	144.9	7.7	0.0	4.2	156.9
Solar Thermal <sup>a</sup>	20	204.7	40.1	0.0	6.2	251.0
Hydro <sup>a</sup>	53	76.9	4.0	6.0	2.1	89.9

<sup>a</sup> Non-dispatchable (Hydro is dispatchable within a season, but nondispatchable overall-limited by site and season)

<sup>b</sup> Costs are expressed in terms of net AC power available to the grid for the installed capacity



**Regional Variation in Levelized Costs of New Generation Resources, 2017<sup>[11]</sup>**

Plant Type	Range for Total System Levelized Costs (2010 USD/MWh)		
	Minimum	Average	Maximum
Conventional Coal	90.1	99.6	116.3
Advanced Coal	103.9	112.2	126.1
Advanced Coal with CCS	129.6	140.7	162.4
Natural Gas Fired			
Conventional Combined Cycle	61.8	68.6	88.1
Advanced Combined Cycle	58.9	65.5	83.3
Advanced CC with CCS	82.8	92.8	110.9
Conventional Combustion Turbine	94.6	132.0	164.1
Advanced Combustion Turbine	80.4	105.3	133.0
Advanced Nuclear	108.4	112.7	120.1
Geothermal	85.0	99.6	113.9
Biomass	101.5	120.2	142.8
Wind - Onshore	78.2	96.8	114.1
Wind - Offshore	307.3	330.6	350.4
Solar PV	122.2	156.9	245.6
Solar Thermal	182.7	251.0	400.7
Hydro <sup>[14]</sup>	57.8	88.9	147.6

- O&M = operation and maintenance.
- CC = combined cycle.
- CCS = carbon capture and sequestration.
- PV = photovoltaics.
- GHG = greenhouse gas.

### (11-B) UK 2010 estimates

In March 2010, a new report on UK levelised generation costs was published by Parsons Brinckerhoff<sup>[15]</sup>. It puts a range on each cost due to various uncertainties. Combined cycle gas turbines without CO<sub>2</sub> capture are not directly comparable to the other low carbon emission generation technologies in the PB study. The assumptions used in this study are given in the report.

#### UK energy costs for different generation technologies in pounds per megawatt hour (2010)

Technology	Cost range (£/MWh) <sup>1</sup>
New nuclear	80–105
Onshore wind	80–110
Biomass	60–120
Natural gas turbines with CO <sub>2</sub> capture	60–130
Coal with CO <sub>2</sub> capture	100–155
Solar farms	125–180
Offshore wind	150–210
Natural gas turbine, no CO <sub>2</sub> capture	55–110
Tidal power	155–390

Divide the above figures by 10 to obtain the price in pence per kilowatt-hour.

More recent UK estimates are the Mott MacDonald study released by DECC in June 2010<sup>[16]</sup> and the Arup study for DECC published in 2011<sup>[17]</sup>.

### (11-C) French 2011 estimates

The International Agency for the Energy and EDF have estimated for 2011 the following costs. For the nuclear power they include the costs due to new safety investments to upgrade the French nuclear plant after the Fukushima Daiichi nuclear disaster; the cost for those investments is estimated at 4 €/MWh. Concerning the solar power the estimate at 293 €/MWh is for a large plant capable to produce in the range of 50-100 GWh/year located in a favorable location (such as in Southern Europe). For a small household plant capable to produce typically around 3 MWh/year the cost is according to the location between 400 and 700 €/MWh. Currently solar power is by far the most expensive renewable source to produce electricity, although increasing efficiency and longer lifespan of photovoltaic panels together with reduced production costs could make this source of energy more competitive.

#### French energy costs for different generation technologies in Euros per megawatt hour (2011)

Technology	Cost (€/MWh)
Hydro power	20
Nuclear	50
Natural gas turbines without CO <sub>2</sub> capture	61
Onshore wind	69
Solar farms	293

### (11-D) Analysis from different sources

A draft report of LECs used by the California Energy Commission is available<sup>[18]</sup>. From this report, the price per MWh for a municipal energy source is shown here:

#### California levelized energy costs for different generation technologies in US dollars per megawatt hour (2007)

Technology	Cost (USD/MWh)
Advanced Nuclear	67
Coal	74–88
Gas	87–346
Geothermal	67
Hydro power	48–86
Wind power	60
Solar	116–312
Biomass	47–117
Fuel Cell	86–111
Wave Power	611

Note that the above figures incorporate tax breaks for the various forms of power plants. Subsidies range from 0% (for Coal) to 14% (for nuclear) to over 100% (for solar).

The following table gives a selection of LECs from two major government reports from Australia<sup>[19, 20]</sup>. Note that these LECs do *not* include any cost for the greenhouse gas emissions (such as under carbon tax or emission trading scenarios) associated with the different technologies.

#### Levelised energy costs for different generation technologies in Australian dollars per megawatt hour (2006)

Technology	Cost (AUD/MWh)
Nuclear (to COTS plan) <sup>[20]</sup>	40–70
Nuclear (to suit site; typical) <sup>[20]</sup>	75–105
Coal	28–38
Coal: IGCC + CCS	53–98
Coal: supercritical pulverized + CCS	64–106
Open-cycle Gas Turbine	101
Hot fractured rocks	89
Gas: combined cycle	37–54
Gas: combined cycle + CCS	53–93
Small Hydro power	55
Wind power: high capacity factor	63
Solar thermal	85
Biomass	88
Photovoltaics	120

In 1997 the Trade Association for Wind Turbines (Wirtschaftsverband Windkraftwerke e.V. – WWV) ordered a study into the costs of electricity production in newly constructed conventional power plants from the Rheinisch-Westfälischen Institute for Economic Research –RWI). The RWI predicted costs of electricity production per kWh for the basic load for the year 2010 as follows:

<b>Fuel</b>	<b>Cost per kilowatt hour in euro cents.</b>
Nuclear Power	10.7 €ct – 12.4 €ct
Brown Coal (Lignite)	8.8 €ct – 9.7 €ct
Black Coal (Bituminous)	10.4 €ct – 10.7 €ct
Natural gas	11.8 €ct – 10.6 €ct.

The part of a base load represents approx. 64% of the electricity production in total. The costs of electricity production for the mid-load and peak load are considerably higher. There is a mean value for the costs of electricity production for all kinds of conventional electricity production and load profiles in 2010 which is 10.9 €ct to 11.4 €ct per kWh. The RWI calculated this on the assumption that the costs of energy production would depend on the price development of crude oil and that the price of crude oil would be approx. 23 US\$ per barrel in 2010. In fact the crude oil price is about 80 US\$ in the beginning of 2010. This means that the effective costs of conventional electricity production still need to be higher than estimated by the RWI in the past.

The WWV takes the legislative feed-in-tariff as basis for the costs of electricity production out of renewable energies because renewable power plants are economically feasible under the German law (German Renewable Energy Sources Act-EEG).

The following figures arise for the costs of electricity production in newly constructed power plants in 2010:

<b>Energy source</b>	<b>Costs of electricity production in euros per megawatt hour</b>
Nuclear Energy	107.0 – 124.0
Brown Coal	88.0 – 97.0
Black Coal	104.0 – 107.0
Domestic Gas	106.0 – 118.0
Wind Energy Onshore	49.7 – 96.1
Wind Energy Offshore	35.0 – 150.0
Hydropower	34.7 – 126.7
Biomass	77.1 – 115.5
Solar Electricity	284.3 – 391.4

## References

- [10] Levelized Cost of New Generation Resources in the Annual Energy Outlook 2011. Released January 23, 2012. Report of the US Energy Information Administration (EIA) of the U.S. Department of Energy (DOE).
- [11] Energy Information Administration, Annual Energy Outlook 2012. June 2012, DOE/EIA-0383(2012).
- [12] Assumptions to the Annual Energy Outlook 2011. U.S. Energy Information Administration of the U.S. Department of Energy.
- [13] Appendix A: Handling of Federal and Selected State Legislation and Regulation in the Annual Energy Outlook. US Energy Information Administration of the U.S. Department of Energy.
- [14] [http://www.eia.gov/forecasts/aeo/electricity\\_generation.cfm](http://www.eia.gov/forecasts/aeo/electricity_generation.cfm)
- [15] "Powering the Nation". Parsons Brinckerhoff. 2010. Retrieved 16 February 2012.
- [16] "Mott MacDonald study released by DECC in June 2010" (PDF). Retrieved 2012-09-04.
- [17] Ove Arup & Partners Ltd (October 2011). "Review of the generation costs and deployment potential of renewable electricity technologies in the UK" (PDF). London: Department of Energy and Climate Change. Retrieved 16 February 2012.
- [18] "Comparative Costs of California Central Station Electricity Generation Technologies" (PDF). Retrieved 2012-09-04.
- [19] Graham, P. The heat is on: the future of energy in Australia CSIRO, 2006
- [20] Switkowski, Z. Uranium Mining, Processing and Nuclear Energy Review UMPNER taskforce, Australian Government, 2006

## (12) Environmental impact of electricity generation

### (12-A) Water usage

The amount of water usage is often of great concern for electricity generating systems as populations increase and droughts become a concern. Still, according to the U.S. Geological Survey, thermoelectric power generation accounts for only 3.3 percent of net freshwater consumption with over 80 percent going to irrigation. Likely future trends in water consumption are covered here<sup>[1]</sup>. General numbers for fresh water usage of different power sources are shown below.

**Water usage (gal/MW-h)**

<b>Power source</b>	<b>Low case</b>	<b>Medium/Average case</b>	<b>High case</b>
Nuclear power	400 (once-through cooling)	400 to 720 (pond cooling)	720 (cooling towers)
Coal	300		480
Natural gas	100 (once-through cycle)		180 (with cooling towers)
Hydroelectricity		1,430	
Solar thermal		1,060	
Geothermal	1,800		4,000
Biomass	300		480
Solar photovoltaic		30	
Wind power	.5	1	2.2

### References

[1] AAAS Annual Meeting 17–21 February 2011, Washington DC. Sustainable or Not? Impacts and Uncertainties of Low-Carbon Energy Technologies on Water. Dr Evangelos Tzimas, European Commission, JRC Institute for Energy, Petten, Netherlands

## **(13) Hydraulic fracturing**

### **(13-A) Air**

The air emissions from hydraulic fracturing are related to methane leaks originating from wells, and emissions from the diesel or natural gas powered equipment such as compressors, drilling rigs, pumps etc.<sup>[34]</sup>. Also transportation of necessary water volume for hydraulic fracturing, if done by trucks, can cause high volumes of air emissions, especially particulate matter emissions<sup>[65]</sup>.

Shale gas produced by hydraulic fracturing causes higher well-to-burner emissions than conventional gas. This is mainly due to the gas released during completing wells as some gas returns to the surface, together with the fracturing fluids. Depending on their treatment, the well-to-burner emissions are 3.5%–12% higher than for conventional gas<sup>[56]</sup>. According to a study conducted by professor Robert W. Howarth et al. of Cornell University, "3.6% to 7.9% of the methane from shale-gas production escapes to the atmosphere in venting and leaks over the lifetime of a well." The study claims that this represents a 30–100% increase over conventional gas production<sup>[66]</sup>. Methane gradually breaks down in the atmosphere, forming carbon dioxide, which contributes to greenhouse gasses more than coal or oil for timescales of less than fifty years<sup>[66,67]</sup>. Howarth's colleagues at Cornell and others have criticized the study's design<sup>[68,69]</sup>, however several other studies have also found higher emissions from shale-gas production than from conventional gas production<sup>[70-73]</sup>. Howarth et al. have responded, "The latest EPA estimate for methane emissions from shale gas falls within the range of our estimates but not those of Cathles et al, which are substantially lower."<sup>[74]</sup>

In some areas, elevated air levels of harmful substances have coincided with elevated reports of health problems among the local populations. In DISH, Texas, elevated substance levels were detected and traced to hydraulic fracturing compressor stations<sup>[75]</sup>, and people living near shale gas drilling sites complained of health problems<sup>[76]</sup>; though a causal relationship to hydraulic fracturing was not established<sup>[76]</sup>.

### **(13-B) Water Consumption**

The large volumes of water required have raised concerns about hydraulic fracturing in arid areas, such as Karoo in South Africa<sup>[57]</sup>. During periods of low stream flow it may affect water supplies for municipalities and industries such as power generation, as well as recreation and aquatic life. It may also require water overland piping from distant sources<sup>[77]</sup>.

Hydraulic fracturing uses between 1.2 and 3.5 million US gallons (4.5 and 13 Ml) of water per well, with large projects using up to 5 million US gallons (19 Ml). Additional water is used when wells are refractured; this may be done several times<sup>[41, 78]</sup>. An average well requires 3 to 8 million US gallons (11,000 to 30,000 m<sup>3</sup>) of water over its lifetime<sup>[34, 77-79]</sup>. Using the case of the Marcellus Shale as an example, as of 2008 hydraulic fracturing accounted for 650 million US gallons per year (2,500,000 m<sup>3</sup>/y) or less than 0.8% of annual water use in the area overlying the Marcellus Shale<sup>[77, 80]</sup>. The annual number of well permits, however, increased by a factor of five<sup>[81]</sup> and the number of well starts increased by a factor of over 17 from 2008 to 2011<sup>[82]</sup>. According to the Oxford Institute for Energy Studies, greater volumes of fracturing fluids are required in Europe, where the shale depths average 1.5 times greater than in the U.S.<sup>[83]</sup>. To minimize water consumption, recycling is one possible option<sup>[56]</sup>.

### **References**

[34] Ground Water Protection Council; ALL Consulting (April 2009) (PDF). Modern Shale Gas Development in the United States: A Primer (Report). DOE Office of Fossil Energy and National Energy Technology Laboratory. pp. 56–66. DE-FG26-04NT15455. Retrieved 24 February 2012.

[41] Andrews, Anthony et al. (30 October 2009) (PDF). Unconventional Gas Shales: Development, Technology, and Policy Issues (Report). Congressional Research Service. p. 7; 23. Retrieved 22 February 2012.

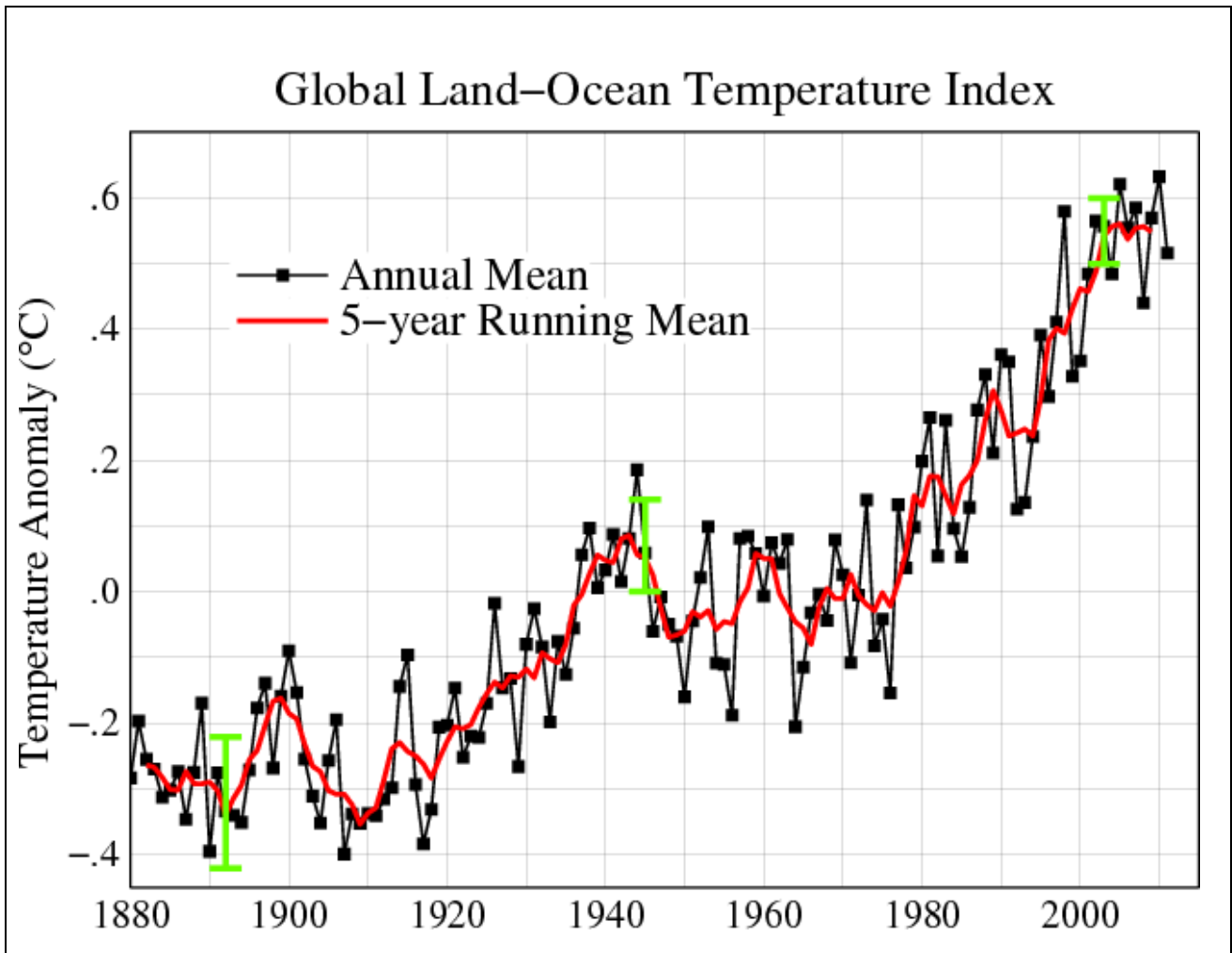
- [56] IEA (2011). *World Energy Outlook 2011*. OECD. pp. 91; 164. ISBN 9789264124134.
- [57] Urbina, Ian (30 December 2011). "Hunt for Gas Hits Fragile Soil, and South Africans Fear Risks". *The New York Times*. Retrieved 23 February 2012. "Covering much of the roughly 800 miles between Johannesburg and Cape Town, this arid expanse – its name [Karoo] means "thirsty land" – sees less rain in some parts than the Mojave Desert."
- [65] Fernandez, John Michael; Gunter, Matthew (PDF). *Hydraulic Fracturing: Environmentally Friendly Practices*. Houston Advanced Research Center. Retrieved 2012-12-29.
- [66] Howarth, Robert W.; Santoro, Renee; Ingraffea, Anthony (13 March 2011). "Methane and the greenhouse-gas footprint of natural gas from shale formations" (PDF). *Climatic Change (Springer)* 106 (4): 679–690. doi:10.1007/s10584-011-0061-5. Retrieved 2012-05-07.
- [67] Howarth, Robert W.; Ingraffea, Anthony (15 September 2011). "Should Fracking Stop? Extracting gas from shale increases the availability of this resource, but the health and environmental risks may be too high. Point: Yes, it's too high risk". *Nature (477)*: 271–275. Bibcode 2011Natur.477..271H. doi:10.1038/477271a.
- [68] Cathles, Lawrence M.; Brown, Larry; Taam, Milton; Hunter, Andrew (2011). *Climatic Change*. doi:10.1007/s10584-011-0333-0.
- [69] Leahy, Stephen (24 January 2012). "Shale Gas a Bridge to More Global Warming". IPS. Retrieved 4 February 2012.
- [70] Skone, Timothy J. (12 May 2011). "Life Cycle Greenhouse Gas Analysis of Natural Gas Extraction & Delivery in the United States" (PDF). National Energy Technology Laboratory. Retrieved 4 February 2012.
- [71] Jiang, Mohan; Griffin, W Michael; Hendrickson, Chris; Jaramillo, Paulina; VanBriesen, Jeanne; Venkatesh, Aranya (2011). "Life cycle greenhouse gas emissions of Marcellus shale gas" (PDF). *Environmental Research Letters (IOP Publishing)* 6 (3). Bibcode 2011ERL.....6c4014J. doi:10.1088/1748-9326/6/3/034014. Retrieved 4 February 2012.
- [72] Hultman, Nathan; Rebois, Dylan; Scholten, Michael; Ramig, Christopher (2011). "The greenhouse impact of unconventional gas for electricity generation" (PDF). *Environmental Research Letters (IOP Publishing)* 6 (4). Bibcode 2011ERL.....6d4008H. doi:10.1088/1748-9326/6/4/044008. Retrieved 4 February 2012.
- [73] Lashof, Dan (12 April 2011). "Natural Gas Needs Tighter Production Practices to Reduce Global Warming Pollution". Natural Resources Defense Council. Retrieved 4 February 2012.
- [74] Howarth, Robert W.; Santoro, Renee; Ingraffea, Anthony (1 February 2012). "Venting and leaking of methane from shale gas development: Response to Cathles et al." (PDF). *Climatic Change (Springer)*. doi:10.1007/s10584-012-0401-0. Retrieved 4 February 2012.
- [75] Biello, David (30 March 2010). "Natural gas cracked out of shale deposits may mean the U.S. has a stable supply for a century – but at what cost to the environment and human health?". *Scientific American*. Retrieved 23 March 2012.
- [76] Schmidt, Charles (1 August 2011). "Blind Rush? Shale Gas Boom Proceeds Amid Human Health Questions". *Environmental Health Perspectives* 119 (8): a348-a353. doi:10.1289/ehp.119-a348. Retrieved 23 March 2012.
- [77] Arthur, J. Daniel; Uretsky, Mike; Wilson, Preston (May 5–6, 2010). "Water Resources and Use for Hydraulic Fracturing in the Marcellus Shale Region" (PDF). Meeting of the American Institute of Professional Geologists. Pittsburgh: ALL Consulting. p. 3. Retrieved 2012-05-09.
- [78] Abdalla, Charles W.; Drohan, Joy R. (2010) (PDF). *Water Withdrawals for Development of Marcellus Shale Gas in Pennsylvania. Introduction to Pennsylvania's Water Resources (Report)*. The Pennsylvania State University. Retrieved 16 September 2012. "Hydrofracturing a horizontal Marcellus well may use 4 to 8 million gallons of water, typically within about 1 week. However, based on experiences in other major U.S. shale gas fields, some Marcellus wells may need to be hydrofractured several times over their productive life (typically five to twenty years or more)"
- [79] Cothren, Jackson (PDF). *Modeling the Effects of Non-Riparian Surface Water Diversions on Flow Conditions in the Little Red Watershed (Report)*. U. S. Geological Survey, Arkansas Water Science Center Arkansas Water Resources Center, American Water Resources Association, Arkansas State Section Fayetteville Shale Symposium 2012. p. 12. Retrieved 16 September 2012. "...each well requires between 3 and 7 million gallons of water for hydraulic fracturing and the number of wells is expected to grow in the future"
- [80] Satterfield, J; Mantell; Kathol, D; Hiebert, F; Patterson, K; Lee, R (September 2008). "Managing Water Resource's Challenges in Select Natural Gas Shale Plays". GWPC Annual Meeting. ALL Consulting.



- [81] "Unconventional well drilling permits". Marcellus Center. Marcellus Center, Pennsylvania State University. 2012. Retrieved 2012-09-16.
- [82] "Horizontal drilling boosts Pennsylvania's natural gas production". EIA. 23 May 2012. Retrieved 2012-09-16.
- [83] Faucon, Benoît (17 September 2012). "Shale-Gas Boom Hits Eastern Europe". WSJ.com. Retrieved 17 September 2012.

**Section 4 – Effects on climate**  
(From Wikipedia, 20 January 2013)

**(1) Global-Land Ocean Temperature Index, from 1880 to present**



**Page: Global Warming**

**Description:** Line plot of global mean land-ocean temperature index, 1880 to present, with the base period 1951-1980. The black line is the annual mean and the red line is the five-year running mean. The green bars show uncertainty estimates. [This is an update of Fig. 1A in Hansen et al. (2006).] The graph shows an overall long-term warming trend. In the 1890s, the global temperature anomaly was on average slightly below  $-0.3\text{ }^{\circ}\text{C}$ , with an error range of roughly  $-0.2$  and  $-0.4\text{ }^{\circ}\text{C}$ . In the 1940s, the global temperature anomaly was on average slightly below  $+0.1\text{ }^{\circ}\text{C}$ , with an error range of roughly  $0.0$  and  $+0.15\text{ }^{\circ}\text{C}$ . In the 2000s, the global temperature anomaly was on average slightly below  $+0.6\text{ }^{\circ}\text{C}$ , with an error range of roughly  $+0.6$  and  $+0.5\text{ }^{\circ}\text{C}$ .

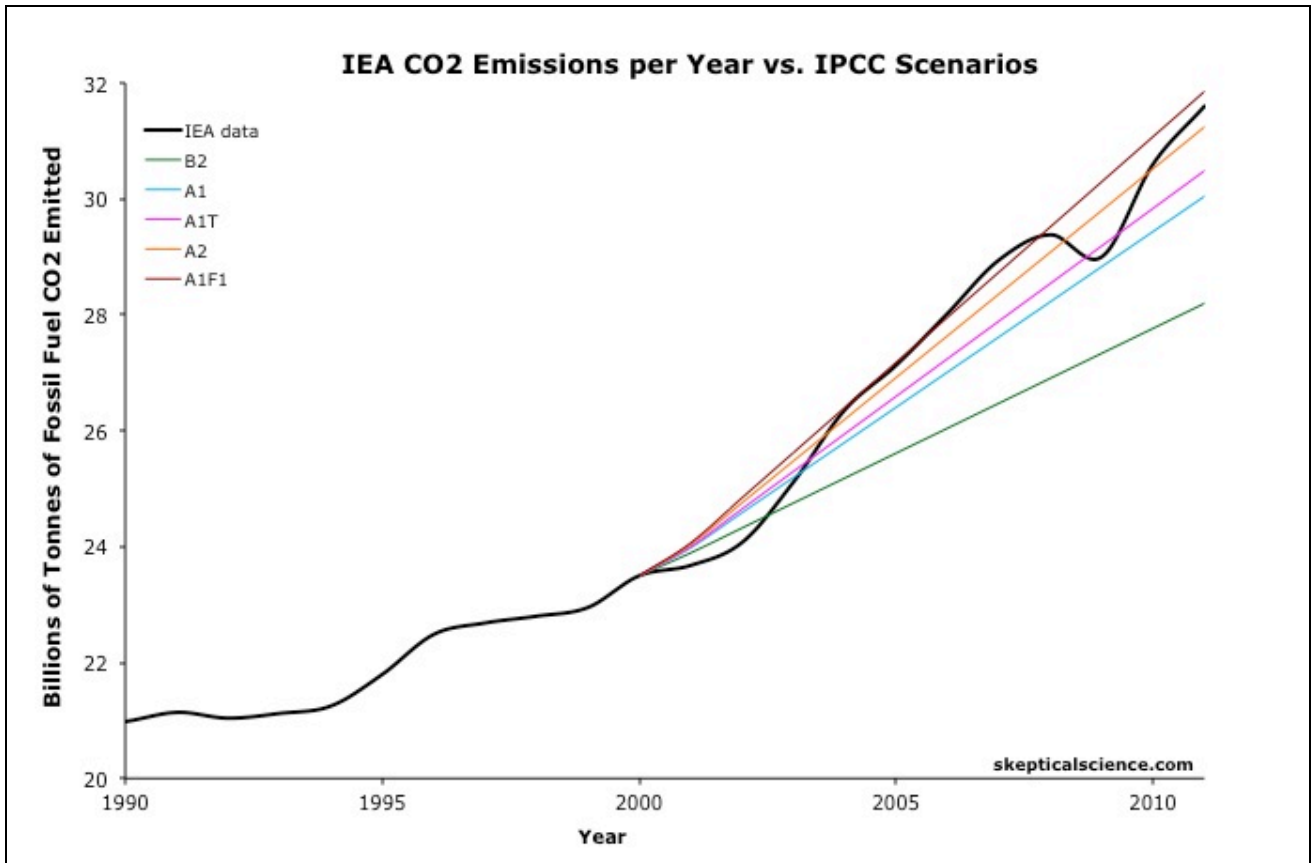
**Date:** 10 February 2011

**Source:** <http://data.giss.nasa.gov/gistemp/>

**Author:** NASA Goddard Institute for Space Studies

**Other versions:** PDF version: File:Global\_Temperature\_Anomaly\_1880-2010\_(Fig.A).pdf. SVG version (1880-2010 data, 1961-1990 base period): File:Instrumental\_Temperature\_Record (NASA).svg

## (2) CO<sub>2</sub> emissions per years vs. IPCC scenarios



### Page: Global Warming

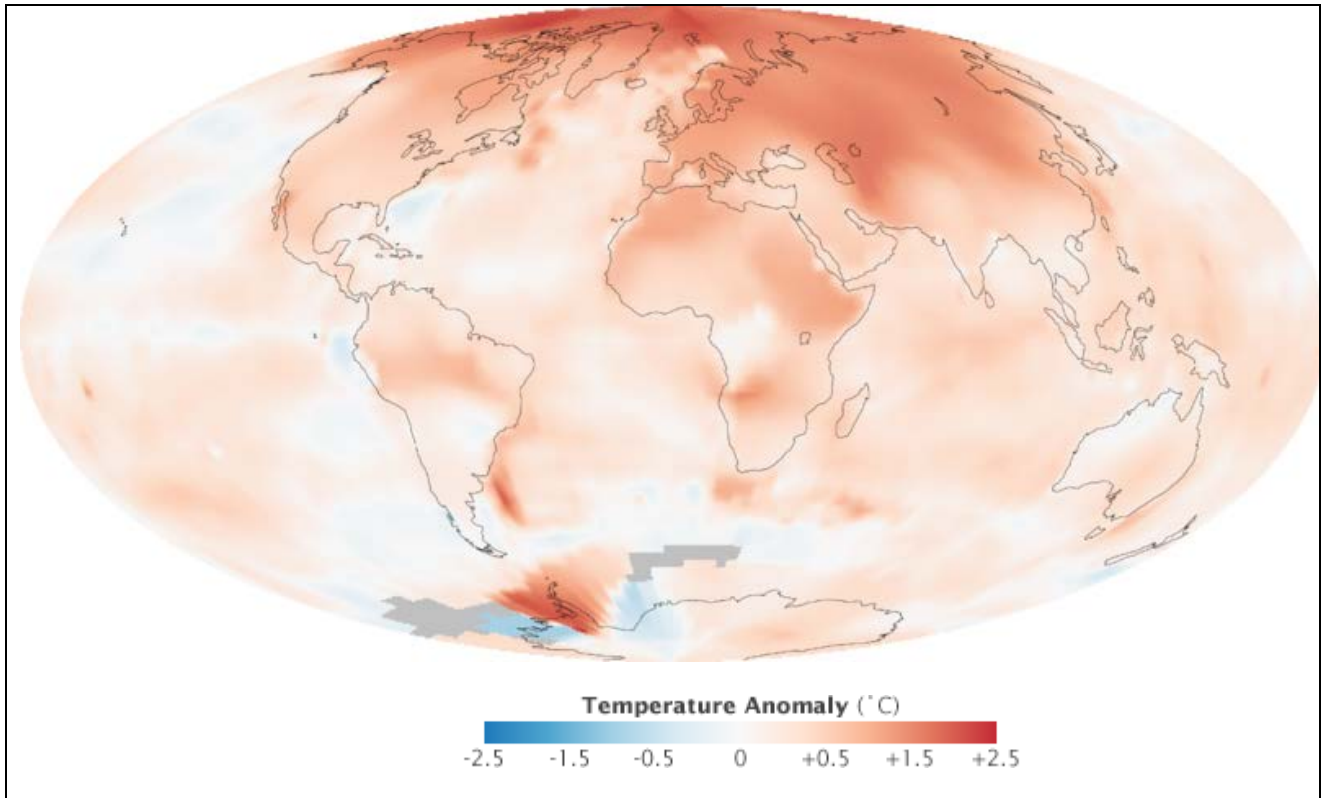
**Description:** Shows in graphic form the projected increase in carbon dioxide (CO<sub>2</sub>) emissions from fossil fuels in five of the emissions scenarios used by the International Panel on Climate Change (IPCC), compared to the International Energy Agency's (IEA's) actual observational CO<sub>2</sub> emissions data from fossil fuel consumption. Data from IPCC emissions scenarios; Data spreadsheet included with International Energy Agency's "CO<sub>2</sub> Emissions from Fuel Combustion 2011 - Highlights"; and Supplemental 2010 IEA data; and Supplemental 2011 IEA data.

**Date:** 2011-06-3

**Source:** <http://www.skepticalscience.com/graphics.php>

**Author:** Dana Nuccitelli

### (3) Temperature variations in the decade 2000-2009



#### **Page: Global Warming**

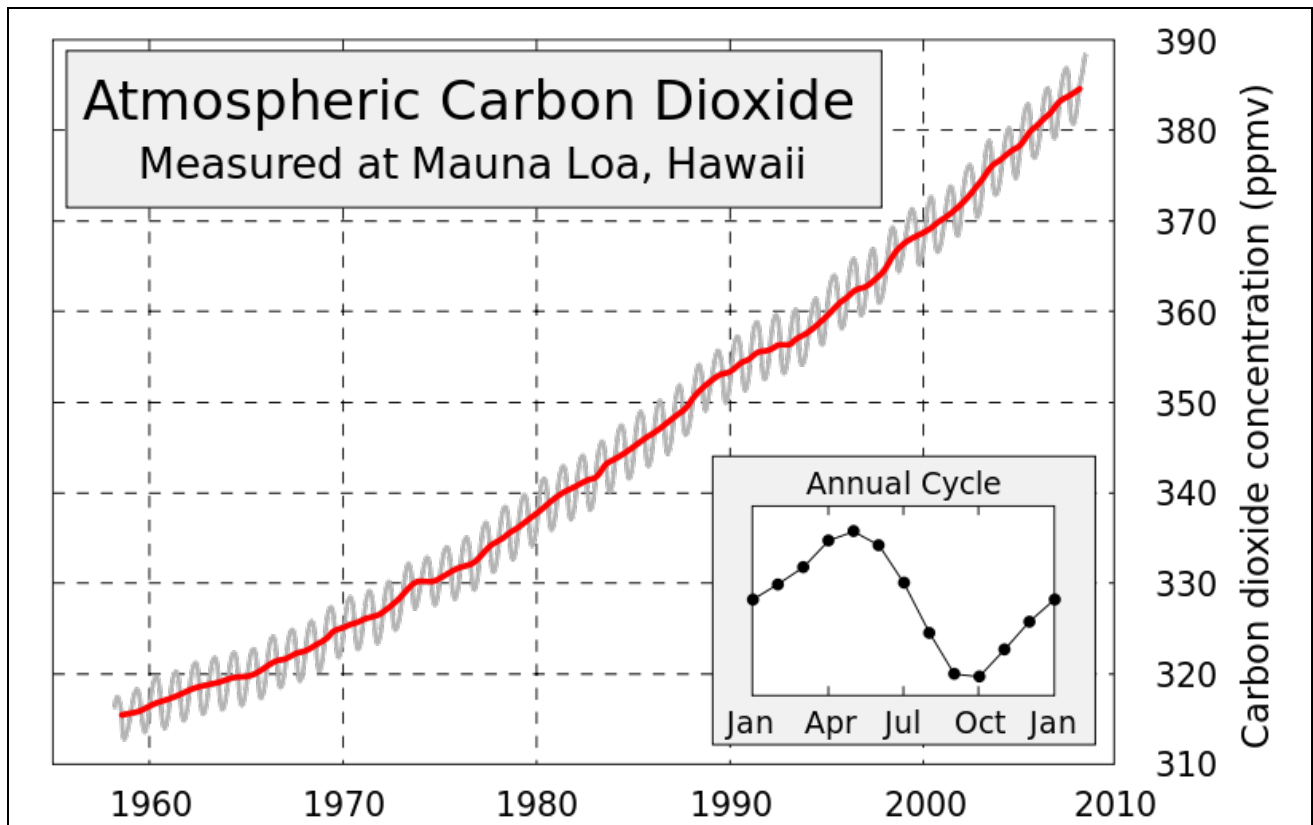
**Description:** The map illustrates just how much warmer temperatures were in the decade (2000-2009) compared to average temperatures recorded between 1951 and 1980 (a common reference period for climate studies). The most extreme warming, shown in red, was in the Arctic. Very few areas saw cooler than average temperatures, shown in blue. Gray areas over parts of the Southern Ocean are places where temperatures were not recorded. The analysis, conducted by the Goddard Institute for Space Studies (GISS) in New York City, is based on temperatures recorded at meteorological (weather) stations around the world and satellite data over the oceans.

**Date:** 22 January 2010

**Source:** NASA Earth Observatory Image of the Day: 2009 Ends Warmest Decade on Record <http://earthobservatory.nasa.gov/IOTD/view.php?id=42392>

**Author:** NASA images by Robert Simmon, based on data from the Goddard Institute for Space Studies.

#### (4) Atmospheric CO<sub>2</sub> measured at Mauna Loa, Hawaii, from 1960 to 2008



#### Page: Carbon dioxide in Earth's atmosphere

**Description:** This figure shows the history of atmospheric carbon dioxide concentrations as directly measured at Mauna Loa, Hawaii. This curve is known as the Keeling curve, and is an essential piece of evidence of the man-made increases in greenhouse gases that are believed to be the cause of global warming. The longest such record exists at Mauna Loa, but these measurements have been independently confirmed at many other sites around the world [<http://cdiac.ornl.gov/trends/co2/contents.htm>].

The annual fluctuation in carbon dioxide is caused by seasonal variations in carbon dioxide uptake by land plants. Since many more forests are concentrated in the Northern Hemisphere, more carbon dioxide is removed from the atmosphere during Northern Hemisphere summer than Southern Hemisphere summer. This annual cycle is shown in the inset figure by taking the average concentration for each month across all measured years.

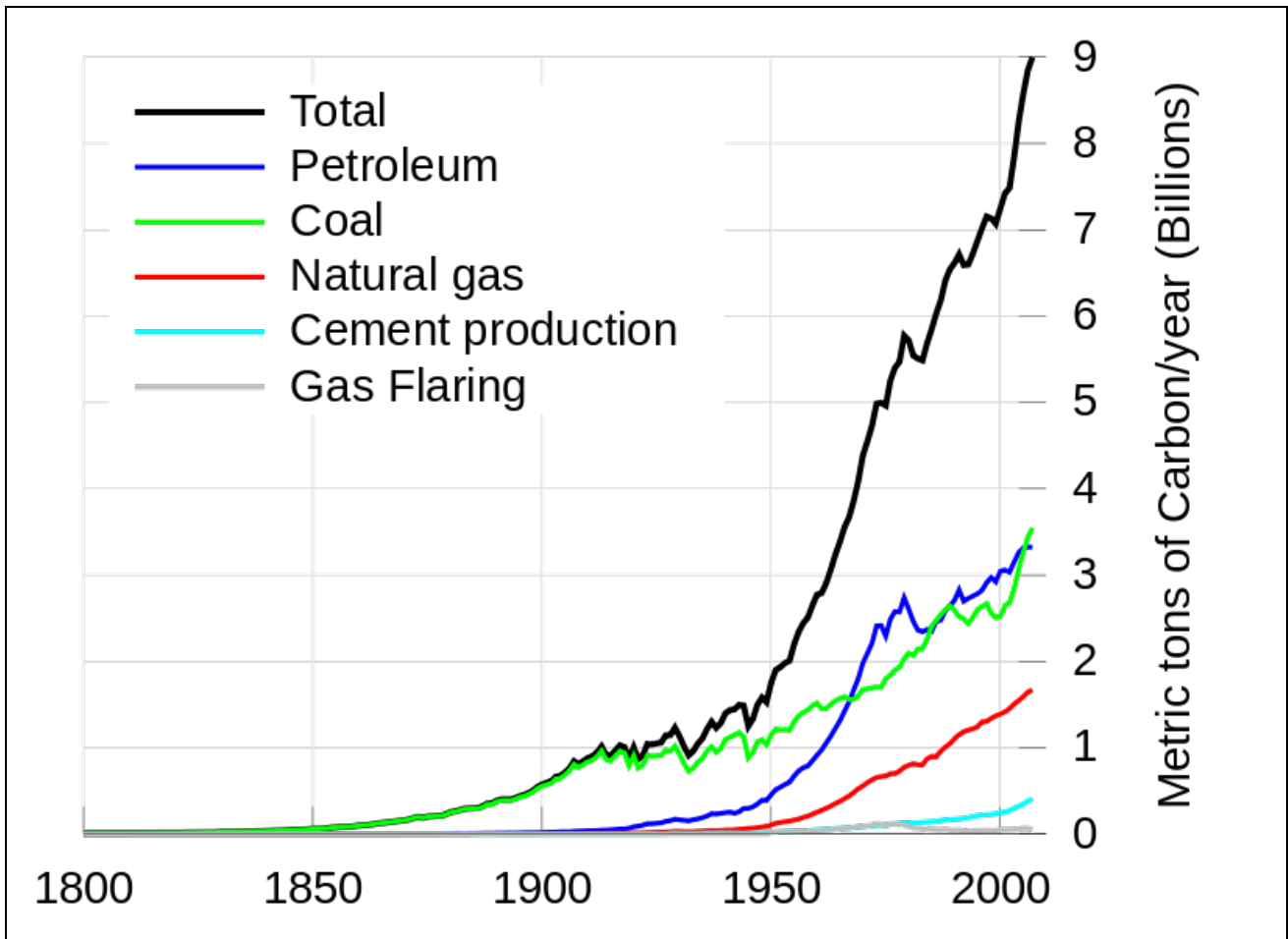
The grey curve shows the average monthly concentrations, and red curve is a moving 12 month average.

**Date:** 23 April 2008

**Source:** Own work, from Image:Mauna Loa Carbon Dioxide.png, uploaded in Commons by Nils Simon under licence GFDL & CC-NC-SA ; itself created by Robert A. Rohde from NOAA published data and is incorporated into the Global Warming Art project.

**Author:** Sémhur

(5) Global annual fossil fuel CO<sub>2</sub> emissions, from 1800 to 2007



**Page: Carbon dioxide in Earth's atmosphere**

**Description:** Global annual fossil fuel carbon dioxide emissions through year 2007, in million metric tons of carbon, as reported by the Carbon Dioxide Information Analysis Center [1].

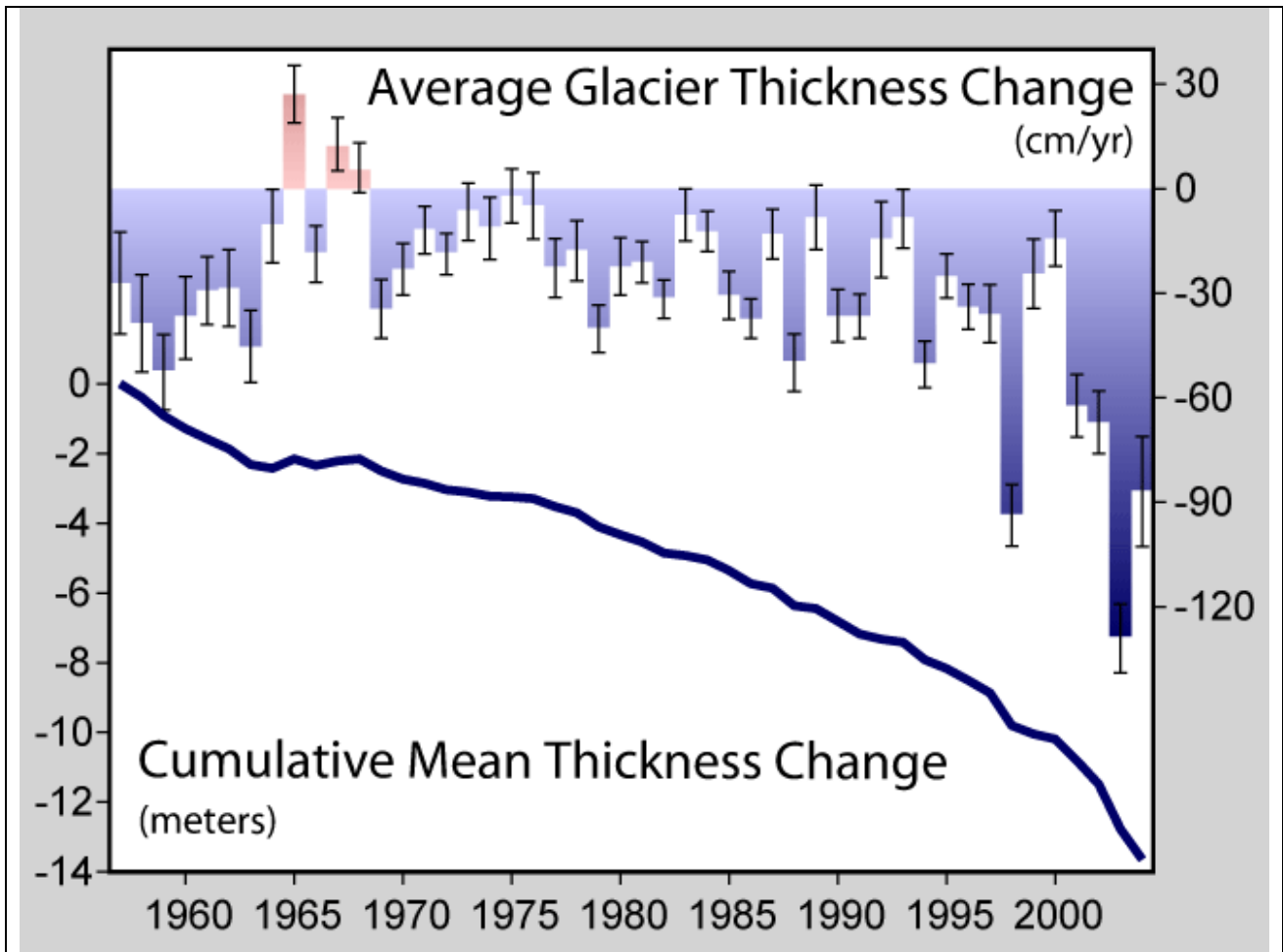
**Date:** 2010-07-12

**Source:** <http://cdiac.ornl.gov/ftp/ndp030/CSV-FILES/>  
and Global\_Carbon\_Emission\_by\_Type\_to\_Y2004.png

**Original Data citation:** "Marland, G., T.A. Boden, and R. J. Andres. 2007. Global, Regional, and National CO<sub>2</sub> Emissions. In Trends: A Compendium of Data on Global Change. Carbon Dioxide Information Analysis Center, Oak Ridge National Laboratory, United States Department of Energy, Oak Ridge, Tenn., U.S.A."

**Author:** Global\_Carbon\_Emission\_by\_Type\_to\_Y2004.png: Mak Thorpe

(6) Average rate of glacier thickness change, from 1955 to 2004



**Page: Retreat of Glaciers since 1850**

**Summary:** This figure shows the average rate of thickness change in mountain glaciers around the world. This information, known as the glaciological mass balance, is found by measuring the annual snow accumulation and subtracting surface ablation driven by melting, sublimation, or wind erosion. These measurements do not account for thinning associated with iceberg calving, flow related thinning, or subglacial erosion. All values are corrected for variations in snow and firn density and expressed in meters of water equivalent (Dyurgerov 2002).

Measurements are shown as both the annual average thickness change and the accumulated change during the fifty years of measurements presented. Years with a net increase in glacier thickness are plotted upwards and in red; years with a net decrease in glacier thickness (i.e. positive thinning) are plotted downward and in blue. Only three years in the last 50 have experienced thickening in the average.

Systematic measurements of glacier thinning began in the 1940s, but fewer than 15 sites had been measured each year until the late 1950s. Since then more than 100 sites have contributed to the average in some years (Dyurgerov 2002, Dyurgerov and Meier 2005). Error bars indicate the standard error in the mean.

Other observations, based on glacier length records, suggest that glacier retreat has occurred nearly continuously since the early 1800s and the end of the little ice age, but variations in rate have occurred, including a significant acceleration during the twentieth century that is believed to have been a response to global warming (Oerlemans 2005).

**Data:** These measurements are described in Dyurgerov (2002), updated in Dyurgerov and Meier (2005), and archived at the World Glacier Monitoring Service at the National Snow and Ice Data Center<sup>[1, 2]</sup>.

**Copyright:** This figure was prepared by Robert A. Rohde from published data and is part of the Global Warming Art project.

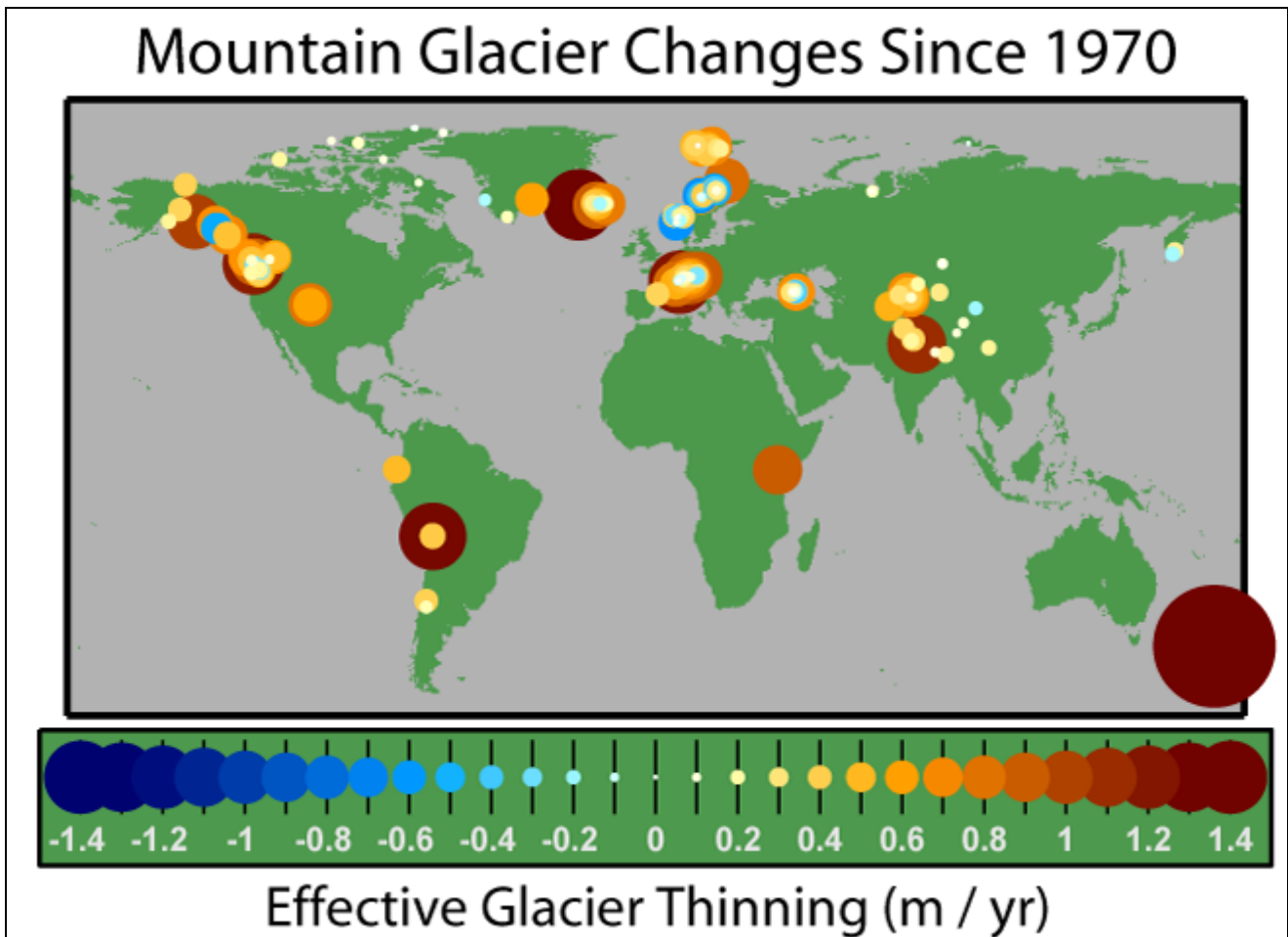
#### **References**

[1] [http://nsidc.org/data/docs/noaa/g10002\\_instaar\\_glacier\\_mass\\_balance\\_regime/index.html](http://nsidc.org/data/docs/noaa/g10002_instaar_glacier_mass_balance_regime/index.html)

[2] <ftp://sidads.colorado.edu/pub/DATASETS/NOAA/G10002/>



(7) Effective glacier thinning, from 1970 to 2004



**Page: Retreat of Glaciers since 1850**

**Summary:** The effective rate of change in glacier thickness, also known as the glaciological mass balance, is a measure of the average change in a glacier's thickness after correcting for changes in density associated with the compaction of snow and conversion to ice. The map shows the average annual rate of thinning since 1970 for the 173 glaciers that have been measured at least 5 times between 1970 and 2004 (Dyurgerov and Meier 2005). Larger changes are plotted as larger circles and towards the back.

All survey regions except Scandinavia show a net thinning. This widespread glacier retreat is generally regarded as a sign of global warming.

During this period, 83% of surveyed glaciers showed thinning with an average loss across all glaciers of 0.31 m/yr. The most rapidly growing glacier in the sample is Engabreen glacier in Norway with a thickening of 0.64 m/yr. The most rapidly shrinking was Ivory glacier in New Zealand which was thinning at 2.4 m/yr. Ivory glacier had totally disintegrated by circa 1988 [<http://www.stats.govt.nz/NR/rdonlyres/B79A90C2-70D6-46AB-8E1F-6D90D0B60544/0/glaciers.pdf>].

**Copyright:** This figure was originally prepared by Rober A. Rohde from published data and is incorporated into the Global Warming Art project.

## **(8) Retreat of glaciers**

### **Page: Retreat of Glaciers since 1850**

#### **(8-A) Greenland**

In Greenland, glacier retreat has been observed in outlet glaciers, resulting in an increase of the ice flow rate and destabilization of the mass balance of the ice sheet that is their source. The net loss in volume and hence sea level contribution of the Greenland Ice Sheet (GIS) has doubled in recent years from 90 km<sup>3</sup> (22 cu mi) to 220 km<sup>3</sup> (53 cu mi) per year<sup>[92]</sup>. Researchers also noted that the acceleration was widespread affecting almost all glaciers south of 70°N by 2005. The period since 2000 has brought retreat to several very large glaciers that had long been stable. Three glaciers that have been researched - Helheim Glacier, Kangerdlugssuaq Glacier, and Jakobshavn Isbræ - jointly drain more than 16% of the Greenland Ice Sheet. In the case of Helheim Glacier, researchers used satellite images to determine the movement and retreat of the glacier. Satellite images and aerial photographs from the 1950s and 1970s show that the front of the glacier had remained in the same place for decades. In 2001 the glacier began retreating rapidly, and by 2005 the glacier had retreated a total of 7.2 km (4.5 mi), accelerating from 20 m (66 ft) per day to 35 m (115 ft) per day during that period<sup>[93]</sup>.

Jakobshavn Isbræ in west Greenland, a major outlet glacier of the Greenland Ice Sheet, has been the fastest moving glacier in the world over the past half century. It had been moving continuously at speeds of over 24 m (79 ft) per day with a stable terminus since at least 1950. In 2002 the 12 km (7.5 mi) long floating terminus of the glacier entered a phase of rapid retreat, with the ice front breaking up and the floating terminus disintegrating and accelerating to a retreat rate of over 30 m (98 ft) per day. On a shorter timescale, portions of the main trunk of Kangerdlugssuaq Glacier that were flowing at 15 m (49 ft) per day from 1988 to 2001 were measured to be flowing at 40 m (130 ft) per day in the summer of 2005. Not only has Kangerdlugssuaq retreated, it has also thinned by more than 100 m (330 ft)<sup>[94]</sup>.

The rapid thinning, acceleration and retreat of Helheim, Jakobshavns and Kangerdlugssuaq glaciers in Greenland, all in close association with one another, suggests a common triggering mechanism, such as enhanced surface melting due to regional climate warming or a change in forces at the glacier front. The enhanced melting leading to lubrication of the glacier base has been observed to cause a small seasonal velocity increase and the release of meltwater lakes has also led to only small short term accelerations<sup>[95]</sup>. The significant accelerations noted on the three largest glaciers began at the calving in front and propagated inland and are not seasonal in nature<sup>[96]</sup>. Thus, the primary source of outlet glacier acceleration widely observed on small and large calving glaciers in Greenland is driven by changes in dynamic forces at the glacier front, not enhanced meltwater lubrication<sup>[96]</sup>. This was termed the Jakobshavns Effect by Terence Hughes at the University of Maine in 1986<sup>[97]</sup>.

#### **(8-B) Antarctica**

The climate of Antarctica is one of intense cold and great aridity. Most of the world's freshwater ice is contained in the great ice sheets that cover the continent of Antarctica. The most dramatic example of glacier retreat on the continent is the loss of large sections of the Larsen Ice Shelf on the Antarctic Peninsula. Ice shelves are not stable when surface melting occurs, and the collapse of Larsen Ice Shelf has been caused by warmer melt season temperatures that have led to surface melting and the formation of shallow ponds of water on the ice shelf. The Larsen Ice Shelf lost 2,500 km<sup>2</sup> (970 sq mi) of its area from 1995 to 2001. In a 35-day period beginning on January 31, 2002, about 3,250 km<sup>2</sup> (1,250 sq mi) of shelf area disintegrated. The ice shelf is now 40% the size of its previous minimum stable extent<sup>[98]</sup>. The recent collapse of Wordie Ice Shelf, Prince Gustav Ice Shelf, Mueller Ice Shelf, Jones Ice Shelf, Larsen-A and Larsen-B Ice Shelf on the Antarctic Peninsula has raised awareness of how dynamic ice shelf systems are. Jones Ice Shelf had an area of

35 km<sup>2</sup> (14 sq mi) in the 1970s but by 2008 it had disappeared<sup>[99]</sup>. Wordie Ice Shelf has gone from an area of 1,500 km<sup>2</sup> (580 sq mi) in 1950 to 1,400 km<sup>2</sup> (540 sq mi) in 2000<sup>[99]</sup>. Prince Gustav Ice Shelf has gone from an area of 1,600 km<sup>2</sup> (620 sq mi) to 1,100 km<sup>2</sup> (420 sq mi) in 2008<sup>[99]</sup>. After their loss the reduced buttressing of feeder glaciers has allowed the expected speed-up of inland ice masses after shelf ice break-up<sup>[100]</sup>. The Wilkins Ice Shelf is another ice shelf that has suffered substantial retreat. The ice shelf had an area of 16,000 km<sup>2</sup> (6,200 sq mi) in 1998 when 1,000 km<sup>2</sup> (390 sq mi) was lost that year<sup>[101]</sup>. In 2007 and 2008 significant rifting developed and led to the loss of another 1,400 km<sup>2</sup> (540 sq mi) of area and some of the calving occurred in the Austral winter. The calving seemed to have resulted from preconditioning such as thinning, possibly due to basal melt, as surface melt was not as evident, leading to a reduction in the strength of the pinning point connections. The thinner ice then experienced spreading rifts and breakup<sup>[23]</sup>. This period culminated in the collapse of an ice bridge connecting the main ice shelf to Charcot Island leading to the loss of an additional 700 km<sup>2</sup> (270 sq mi) between February and June 2009<sup>[102]</sup>.

Pine Island Glacier, an Antarctic outflow glacier that flows into the Amundsen Sea, thinned 3.5 m (11 ft) ± 0.9 m (3.0 ft) per year and retreated a total of 5 km (3.1 mi) in 3.8 years. The terminus of the Pine Island Glacier is a floating ice shelf, and the point at which it starts to float retreated 1.2 km (0.75 mi) per year from 1992 to 1996. This glacier drains a substantial portion of the West Antarctic Ice Sheet and along with the neighboring Thwaites Glacier, which has also shown evidence of thinning, has been referred to as the weak underbelly of this ice sheet<sup>[103]</sup>. Additionally, the Dakshin Gangotri Glacier, a small outlet glacier of the Antarctic ice sheet, receded at an average rate of 0.7 m (2.3 ft) per year from 1983 to 2002. On the Antarctic Peninsula, which is the only section of Antarctica that extends well north of the Antarctic Circle, there are hundreds of retreating glaciers. In one study of 244 glaciers on the peninsula, 212 have retreated an average of 600 m (2,000 ft) from where they were when first measured in 1953<sup>[104]</sup>. The greatest retreat was seen in Sjogren Glacier, which is now 13 km (8.1 mi) further inland than where it was in 1953. There are 32 glaciers that were measured to have advanced; however, these glaciers showed only a modest advance averaging 300 m (980 ft) per glacier, which is significantly smaller than the massive retreat observed<sup>[105]</sup>.

### **(8-C) Impacts of glacier retreat**

The continued retreat of glaciers will have a number of different quantitative impacts. In areas that are heavily dependent on water runoff from glaciers that melt during the warmer summer months, a continuation of the current retreat will eventually deplete the glacial ice and substantially reduce or eliminate runoff. A reduction in runoff will affect the ability to irrigate crops and will reduce summer stream flows necessary to keep dams and reservoirs replenished. This situation is particularly acute for irrigation in South America, where numerous artificial lakes are filled almost exclusively by glacial melt<sup>[106]</sup>. Central Asian countries have also been historically dependent on the seasonal glacier melt water for irrigation and drinking supplies. In Norway, the Alps, and the Pacific Northwest of North America, glacier runoff is important for hydropower.

Some of this retreat has resulted in efforts to slow down the loss of glaciers in the Alps. To retard melting of the glaciers used by certain Austrian ski resorts, portions of the Stubai and Pitztal Glaciers were partially covered with plastic<sup>[107]</sup>. In Switzerland plastic sheeting is also used to reduce the melt of glacial ice used as ski slopes<sup>[108]</sup>. While covering glaciers with plastic sheeting may prove advantageous to ski resorts on a small scale, this practice is not expected to be economically practical on a much larger scale.

Many species of freshwater and saltwater plants and animals are dependent on glacier-fed waters to ensure the cold water habitat to which they have adapted. Some species of freshwater fish need cold water to survive and to reproduce, and this is especially true with salmon and cutthroat trout. Reduced glacial runoff can lead to insufficient stream flow to allow these species to thrive. Alterations to the ocean currents, due to increased freshwater inputs from glacier melt, and the

potential alterations to thermohaline circulation of the World Ocean, may impact existing fisheries upon which humans depend as well<sup>[109]</sup>.

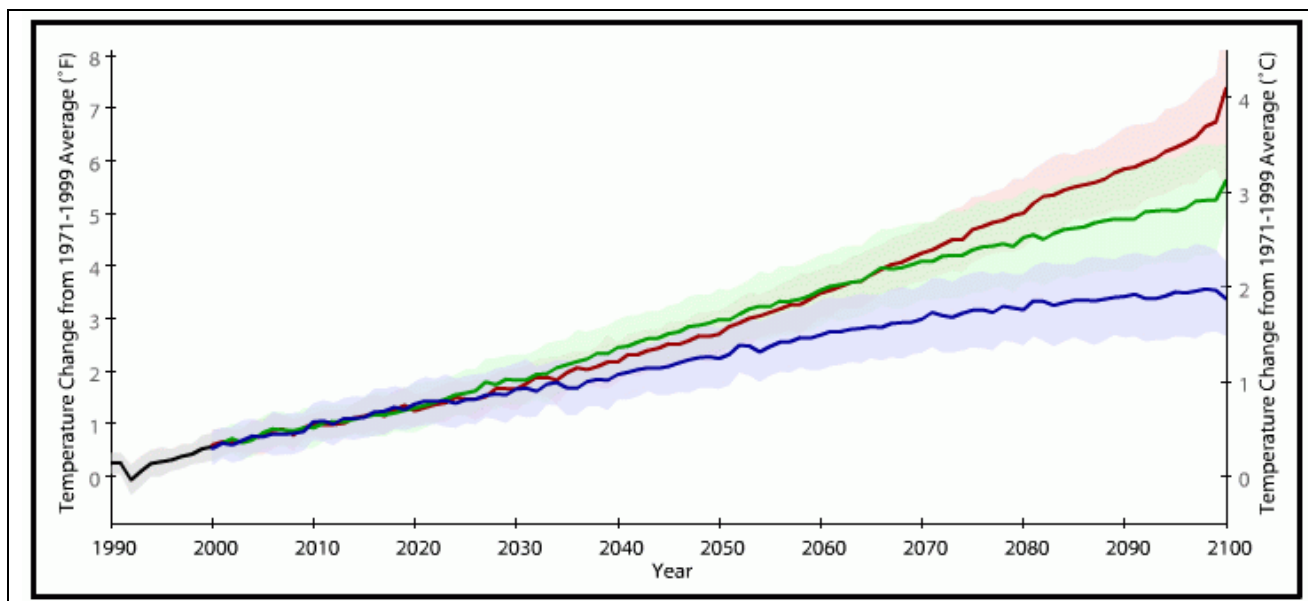
**The potential for major sea level rise depends mostly on a significant melting of the polar ice caps of Greenland and Antarctica, as this is where the vast majority of glacial ice is located. If all the ice on the polar ice caps were to melt away, the oceans of the world would rise an estimated 70 m (230 ft).** Although previously it was thought that the polar ice caps were not contributing heavily to sea level rise (IPCC 2007), recent studies have confirmed that both Antarctica and Greenland are contributing 0.5 millimetres (0.020 in) a year each to global sea level rise<sup>[110-112]</sup>. The fact that the IPCC estimates did not include rapid ice sheet decay into their sea level predictions makes it difficult to ascertain a plausible estimate for sea level rise but recent studies find that the minimum sea level rise will be around 0.8 metres (2.6 ft) by 2100<sup>[113]</sup>.

## References

- [23] Mauri S. Pelto. "Ice Shelf Instability". Retrieved 2009.
- [92] Rignot, E. and Kanagaratnam, P. (February 17, 2006). "Changes in the Velocity Structure of the Greenland Ice Sheet". *Science* 311 (5763): 986–990. Bibcode 2006Sci...311..986R. doi:10.1126/science.1121381. PMID 16484490. Retrieved November 2009.
- [93] Ian Howat. "Rapidly accelerating glaciers may increase how fast the sea level rises". UC Santa Cruz, November 14–27, 2005 Vol. 10, No. 14. Retrieved November 27, 2007.
- [94] M Truffer, University of Alaska Fairbanks; M Fahnestock, University of New Hampshire. "The Dynamics of Glacier System Response: Tidewater Glaciers and the Ice Streams and Outlet Glaciers of Greenland and Antarctica I". Retrieved 2007.
- [95] S.Das, I, Joughin, M. Behm, I. Howat, M. King, D. Lizarralde, M. Bhatia. "Fracture Propagation to the Base of the Greenland Ice Sheet During Supraglacial Lake Drainage". Retrieved 2009.
- [96] M. Pelto. "Moulins, Calving Fronts and Greenland Outlet Glacier Acceleration". Retrieved 2009.
- [97] T. Hughes (1986). "The Jakobshavn effect". *Geophysical Research Letters* 13 (1): 46–48. Bibcode 1986GeoRL..13...46H. doi:10.1029/GL013i001p00046.
- [98] National Snow and Ice Data Center (March 21, 2002). "Larsen B Ice Shelf Collapses in Antarctica". *The Cryosphere, Where the World is Frozen*. Retrieved November 5, 2009.
- [99] A. J. Cook and D. G. Vaughan. "Overview of areal changes of the ice shelves on the Antarctic Peninsula over the past 50 years". *The Cryosphere Discussions* 3 (2): 579–630. doi:10.5194/tcd-3-579-2009. Retrieved January, 2010.
- [100] Rignot, E.; Casassa, G.; Gogineni, P.; Krabill, W.; Rivera, A.; Thomas, R. (2004). "Accelerated ice discharge from the Antarctic Peninsula following the collapse of Larsen B ice shelf". *Geophysical Research Letters* 31 (18): L18401. Bibcode 2004GeoRL..3118401R. doi:10.1029/2004GL020697. Retrieved 2011-10-22.
- [101] M. Humbert, A. Braun and A. Moll (2008). "Changes of Wilkins Ice Shelf over the past 15 years and inferences on its stability". *The Cryosphere* 2 (3): 341–382. doi:10.5194/tcd-2-341-2000.
- [102] "Satellite imagery shows fragile Wilkins Ice Shelf destabilised". European Space Agency. June 13, 2009.
- [103] Rignot, E. J. (July 24, 1998). "Fast Recession of a West Antarctic Glacier". *Science* 281 (5376): 549–551. Bibcode 1998Sci...281..549R. doi:10.1126/science.281.5376.549. PMID 9677195.
- [104] News, AAAS (April 21, 2005). "New Study in Science Finds Glaciers in Retreat on Antarctic Peninsula". American Association for the Advancement of Science.
- [105] News, BBC (April 21, 2005). "Antarctic glaciers show retreat". BBC News.
- [106] News, BBC (October 9, 2003). "Melting glaciers threaten Peru". BBC News.
- [107] M. Olefs and A. Fischer. "Comparative study of technical measures to reduce snow and ice ablation in Alpine glacier ski resorts". in "Cold Regions Science and Technology, 2007". Retrieved September 6, 2009.
- [108] ENN (July 15, 2005). "Glacial Cover-Up Won't Stop Global Warming, But It Keeps Skiers Happy". Environmental News Network.
- [109] *The Economics of Adapting Fisheries to Climate Change*. OECD Publishing. 2011. pp. 47–55. ISBN 92-64-09036-3. Retrieved 2011-10-15.

- [110] Rahmstorf S, Cazenave A, Church JA, et al. (May 2007). "Recent climate observations compared to projections". *Science* 316 (5825): 709. Bibcode 2007Sci...316..709R. doi:10.1126/science.1136843. PMID 17272686.
- [111] Velicogna, I. (2009). "Increasing rates of ice mass loss from the Greenland and Antarctic ice sheets revealed by GRACE". *Geophysical Research Letters* 36 (19). Bibcode 2009GeoRL..3619503V. doi:10.1029/2009GL040222. edit
- [112] Cazenave, A.; Dominh, K.; Guinehut, S.; Berthier, E.; Llovel, W.; Ramillien, G.; Ablain, M.; Larnicol, G. (2009). "Sea level budget over 2003–2008: A reevaluation from GRACE space gravimetry, satellite altimetry and Argo". *Global and Planetary Change* 65: 83–88. Bibcode 2009GPC....65...83C. doi:10.1016/j.gloplacha.2008.10.004. edit
- [113] Pfeffer WT, Harper JT, O'Neel S (September 2008). "Kinematic constraints on glacier contributions to 21st-century sea-level rise". *Science* 321 (5894): 1340–3. Bibcode 2008Sci...321.1340P. doi:10.1126/science.1159099. PMID 18772435.

## (9) Projected temperature variations in the 21<sup>st</sup> century on a range of emissions scenarios



### Page: Effects of Global Warming

**Description:** Based on the cited public-domain source: The graph shows the average of a set of temperature simulations for the 20th century (black line), followed by projected temperatures for the 21st century based on a range of emissions scenarios (colored lines). The shaded areas around each line indicate the statistical spread (one standard deviation) provided by individual model runs. (Data processing by Jay Hnilo, CICS-NC, using data courtesy the Coupled Model Intercomparison Project, or CMIP3.) Temperature changes are measured against the 1971-1999 average. Results from a wide range of climate model simulations suggest that our planet's average temperature could be between 2 and 9.7°F (1.1 to 5.4°C) warmer in 2100 than it is today.

The net impacts of human actions and choices on future greenhouse gas concentrations are fed into models as different “scenarios.” For example, the scenario represented by the blue trend line above (IPCC Scenario B1) assumes that humans worldwide will make more sustainable development choices by using a greater range of, and more efficient, technologies for producing energy. In this scenario, carbon emissions are projected to increase from today's rate of about 9 billion metric tons per year to about 12 billion tons per year in 2040, and then gradually decline again to 1990 levels—5 billion tons per year—by 2100.

The scenario represented by the red trend line (IPCC Scenario A2) assumes humans will continue to accelerate the rate at which we emit carbon dioxide. This is consistent with a global economy that continues to rely mainly on coal, oil, and natural gas to meet energy demands. In this scenario, our carbon emission increases steadily from today's rate of about 9 billion tons per year to about 28 billion tons per year in 2100. The middle trend (green, IPCC Scenario A1b) assumes humans will roughly balance their use of fossil fuels with other, non-carbon emitting sources of energy.

For B1, the projected temperature in 2030 is around 1.6 °F, with a statistical spread (s.s.) (one standard deviation) ranging between 1.2-2.2 °F. The other two scenarios (A2 and A1b) are very similar to this. By 2060, B1 increases to around 2.7 °F, with a s.s. of around 2-3.3 °F. A1b increases to around 3.5 °F, with a s.s. of around 2.9-4.2 °F. A2 increases to around 3.5 °F, with a s.s. of around 3-3.9 °F. A1b increases to around 3.5 °F, with a s.s. of around 2.9-4.2 °F. By 2090, B1 increases to around 3.4 °F, with a s.s. of around 2.6-4.2 °F. A1b increases to around 4.8 °F, with a s.s. of around 3.9-5.8 °F. A2 increases to around 5.8 °F, with a s.s. of around 5.1-6.6 °F.

Because temperature projections depend on the choices people make in the future, climate scientists can't say which one of the scenarios is more likely to come to pass by the end of the century. These

scenarios are estimates, and greenhouse gas concentrations may grow at rates that are higher or lower than the scenarios shown in the graph. If future carbon dioxide emissions follow the same trajectory as they have over the last decade, increasing at a rate of more than 3 percent per year, carbon dioxide levels in the atmosphere would exceed the scenario represented by the red line (IPCC scenario A2) by the end of this century, if not before.

The source website (requires Flash) allows the graph's axes to be adjusted in scale, the x-axis moved left and right, and the y-axis up and down.

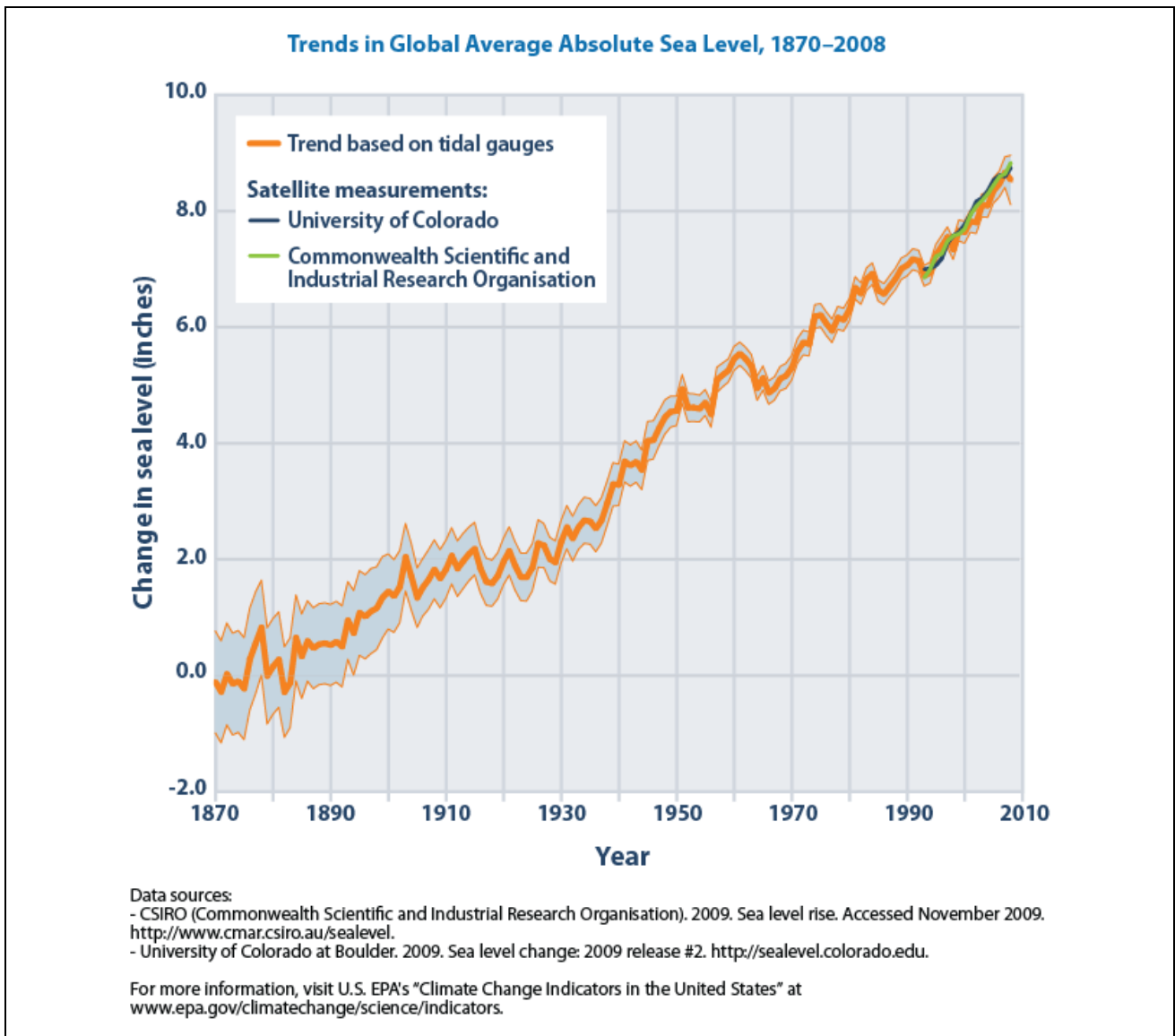
File:Map of projected global warming across the globe by the 2050s. Projections based on three SRES greenhouse gas emissions scenarios. Data from CMIP3 (2007).jpg shows maps of temperature changes across the world for these three scenarios.

**Date:** 6 March 2012

**Source:** ClimateWatch Magazine » Global Temperature Projections. NOAA Climate Portal.

**Author:** Jay Hnilo

(10) Global average absolute seas level, from 1870 to 2008



**Page: Effects of Global Warming**

**Description:** This image shows trends in global average absolute sea level between 1870 and 2008. From the cited public-domain source (US Environmental Protection Agency (US EPA), 2010): "After a period of approximately 2,000 years of little change, average sea levels rose worldwide throughout the 20th century, and the rate of change has accelerated in recent years. [...] When averaged over all the world's oceans, absolute sea level increased at an average rate of 0.06 inches per year from 1870 to 2008 [...] From 1993 to 2008, however, average sea level rose at a rate of 0.11 to 0.13 inches per year—roughly twice as fast as the long-term trend.

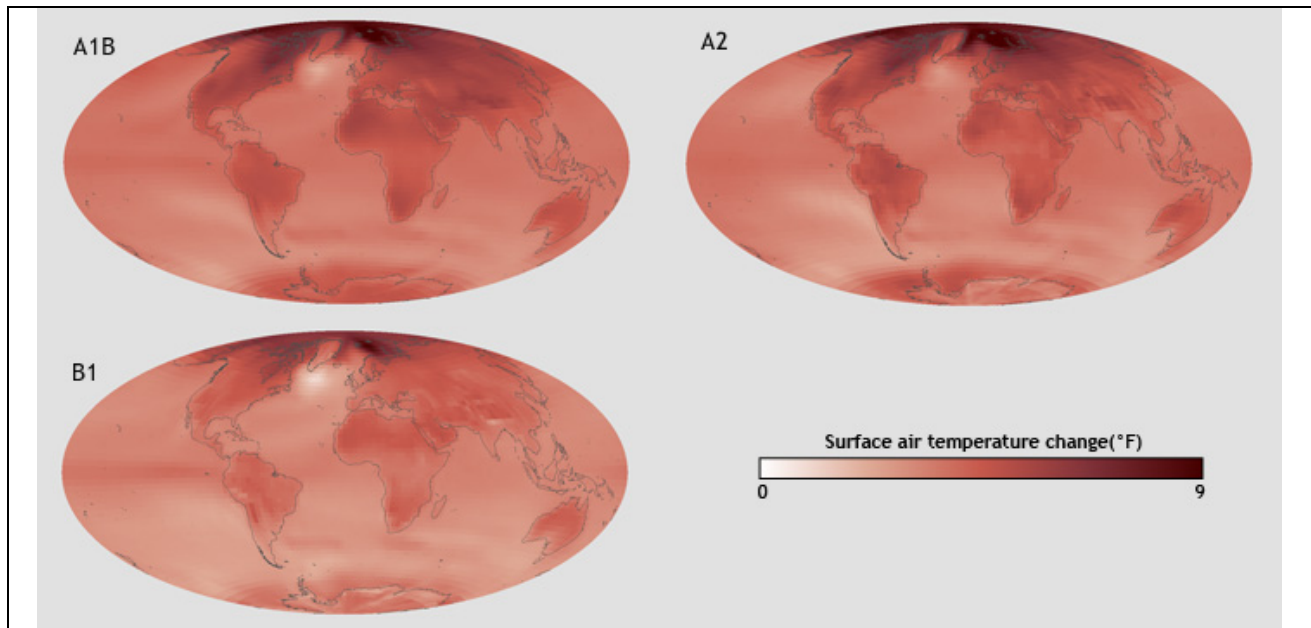
**Date:** 2010

**Source:** Sea level: Climate Change: US EPA. Publisher: US EPA

**Author:** US EPA



## (11) Projected surface temperatures for the period 2050-2059 in different scenarios



### Page: Effects of Global Warming

**Description:** The following description is based on the cited public-domain source (Gardiner et al, 2012): These maps show the average of a set of climate model experiments projecting changes in surface temperature for the period 2050-2059, relative to the period from 1971-1999. There are three different maps. Each map shows projected temperatures for a different scenario of future greenhouse gas emissions. The top left map corresponds with IPCC emissions scenario A1B; the top right map IPCC emissions scenario A2; and the bottom left map IPCC emissions scenario B1. These emissions scenarios are described in the following paragraphs. All models project some warming for all regions, with land areas warming more than oceans.

"The net impacts of [...] human actions and choices on future greenhouse gas concentrations are fed into models as different "scenarios." For example, [IPCC Scenario B1] assumes that humans worldwide will make more sustainable development choices by using a greater range of, and more efficient, technologies for producing energy. In this scenario, carbon emissions are projected to increase from today's rate of about 9 billion metric tons per year to about 12 billion tons per year in 2040, and then gradually decline again to 1990 levels—5 billion tons per year—by 2100.

[IPCC Scenario A2] assumes humans will continue to accelerate the rate at which we emit carbon dioxide. This is consistent with a global economy that continues to rely mainly on coal, oil, and natural gas to meet energy demands. In this scenario, our carbon emission increases steadily from today's rate of about 9 billion tons per year to about 28 billion tons per year in 2100. [IPCC Scenario A1b] assumes humans will roughly balance their use of fossil fuels with other, non-carbon emitting sources of energy.

Because temperature projections depend on the choices people make in the future, climate scientists can't say which one of the scenarios is more likely to come to pass by the end of the century. These scenarios are estimates, and greenhouse gas concentrations may grow at rates that are higher or lower than the scenarios shown in the graph. If future carbon dioxide emissions follow the same trajectory as they have over the last decade, increasing at a rate of more than 3 percent per year, carbon dioxide levels in the atmosphere would exceed [the IPCC A2 scenario] by the end of this century, if not before."

Projected changes in global mean temperature over the 21st century for these three emissions scenarios can be accessed at: [File:Projected global warming over the 21st century using three SRES greenhouse gas emissions scenarios. Data from CMIP3 \(2007\).png](#).

**Date:** 6 March 2012

**Source:** ClimateWatch Magazine » Global Temperature Projections. NOAA Climate Portal.

**Author:** Ned Gardiner, Hunter Allen, and Jay Hnilo

## **(12) Global warming and irreversible effects**

### **Page: Effects of Global Warming**

#### **(12-A) Abrupt or irreversible changes**

Physical, ecological and social systems may respond in an abrupt, non-linear or irregular way to climate change<sup>[145]</sup>. This is as opposed to a smooth or regular response. A quantitative entity behaves "irregularly" when its dynamics are discontinuous (i.e., not smooth), nondifferentiable, unbounded, wildly varying, or otherwise ill-defined<sup>[145]</sup>. Such behaviour is often termed "singular." Irregular behaviour in Earth systems may give rise to certain thresholds, which, when crossed, may lead to a large change in the system.

Some singularities could potentially lead to severe impacts at regional or global scales<sup>[146]</sup>. Examples of "large-scale" singularities are discussed in the articles on abrupt climate change, climate change feedback and runaway climate change. It is possible that human-induced climate change could trigger large-scale singularities, but the probabilities of triggering such events are, for the most part<sup>[147]</sup>, poorly understood<sup>[146]</sup>.

With low to medium confidence, Smith et al. (2001)<sup>[145]</sup> concluded that a rapid warming of more than 3 °C above 1990 levels would exceed thresholds that would lead to large-scale discontinuities in the climate system. Since the assessment by Smith et al. (2001), improved scientific understanding provides more guidance for two large-scale singularities: the role of carbon cycle feedbacks in future climate change (discussed below in the section on biogeochemical cycles) and the melting of the Greenland and West Antarctic ice sheets<sup>[134]</sup>.

#### **(12-B) Irreversible impacts**

Human-induced climate change may lead to irreversible impacts on physical, biological, and social systems<sup>[156]</sup>. There are a number of examples of climate change impacts that may be irreversible, at least over the timescale of many human generations<sup>[157]</sup>. These include the large-scale singularities described above - changes in carbon cycle feedbacks, the melting of the Greenland and West Antarctic ice sheets, and changes to the AMOC<sup>[157]</sup>. In biological systems, the extinction of species would be an irreversible impact<sup>[157]</sup>. In social systems, unique cultures may be lost due to climate change<sup>[157]</sup>. For example, humans living on atoll islands face risks due to sea-level rise, sea-surface warming, and increased frequency and intensity of extreme weather events<sup>[158]</sup>.

### **References**

[134] Schneider et al, "Chapter 19: Assessing key vulnerabilities and the risk from climate change", Sec. 19.3.7 Update on 'Reasons for Concern', p. 796, in IPCC AR4 WG2 2007.

[145] Smith et al., "Chapter 19: Vulnerability to Climate Change and Reasons for Concern: A Synthesis", Sec. 19.6.1. The Irregular Face of Climate Change, in IPCC TAR WG2 2001.

[146] White et al., "Technical summary", Sec. 7.2.5, Large-Scale Singular Events, in IPCC TAR WG2 2001.

[147]"[F]or the most part" refers to improved scientific understanding of singularities since the assessment by White et al. (2001). See: Schneider et al, "Chapter 19: Assessing key vulnerabilities and the risk from climate change", Sec. 19.3.7 Update on 'Reasons for Concern', in IPCC AR4 WG2 2007.

[156] IPCC, "5.14", Question 5, in IPCC TAR SYR 2001.

[157] Schneider et al., "Chapter 19: Assessing key vulnerabilities and the risk from climate change", Sec.19.2 Criteria for selecting 'key' vulnerabilities: Persistence and reversibility, in IPCC AR4 WG2 2007.

[158] Barnett, J and WN Adger (2003). "Climate dangers and atoll countries". Climatic Change (Kluwer Academic Publishers) 61: 321. This paper was published in 2001 as Tyndall Centre Working Paper 9

## (13) Risks from climate change

### Page: Runaway climate change

#### (13-A) Current risk

The scientific consensus in the IPCC Fourth Assessment Report<sup>[16]</sup> is that "Anthropogenic warming could lead to some effects that are abrupt or irreversible, depending upon the rate and magnitude of the climate change." Note however that this statement is about situations weaker than "runaway change". Text prepared for the IPCC Fifth Assessment Report states that "a 'runaway greenhouse effect' - analogous to Venus - appears to have virtually no chance of being induced by anthropogenic activities."<sup>[17]</sup>

Estimates of the size of the total carbon reservoir in Arctic permafrost and clathrates vary widely. It is suggested that at least 900 gigatonnes of carbon in permafrost exists worldwide<sup>[18]</sup>. Furthermore, there are believed to be another 400 gigatonnes of carbon in methane clathrates in permafrost regions<sup>[19]</sup> with 10,000 to 11,000 gigatonnes worldwide<sup>[19]</sup>. This is large enough that if 10% of the stored methane were released, it would have an effect equivalent to a factor of 10 increase in atmospheric CO<sub>2</sub> concentrations<sup>[20]</sup>. Methane is a potent greenhouse gas with a higher global warming potential than CO<sub>2</sub>.

Worries about the release of this methane and carbon dioxide is linked to arctic shrinkage. Recent years have seen record low Arctic sea ice. It has been suggested that rapid melting of the sea ice may initiate a feedback loop that rapidly melts arctic permafrost<sup>[21, 22]</sup>. Methane clathrates on the sea-floor have also been predicted to destabilise, but much more slowly<sup>[19]</sup>.

A release of methane from clathrates, however, is believed to be slow and chronic rather than catastrophic and that 21st-century effects of such a release are therefore likely to be 'significant but not catastrophic'<sup>[20]</sup>. It is further noted that 'much methane from dissociated gas hydrate may never reach the atmosphere'<sup>[23]</sup>, as it can be dissolved into the ocean and be broken down biologically<sup>[23]</sup>. Other research<sup>[24]</sup> demonstrates that a release to the atmosphere can occur during large releases. These sources suggest that the clathrate gun effect alone will not be sufficient to cause 'catastrophic'<sup>[20]</sup> climate change within a human lifetime.

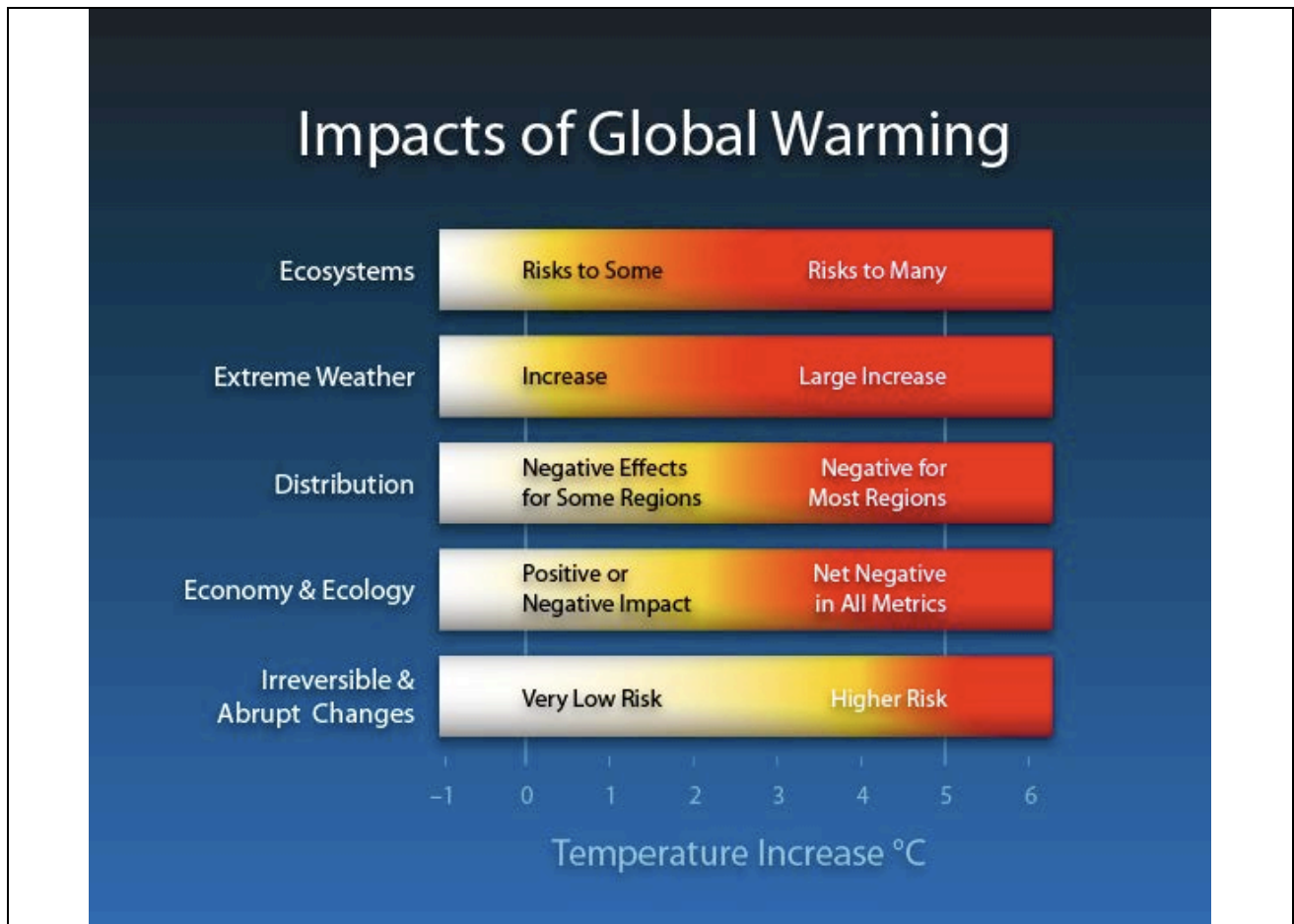
James E. Hansen has suggested that the Earth could experience a runaway greenhouse effect and adopt a climate like that of Venus if fossil-fuel use continues until reserves are exhausted<sup>[25]</sup>.

#### References

- [16] "Summary for Policymakers" (PDF). Climate Change 2007: Synthesis Report. IPCC. November 17, 2007.
- [17] <http://www.ipcc.ch/meetings/session31/inf3.pdf>
- [18] "Melting permafrost methane emissions: The other threat to climate change". TerraNature. 2006-09-15.
- [19] Macdonald, G. J. (1990). "Role of methane clathrates in past and future climates". *Climatic Change* 16 (3): 247–243. doi:10.1007/BF00144504. edit
- [20] Archer, David (2007). "Methane hydrate stability and anthropogenic climate change" (PDF). *Biogeosciences* 4 (4): 521–544. doi:10.5194/bg-4-521-2007. Retrieved 2009-05-25.
- [21] Lawrence, D. M.; Slater, A. G.; Tomas, R. A.; Holland, M. M.; Deser, C. (2008). "Accelerated Arctic land warming and permafrost degradation during rapid sea ice loss". *Geophysical Research Letters* 35 (11): L11506. Bibcode 2008GeoRL..3511506L. doi:10.1029/2008GL033985. edit
- [22] "Permafrost Threatened by Rapid Retreat of Arctic Sea Ice, NCAR Study Finds" (Press release). UCAR. June 10, 2008. Retrieved 2009-05-25.
- [23] Kvenvolden, Keith A. (March 30, 1999). "Potential effects of gas hydrate on human welfare". *PNAS* 96 (7): 3420–3426. Bibcode 1999PNAS...96.3420K. doi:10.1073/pnas.96.7.3420. PMC 34283. PMID 10097052. Retrieved 2009-05-23.
- [24] De Garidel-Thoron, T.; Beaufort, L.; Bassinot, F.; Henry, P. (Jun 2004). "Evidence for large methane releases to the atmosphere from deep-sea gas-hydrate dissociation during the last glacial episode" (Free full text). *Proceedings of the National Academy of Sciences of the United States of America* 101 (25): 9187–

9192. Bibcode 2004PNAS..101.9187D. doi:10.1073/pnas.0402909101. ISSN 0027-8424. PMC 438951. PMID 15197255. edit  
[25] Hansen, James (2008-12-17). "Climate Threat to the Planet" (PDF). Retrieved 2009-10-10.

## (14) Impacts of global warming



### Page: Global warming (Portal)

**Description:** Graph summarizing some of the expected impacts of Global Warming according to IPCC. Temperature deviations from 1990 readings.

**Date:** 20 July 2008

**Source:** Own work, estimates by IPCC

**Author:** Markus Koljonen (Dilaudid)

**(15) If all the ice melted**

(From an article by Tim Folger, National Geographic, September 2013, pp. 30-59)

If all the ice melted, the sea-level would rise 216 feet (65.83 meters).

In particular:

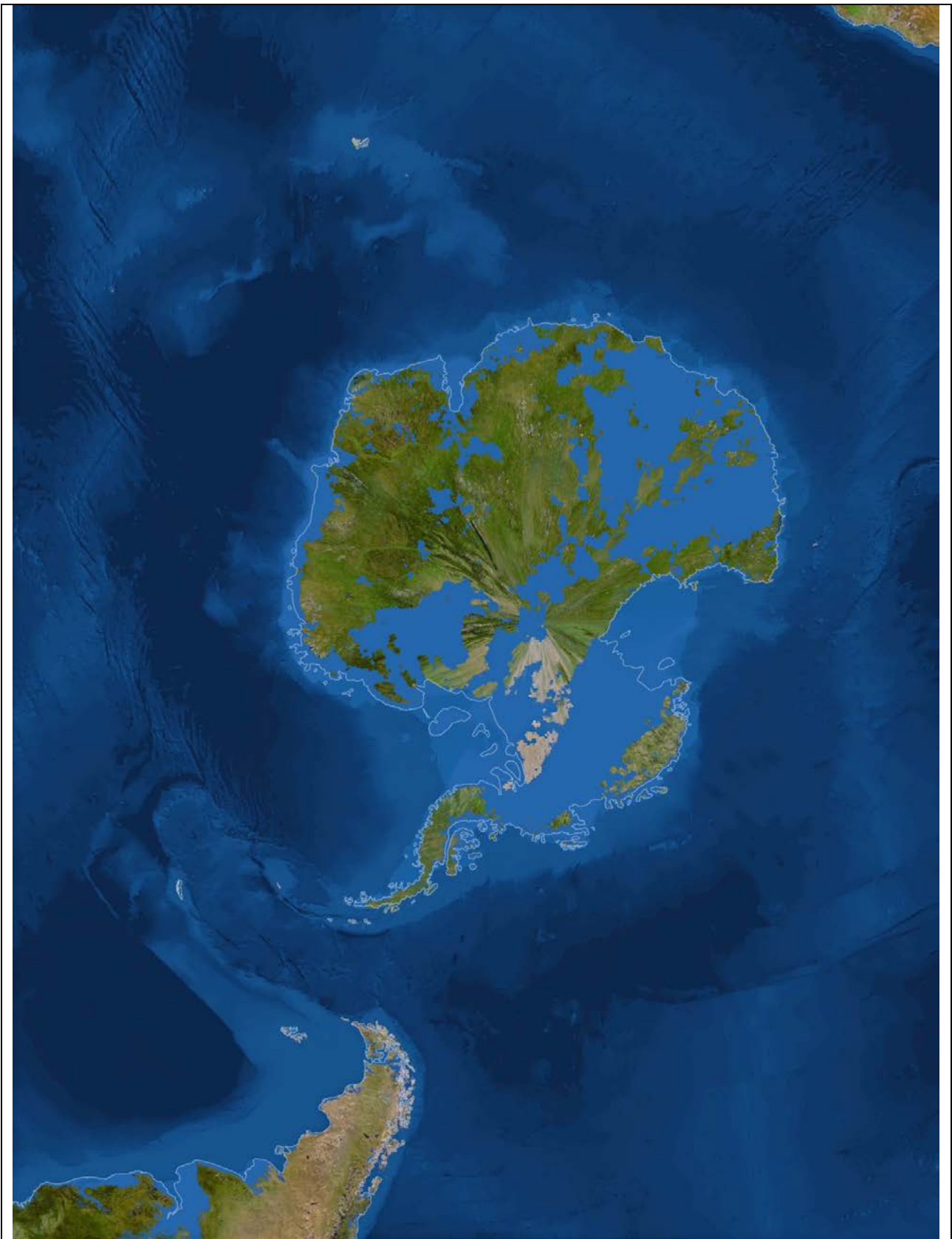
Area with ice melted	Sea-level rising	
	(feet)	(meters)
East Antarctica	175	53,34
West Antarctica	14	4,27
Greenland	25	7,62
Other ice	1	0,61
Total	216	65,84



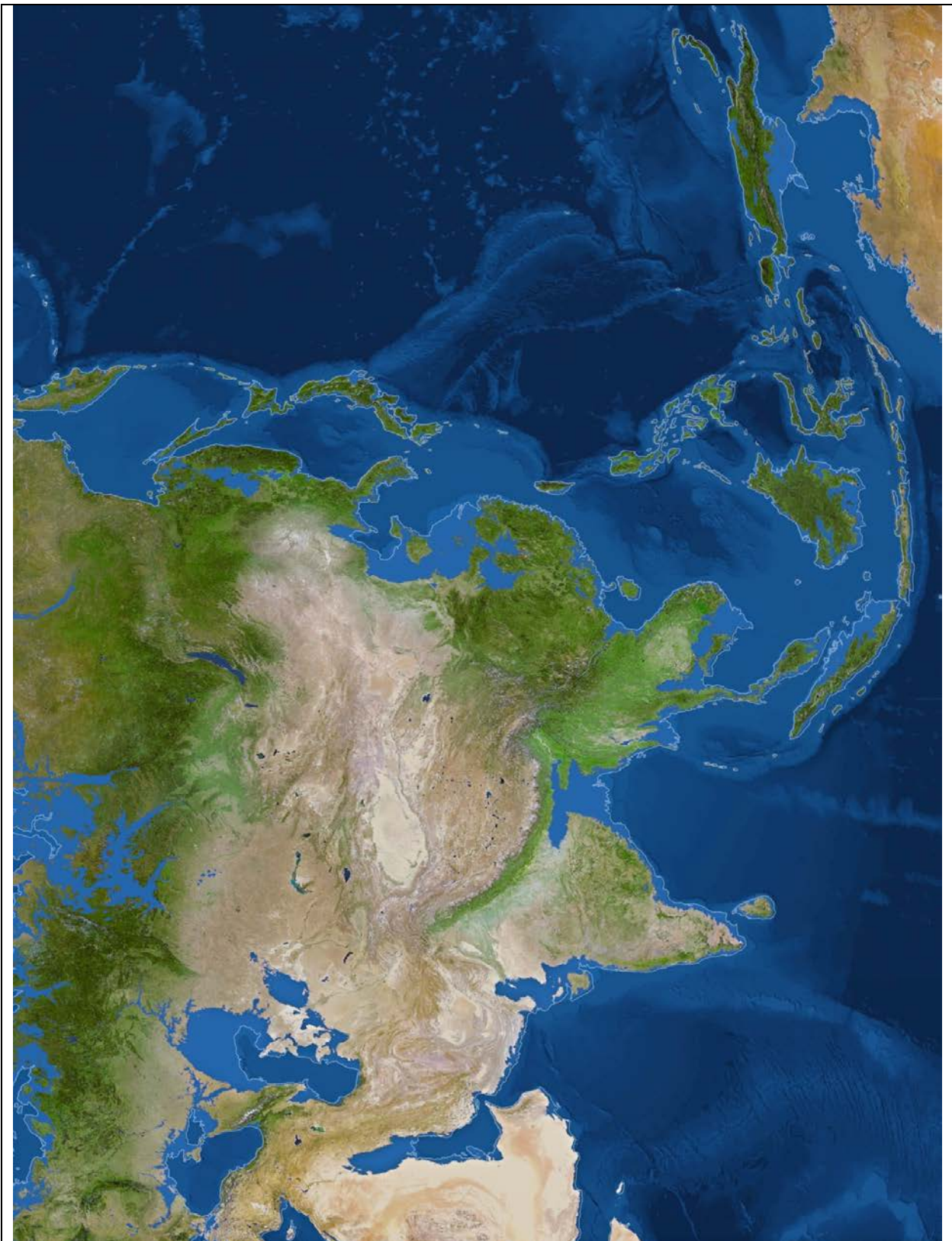


Effects of sea-level rising on Africa



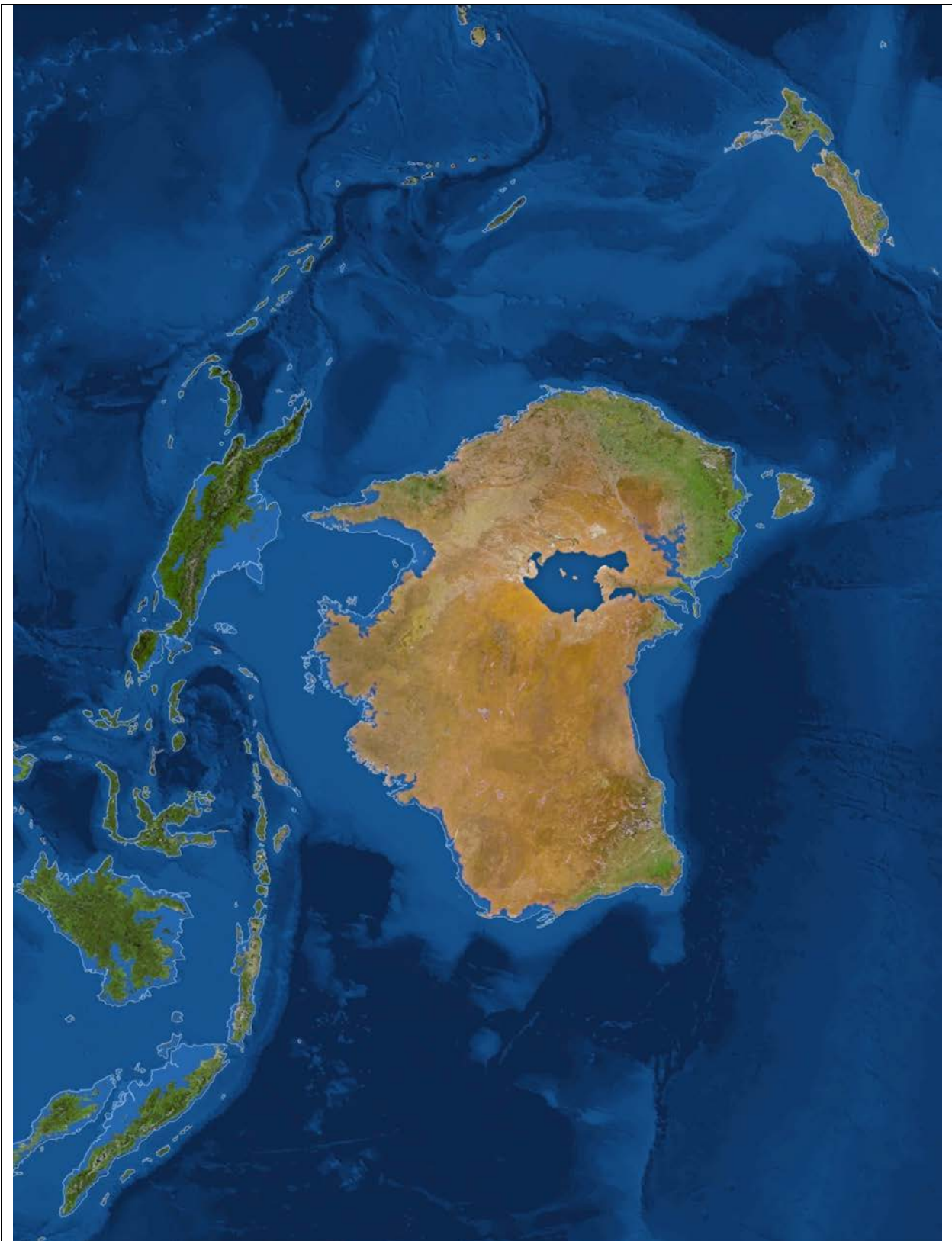


Effects of sea-level rising on Antarctica



Effects of sea-level rising on Asia





Effects of sea-level rising on Australia



Effects of sea-level rising on Europa





Effects of sea-level rising on North America



Effects of sea-level rising on South America



## **Summary**

83% of total world energy production for all purposes is, today, based on the use of non-renewable resources. This is becoming increasingly problematic, both in terms of the gradual depletion of the resources themselves, but even more so because of the progressive climate warming that, within a few decades, could lead to the complete destruction of large part of many of the world's most important cities. A transition to massive use of renewable resources as soon as possible is, therefore, essential.

The use of wind power plants would potentially appear as the best possible solution but today's plants have severe limitations. If, on one hand, we need to build plants that are as powerful as possible, costs grow exponentially, for the type of plant currently in use, in relation to the height (i.e., power) of the plants and so the construction of plants noticeably more powerful than those so far constructed, does not seem feasible.

This work proposes an entirely new type of plants, with a vertical axis of rotation, and with reduced costs, due to the method of construction and to the reduction in materials used.

In addition, the most interesting aspect is the possibility of constructing plants that are much more powerful than those existing at present with a linear increase of the costs/power ratio.

In fact, by building plants with an effective power 20 times greater than that of the most powerful current wind power plants built to date, about 68,000 plants would be sufficient to meet today's world energy needs satisfied by non-renewable sources. Furthermore, in a future scenario with world population increased to 10 billion and average consumption per capita equal to that of the most industrialized countries (but excluding countries with high consumption of energy), the overall energy needs would be covered by about 165,000 plants. The building of these plants would not constitute a heavy economic burden but could, indeed, be amortized in less than two years.